AN INVESTIGATION INTO THE USEFULNESS OF A METHOD OF ANALYSIS FOR STRAIGHT, UNIFORM-SECTION, BOX-GIRDER BRIDGE DECKS WITH SIDE CANTILEVERS

by F J RETIEF BSc (Civil) Engineering

A thesis submitted in partial fulfillment of the requirements for the degree of Master of Science in Engineering

Department of Civil Engineering
UNIVERSITY OF CAPE TOWN
April 1991

DECLARATION BY THE CANDIDATE

I, FRANCOIS JACQUES RETIEF, hereby declare that this Thesis is my own work and that it has not been submitted for a Degree at any other University.

Signed by candidate

F J RETIEF

April 1991

SYNOPSIS

Maisel and Roll, in a technical report for the London Cement and Concrete Association, proposed a method of analysis, in the form of an extension of simple beam theory, which is suitable for application to straight, rectangular, single-cell, uniform-section concrete box-girder bridge-decks with side cantilevers. This method only requires a calculator for execution and if a computer is used, results for maximum stresses may be obtained almost immediately. The authors state that since their method does not discretize the structure as in the case of finite element methods, the requirements in terms of computer capacity and therefore computation time is considerably reduced. Maisel, in a later Cement and Concrete Association development report, examining the use of small computer capacity for the analysis of concrete boxbeams, indicates that the hand method was being programmed.

Since the usefulness of such a method is obvious, especially if available in program form, it remains to confirm the accuracy and range of application of the method. For this purpose, four Perspex box-girder models of different depths were constructed and tested. Strain gauges were fitted at the mid- and quarter-span sections and readings for four to five loadcases per model were taken. Several problems relating to the creep and thermal properties of Perspex had to be overcome during the experimental phase.

Strain values obtained from the model tests were converted to stresses and these were compared to the stresses calculated by the recommended method of analysis proposed by Maisel and Roll. Generally, the experimental results showed a very good correlation with the analytical values and thus adequately confirmed the accuracy of the method.

The analysis for the model loadcases were performed using a programmable calculator and although some of the more complex equations were individually programmed to save calculation time, it still took about 6 hours to do an analysis for a loadcase comprising only point loading at a single position on the span. However, once the method has been programmed for small-capacity computers, the time required for analysis will be consideraly shorter, even for more complex load arrangements and this will provide the Engineer with a fast and inexpensive analytical tool.

ACKNOWLEDGEMENTS

The author especially wishes to thank Associate Professor M O de Kock for his valuable assistance and support as Supervisor in the execution of this Thesis.

Futhermore, the efforts of the following people in giving assistance are appreciated:

Mr G Bertuzzi	Dept of Civil Engineering (Workshop)
Mr H A Fagan	Principal Partner, Henry Fagan Consulting Engineers
Assoc Prof R D Kratz	Consultant, Henry Fagan Consulting Engineers
Assoc Prof R Tait	Dept of Mechanical Engineering
Mrs E van Niekerk	Henry Fagan Consulting Engineers
Miss A Serdyn	Henry Fagan Consulting Engineers

Finally the author wishes to express his gratitude to the Council for Scientific and Industrial Research for their financial assistance towards this Thesis.

CONTENTS

LIST OF FIGURES

NOTATION

a_{dis}	vertical deflection of web associated with distortion
a_{lbg}	vertical deflection of web associated with longitudinal bending
a_{svt}	vertical deflection of web associated with St Venant torsion
a_t	vertical deflection of web occurring in torsion without distortion
a_{twr}	vertical deflection of web associated with torsional warping
a_{vlg}	differential longitudinal deflection in flange associated with shear lag
a_x	displacement in the direction of the x axis
a_y	displacement in the direction of the y axis
a_z	displacement in the direction of the z axis
a_{1-6}	dimensions relating to longitudinal position of load
a_8	perpendicular distance from shear centre to tangent to mid-line of wall at the point considered
A	total area of cross-section including side cantilevers
A_{bot}	bh_{bot}
A_{cant}	$b_{cant}h_{top}$
A_{enc}	area enclosed by mid-line of wall of closed portion of cross-section = bd
A_{top}	bh_{top}
A_{web}	dh_{web}
$(\overline{Ay})_{½}$	first moment of area of partial half-cross-section about centroidal x axis
b	breadth between mid-lines of webs
b_{cant}	breadth of cantilever
B	internal bimoment
B_{dwr}	distortional warping bimoment
$B_{dwr,o}$	term in expression for B_{dwr}
B_{ext}	concentrated applied bimoment
B_{twr}	torsional warping bimoment
C_{cen}	central torsional moment of inertia of cross-section

C_{dwr}	distortional warping moment of inertia of cross-section
C_{svt}	torsional moment of inertia of cross-section in St Venant torsion
C_{twr}	torsional warping moment of inertia of cross-section
C_{twr}	$K_{19}C_{twr}$
d	depth between mid-lines of top and bottom slabs
d_{shc}	depth of shear centre below mid-line of top slab
D	overall depth of section
E	Young's modulus of elasticity
EI_{fra}	frame stiffness
f_{dwr}	distortional warping stress
f_{lbg}	longitudinal bending stress, calculated by engineers' theory of bending
f_{trb}	transverse bending stress
f_{twr}	torsional warping stress
f'_{lbg}	longitudinal bending stress, considering shear lag effect by the method of Schmidt et al[11]
F_x	concentrated applied load in the direction of the x axis
F_y	concentrated applied load in the direction of the y axis
F_z	concentrated applied load in the direction of the z axis
G	shear modulus of elasticity
h	thickness of wall
h_{bot}	thickness of bottom slab
h_{top}	thickness of top slab
h_{web}	thickness of web
I_{bot}	$h^3_{bot}/12(1-v^2)$
I_{fra}	1/E x frame stiffness
I_{top}	$h^3_{top}/12(1-v^2)$
I_{web}	$h^3_{web}/12(1-v^2)$
I_x	moment of inertia of entire cross-section about the centroidal x axis
I_y	moment of inertia of entire cross-section about the centroidal y axis

K_{1-34}	constants arising in various analyses
l	span
$m_{x,ext}$	distributed applied bending moment about the x axis
$m_{y,ext}$	distributed applied bending moment about the y axis
$M_{applied}$	applied bending moment (shear lag analysis)
$M_{bot\ flange}$	Resisting moment due to bending stresses in the bottom flange (shear lag analysis)
$M_{top\ flange}$	Resisting moment due to bending stresses in the top flange (shear lag analysis)
$M_{top\ webs}$	Resisting moment due to bending stresses in the webs above the neutral axis (shear lag analysis)
M_{trb}	transverse bending moment
$M_{trb,B}$	transverse bending moment at top of web due to distortional load system
$M_{trb,D}$	transverse bending moment at bottom of web due to distortional load system
M_x	internal bending moment about the x axis
$M_{x,ext}$	concentrated applied bending moment about the x axis
M_y	internal bending moment about the y axis
$M_{y,ext}$	concentrated applied bending moment about the y axis
n	index in summation of series
n_x	intensity of distributed loading in the x direction
n_y	intensity of distributed loading in the y direction
n_z	intensity of distributed loading in the z direction
N	internal axial force
s_{per}	peripheral coordinate along mid-line of wall
t_{ext}	distributed applied torsional moment
T	internal torsional moment
T_{ext}	concentrated applied torsional moment
T_{svt}	internal torsional moment in St Venant torsion
T_{twr}	internal torsional moment due to torsional warping shear stresses

v_{dwr}	distortional warping shear stress
v_{lbg}	shear stress in longitudinal bending
$(v_{lbg}h)$	shear flow in longitudinal bending
v_{svt}	shear stress in St Venant torsion at mid-line of wall
$(v_{svt}h)$	shear flow in St Venant torsion of thin-walled section
v_{twr}	torsional warping shear stress
V_x	shear force in the x direction
V_y	shear force in the y direction
x	horizontal coordinate referred to centroidal axes
y	vertical coordinate referred to centroidal axes
z	longitudinal coordinate
β_{trb}	angle of distortion of cross-section
$\beta_{trb,o}$	term in expression for β_{trb}
δC_{svt}	increment in C_{svt} due to antisymmetric shear stress distribution measured by δv_{svt}
δT_{svt}	increment in T_{svt} due to antisymmetric shear stress distribution measured by δv_{svt}
δv_{svt}	increment in v_{svt} over half thickness of wall
ϵ_x	strain in x direction for plane stress analysis
ϵ_y	strain in y direction for plane stress analysis
τ_{xy}	shear strain for plane stress analysis
λ	term used in shear lag analysis of Schmidt et al[11]
σ_x	normal stress in x direction for plane stress analysis
σ_y	normal stress in y direction for plane stress analysis
t_{xy}	shear stress for plane stress analysis
θ_{svt}	rotation due to St Venant torsion
θ_x	rotation about the x axis
θ_y	rotation about the y axis
θ_z	rotation about the z axis
v	Poisson's ratio

w_{dwr} distortional warping coordinate

w_{twr} sectorial coordinate in torsional warping, referred to the shear centre

$\int_A dA$ integral over the entire cross-sectional area

$\oint$ integral along the mid-line of wall of the closed portion of cross-section

dw_{twr}/ds_{per} derivative of w_{twr} with respect to s_{per}

TERMINOLOGY

The definitions for the various terms and expressions used in the text are as follows:

distortion	deformation of a cross-section (Figure 3.1)
warping	the out-of-plane displacement of points on a cross-section (Figure 3.2c)
torsional warping	warping of cross-section associated with shear deformations in planes of flanges and webs caused by torsion
distortional warping	warping of cross-section associated with in-plane bending of flanges and webs caused by torsion
shear lag	a form of warping associated with bending without torsion as a result of shear deformations in the planes of the flanges (can also occur under torsional loading) (Figure 3.3)
St Venant torsion	pure torsion, theory assumes zero warping restraint and therefore no longitudinal normal stresses
longitudinal	in the direction of the span or z axis
transverse	in directions perpendicular to the span
centreline	vertical line through axis of symmetry (centroid) of cross-section
mid-line	centrelines of flanges and webs in section
midpoint	a point halfway between reference points

The terms **measured, experimental and observed readings** refer to the stresses determined from the strain readings from the model tests.

The terms **analytical, theoretical and calculated values** refer to stresses determined by using the hand method of analysis.

1 INTRODUCTION

Torsional loading in box-girders introduce longitudinal warping stresses over and above those found from the simple bending and torsional analyses. Additionally, transverse bending stresses due to the distortion of the cross-section as well as local bending also occurs. These stresses must be taken into account in the design of such members since they represent a major portion of the total stresses that are present.

Several methods are available whereby the warping and transverse bending stresses can be determined. The most accurate method and also the method with the widest application is the finite element method which requires a computer of sufficient capacity. These methods involve extensive calculations and as such use considerable computational time and therefore have high costs. Also, the time required for preparing the input for such programs may be substantial, especially if a facility for automatically discretizing the structure is not available.

The finite strip method also involves discretizing the structure and considerable computation but according to Maisel [6], has been developed into an economical method for dealing with box-giders of uniform section as well as curved and skew girders and continuous members.

Maisel and Roll[7], in the method that they proposed, selected the most suitable methods available, in their assessment, for dealing with each of the structural actions that typically occur in box-girder structures. The structural action types are the following: simple bending and shear, St Venant torsion, torsional warping, distortional warping, transverse bending, shear lag in bending and local plate bending. The final result is obtained by superimposing the relevant stresses from each of the above effects. The method is limited to rectangular, single-cell, constant-section members and requires considerable calculation time if done by hand. However, if it is programmed for a small computer, and it is suitable for this purpose, it will be a fast and inexpensive analytical method which is competitive with the finite element procedures within its scope of application. The only question remaining therefore is with regard to accuracy and whether the method can produce suitable results for use in the actual design of members.

Maisel and Roll performed tests on a single Perspex model with successive single point-loads applied at various points on the deck of the model and in addition did have some results available from tests performed by Steinle. The Maisel and Roll model represented a box-girder of average proportions and the tests gave satisfactory although sparse results.

In order to broadly assess the accuracy of the method, it was decided to test four Perspex models ranging from extremely deep to extremely shallow sections with the in-between models slightly deeper and slightly shallower than normal. The support conditions in all cases represented a system preventing distortion but not warping. Loading was in the form of single point loads or pairs of point loads (mostly) applied at either midspan or quarter-span. Where possible, loadcases were devised to be able to separately examine individual structural action types. Electrical strain gauges around the midspan and quarter-span sections were used to find stresses which were compared to those found from analysis.

The tests on the models may have been extended to include distributed loading as well as support conditions which provided full warping restraint as in the case of continuous members. It was however felt that in the first instance, if good results are achieved with point loading, good results should also be achieved for distributed loading since this merely represents a superposition of a number of point loads. In the second instance, Maisel and Roll refer to an example by Steinle in which the warping stresses at midspan under concentrated midspan torsional loading differ by only 5% when calculated for no warping restraint at the supports and then for full warping restraint at the supports. This is a relatively small influence and as such less important than the other effects examined here.

2 EXPERIMENTAL PROCEDURE AND RESULTS

2.1 GENERAL

The purpose of the experimental work was to establish the accuracy of the hand method of analysis proposed by Maisel and Roll[7] and this was done by testing four box-girder models with different (but realistic) cross-sectional dimensions.

It was decided to construct the models using Perspex sheets mainly because of the ease in accurately machining and assembling this type of material.

A further consideration in selecting Perspex was that Maisel and Roll had also tested their proposed analytical method against the results of tests on Perspex models. According to their report[7], these tests yielded results which compared favourably with those from the analysis.

For simplicity, the loading type was restricted to point loads applied at the mid- and quarter-span sections of the models to give the required combinations of torsional, distortional and bending effects. The support conditions for the models were chosen so as to restrain both torsion and distortion but not warping. In terms of longitudinal bending, the models were all simply supported single-span structures.

2.2 SELECTION OF MODEL DIMENSIONS

2.2.1 Design Considerations

The selection of proportions for the box-girder models was based on the results of a feature survey by Swann[13] of 173 concrete box-girder bridges constructed between 1957 and 1972.

From the above publication it was found that the preferred range of spans for uniform-section, single-spine box girders lie between 25 and 50 metres and that span to depth ratios vary between about 12 (economic limit) and 32 (flexural stress limit).

In order to keep model-making to a minimum and to re-use strain gauges as far as possible, it was decided to initially build and test the deepest model (l/D = 8) and to subsequently modify this model by cutting the webs to the depth required for the next deepest model(l/D = 14). After accurately milling the shortened webs, the bottom flange, either the one used previously or a new one if a different thickness was required, was re-glued. This process was repeated three times to yield the four models.

In this way it was possible to retain the top flange (deck) and web portions from one model to the next and since these had the most gauges attached to them and consequently were the most expensive and time-consuming to replace, considerable savings were achieved.

The modification procedure described above, imposed restrictions on the selection of dimensions for the various models in that it fixed the thicknesses of the top flanges and the webs, h_{top} and h_{web}, as well as the width of deck, b, and length of the cantilevers, b_{cant}. Therefore, it was also necessary to check whether these fixed dimensions and thicknesses did not result in abnormal values for some models, especially the ones with the deepest and shallowest sections, in terms of the various Swann criteria. However, it was found that by selecting suitable scaling factors, the full scale dimensions for all models could be made to fall within the normal range.

2.2.2 Design Procedure

Firstly, the dimensions for a box-girder of average proportions was determined using results from the Swann survey.

A span length of 48 m, which is relatively large for this type of deck, was selected so that the member sizes and thicknesses would be determined in terms of structural requirements rather than nominal sizes. This gave a model length of 1.200 m when using a scaling factor of 40. The above length was found to be suitable in terms of the available Perspex sheet sizes and the size of milling machine.

A span to depth ratio of 21, which is approximately the mean value for this length of span, was chosen from a diagram of maximum span/depth ratio at the piers versus maximum span for the various bridge structures included in the survey[13]. This gave an overall depth of section of about 2.3 m and a model depth of 57.5 mm.

The deck width b, was found from a diagram of ratio of total breadth/maximum span versus maximum span. The approximate mean ratio given for single-cell structures is 0.21 for a 48 m span, giving a deck width of about 10,1 m and a model dimension of 252.5 mm.

The the cantilever length, b_{cant}, was calculated using the following equation given for single-cell box-girders:

$$b_{cant}/b = 0.24 - 0.00048\ l_{max} + 0.0058\ b$$

where

l_{max} = maximum span length

b_{cant} = length of cantilever measured from the web centreline

b = breadth of deck including the cantilevers

The above equation gives a value of approximately 2.80 m for b_{cant} and an equivalent model dimension of 70.0 mm.

The thicknesses of deck slabs are largely dictated by transverse bending design considerations. Swann considers this dimension at two critical positions: at the root of the cantilever and between webs. In both instances plotted diagrams of slab thickness versus span and which differentiate between transversely reinforced and transversely prestressed deck slabs, are given for the structures surveyed. For a cantilever length of about 2.6 m (measured from the outside of the webs, assuming a web thickness of 400 mm) the average thickness at the root was found to be about 320 mm. In terms of the second consideration, the average thickness for a deck slab with a 4.10 m clear span between webs, again assuming a web thickness of 400 mm and with haunches present between flange and webs, was found to be about 240 mm. The thickness selected for the top flange was based on an average of the above, i.e. 280mm, which translated to a model dimension of 7 mm.

The web thickness was found from a diagram of $2h_{web}D/bl_{max}$ versus maximum span, l_{max}, and which distinguishes between box-girder structures with constant section, varying slab thicknesses and varying depth of section. The parameter given above is a dimensionless expression taking web shear area at the supports (proportional to shear resistance) and deck area (proportional to load) into account. For a constant section with a span of 48 m, the diagram gives a value of about 3.8×10^{-3} which works out to a web thickness of 0.801 m for both webs or 400 mm per web. This gave a model dimension of 10 mm.

The final stage in finding dimensions for the average box-girder was determining the thickness of the bottom flange. A diagram similar to that for the webs but with parameters of $D\,A_{bot}/bl_{max}^2$ versus maximum span l_{max}, where A_{bot} is the area of the bottom flange, is provided. This gives a value of about 1.0×10^{-4} for a constant section member with a 48 m span. The thickness of the bottom flange was then 210 mm which for the model became 5.3 mm.

The dimensions for the average section from the above calculations are illustrated in Figure 2.1.

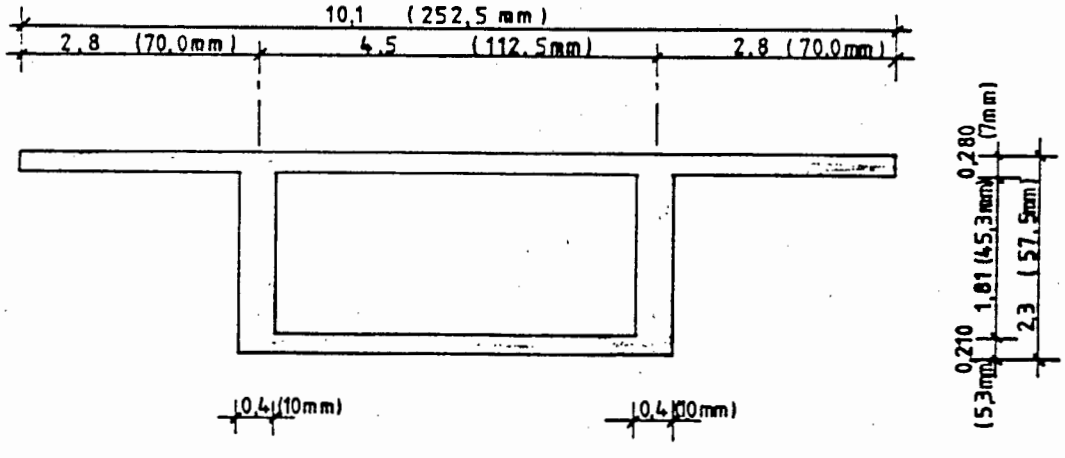

MODEL DIMENSIONS (1 IN 40 SCALE) GIVEN IN BRACKETS
FULL SCALE DIMENSIONS IN m

Figure 2.1 **Average cross-section for a single-spine, uniform-section box-girder spanning 48 m.**

Secondly, span to depth ratios were chosen for the four models so that these would be spaced towards the upper and lower portions of the range of values presented in the Swann survey, i.e. from 12 to about 28. Values of 8, 14, 27 and 32 were selected.

The cross-sectional dimensions for all the models with the exception of the bottom flange thicknesses were therefore known at this stage: the width of the deck, length of cantilever and thicknesses for webs and deck were taken from the sizes found for the average model above and remained the same throughout and the depths were calculated from the above span to depth ratios.

The required bottom flange thicknesses were provided for each of the models according to the Swann survey since these panels had to be removed for the modification from one model to the next in any case.

Thirdly, as a check, it was seen whether suitable scaling factors could be found on a trial and error basis to give full scale dimensions that would fall within the range of values described by the Swann survey. These factors were found to be 30, 33.3, 40 and 40 for models 1 to 4.

The models were made, as described in the next section, using the Perspex sheet thicknesses nearest to the values found above. See Figure 2.2 for the as-built model cross-sections.

2.3 PRODUCTION OF MODELS AND MEASUREMENTS

As described previously, Model 1 (deepest section) had to be made first and tested before being modified by cutting through the webs to produce the next model - ie Model 2. This process was then repeated twice more to obtain the other models.

The various panels for the deck, webs and bottom flange were cut with a bandsaw from 6, 10 and 3mm Perspex sheets respectively and accurately machined down to the required sizes using a milling machine. The panels were then glued together using Tensol cement for Perspex - a chloroform based adhesive. The as-built cross-sectional dimensions of the models are given in Figure 2.2.

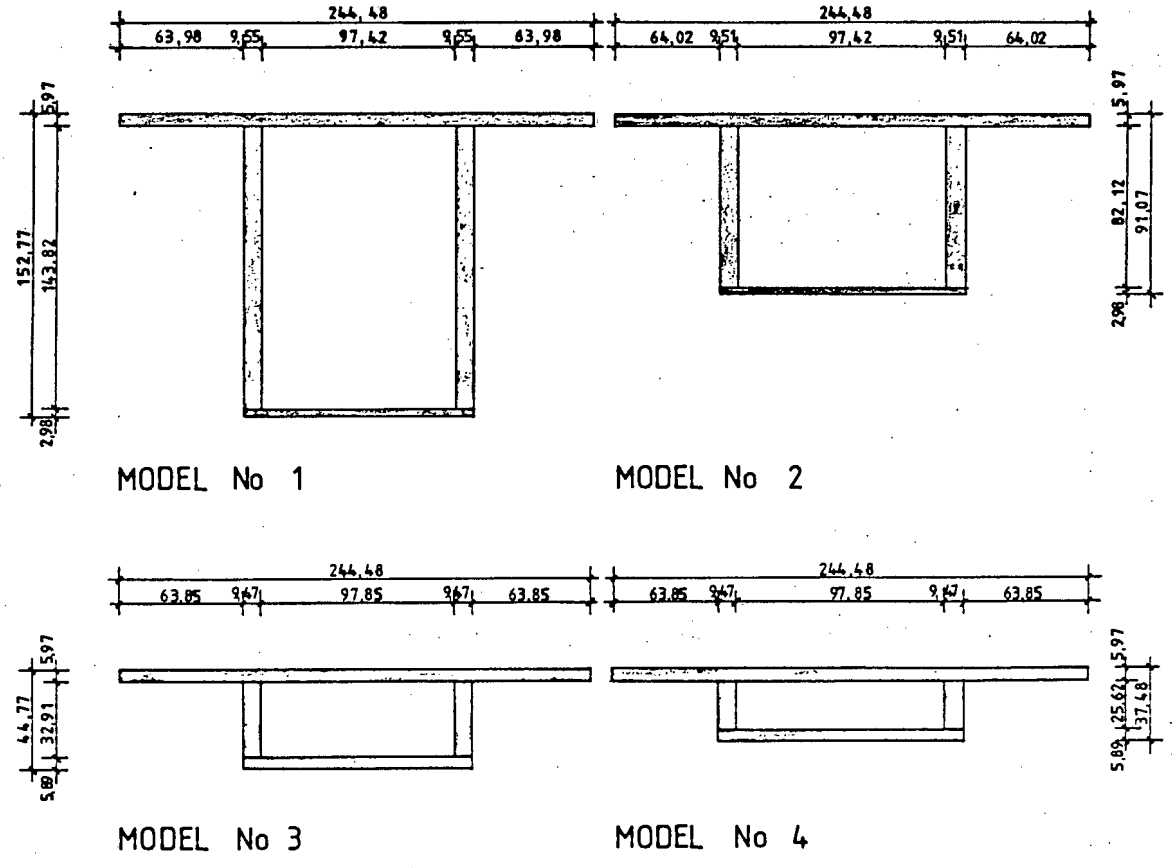

Figure 2.2 As-built model cross-sectional dimensions.

For the modification, the webs were cut 2 to 3mm below the required depth with a bandsaw and the excess material machined off accurately with a milling machine. The bottom flange, which could either be from the previous model from which the residual web portions had been carefully machined down or a completely new panel depending on the thickness required, was then glued on.

2.4 INSTRUMENTATION

2.4.1 Strain Gauges

2.4.1.1 Selection of strain gauges

The strain gauges that were used had to be compatible with both Perspex as base material and with the available measuring instruments (see 2.4.2) and in addition had to be small enough in relation to the size of the models to give sufficiently localized strain values.

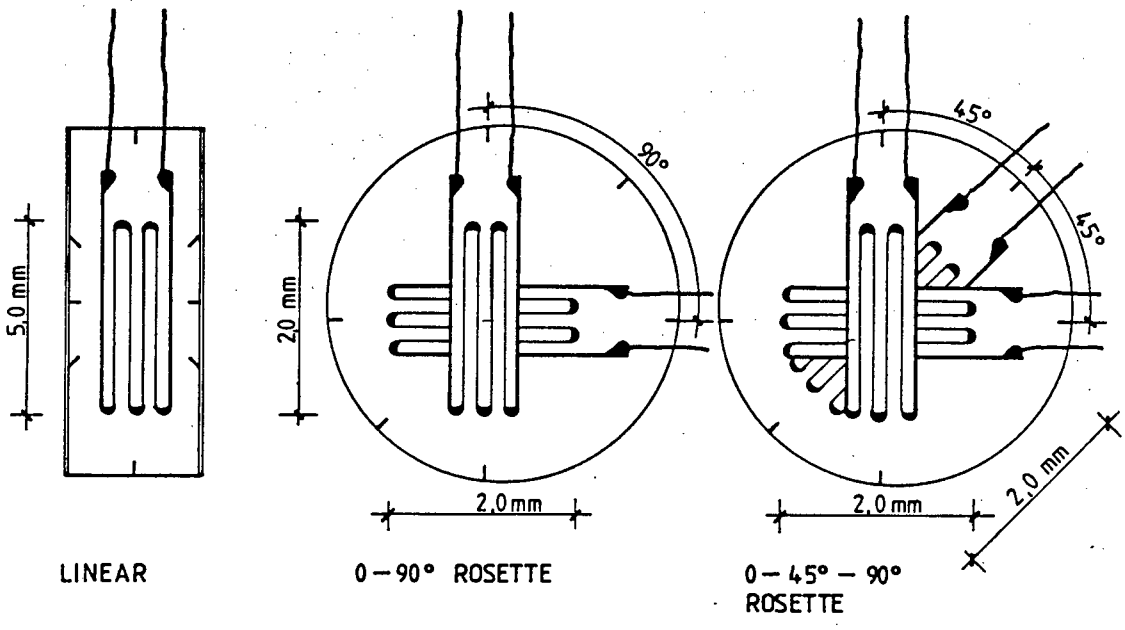

Figure 2.3 Strain gauge configurations.

Strain gauges produced by KYOWA ELECTRONIC INSTRUMENTS COMPANY of Japan were chosen since they satisfied both the above requirements - see Figure 2.3 above. These gauges were available in 2 and 5 mm lengths for the rosettes and the linear types respectively and were small when compared to a model span of 1200 mm or deck width of 245 mm.

2.4.1.2 Choosing the strain gauge positions

For simplicity and ease of making direct comparisons with the results from other published sources, it was decided to mount the strain gauges at the midspan and quarter-span sections for all four of the models tested.

These gauge positions also coincided with the loading points, which were on the web centrelines at either midspan or quarter-span sections. This form of loading was chosen to provide results for the most elementary loading configurations. Hence, it was anticipated that some local stress concentrations would occur in the immediate vicinity of the loads but that these would not affect gauge readings lower down on the webs, on the bottom flange or at the edges and centre-line of the deck at the same section.

The transverse arrangement of gauges on the cross-sections depended on several factors, the most important of which was the amount of information that could be obtained from the various types i.e. linear strain gauges, 0-90 degree two-gauge strain rosettes and the 0-45-90 degree three-gauge strain rosettes.

To find the normal stress at a point, it was necessary to know the strain in the direction considered as well as either the strain or the stress in the perpendicular direction - see Section 2.6.1. Therefore, perpendicular normal stresses could be calculated readily when using rosettes which measured the strains in perpendicular directions. However, in the case of the linear gauges, either the stress or strain for the perpendicular direction had to be known or assumed before the normal stresses could be determined.

Since the side cantilevers were not loaded, normal stresses in the transverse direction in these members remained zero and thus only linear gauges were required to find the longitudinal stresses.

Similarly, when the webs were loaded symmetrically, transverse normal stresses in the top and bottom flanges remained zero and so again only the linear gauges were needed to find the longitudinal normal stresses. However, under torsional loading conditions, transverse bending stresses occured in the flanges between webs in addition to the longitudinal normal stresses and therefore strain rosettes were required to find the perpendicular normal stresses at these positions.

To find the shear stress at a point, it was necessary to know the strains in at least three separate (and preferably widely spaced) directions at that point. These strains could be found by making use of a 0-45-90 degree three-gauge rosette. These gauges were consequently provided at positions where significant shear stresses were expected to occur, such as in the webs under symmetrical vertical loading conditions and in the top and bottom flanges as well as the webs under torsional loading conditions. Figure 2.4 shows the layout of gauge-positions used for Model 3, which was typical for all the models.

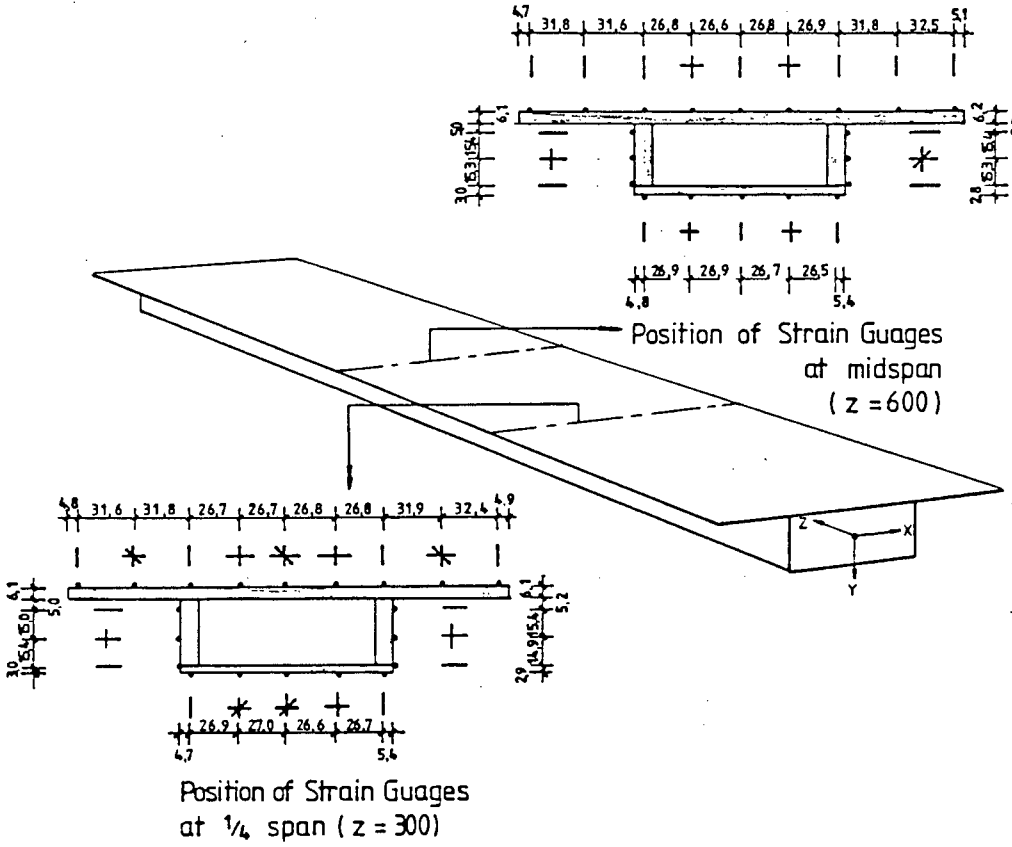

Figure 2.4 Typical strain gauge positions (Model No 3 shown).

2.4.1.3 Mounting and wiring of strain gauges

The strain gauges were cemented to the Perspex models in accordance with the procedure prescibed by the gauge manufacturer. Also, a gauge from each lot number was cemented to a spare piece of Perspex by the same procedure to act as temperature compensation or dummy gauge and was to be used when reading active gauges on the models with the same lot number.

The leads for each gauge comprised two eight-strand (200 micron) copper wire conductors sheathed in insulating plastic and were approximately 1.2 m long to reach the reading instruments.

Finally KYOWA C5 protective silicone coating was used to seal the gauges after first driving off moisture with a blow drier.

2.4.2 Equipment for reading strain gauges

The basic instrument for taking strain readings was a Wheatstone (strain) bridge, in this case manufactured by HUGGENBERGER of Zurich, which measures the change in the electrical resistance of a strain gauge due to a change in length.

Initially only one of these instruments was used and was connected to the strain gauges via a HUGGENBERGER switching unit which could accomodate up to 22 gauges at a time together with a single dummy gauge. The strain bridge could only monitor one gauge reading at a time and the switching unit therefore enabled one to switch rapidly from one gauge to the next and so reduce the time for taking readings. This however only applied if the dummy gauge already matched the lot number of the chosen active gauge.

A typical Huggenberger strain bridge is read by adjusting a meter to the centre-zero position using a selector switch and a rotating dial for fine adjustments. See Plate 1 and Figure 2.5.

Plate 1 Huggenberger strain bridge and switching unit.

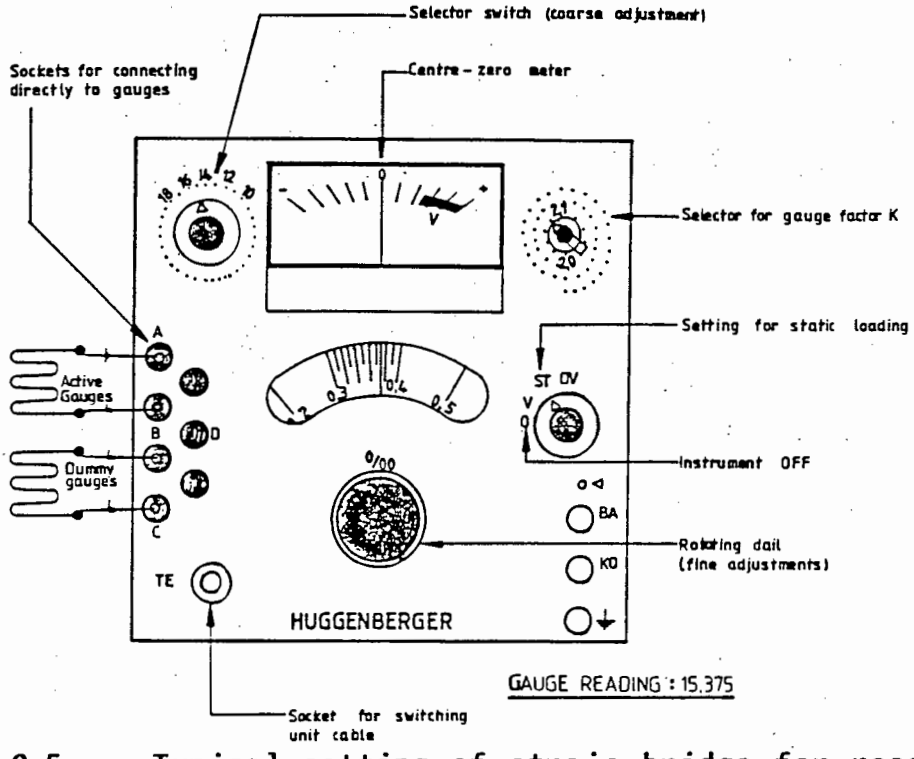

Figure 2.5 Typical setting of strain bridge for reading strains.

A instability problem was encountered with the gauge readings, which was the result of the heating influence of the reading current and which severely slowed the rate of taking readings. The result was that two more strain bridges similar to the above had to be used to speed up the reading process. Each additional instrument was connected directly to a single active gauge and the appropriate dummy gauge. See figure 2.6 below for a basic layout of the arrangement of instruments and their connecting circuitry.

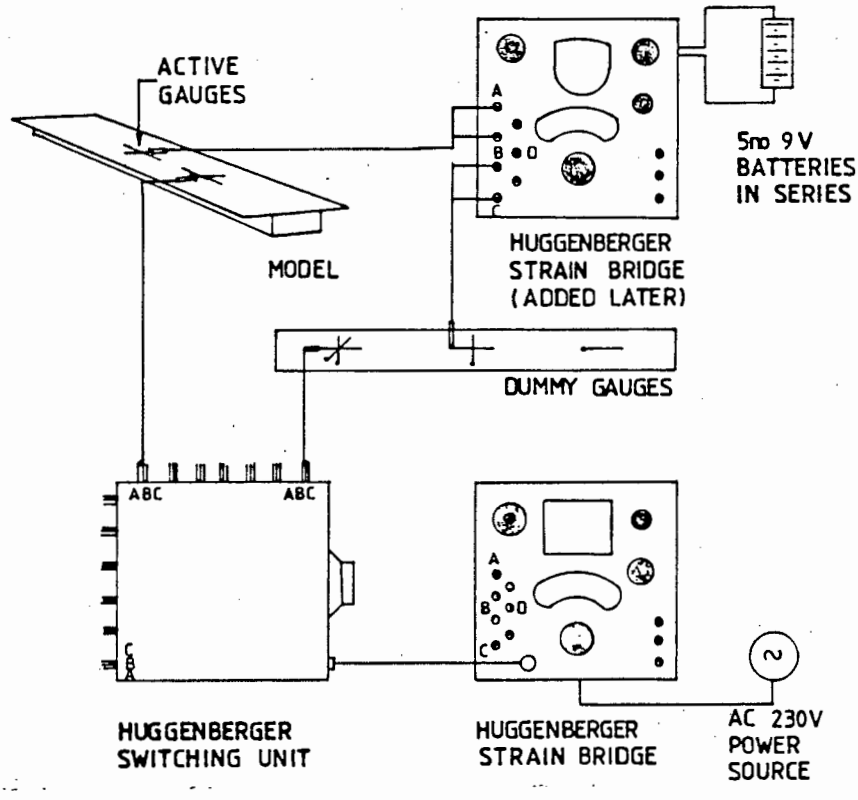

Figure 2.6 Layout of instruments and connections.

2.5 TESTING PROCEDURE AND RESULTS

2.5.1 Setting up for testing

The support conditions for all the models and loadcases were identical - i.e. the models were simply supported on pinned supports at one end and on roller or vertical supports at the other. In addition, the supports also provided full torsional restraint but not warping restraint. Since the model span lengths (1.200m) were identical it followed that the same support configuration could be used throughout.

A 50 x 50 angle-section with the legs turned downwards was used to make the pinned or knife-edge support. The roller support was made by sandwiching two 10 mm diameter steel rollers between two 6 mm thick glass plates and mounting this assembly on a 10 mm thick flat steel plate with levelling screws. These supports were set on a rigid steel frame at the required distance apart and adjusted with shims and the levelling screws to be at the same level. Finally the model under test was positioned on the supports and weights applied on the web centrelines directly above the line of the supports in order to provide the required torsional restraints. Diaphragms (aluminium cross-braces) were fitted inside the closed elements of the models at supports to prevent distortion of the cross-section.

Plate 2 Roller support details.

2.5.2 System of loading

The models were loaded as follows:

The downward loading was provided by using a system of weights on hangers and suspending these from the models. Upward loading was also by weights on a hanger but these acted on the models via a thin flexible cable running over two pulleys mounted on greased ball-bearings and fastened to a steel beam. The steel beam was supported by stands on either side of the model and could be moved to position the one pulley (from which the cable ran down to the model) directly above the point required i.e. so that cable pulled up vertically. The cable was hooked onto anchors threaded through the deck into the web.

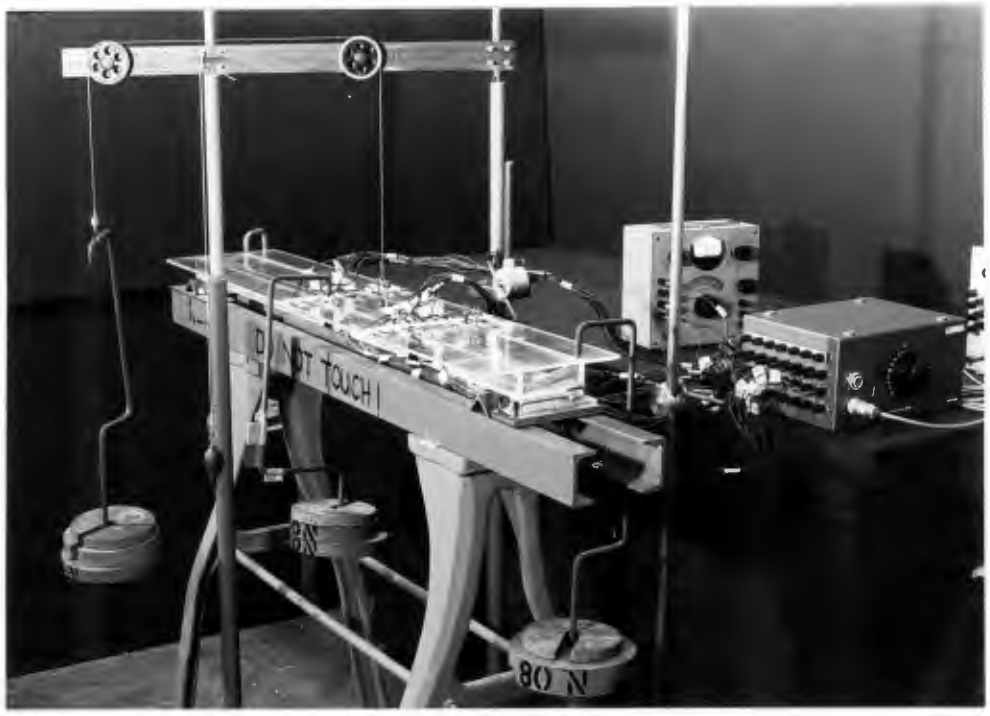

Plate 3 Loading system.

2.5.3 Reading procedure

The typical steps for reading a strain gauge was as follows:

Before loading up the model, an active gauge (on model) and matching temperature compensation (dummy) gauge were selected and connected, either directly or through the switching unit, to a strain bridge and the instrument switched on.

The gauges were allowed to reach thermal equilibrium in order to obtain a constant reading by leaving them switched on for about 20 minutes.

After taking the initial reading, the loading was applied and the gauge reading taken again and finally the loading removed and another gauge reading taken. This loading process was then repeated with the loading sequence reversed for those loadcases in which two point loads were used - see Section 2.5.4 for presentation of results.

The complete procedure above was repeated until all the gauges for the model being tested had been read, i.e for about 45 to 50 gauges per model.

It was obviously important to minimise the build-up of friction at the roller support and for this reason the model was tapped lightly a few times at this position before taking any readings in order to release the rollers.

The time taken to load a model and take readings for a single loading sequence took approximately two minutes and had a direct influence on the amount of creep that would occur during the period for which the loads were applied. The amount of creep was reflected in the difference between the first (just before loading) and the third (just after removing the loading) readings. This generally small creep component could therefore be eliminated by taking the average of the first and third readings and subtracting this from the second reading (under loading) to give the actual elastic strain - see 2.5.4.

The reading process was speeded up by using three strain bridges simultaneously i.e. two gauges could be switched on and be left to stabilize while a third gauge was being read. This increased the rate of reading gauges from about one every 25 minutes to about three per 25 minutes.

2.5.4 Presentation of results

The strain readings as well as the derived stress values for each of the models and loadcases tested are presented in tables given in APPENDIX A.

A typical reading is presented in the tables as follows:

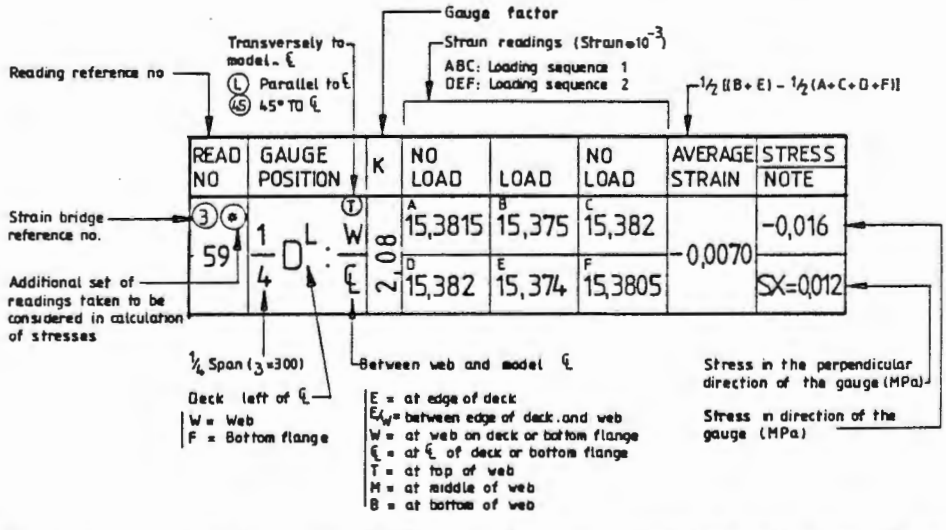

Figure 2.7 **Typical notation and presentation of strain gauge readings as given in the tables in APPENDIX A.**

The theory and calculation procedure for finding the experimental stress values are given in Section 2.6. These stress values are plotted together with the theoretical stress diagrams in Figures 5.1 to 5.8, Figures 5.10 to 5.16 and Figures 5.18 and 5.19.

2.6 DERIVATION OF STRESSES AND PRESENTATION

2.6.1 Theory of elastic stress-strain relations

The theory describing elastic stress - strain relations as well as strain - strain relations in two- dimensional stress systems is well documented in most literature dealing with the strength of materials and structures[1] and can be summarised as follows:

2.6.1.1 Normal stresses acting in perpendicular directions

Assume the tensile stresses σ_x and σ_y are acting separately in mutually perpendicular directions at a point in an elastic body. The resulting strains are indicated in Figure 2.8 below.

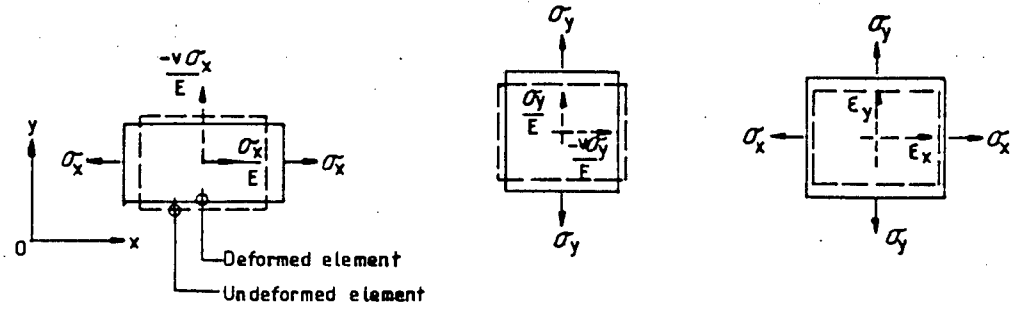

Stress in x direction | Stress in y direction | Stresses combined

Figure 2.8 Stresses and strains acting on a rectangular element in a two-dimensional linear elastic stress system.

The total strains in these directions, ϵ_x and ϵ_y, are found by superimposing the strains due to σ_x and σ_y acting separately. Taking tensile strain as positive, the equations for the strains in each of the x- and y-directions can be written thus

$$\epsilon_x(x) = (\sigma_x - v\sigma_y)/E$$

$$\epsilon_y(x) = (\sigma_y - v\sigma_x)/E \qquad (1)$$

and rewritten as

$$\sigma_x(x) = E(\epsilon_x + v\epsilon_y)/(1 - v^2)$$

$$\sigma_y(x) = E(\epsilon_y + v\epsilon_x)/(1 - v^2) \qquad (2)$$

Note that when a shearing stress t_{xy} is present in addition to the direct or normal stresses σ_x and σ_y, it is assumed that the shearing stress has no effect on the direct strains ϵ_x and ϵ_y nor does the direct stresses σ_x and σ_y have an effect on the shearing strain τ_{xy}.

It is clear from the above equations that in order to find the normal stresses at a point, at least two of the variables σ_x, σ_y, ϵ_x or ϵ_y must be known.

2.6.1.2 Derivation of shear stress from known strains in 3 directions

For a two-dimensional system of strains, the Mohr's circle of strain can be constructed if the direct and shearing strains in two mutually perpendicular directions are known. Hence, it follows that the direct and shearing strains in any direction can be found if the direct and shearing strains in two mutually perpendicular directions are known.

Consider a rectangular element of material, OPQR, in the xy-plane as given in Figure 2.9 below. All strains are considered to be small.

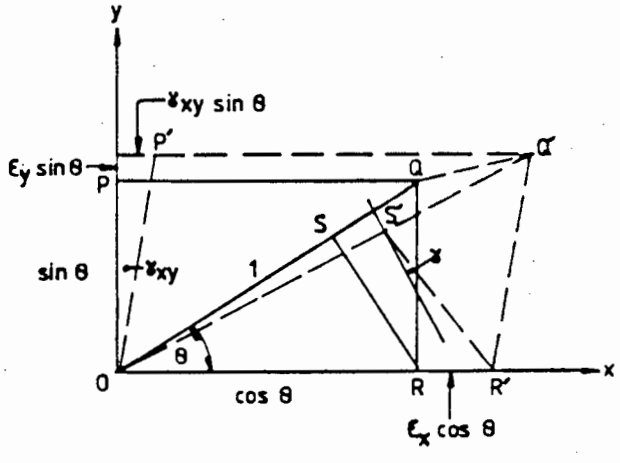

Figure 2.9 Strains in the Ox and Oy directions and along the inclined direction, OQ.

The direct strain on the diagonal OQ can be determined as follows, given that the direct strains, ϵ_x and ϵ_y, and shearing strains τ_{xy} in the Ox and Oy directions are known.

When the rectangular element is strained, side OR extends by $\epsilon_x \cos\theta$ and side OP by $\epsilon_y \sin\theta$. Also, the side OP rotates through a small angle τ_{xy} due to the shearing strain and point Q moves to point Q'.

Therefore, the movement of Q parallel to Ox is

$\epsilon_x \cos\theta + \tau_{xy} \sin\theta$

and the movement parallel to Oy is

$\epsilon_y \sin\theta$

The movement of Q parallel to OQ then is

$(\epsilon_x \cos\theta + \tau_{xy} \sin\theta)\cos\theta + (\epsilon_y \sin\theta)\sin\theta$

Since the strains are small, this is approximately equal to the extension of OQ in the strained condition and since OQ is of unit length, the extension is also the direct or normal strain in the direction of OQ. This can therefore be denoted as follows

$$\epsilon = (\epsilon_x \cos\theta + \tau_{xy} \sin\theta)\cos\theta + (\epsilon_y \sin\theta)\sin\theta$$

and may be written in the form

$$\epsilon = \epsilon_x \cos^2\theta + \epsilon_y \sin^2\theta + \tau_{xy} \sin\theta\cos\theta \qquad (3)$$

The above equation can be used to find the shearing strains as well as the perpendicular normal strains for any orientation of the x and y axes by using the three strain readings given by the 0-45-90 degree rosettes at the same point. Since the 0- and 90-degree gauges were always lined up with the x and y axes on the model and using the above equation, the following three equations could be written for the three gauges

$$\epsilon_0 = \epsilon_x .1^2 + \epsilon_y .0 + \tau_{xy} .0.1$$

$$\epsilon_{45} = \epsilon_x (0.71)^2 + \epsilon_y (0.71)^2 + \tau_{xy} (0.71)^2$$

$$\epsilon_{90} = \epsilon_x .0 + \epsilon_y .1^2 + \tau_{xy} .1.0$$

and more conveniently rewritten as

$$\epsilon_x = \epsilon_0$$

$$xy = 2(\epsilon_{45} - 0.5\epsilon_0 - 0.5\epsilon_{90})$$

$$\epsilon_y = \epsilon_{90} \qquad (4)$$

From the above the direct stresses could be found using the equations developed in 2.6.1.1 above. The shearing stress is found using the following equation

$$t_{xy} = G\tau_{xy} \qquad (5)$$

where

$$G = E/2(1 + v) \qquad (6)$$

2.6.2 Calculator program for strain-stress conversion

A program was written for a Hewlett-Packard 41C calculator whereby a single average strain was calculated using the six readings taken per gauge(i.e. for the unloaded, loaded and again unloaded conditions repeated for two loading sequences) and from which the stress was then calculated.

2.7 PROPERTIES OF PERSPEX

2.7.1 General

Initially, after a lengthy but unsuccessful search for suitable literature on the properties of Perspex, it was decided to do tensile tests to establish a value for the Young's modulus and to use certain of the strain rosette readings from the model tests to determine the Poisson's ratio.

Later, following completion of the tests, enquiries to the AECI company, which manufactures Perspex, produced a comprehensive brochure[9] giving all the important properties of this material. This brochure shows that both temperature and the rate of application of stress or straining have a considerable influence on the elastic modulus and Poisson's ratio values. The effects of these are briefly discussed in 2.7.2.

The values derived from the tests were found to be close to those given in the AECI brochure for a temperature of 20°C and short term testing, which are the conditions nearest to those in the laboratory where the tests were done. Sections 2.7.3 and 2.7.4 deal with the selection of appropriate values for E and v.

2.7.2 The effects of temperature and straining rate on the elastic modulus and Poisson's ratio of Perspex

2.7.2.1 Elastic modulus

The AECI brochure[9] considers several types of elastic moduli - the initial tangent, tangent and 1% secant moduli in tension; the flexural modulus; the compressive modulus and the apparent Young's modulus - for a range of temperatures and straining rates.

Figure 2.10 below illustrates the influence of temperature on some of the moduli and shows the similarity of the rates of change of the various moduli with temperature. It is also clear from the graph that the magnitudes of initial tangent moduli in tension and compression as well as the flexural modulus are substantially similar at a given temperature and rate of strain.

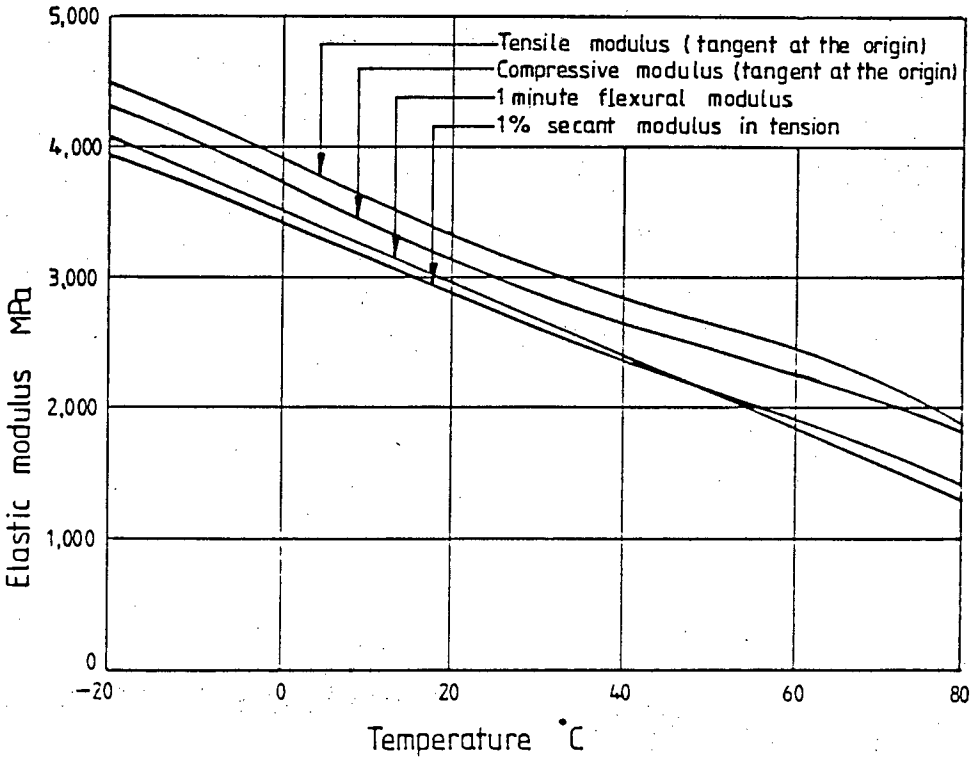

Figure 2.10 **Effect of temperature on the 1 minute flexural modulus and the tensile and compressive elastic moduli for a straining rate of 1 % per minute.**

The influence of the rate of straining on the 1% secant modulus at a given temperature is shown by Figure 2.11 and it can be assumed that the effect of straining rate on the other types of moduli referred to above will be similar on a pro rata basis.

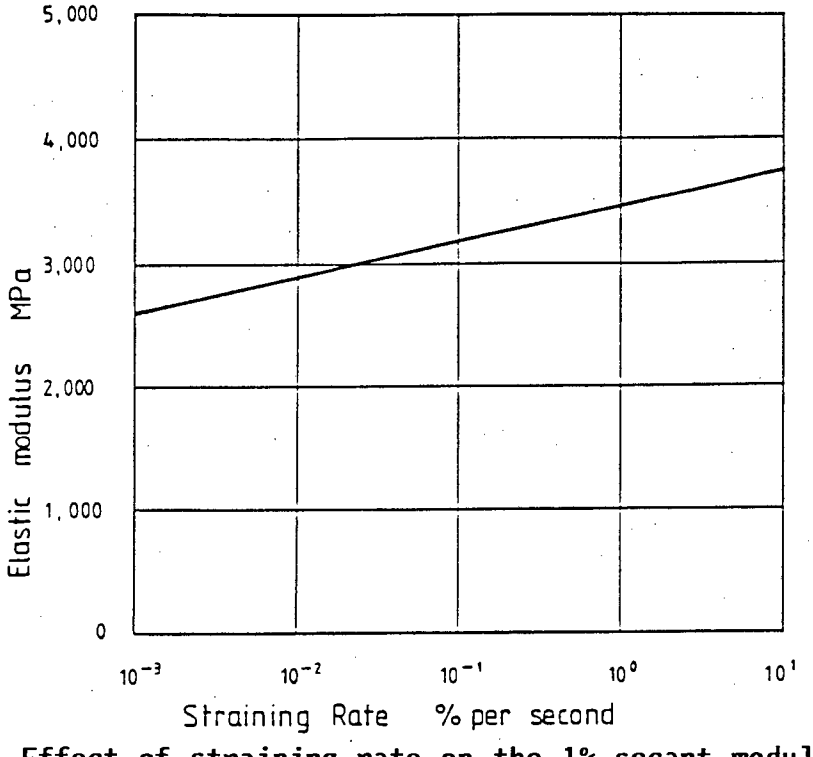

Figure 2.11 **Effect of straining rate on the 1% secant modulus at 20 °C.**

2.7.2.2 Poisson's ratio

Essentially, according to the brochure[9], for small values of strain, the Poissons's ratio for Perspex remains constant over the -25°C to +50°C temperature range. At temperatures above 100° C, where large deformations can occur, Poisson's ratio approaches a value of 0.5.

As far as the influence of straining rate is concerned, a short term (6 hours) design value of 0.39 and a long term (10 years) design value 0.40 is given.

2.7.3 Choosing a suitable value for the Modulus of Elasticity of Perspex

The tensile tests, performed on samples taken from the same sheets of Perspex as used for building the box-girder models, produced a value of 2918 MPa for the Elastic modulus. This value represents the initial tangent modulus in tension for a temperature of between 18°C to 22°C and a straining rate of about 0.3% per minute.

The equivalent value given in the brochure is 3357 MPa for a temperature of 20°C and a straining rate of 1% per minute and which, if adjusted for a straining rate of 0.3% per minute, using figure 2.11 above, becomes 3185 MPa. This figure is about 9% higher than the test value.

However, since the tensile tests were carried out using samples from the same sheets of Perspex as used for making the models and since the test values compared closely to those given in the brochure in any case, it was decided to rather use the test value for this thesis, i.e. **2918 MPa.**

2.7.4 Choosing a suitable value for the Poissons's Ratio of Perspex

The value of Poisson's ratio, derived from the strain rosette readings of the model tests with symmetrical loading - i.e. for which the transverse normal stresses were theoretically zero - was 0.39. This value represents the Poisson's ratio for short term testing at a temperature of between 18°C and 22°C.

The equivalent value from the brochure, defined as being for short term testing at a temperature of 20°C, is 0.38, which is close to the value from the model tests given above. The brochure also gives short term (6 hours) and long term(10 years) design values of 0.39 and 0.40 respectively.

Since the test value is confirmed by the information from the AECI brochure, it was decided to use this value of **0.39** for this thesis.

3 REVIEW OF THEORY OF ANALYTICAL METHOD

3.1 GENERAL

The hand method proposed by Maisel and Roll[7], the theory of which is discussed here, basically treats the analysis of box-beams as the summation of the stresses arising from a number of independant structural actions. Typical examples of using the hand method in analysing the loadcases used for the experimental testing of models are given in APPENDIX E.

3.1.1 Distortion and warping

Apart from simple beam action, there are two major types of structural action that occur in box-girders: distortion or deformation of the cross-section and warping of the cross-section (defined as an out-of-plane displacement of points on the cross-section).

The typical forms of loading giving rise to distortion are shown in Figure 3.1 below.

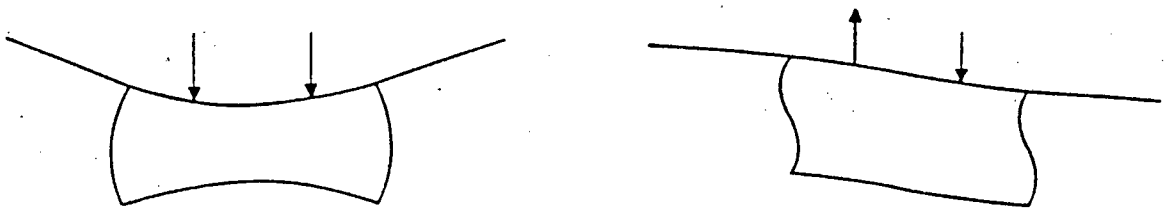

Figure 3.1 Distortion of cross-section due to symmetric (bending) and anti-symmetric (torsional) loading.

Warping of the cross-section is most conveniently described with the aid of Figures 3.2, which are for a box-girder under torsional loading.

Firstly, consider a box-girder with cross-sections which are prevented from distorting by the presence of rigid diaphragms. The diaphragms are assumed not to restrict longitudinal displacements from taking place. Figure 3.2 (a) shows the twisting of the cross-section without distortion and Figure 3.2 (c) shows the resulting longitudinal warping (torsional warping) displacements (dashed line) which are associated with shear deformations in the planes of the webs and flanges. The midspan deflections of the webs are denoted by a_t. Note that, due to symmetry, no warping occurs at the midspan section.

The second stage is to assume that the rigid diaphragms are removed so that distortion of the cross-sections can occur. This is shown in Figure 3.2 (b), with the additional vertical deflection of each web denoted by a_{dis}. As a result, additional twisting of the cross-sections take place and therefore also additional warping displacements (distortional warping) which are associated with bending in the planes of the flanges and webs - see Figure 3.2 (c). Again, due to symmetry, no longitudinal dispacements occur at midspan.

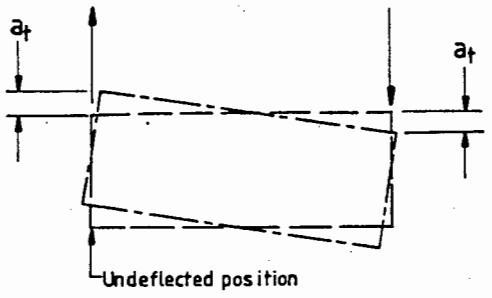

Figure 3.2(a) Twisting of midspan cross-section without distortion

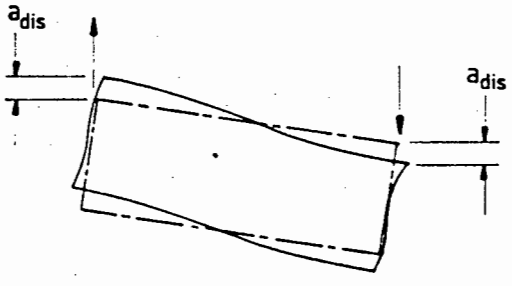

Figure 3.2(b) Additional twisting of midspan cross-section with distortion

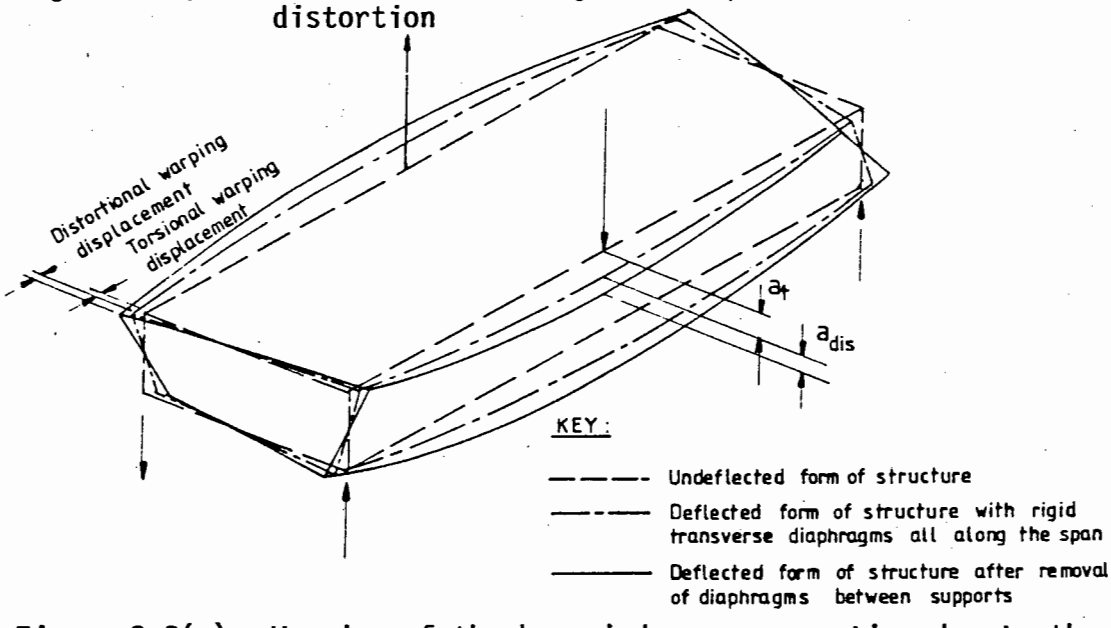

Figure 3.2(c) Warping of the box-girder cross-section due to the midspan twisting components in (a) and (b) above.

The two components of warping displacements, described above and which occur in box-girders under torsional loading conditions, give rise to longitudinal normal stresses (warping stresses) when the warping displacements are prevented, for example by symmetry at the midspan section or at a support where there is continuity.

The longitudinal normal warping stresses can significantly increase the total longitudinal stresses above those values predicted by simple bending theory. The authors state that distortion of the cross-section is the main source of warping stress in concrete box-girder construction, in those situations where distortion is resisted mainly by transverse bending.

A third form of warping arises when a box-girder is subjected to bending without torsion. This type of warping, known as shear lag in bending, results from shear deformation in the planes of the flanges and causes the longitudinal bending stresses to decrease away from the webs. This effect is more pronounced in configurations with wide side cantilevers and widely spaced webs and affects the effective widths of the flanges in bending.

Shear lag can also occur in box-girders subjected to torsion, but this aspect is not taken into account by this analysis. See Figure 3.3 for an illustration of shear lag in bending.

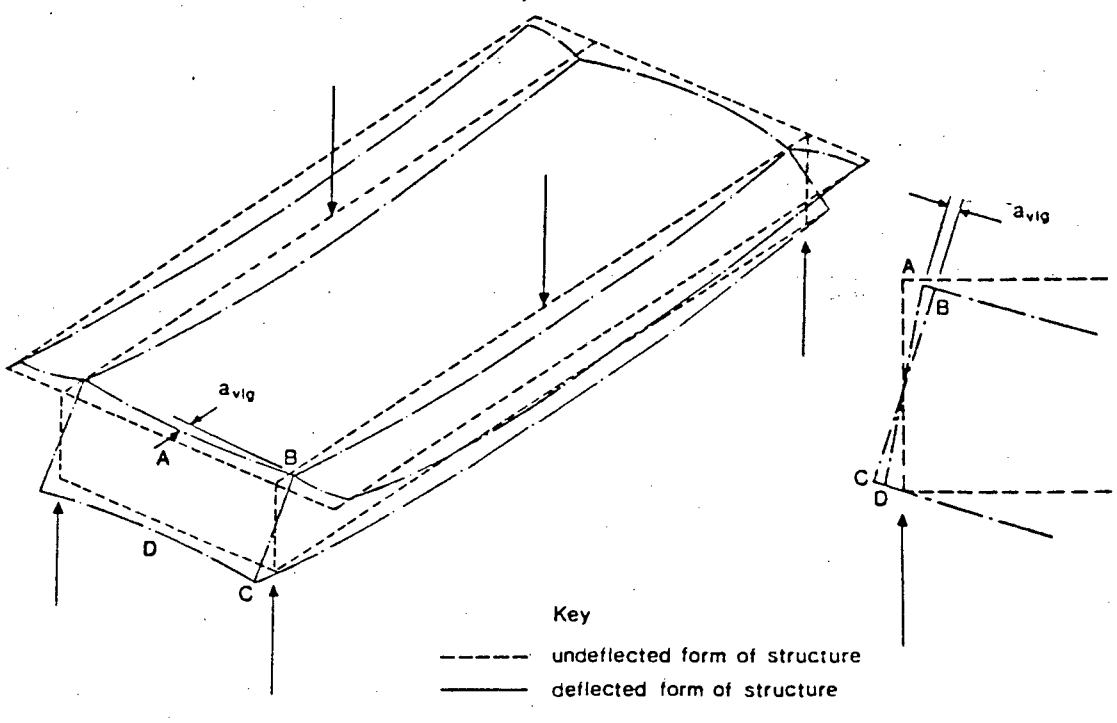

Figure 3.3 Shear lag in bending.

3.1.2 Methods of elastic analysis

The following methods of analysis are used to analyse the various structural action types and collectively make up the **recommended method.**

Longitudinal bending and shear and **St Venant torsion** is analysed by using simple beam theory.

Torsional warping is dealt with by a method developed by Kollbrunner, Hajdin[5] and Heilig[2] from work originally done by Vlasov.

Distortional warping together with **transverse bending** analysis is by the beam-on-elastic-foundation analogy[12].

Shear lag is dealt with by the method given by Schmidt, Peil and Born[11]. Note that this method was chosen after the method presented by Maisel and Roll in their technical report[10] was found to be unsuitable - see Section 3.5.

Local bending effects due to loading between webs and on the cantilevers are determined by means of influence surfaces for plates.

The various calculated stresses found for the above effects are superimposed to give the total or combined stresses.

These individual methods are discussed in detail in the following sections.

3.1.3 Definitions for thin-walled members

The theories relating to torsional warping and St Venant torsion, were originally developed for thin-walled members. Criteria for the definition of thin-walled members, associated with each of these, are given.

Vlasov, on whose work the torsional warping theory is based, defines a thin-walled beam as a structure having the form of a long prismatic shell where the shell thickness is small when compared to any characteristic cross-sectional dimension and the cross-sectional dimensions are also small in comparison to the length of the shell. His criteria are as follows:

$$\frac{\text{shell thickness}}{\text{width or depth of cross-section}} \leq 0.1$$

and

$$\frac{\text{width or depth of cross-section}}{\text{length of shell}} \leq 0.1 \qquad (7)$$

Maisel and Roll claim that the first criterion is often not satisfied by concrete boxbeams but that Vlasov's theory has nonetheless been used for analysing them.

Kollbrunner and Basler[4], in dealing with the theory for St Venant torsion, give the following criteria for identifying thin-walled sections:

The first is: "There is less than 10 % error in calculating the shear stresses for a hollow cross-section with constant wall thickness, if the effective area of cross-section is less than one-fifth of the area enclosed by the wall centre-lines". This condition is usually not satisfied by concrete boxbeams. Note that the effective area of cross-section is the area of the cross-section without the side-cantilevers, i.e that of the closed section.

The second criterion is: · "There less than 10% error in the calculated internal torsional moment if the effective area of cross-section does not exceed the area enclosed by the wall centre-lines" - a condition which is usually satisfied by concrete boxbeams. A more general form of the above criterion for cases where the wall thickness varies around the perimeter is given in 3.2.2.

3.1.4 Notation and sign convention

3.1.4.1 Notation

The notation used by Maisel and Roll, and also used here, is in accordance with an internationally agreed procedure for the selection of symbols. Where equations and algebraic expressions were taken from sources other than the Maisel and Roll report, these were adapted in order to maintain conformity.

A list of the symbols used here, together with the appropriate descriptions and definitions are given in the "Notation" section on page (viii).

The symbols for cross-sectional dimensions and the positions of selected reference points on the cross-section at which the various stresses are determined, are shown in Figure 3.4.

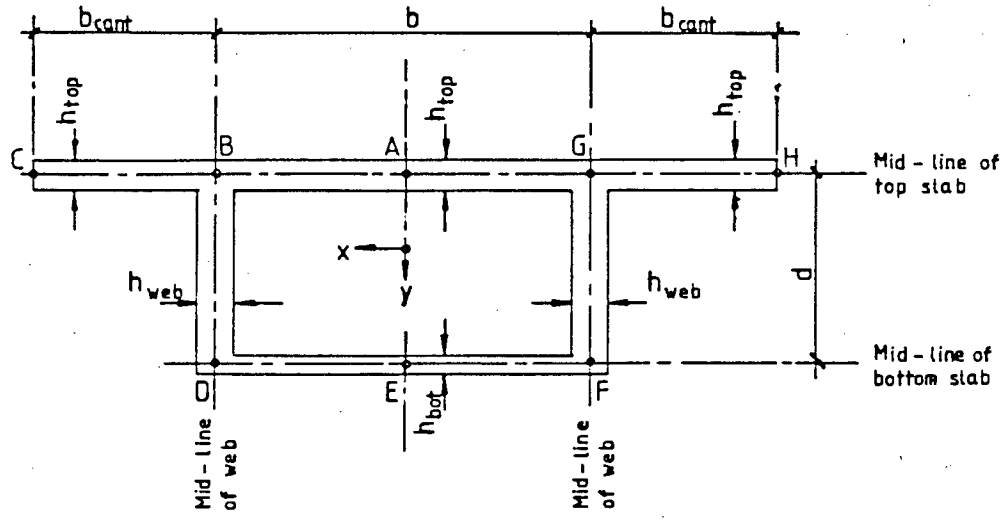

Figure 3.4 **Cross-sectional dimensions and reference points.**

3.1.4.2 Sign Convention

A right-handed system is used for the coordinate axes so that, for a horizontal beam, the x and y axes are the horizontal and vertical axes of the cross-section respectively and the z axis the longitudinal axis in the direction of the span.

The y axis is taken as positive downwards so that loads and deflections due to gravity are positive quantities. Figure 3.5 shows the typical orientation of the coordinate axes in relation to a box-girder.

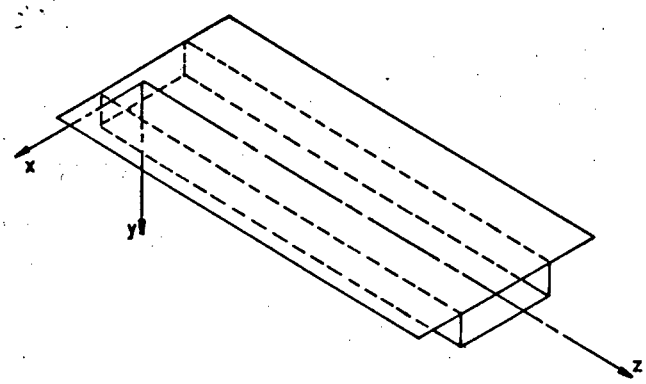

Figure 3.5 Orientation of the Coordinate axes.

The position of the origin of the x and y axes within the cross-section is taken as the centroid for longitudinal bending analysis, as the shear centre for torsional warping analysis and as the geometric midpoint of the closed portion of the cross-section for the distortional warping analysis.

The origin and positive directions for the **peripheral coordinate**, s_{per}, is shown in Figure 3.6.

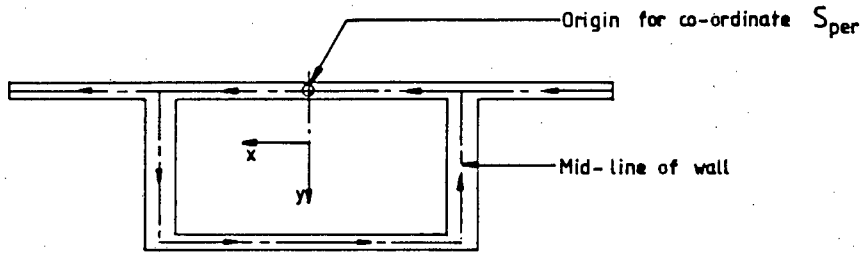

Figure 3.6 **Origin and positive directions for the peripheral coordinate, s_{per}.**

Displacements and rotations are positive if they are in the directions shown in Figure 3.7 (a). The positive direction for distortional displacement of the cross-section under antisymmetric loading is given by Figure 3.7 (b).

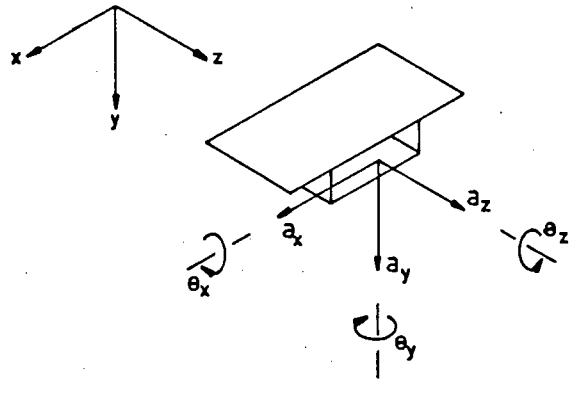

Figure 3.7(a) **Positive directions for diplacements and rotations.**

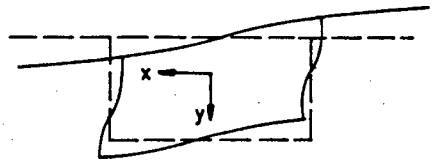

Figure 3.7(b) Positive distortional displacement under antisymmetric loading.

A positive face of cross-section is a section on which the external normal is in the positive direction of the longitudinal or z axis. Similarly a negative face is one for which the external normal is in the negative direction of the z axis. Generally a positive face is used when analysing a section within the span and a negative face for analysing a section at a support.

The positive directions for **internal stresses, stress resultants** and **applied** or **external loading** are shown in Figure 3.8 below.

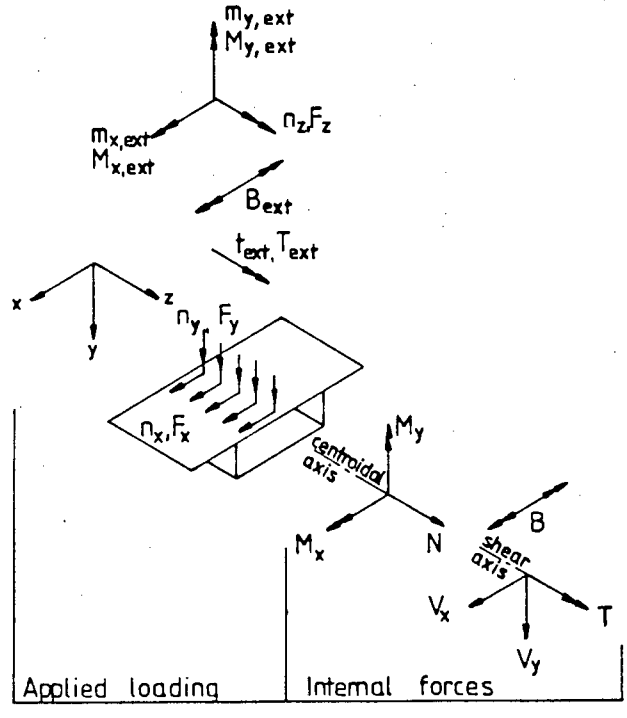

Figure 3.8 **Positive directions for internal stress-resultants and external applied loading.**

All stresses referred to in this thesis are internal resistive stresses arising from the application of the external loading.

The sign convention for **normal stresses** and **shear stresses** acting on a cross-section is as follows:

Normal stresses are regarded as positive if, for a positive face of cross-section, they act in the direction of the positive z-axis. Also, normal stresses acting in the negative direction of the z axis for a negative face of cross-section are positive. It thus follows that tensile stresses on a cross-section are always positive.

Shear stresses are positive if for a positive face of cross-section they act in the positive direction of s_{per}, the peripheral coordinate.

Transverse bending stresses, associated with distortion of the cross-section and hence also with the deflected shapes shown in Figure 3.1, are simply plotted on the tension face of the cross-section and therefore do not require signs.

Note that since the stress resultants or internal forces are summations of internal stresses, they must naturally follow the same signs.

In Figure 3.8 above it may be noted that the positive directions for the internal stress resultants acting on the positive face and those for the external loads acting on the member are the same.

3.2 ANALYSIS OF SIMPLE BENDING AND ST VENANT TORSION

The structural effects ignored in this analysis are torsional and distortional warping, shear lag and distortion.

3.2.1 Simple longitudinal bending and shear

In this section, the torsional components of external loading and their effects are not considered. For example, in horizontal beams, vertical loads are treated as if they are equally shared between webs, irrespective of their actual lateral position.

The bending moments and shear forces along the length of the beam are determined by simply using the basic equilibrium equations for statically determinate structures or in the case of continuous structures, any convenient method of elastic analysis - e.g. moment distribution or virtual work.

Once the bending moments and shear forces are known, the longitudinal normal stresses at the midlines are found from the following equation, assuming section is thin-walled and that cross-sections remain plane.

$$f_{lbg} = \frac{M_x y}{I_x} + \frac{M_y x}{I_y} \qquad (8)$$

where

f_{lbg} = midline normal stress in longitudinal bending

x,y = coordinates of a point on the mid-line, referred to the centroidal axes

I_x, I_y = moments of inertia of the entire cross-section about the centroidal x and y axes respectively

M_x, M_y = bending moments about the centroidal x and y axes

In practice, the horizontal loads which give rise to bending about the y-axis, i.e. M_y, are generally small in comparison with the vertical loading and their effects are as such not considered here.

The shear stresses arising in longitudinal bending are found by establishing boundary conditions for shear at points A,C and E and then analysing the half-section, ABCDE, as an open section - see Figure 3.9. By symmetry, the longitudinal shear at points A and E are zero and it follows that the complementary shear stresses in the plane of the cross-section at these points are then also zero. Similarly, since there is a free edge at point C, the longitudinal and complementary shear stresses are zero.

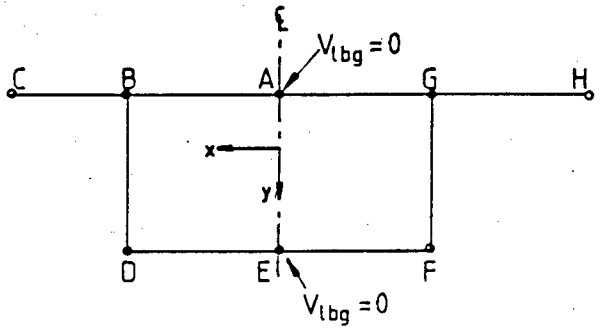

Figure 3.9 Boundary conditions for shear stresses.

The half section, ABCDE, is analysed by means of the following equation given by Kollbrunner and Basler[3]:

$$v_{lbg} = - \frac{V_y \, (\overline{Ay})_{\frac{1}{2}}}{I_x \, h} \qquad (9)$$

where

v_{lbg} = shear stress in longitudinal bending

V_y = shear force in the vertical or y direction acting on the half cross-section

h = thickness of wall at the section being considered

$(\overline{Ay})_{\frac{1}{2}}$ = first moment of area of the partial half cross-section about the centroidal x axis - see Figure 3.10

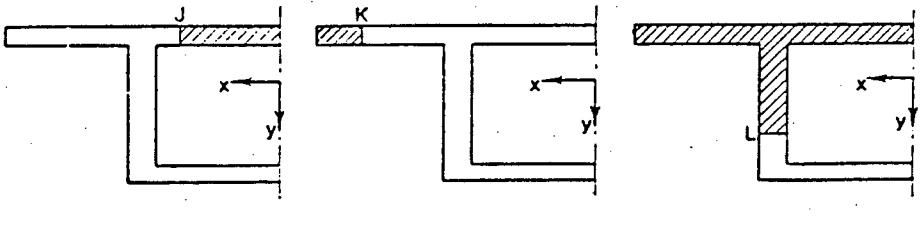

Figure 3.10 $(\overline{Ay})_{\frac{1}{2}}$ at J,K or L is the first moment of area of the shaded areas about the centroidal x axis.

Typical diagrams, showing how both the bending and shear stresses in longitudinal bending are plotted, are shown in Figure 3.11.

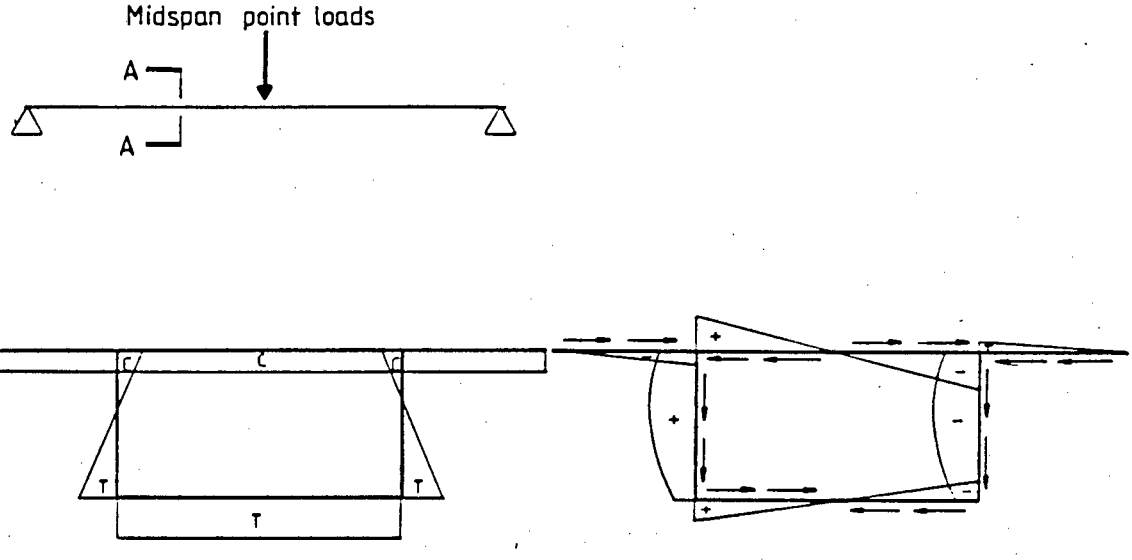

(a) Bending stresses (b) Shear stresses

Figure 3.11 Typical bending and shear stresses in longitudinal bending.

3.2.2 St Venant torsion

For single span members, where no torsional rotation is possible at the supports, the internal torsional moment diagram is found by simply using a ratio of the relative torsional stiffnesses of the member between the section being loaded and the supports on either side. These ratios are expressed in terms of longitudinal dimensions and are given for both concentrated and distributed loading - see Figure 3.12.

	$0 \leq z < a_1$	$a_1 < z \leq \iota$
T_{svt}	$+ T_{ext} \frac{a_2}{\iota}$	$- T_{ext} \frac{a_1}{\iota}$

Uniformly distributed torsional loading t_{ext} over portion of span

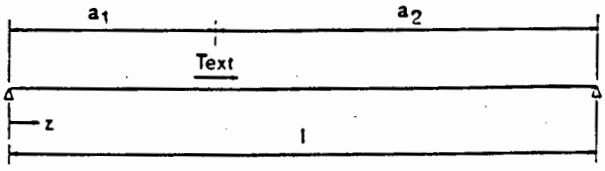

Elevation of beam

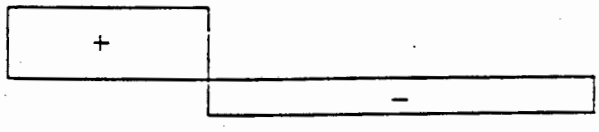

Diagram of torsional moment, T_{svt}

(a) Concentrated torsional loading, T_{ext}

	$0 \leq z \leq a_3$	$a_3 \leq z \leq (a_3 + a_4)$	$(a_3 + a_4) \leq z \leq \iota$
T_{svt}	$+ t_{ext} a_4 \frac{a_5 + \frac{a_4}{2}}{\iota}$	$t_{ext} a_4 (\frac{a_5 + \frac{a_4}{2}}{\iota} - \frac{z - a_3}{a_4})$	$- t_{ext} a_4 \frac{a_3 + \frac{a_4}{2}}{\iota}$

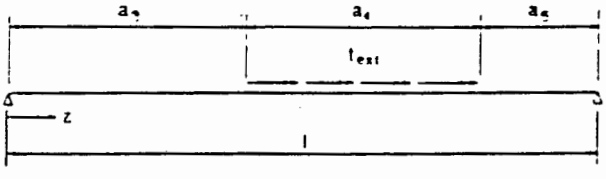

Elevation of beam

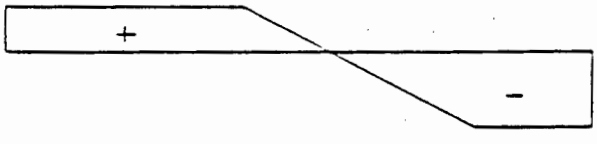

Diagram of torsional moment, T_{svt}

(b) Uniformly distributed torsional loading t_{ext} over portion of span

Figure 3.12 Internal torsional moment diagrams.

In continuous members subjected to torsional loading, supports preventing torsional rotation also prevent the carry over of torsion into the next span and hence the internal torsional moment can be determined as for a discontinuous member. Supports not affecting rotation can be neglected in the torsional analysis altogether. The special case of elastically rotating supports is not considered in this analysis.

(It is important to note here that the internal torsional moment resisting the externally applied torsional loading at a section is made up of the sum of the moments due to St Venant shear stresses and to torsional warping shear stresses.)

The following expression, given by Kollbrunner and Basler[4], is used to find the St Venant shear stresses for a section that can warp freely:

$$v_{svt} = \frac{T_{svt}}{2 A_{enc} h} \qquad (10)$$

where

v_{svt} = shear stress in St Venant torsion at the mid-line of wall

h = thickness of wall of closed portion of cross-section at the point considered

T_{svt} = internal torsional moment in St Venant torsion at the section being considered

A_{enc} = area enclosed by the mid-lines of the walls of the closed portion of the cross-section

For thicker-walled sections, the authors give the following equation for adjusting the values found in equation 10 above:

$$\delta v_{svt} = \frac{h T_{svt}}{C_{svt}} \qquad (11)$$

where

δv_{svt} = the increment in St Venant shear stress over half the thickness of the wall

C_{svt} = torsional moment of inertia of the cross-section in St Venant torsion

$$= \frac{4 A^2_{enc}}{\oint ds_{per}/h}$$

and where

$$\oint \frac{ds_{per}}{h} = \frac{b}{h_{top}} + \frac{b}{h_{bot}} + \frac{2d}{h_{web}}$$

s_{per} = peripheral coordinate along the mid-line of the wall

$\oint$ = integral along the midline of the wall of the closed portion of the cross-section.

See Figure 3.4 for the notation of cross-sectional dimensions.

Typical St Venant shear stress diagrams for both thin- and thick-walled sections are given in Figure 3.13 below.

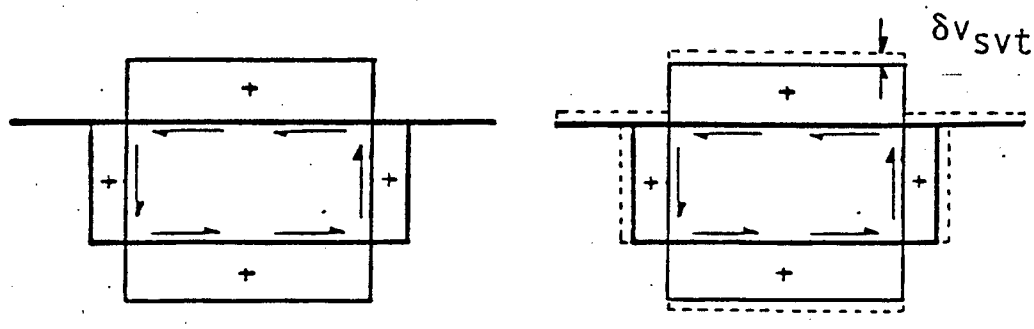

(a) thin-walled **(b)thick-walled**

Figure 3.13 **Typical diagrams for shear stresses in St Venant torsion.**

From equations 10 and 11 above, a more refined form of the Kolbrunner and Basler criterion for thin-walled sections referred to in 3.1.3, which takes the effect of varying wall thicknesses around the perimeter of the cross-section into account, can be derived.

$$\frac{\delta v_{svt}}{v_{svt}} = \frac{h^2}{2A_{enc}}\left[\frac{b}{h_{top}} + \frac{b}{h_{bot}} + \frac{2d}{h_{web}}\right] \qquad (12)$$

and also

$$\delta T_{svt}/T_{svt} = [b(h^3_{top} + h^3_{bot}) + 2dh^3_{web}]/3C_{svt} \qquad (13)$$

where

δT_{svt} = increment in T_{svt} due to the antisymmetric shear stress distribution measured by δv_{svt}.

These equations can therefore be used to calculate the percentage errors in the shear stresses and the torsional moment due to the influence of wall thickness.

It is recommended that if the error in the torsional moment exceeds 10%, the section should be regarded as being thick-walled and that the value of C_{svt} should be modified by adding on a correcting factor δC_{svt} which is found thus:

$$\delta C_{svt} = \int h^3 \, ds_{per} / 3$$

$$= [(b + 2b_{cant})h^3_{top} + bh^3_{bot} + 2dh^3_{web}]/3 \qquad (14)$$

where

b_{cant} = breadth of cantilever

3.3 ANALYSIS OF TORSIONAL WARPING

(Kollbrunner, Hajdin[5] and Heilig[2])

For the torsional warping analysis it is assumed that no deformation of the cross-section occurs. Shear lag in warping as well as a minor effect causing transverse normal stresses constant through the wall thickness, are not considered.

The theory of torsional warping presented here was developed by Kollbrunner and Hajdin[5] from work by Vlasov for thin-walled beams of both open and closed undeformable sections. Their method, in which the shear deformation due to torsional warping is taken into account, determines the longitudinal torsional warping stresses, torsional warping shear stresses and indirectly also the St Venant shear stresses at any section along the span.

Torsional warping occurs when a box-girder is loaded by torsional moments within the span as shown in Figure 3.14. Torsional warping stresses, which act normally to the cross-section in the longitudinal direction, arise when the warping displacements are restrained, for example by symmetry at midspan of a member or at a continuous or built-in end. These stresses vary around the perimeter of the cross-section as well as along the beam. As a result torsional warping shear stresses also occur in the longitudinal direction together with complementary shear stresses in the plane of the cross-section. Both the torsional warping stresses and torsional warping shear stresses are assumed to be constant through the wall thickness. Typical diagrams of torsional warping stresses and torsional warping shear stresses are shown in Figure 3.14.

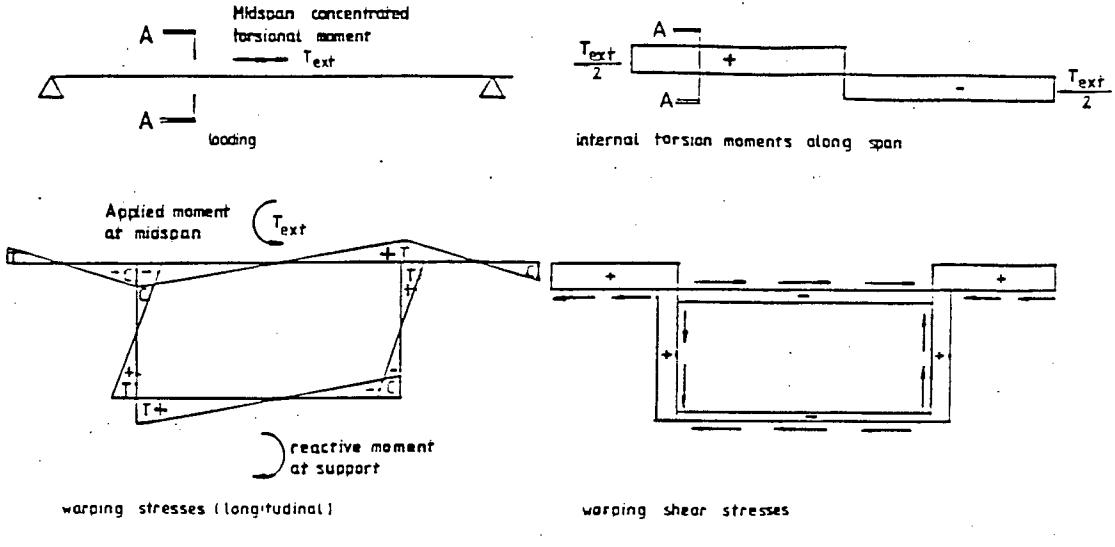

Figure 3.14 Typical torsional loading, torsional warping stresses and torsional warping shear stresses.

As stated before, the internal torsional moment resisting the externally applied torsional loading at any section is made up of the sum of the torsional moments due to St Venant shear stresses and due to the torsional warping shear stresses. Figure 3.15 illustrates a typical distribution of torsional warping stresses along the span and the relationship between the torsional moments due to torsional warping shear stresses and the St Venant shear stresses. The longitudinally localized nature of torsional warping stresses is also apparent from this diagram. It will be shown later that the resultant internal torsional moment due to distortional warping shear stresses is zero since the applied torsional moment is only equilibrated by the sum of the moments from the St Venant shear stresses and the torsional warping shear stresses.

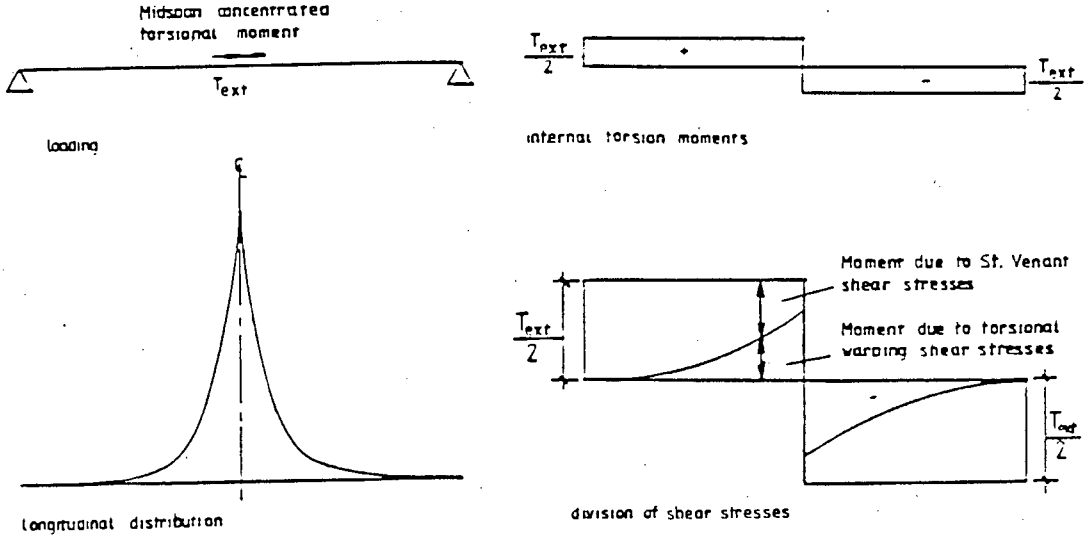

Figure 3.15 **Typical longitudinal distribution of torsional warping stresses and the relationship between the internal torsional moments due to torsional warping shear stresses and due to St Venant shear stresses.**

The following definitions and expressions form the essence of the method proposed for the torsional warping analysis of box-girders:

The **bimoment** B_{twr} is a pair of equal and opposite moments in parallel planes which represent a warping force group with zero longitudinal force resultant and zero moment resultant by definition. Figure 3.16 shows a positive bimoment for the horizontal or x-axis.

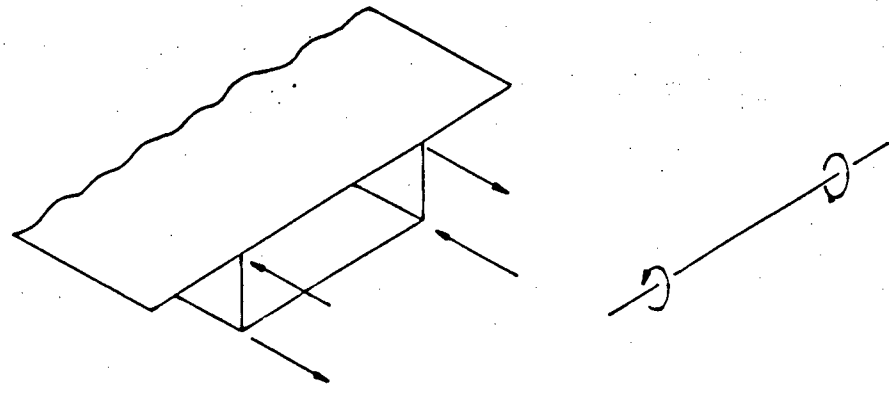

Figure 3.16 Warping force group and bimoment.

It follows that bimoments cannot be found from the equilibrium conditions of a beam, since self-equilibrating quantities do not affect equilibrium. Therefore, the bimoments of torsional warping can only be found when the deformations representing angle of twist and the second derivatives with respect to the longitudinal coordinate are known. The torsional warping bimoment is given by the expression:

$$B_{twr} = \int_A f_{twr}\, w_{twr}\, dA \qquad (15)$$

where

A = total area of the cross-section including the side cantilevers

f_{twr} = torsional warping stresses

w_{twr} = sectorial coordinate in torsional warping, referred to the shear centre

The **sectorial coordinate** w_{twr} is defined as

$$w_{twr} = \int_0^{s_{per}} (a_8 - C_{svt}/2\, A_{enc}\, h)\, ds_{per} \qquad (16)$$

where

a_8 = the perpendicular distance from the shear centre to the tangent on the mid-line of wall at the point considered

C_{svt} is defined for equation 11

A_{enc} is defined for equation 10

h is the wall thickness at the point considered

s_{per} = the sectorial coordinate along the mid-line of the wall - see Figure 3.6

Note that the term $C_{svt}/2A_{enc}.h$ is included in the integrand for integration around the wall of the closed section only - not the side cantilevers. Also, w_{twr} can be regarded as being positive if anti-clockwise integration about the shear centre produces a positive quantity. See Appendix E for a typical diagram of the sectorial coordinate plotted around the cross-section of Model 3.

The position of the **shear centre** is given by the expression:

$$d_{shc} = b^2 d \left[(K_{13} + K_{14} + K_{15} + K_{16})/ K_{17} \right] / I_y \qquad (17)$$

where

d_{shc} = depth of the shear centre below mid-line of top slab

I_y = moment of inertia of the entire cross-section about the centroidal y-axis

b, b_{cant}, d, h_{top}, h_{web} and h_{bot} are shown in Figure 3.4

$K_{13} = \frac{1}{4} b h_{bot} h_{web}(b h_{bot}/3 + 3 d h_{web})$

$K_{14} = b d h_{top} (h^2_{bot}/6 - \frac{1}{4} h^2_{web})$

$K_{15} = \frac{1}{2} h_{top} h_{bot} h_{web}(b^2/6 + d^2)$

$K_{16} = b_{cant} h_{top} h_{bot} h_{web}(b_{cant} + b)$

$K_{17} = b h_{web}(h_{top} + h_{bot}) + 2 d h_{top} h_{bot}$

The **torsional warping moment of inertia of cross-section Ctwr** is defined as:

$$C_{twr} = \int_A w^2_{twr} dA \qquad (18)$$

The torsional warping stresses and torsional warping shear stresses are formulated in terms of internal stress resultants represented by the bimoment B_{twr} and the torsional moment T_{twr} respectively. The sectorial coordinate w_{twr} and the various torsional moments of inertia of cross-section, C_{twr} ,C_{cen} and C_{svt}, also appear in these equations which are given later on.

Algebraic expressions for B_{twr} and T_{twr}, as well as for the torsional moment due to St Venant shear stresses T_{svt} and twist about the shear axis θ_z, are given in Tables 9 to 15 in the Maisel and Roll report[7] for the various loading types and support conditions shown in Figure 3.17. These expressions are presented in terms of the applied torsional loading as well as the following:

$$K_{18} = \sqrt{GC_{svt}/E\bar{C}_{twr}} \qquad (19)$$

and

$$K_{19} = \frac{C_{cen}}{C_{cen} - C_{svt}} \qquad (20)$$

where

$$\bar{C}_{twr} = K_{19}\, C_{twr} \qquad (21)$$

C_{cen} = central torsional moment of inertia of cross-section

$$= \int_A a_8^2\, dA \qquad (22)$$

The functions for $B_{twr}(z)$, $T_{twr}(z)$, $T_{svt}(z)$ and $\theta_{twr}(z)$ applicable to this thesis, i.e. for concentrated applied torsional loading with no warping restraints at the ends, are reproduced in Appendix B.

In the case of continuous box-girders, only supports providing full torsional restraint are dealt with - elastically rotating supports are not considered. Also, for the torsional warping analysis of continuous members, it is assumed that full warping restraint occurs at continuous ends.

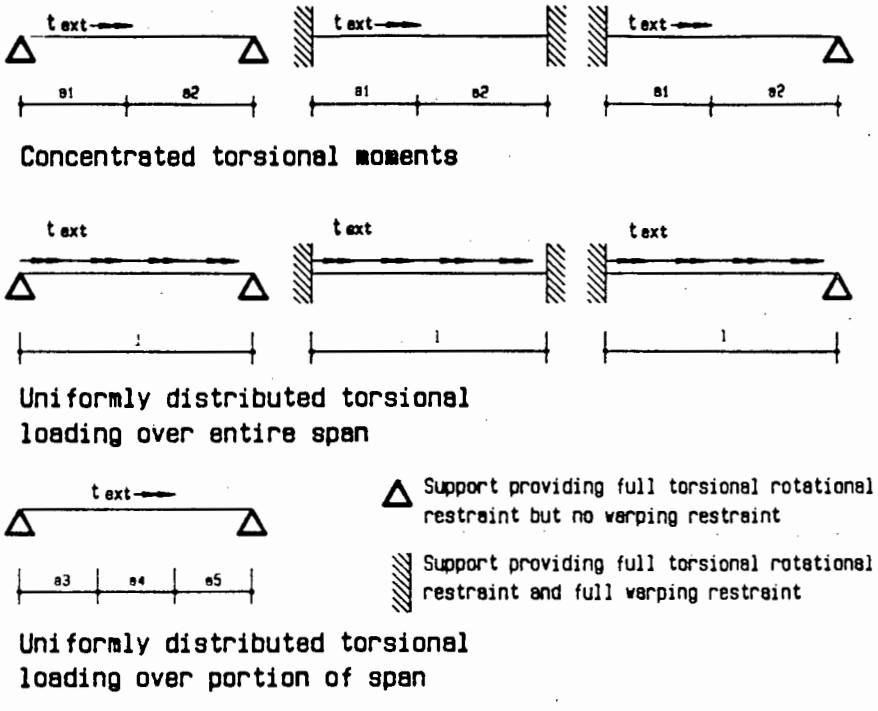

Figure 3.17 Configurations of loading types and support conditions for which expressions for $B_{twr}(z)$, $T_{twr}(z)$, $T_{svt}(z)$ and $\theta_{twr}(z)$ are given.

The torsional warping stresses f_{twr} are found from the following:

$$f_{twr} = \frac{B_{twr}\, w_{twr}}{C_{twr}} \qquad (23)$$

The form of this expression is similar to that of equation 8 for simple bending. In loadcases where eccentric loading is applied (torsion and bending), the longitudinal normal stresses f_{twr} due to torsional warping and f_{lbg} due to simple bending are superimposed to give the total longitudinal normal stresses.

The **torsional warping shear stresses** v_{twr} are given by:

$$v_{twr} = \frac{T_{twr}\, dw_{twr}/ds_{per}}{C_{cen} - C_{svt}} \qquad (24)$$

where, for a single-cell section

$$dw_{twr}/ds_{per} = a_8 - C_{svt}/2\, A_{enc}\, h \qquad (25)$$

The method for evaluating dw_{twr}/ds_{per} is shown in Appendix E as part of the analysis example for Model 3 Loadcase 2.

Finally, the **St Venant shear stresses** v_{svt} and δv_{svt} are found using equations 10 and 11 from section 3.2.2 and T_{svt} calculated by means of the appropriate expression from Tables 9 to 15.

3.4 ANALYSIS OF DISTORTIONAL WARPING (Beam-on-elastic-foundation analogy[12])

Torsional warping and shear lag in warping as well as a small effect giving rise to transverse normal stresses constant through the wall thickness are not considered here.

An analogy exists between the distortion of the cross-sections of a single-cell boxbeam and the flexural behaviour of a beam on an elastic foundation. The basis of the analogy is that under torsional loading the top and bottom slabs provide a continuous elastic support along the webs which then behave like beams supported on an elastic foundation.

Shear deformations in the planes of the flange and web elements become important for distortional analysis as the distortional stiffness increases, but according to the Maisel and Roll report it may be neglected for the distortional analysis of concrete boxbeams.

As in the case of torsional warping, the pattern of warping displacement is such that the distortional warping stresses, which act normally to the cross section, vary around both the perimeter of the cross-section as well as along the length of the box-girder. Hence longitudinal shear stresses arise resulting in complementary shear stresses in the plane of the cross-section - i.e. distortional warping shear stresses. These stresses are assumed to be constant through the wall thickness in the theory presented here. Concurrent with the above stresses, and as a result of the distortion of the cross-section, transverse bending stresses occur which vary through the thickness of the flange and web elements. Typical diagrams of all these types of stresses are shown in Figure 3.18.

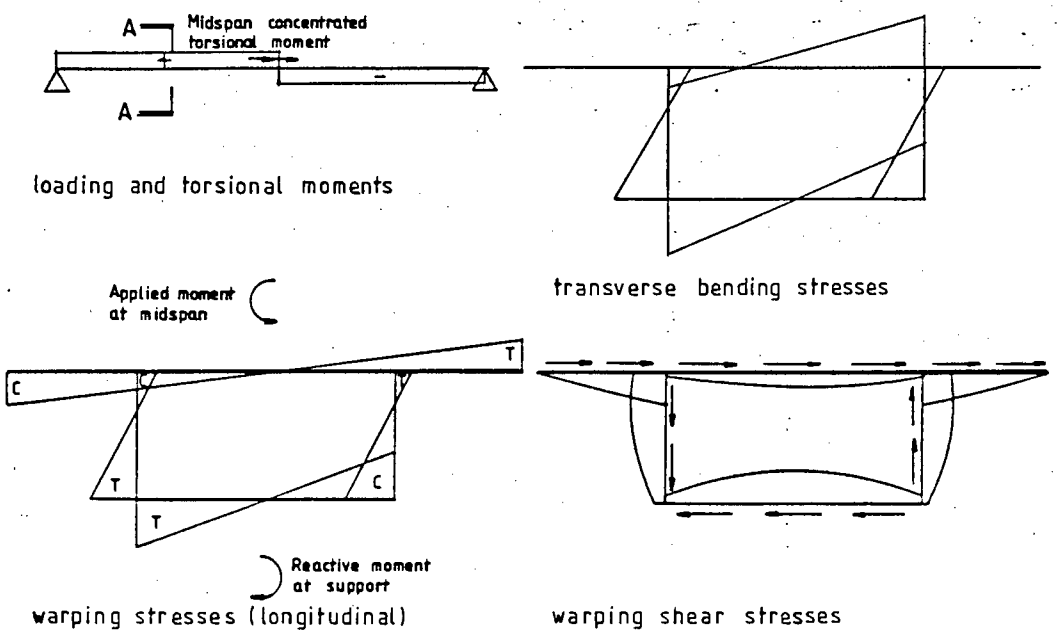

Figure 3.18 **Typical torsional loading, distortional warping stresses, distortional warping shear stresses and transverse bending stresses.**

Note that there is a zero resultant internal torsional moment due to distortional warping shear stresses since the applied torsional moment is equilibrated by the sum of the torsional moments due to torsional warping shear stresses and St Venant shear stresses.

Figure 3.19 illustrates the typical longitudinal distribution of distortional warping stresses. It can be seen from the figure that the distortional warping stresses are less localized longitudinally than the torsional warping stresses are.

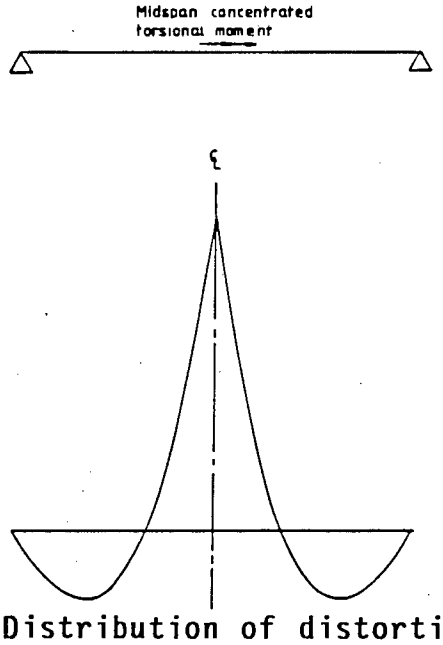

Figure 3.19 **Distribution of distortional warping stresses along the span of the beam.**

The following definitions and expressions are used in the method proposed for distortional warping analysis for box-girders:

The **bimoment** B_{dwr}, defined before for torsional warping, is a pair of equal and opposite moments, acting in parallel planes, which represent a warping force with zero longitudinal force resultant and zero moment resultant - see Figure 3.16. In the context of the beam-on-elastic-foundation analogy, the bimoment B_{dwr} is analogous to the bending moment in the beam. Similarly, the distortion of the cross-section is analogous to the deflection of the beam. Diaphragms in the beam which prevent distortion but not longitudinal warping correspond to unyielding simple supports of the beam. End supports which prevent both distortion and warping are analogous to built-in supports of the beam.

The **distortional warping coordinate** w_{dwr} is shown in Figure 3.20 below.

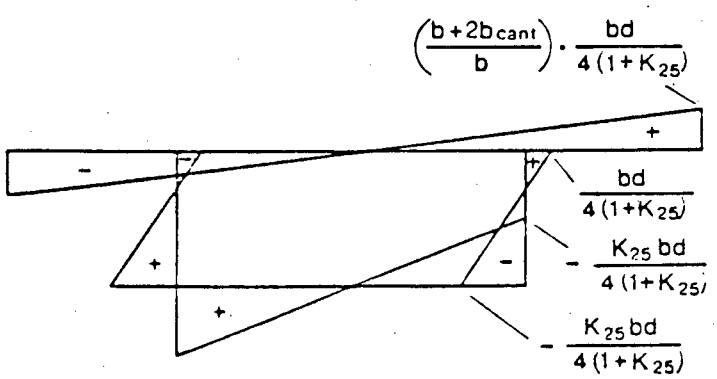

Figure 3.20 Distortional warping coordinate w_{dwr}.

K_{25} is found from:

$$K_{25} = \frac{3 + K_6}{3 + K_7} \tag{26}$$

where

$$K_6 = \frac{bh_{top}}{dh_{web}}\left[\frac{b + 2b_{cant}}{b}\right]^3 \tag{27}$$

$$K_7 = \frac{bh_{bot}}{dh_{web}} \tag{28}$$

The **distortional warping moment of inertia of cross-section** C_{dwr} is given by:

$$C_{dwr} = \frac{b^2 d^3 h_{web} K_4}{48} \tag{29}$$

with

$$K_4 = \frac{3 + 2(K_6 + K_7) + K_6 K_7}{6 + K_6 + K_7} \tag{30}$$

The **frame stiffness** EI_{fra} is obtained from:

$$I_{fra} = \frac{24\ I_{web}}{K_{26} d} \tag{31}$$

where

$$K_{26} = 1 + \frac{2b/d + 3(I_{top} + I_{bot})/I_{web}}{(I_{top} + I_{bot})/I_{web} + 6d\ I_{top} I_{bot}/bI^2_{web}} \tag{32}$$

and

$$I_{top} = \frac{h^3_{top}}{12(1 - v^2)} \tag{33}$$

$$I_{bot} = \frac{h^3_{bot}}{12(1 - v^2)} \tag{34}$$

$$I_{web} = \frac{h^3_{web}}{12(1 - v^2)} \tag{35}$$

v = Poisson's ratio

E = Young's modulus of elasticity

The various stresses associated with distortional warping and transverse bending, as described, are formulated in terms of the bimoment B_{dwr}, the first derivative of the distortional warping bimoment dB_{dwr}/dz and the angle of distortion of the cross-section β_{trb}. The sectorial coordinate w_{dwr}, the distortional moment of inertia of the cross-section C_{dwr} as well as material properties and terms based on cross-sectional dimensions, some of which are shown above, also appear in the equations which are given later on.

Algebraic expressions for B_{dwr}, dB_{dwr}/dz and β_{trb} are given in Tables 16 to 20 in the Maisel and Roll[7] report for the various loading types and support conditions shown in Figure 3.21. These expressions are given in terms of the applied torsional moments T_{ext}, the frame stiffness I_{fra}, the modulus of elasticity E, C_{dwr} as well as trigonometric functions involving span length and loading positions.

The functions for $B_{dwr}(z)$, $dB_{dwr}(z)/dz$ and $\beta_{trb}(z)$ applicable to this thesis, i.e. for concentrated applied torsional loading with no warping restraints at the ends, are reproduced in Appendix C.

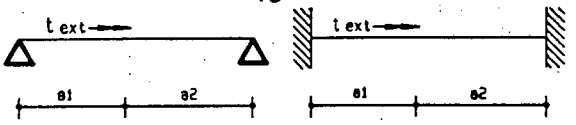

Concentrated torsional moments

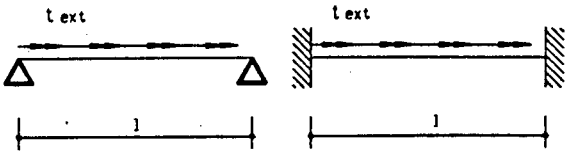

Uniformly distributed torsional loading over entire span

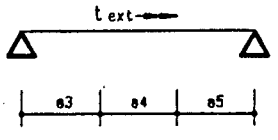

Support providing full torsional rotational restraint but no warping restraint

Support providing full torsional rotational restraint and full warping restraint

Uniformly distributed torsional loading over portion of span

Figure 3.21 Configurations of loading types and support conditions for which expressions for $B_{dwr}(z)$, $dB_{dwr}(z)/dz$ and $\beta_{trb}(z)$ are given.

The **distortional warping stresses** f_{dwr} are found using the expression:

$$f_{dwr} = \frac{B_{dwr} w_{dwr}}{C_{dwr}} \qquad (36)$$

Again, as in the case of equation 23, the form of the above expression is similar to that of equation 8. In loadcases where eccentric loading is applied (bending and torsion), the longitudinal normal stresses f_{dwr} due to distortional warping and f_{lbg} due to simple bending are superimposed to give the total longitudinal normal stresses.

The **distortional warping shear stresses** v_{dwr} are given by the following:

$$v_{dwr} = - \frac{dB_{dwr}/dz \times K_{28} bd}{hC_{dwr} \times 4(1 + K_{25})} \qquad (37)$$

where

K_{25} is as defined above

K_{28} is given for various points on the cross-section in Table 2 of the Maisel and Roll report[7] which is reproduced here in Appendix D. The equations for K_{28} are written in terms of the following:

$$K_{29} = \frac{b + 2b_{cant}}{b} \qquad (38)$$

and

$A_{top} = bh_{top}$

$A_{cant} = b_{cant}\, h_{top}$

$A_{web} = dh_{web}$

$A_{bot} = bh_{bot}$ (39)

Finally, the **transverse bending stresses** f_{trb} are determined by means of the following:

$$f_{trb} = 6\, M_{trb}/h^2 \quad (40)$$

where

M_{trb} = transverse bending moment due to the loading causing distortion

h = wall thickness

f_{trb} = transverse bending stress at the surface of web or flange elements

The transverse bending moments due to the loading causing distortion are:

at the top of the left-hand web

$$M_{trb,B} = \frac{E\, I_{fra}\, \beta_{trb}}{2(1 + K_{30})} \quad (41)$$

and at the bottom of the left-hand web

$$M_{trb,D} = -\frac{K_{30} E\, I_{fra}\, \beta_{trb}}{2(1 + K_{30})} \quad (42)$$

where

$$K_{30} = \frac{3 + bI_{web}/dI_{top}}{3 + bI_{web}/dI_{bot}} \quad (43)$$

and

β_{trb} is the distortional angle (a measure of the distortion of the cross-section) found from the expressions given in the tables referred to above.

$M_{trb,B}$ is positive for positive β_{trb} which gives compressive transverse stresses on the outer surfaces of the top flange and webs at B. $M_{trb,D}$ is negative for positive β_{trb} and gives tensile transverse stresses on the outer surfaces of the web and bottom flange at D. Note that B and D are reference points on the cross-section as given in Figure 3.4. Figure 3.18 above shows a typical transverse bending stress diagram.

3.5 ANALYSIS OF SHEAR LAG (Schmidt, Peil and Born[11])

The structural effects not considered here are shear lag in torsional and distortional warping.

Although shear lag can arise in torsion, Maisel and Roll[7] only consider it for the case of bending without torsion. A method of analysis for shear lag based on the work of Reissner[10] is presented in their report. Reissner uses the principle of minimum potential energy to obtain expressions for the longitudinal bending stresses in a doubly symmetric rectangular box-section (i.e. without side cantilevers) with uniformly distributed loading over the full length of the span. The expressions cover the cases for the stresses at the midspan section of a simply supported member and at both the midspan and support sections of a member built in at both ends.

From the above, it is clear that shear lag is not dealt with adequately by this method, especially with respect to the presence of side cantilevers, but also in terms of a wider range of load configurations, for example point loads or uniformly distributed loading over a portion of the span only. Maisel and Roll recognise the limitations and make reference to a study performed at Imperial College[8] for shear lag in steel box-girders with side cantilevers. Unfortunately this literature was not available and consequently it was necessary to find another method to deal with this aspect of the analysis.

Schmidt, Peil and Born[11] in their paper, give a practical method for determining the distribution of bending stresses for varying flange and cantilever widths. A brief description of the method follows.

The cross-section of the box-girder is divided into a number of individual flange elements of width b′ as shown in Figure 3.22 below.

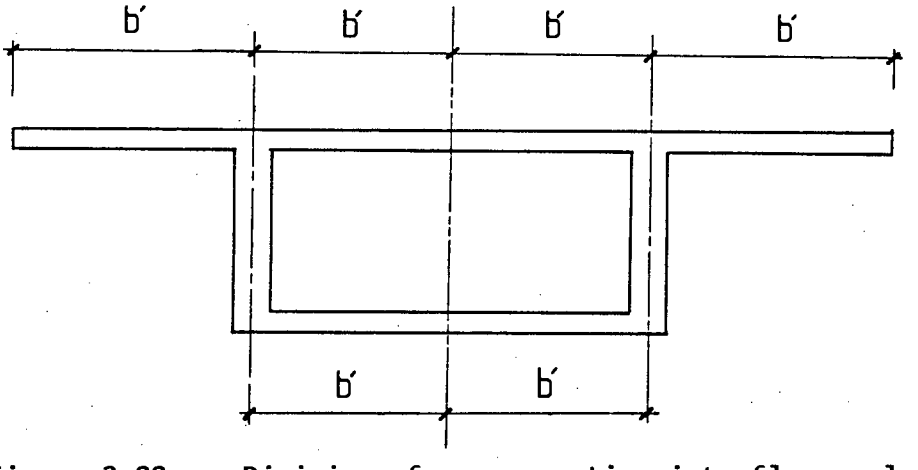

Figure 3.22 Division of cross-section into flange elements.

The basic equation governing the ratio of the magnitude of the longitudinal bending stress at the edge of a flange element to that at the web for symmetrical loading conditions (no torsional loading), is given by:

$$\frac{f'_{lbg}(edge)}{f'_{lbg}(web)} = 1{,}25(\lambda_f - 0{,}20) \text{ or } 1{,}25(\lambda_s - 0{,}20) \qquad (44)$$

where

$f'_{lbg}(edge)$ = longitudinal bending stress at the edge of the flange element

$f'_{lbg}(web)$ = longitudinal bending stress at the web

λ_f, λ_s = factors dependant on the shape of the bending moment diagram (type F or S) and the ratio of span length to flange width, L/b'. See Figure 3.23.

Values for λ_f and λ_s for use in the above equation can be found from the graphs presented in the following figure:

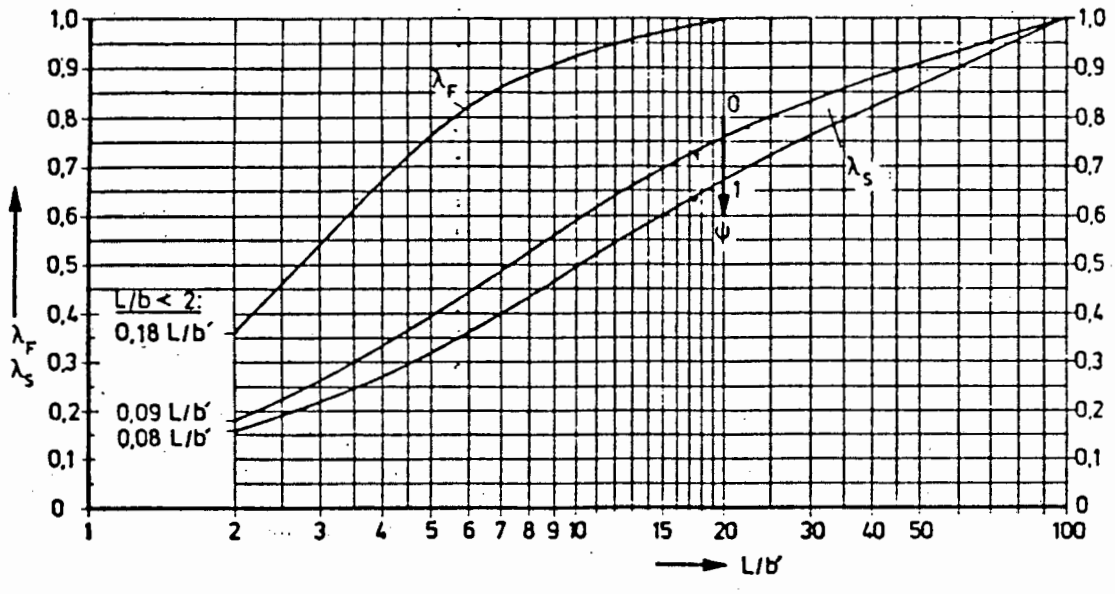

Figure 3.23 Graphs for evaluation of λ_f and λ_s.

The nature of the bending moment diagram along the longitudinal axis must be taken into consideration when selecting values from the above graphs. For this purpose, bending moment diagrams are classified as type F or type S depending on their form which is governed by the loading configuration and by the support conditions. The correspondence of moment types to the diagrams as well as the variation of λ_f and λ_s along the span is illustrated in Figure 3.24 below.

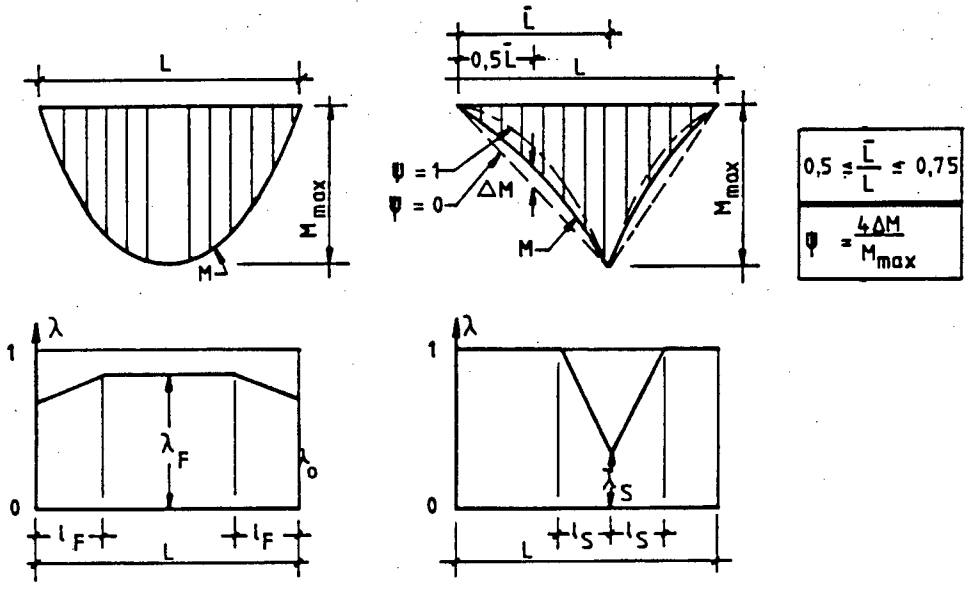

Figure 3.24 Moment types and associated λ values.

For continuous beams the spans are divided into portions within which specific moment types occur. Hence appropriate values of λ and therefore also the shear lag effect can be determined at any point along the span of such members. A typical example of the method of dealing with a continuous beam is given in Figure 3.25.

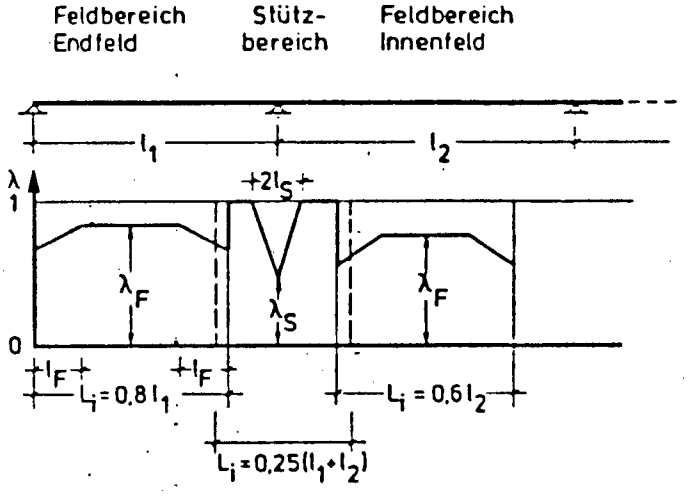

Figure 3.25 Derivation of λ values for continuous beams.

The variation of the longitudinal bending stresses from the edge of a flange element to the web (i.e. transversely) is close to a fourth degree parabola, the equation of which can be written in terms of the stress values at the webs. The form of the equation is:

$$y = ax^4 + c \qquad (45)$$

and is illustrated in Figure 3.26

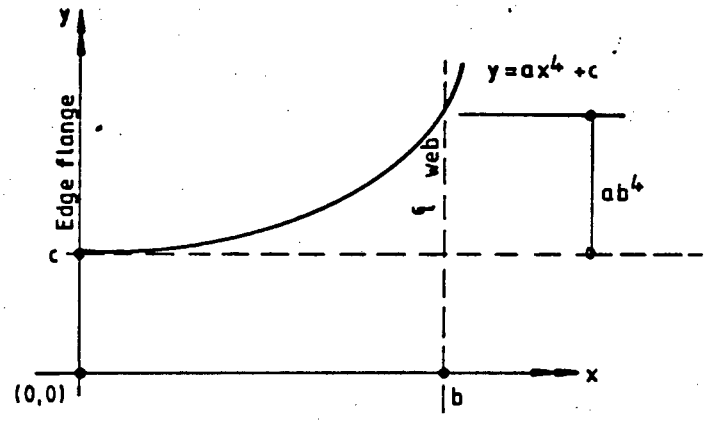

Figure 3.26 **Function for variation of longitudinal bending stresses from edge of flange element to web.**

Since the ratio of the longitudinal bending stress at the edge of a flange element to that at the web is known from equation 44 above, the values of c and a can also be determined in terms of f'_{lbg} (top web) or f'_{lbg}(bot web) as follows:

At $x = 0$, $y = c = f'_{lbg}(edge) = f'_{lbg}(web).1,25(\lambda - 0,2)$

At $x = b$, $y = ab^4 + c = f'_{lbg}(web)$

from which a is found:

$a = f'_{lbg}(web)[\ 1 - 1,25(\lambda - 0,2)]/b^4$

The longitudinal bending stresses f'_{lbg} can therefore be calculated in terms of f'_{lbg} (top web) or f'_{lbg}(bot web) for any point across the flange.

A typical diagram of the longitudinal bending stresses expressed in terms of f'_{lbg} (top web) and f'_{lbg}(bot web) is given in Figure 3.27.

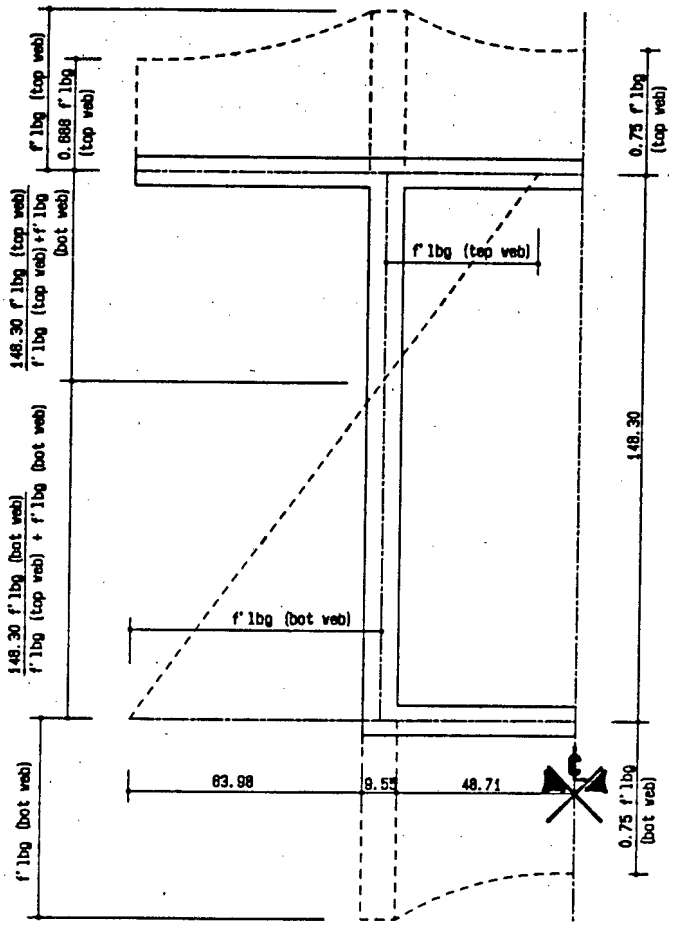

Dimensions shown are for MODEL 1

Figure 3.27 Typical longitudinal bending stress diagram, in terms of f'_{lbg} (top web) and f'_{lbg}(bot web), taking shear lag into account.

The values for f'_{lbg} (top web) and f'_{lbg}(bot web), given that the moment due to the applied loading is known for the section being considered, can be determined on a trial and error basis by using the equilibrium conditions for longitudinal bending.

The first equilibrium equation is that the sum of the axial forces arising from the longitudinal bending stresses must be zero in a beam without axial loads.

$$N_{top\ flange} + N_{top\ webs} + N_{bottom\ flange} + N_{bottom\ webs} = 0 \quad (46)$$

where

$N_{top\ flange}$ = Axial force due to bending stresses in the top flange

$N_{top\ webs}$ = Axial force due to bending stresses in the portions of the webs above the neutral axis

$N_{bottom\ flange}$ = Axial force due to bending stresses in the bottom flange

$N_{bottom\ webs}$ = Axial force due to bending stresses in the portions of the webs below below the neutral axis

The second equation is that the resisting moment due to the longitudinal bending stresses must equal the applied moment.

$$M_{applied} = M_{top\ flange} + M_{top\ webs} + M_{bot\ flange} + M_{bot\ webs} \quad (47)$$

where

$M_{applied}$ = Applied bending moment

$M_{top\ flange}$ = Resisting moment due to bending stresses in the top flange

$M_{top\ webs}$ = Resisting moment due to bending stresses in the webs above the neutral axis

$M_{bot\ flange}$ = Resisting moment due to bending stresses in the bottom flange

$M_{bot\ webs}$ = Resisting moment due to bending stresses in the webs below the neutral axis

Equations 46 and 47 may be written in terms of the two variables f'_{lbg} (top web) and f'_{lbg}(bot web) and solved by trial and error. The example of shear lag analysis given in APPENDIX E illustrates the trial and error procedure. In this example the distribution of stresses between the flange edges and webs are taken as linear with a single intermediate point on the 4^{th} degree curve as a simplification for solving the equilibrium equations.

Schmidt et al[11] also present equations for dealing with shear lag under conditions of torsional loading, but since Maisel and Roll do not treat this aspect, it is not discussed here.

4 ANALYTICAL RESULTS

4.1 GENERAL

The four Perspex models, described in Chapter 2, were each subjected to four different loadcases in order to check the accuracy of the proposed analytical method for simple loading configurations. These loadcases, shown in Figure 4.1, were selected to, as far as possible, individually examine the accuracy of analysis for the different structural actions. In this context it is possible to isolate shear lag in bending as well as the torsional warping action but the distortional warping action cannot take place without the torsional warping action. Loadcases 1.1, 2.1, 3.1 and 4.1 focus on simple bending together with shear lag in bending; loadcases 1.4, 2.4, 3.4 and 4.5 isolate torsional warping effects without distortion by making use of rigid diaphragms at the load positions and loadcases 1.2, 1.3, 2.2, 2.3, 3.2, 3.3 and 4.2 include actions for torsional warping as well as for distortional warping. Loadcase 4.4 includes all action types, i.e. torsional and distortional warping together with simple bending and shear lag in bending. Loadcase 4.6 is the same as loadcase 4.4 except there is a diaphragm at the loaded section.

Examples of typical analyses, done in accordance with the theory given in Chapter 3 for the analytical method, are shown in Appendix E. These are for Model 1 Loadcase 1B (simple bending and shear lag in bending) and for Model 3 Loadcase 2 (torsional and distortional warping), which between them cover all aspects of analysis.

4.2 SECTION PROPERTIES

The cross-sectional dimensions for the as-built models were given in Figure 2.2 and the main cross-sectional properties used in the different analyses are given in Table 4.1.

Note that the position of the origin of the x and y axes within the cross-section is taken as the centroid for longitudinal bending analysis, as the shear centre for torsional warping analysis and as the geometric midpoint of the closed portion of the cross-section for the distortional warping analysis.

4.3 LOADING CASES

The applied loading and support conditions constituting the various loadcases are shown in Figure 4.1. Support conditions are the same throughout, i.e providing full torsional restraint with no warping restraint. Load magnitudes were selected for each loadcase in order to give a suitable range of strain readings.

	Model 1	Model 2	Model 3	Model 4
A	$4.554.10^3$ mm^2	$3.368.10^3$	$2.771.10^3$	$2.633.10^3$
A_{enc}	$15.864.10^3$ mm^2	$9.260.10^3$	$4.168.10^3$	$3.386.10^3$
I_{xx}	13.254 mm^4	$3.614.10^6$	$0.792.10^6$	$0.511.10^6$
y_c	93.30 mm	58.74	27.77	23.34
C_{svt}	11 861.10^{3}mm^4	4 763.10^3	1 565.10^3	1 070.10^3
C_{twr}	2 069.10^{6}mm^6	1 355.10^6	404.10^6	292.10^6
C_{dwr}	9 869.10^{6}mm^6	2 433.10^3	390.10^6	238.10^6
I_{fra}	1.79 mm^2	2.04	4.20	4.27

Table 4.1 Cross-sectional properties for models.

4.4 DIAGRAMS FOR COMBINED STRESSES FROM ANALYSIS

The diagrams for the combined or total stresses, derived from the analyses, are shown in Figures 4.2 to 4.18 for all the loadcases. The diagrams typically show the various stress types, i.e longitudinal normal, shear and transverse bending, for both the midspan (z = 600 mm) and quarter-span (z = 300 mm) sections and are again used in Chapter 5, omitting the stress values for more clarity, as a background for plotting the experimentally derived stresses as points.

The method of the construction of the combined stress diagrams from the various structural actions as well as the use of the sign convention, can be seen in the analysis examples given in Appendix E.

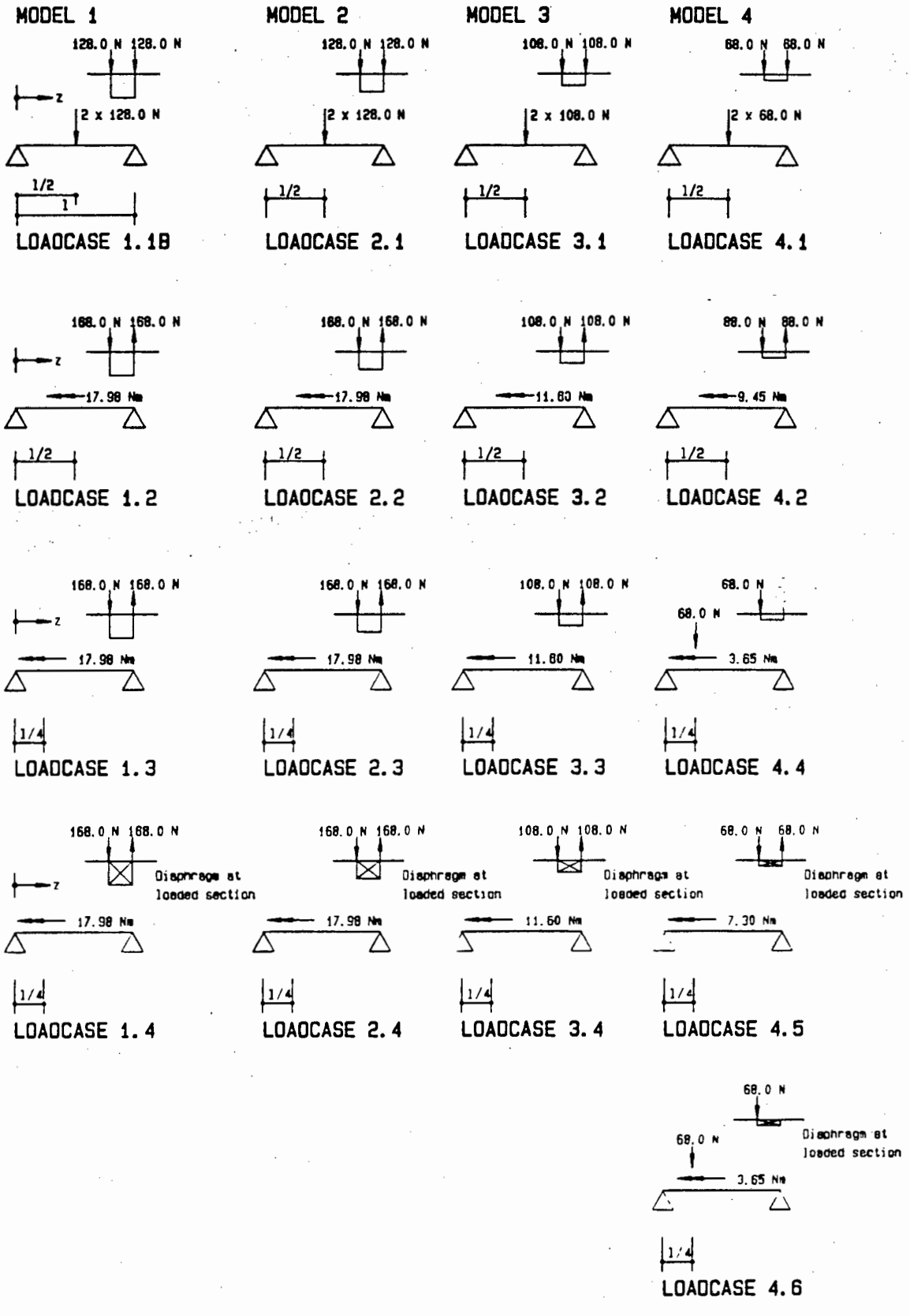

Figure 4.1 Loadcases for which models were tested and analysed.

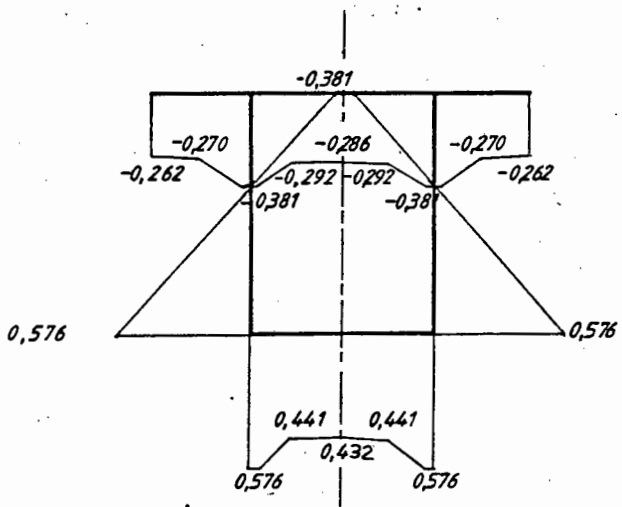

a) Longitudinal stresses at midspan (midlines)

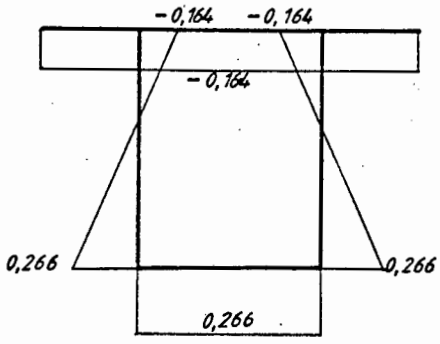

b) Longitudinal stresses at ¼ -span (z = 300 mm) (midlines)

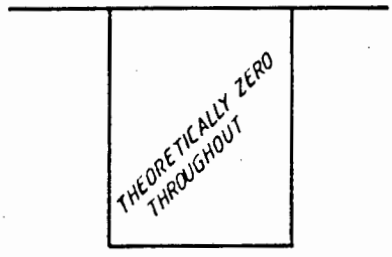

c) Transverse stresses at midspan

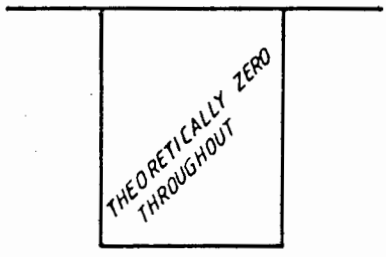

d) Transverse stresses at ¼ - span (z = 300 mm)

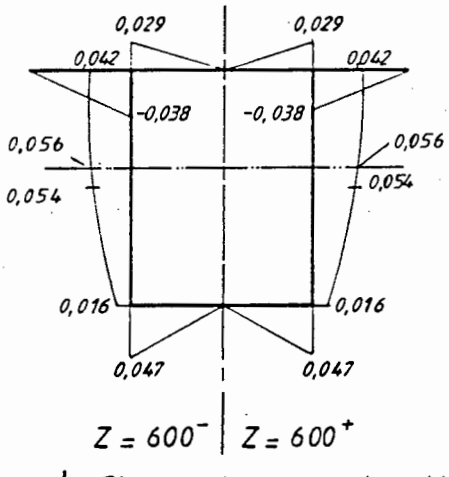

e) Shear stresses at midspan

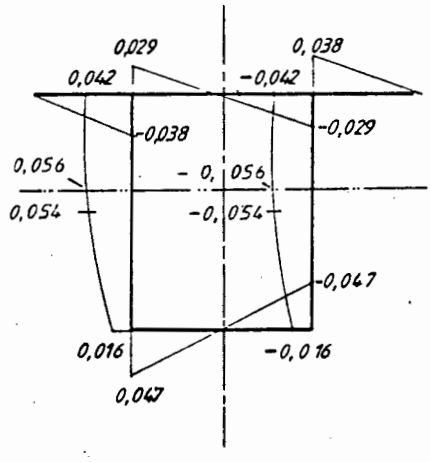

f) Shear stresses at ¼ - span (z = 300 mm)

FIGURE 4.2: Model 1 Loadcase 1B
Combined stresses from analysis MPa

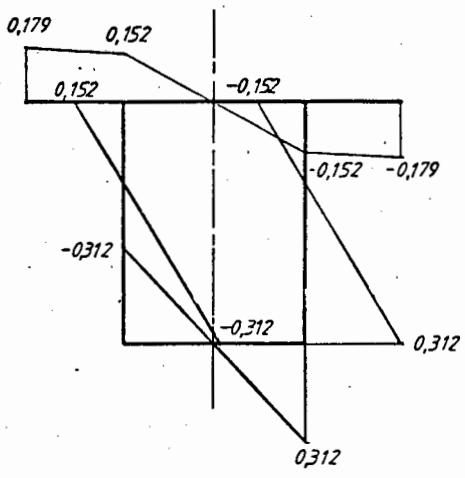

a) Longitudinal stresses at midspan

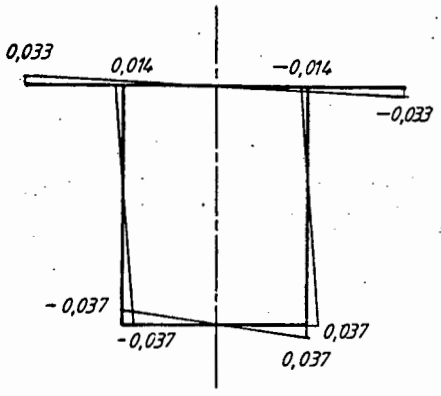

b) Longitudinal stresses at ¼ -span (z = 300 mm)

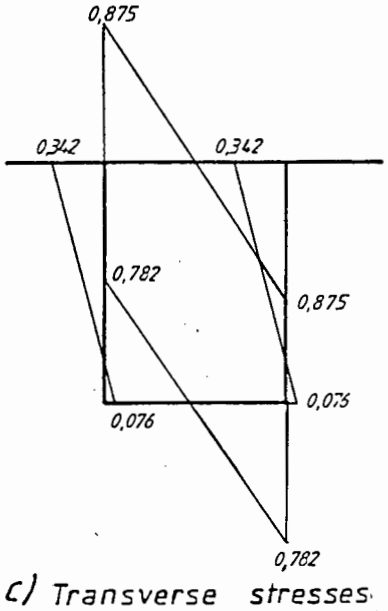

c) Transverse stresses at midspan

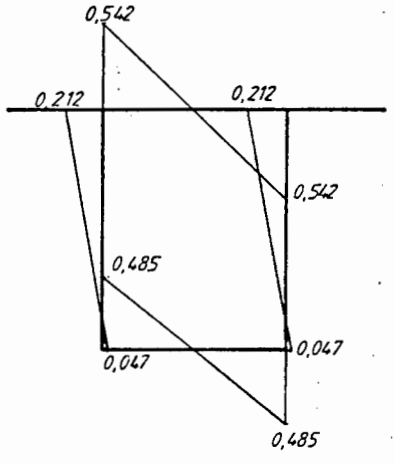

d) Transverse stresses at ¼ - span (z = 300 mm)

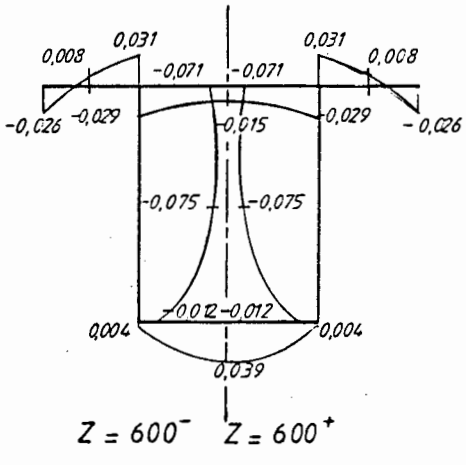

e) Shear stresses at midspan

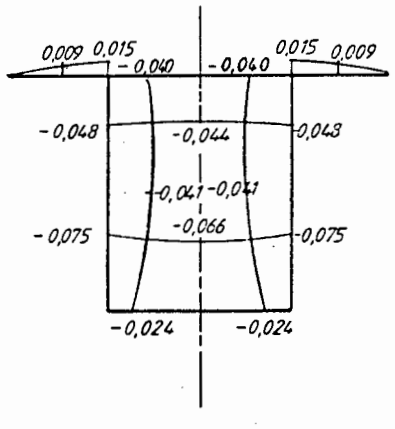

f) Shear stresses at ¼ - span (z = 300 mm)

FIGURE 4.3: Model 1 Loadcase 2
Combined stresses from analysis MPa

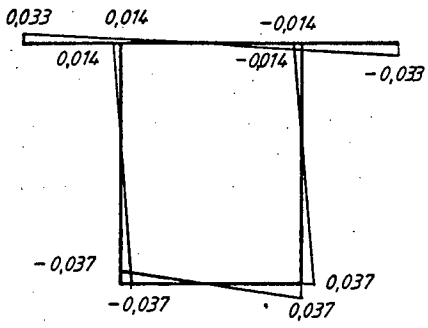

a) Longitudinal stresses at midspan

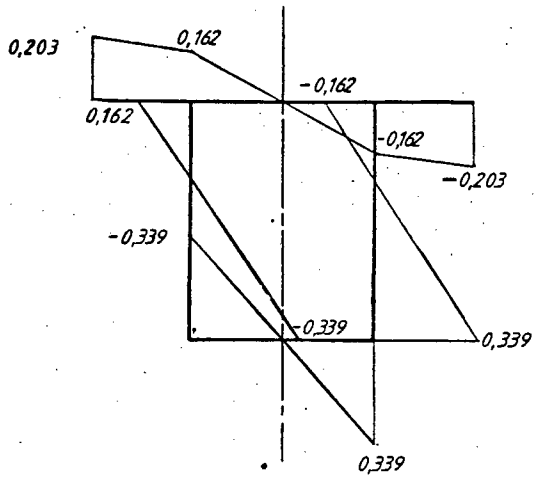

b) Longitudinal stresses at ¼ -span (z = 300 mm)

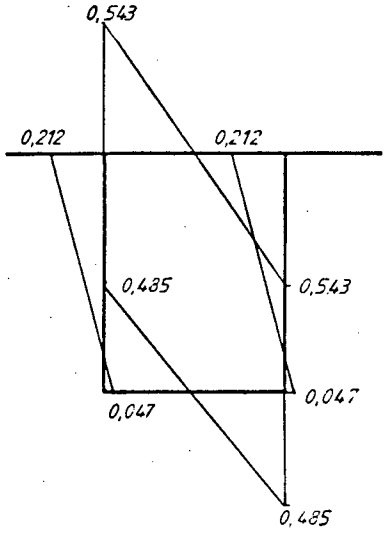

c) Transverse stresses at midspan

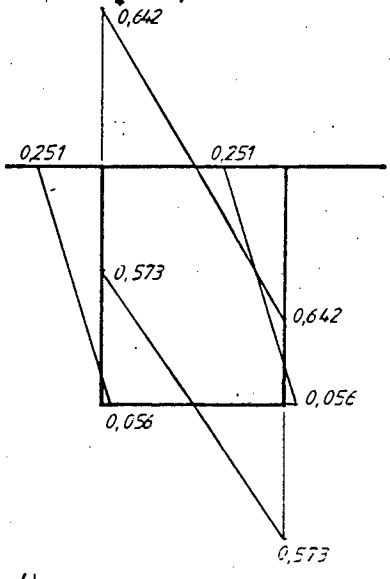

d) Transverse stresses at ¼ - span (z = 300 mm)

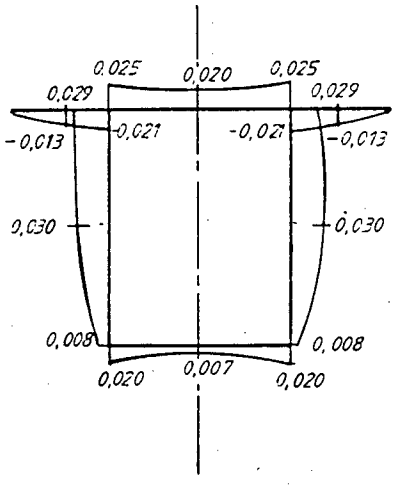

e) Shear stresses at midspan

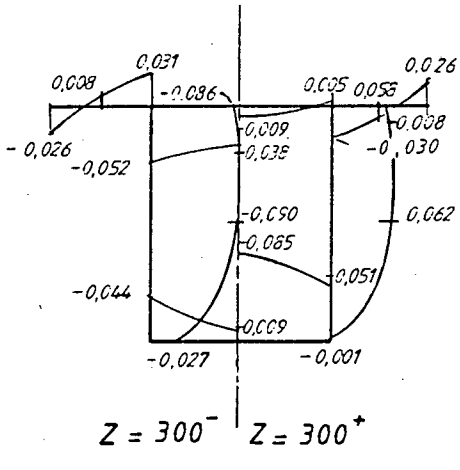

f) Shear stresses at ¼ - span (z = 300 mm)

FIGURE 4.4: Model 1 Loadcase 3
Combined stresses from analysis MPa

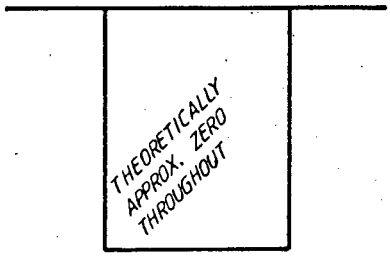

a) Longitudinal stresses at midspan

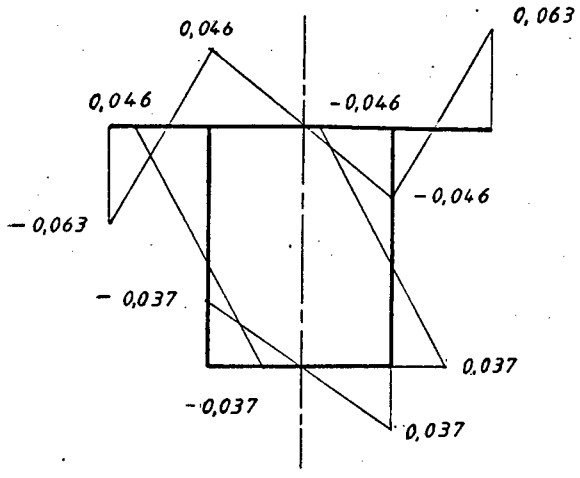

b) Longitudinal stresses at ¼ -span (z = 300 mm)

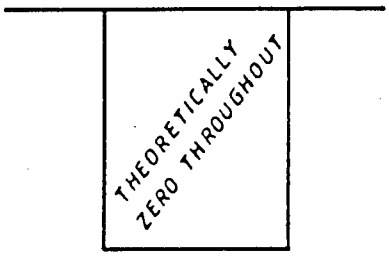

c) Transverse stresses at midspan

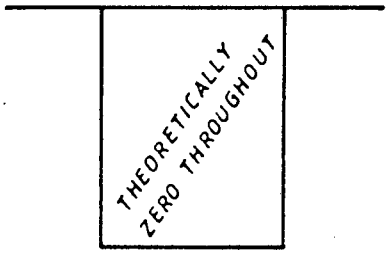

d) Transverse stresses at ¼ - span (z = 300 mm)

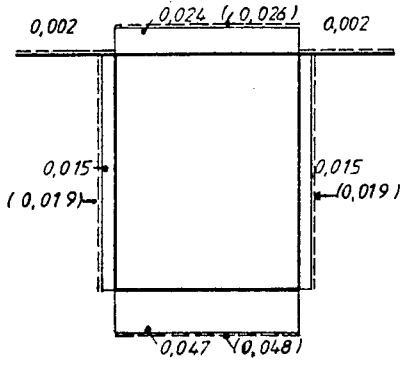

(--- outer fibre stresses)

e) Shear stresses at midspan

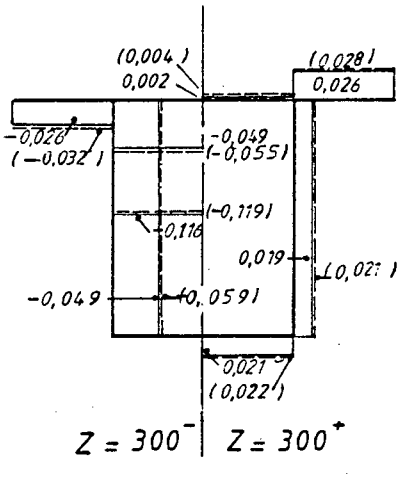

f) Shear stresses at ¼ - span (z = 300 mm)

FIGURE 4.5: Model 1 Loadcase 4
Combined stresses from analysis MPa

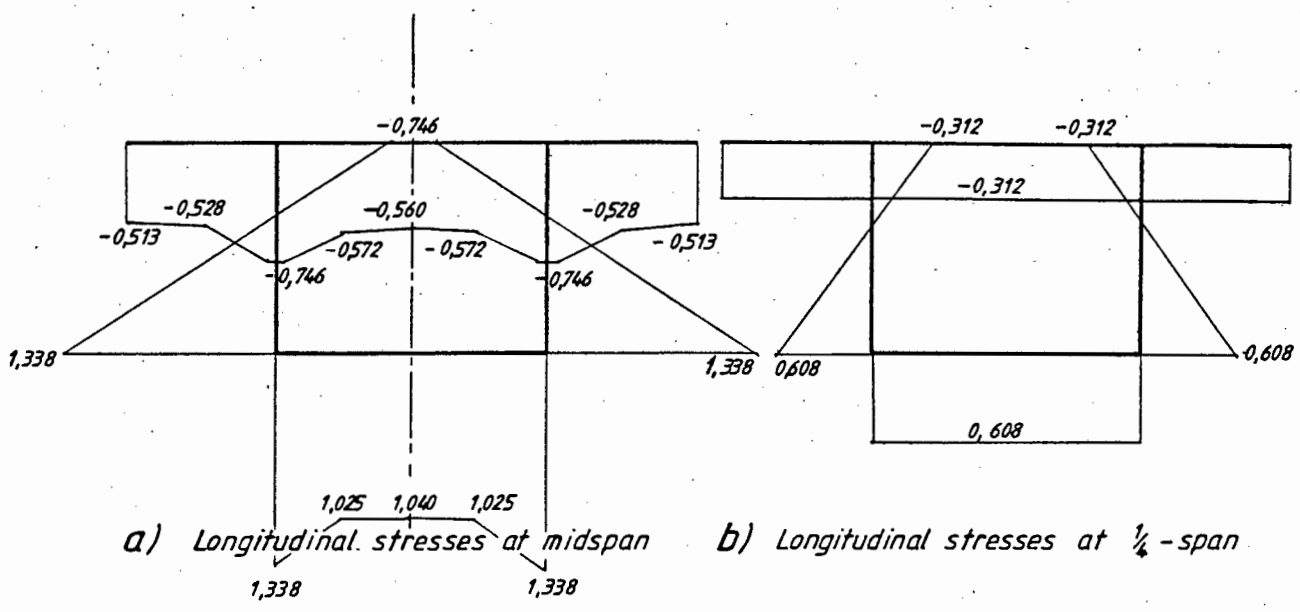

a) Longitudinal stresses at midspan

b) Longitudinal stresses at ¼-span

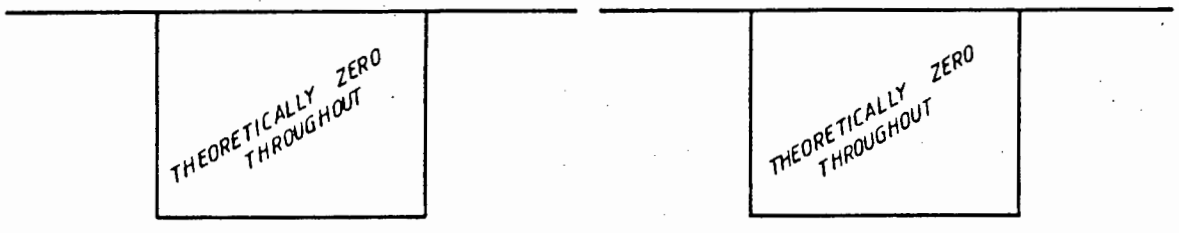

c) Transverse stresses at midspan

d) Transverse stresses at ¼-span (z = 300 mm)

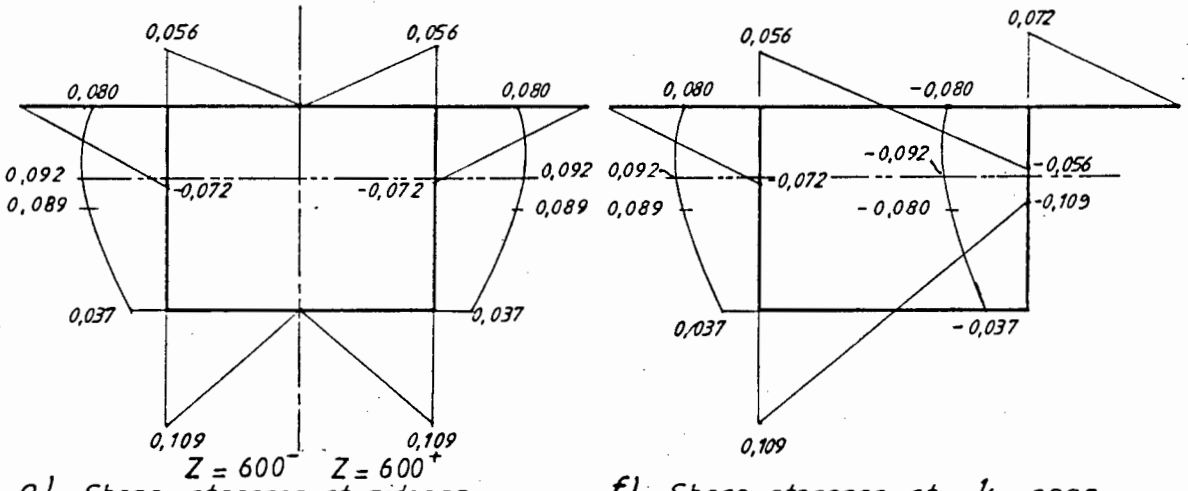

e) Shear stresses at midspan

f) Shear stresses at ¼-span

FIGURE 4.6: Model 2 Loadcase 1
Combined stresses from analysis MPa

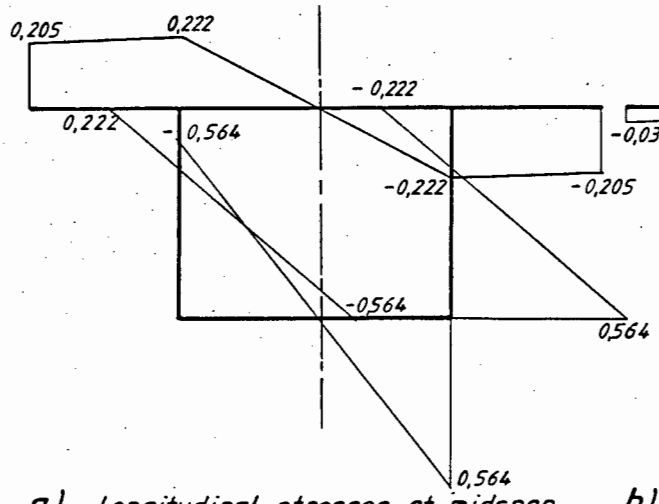

a) Longitudinal stresses at midspan

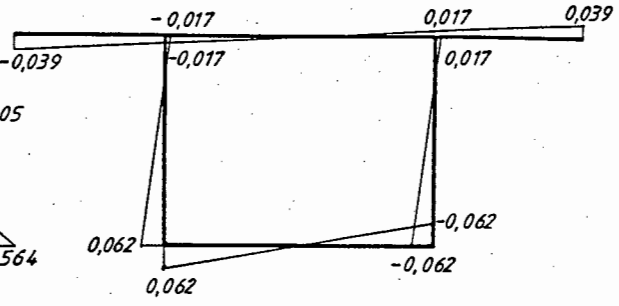

b) Longitudinal stresses at ¼ - span

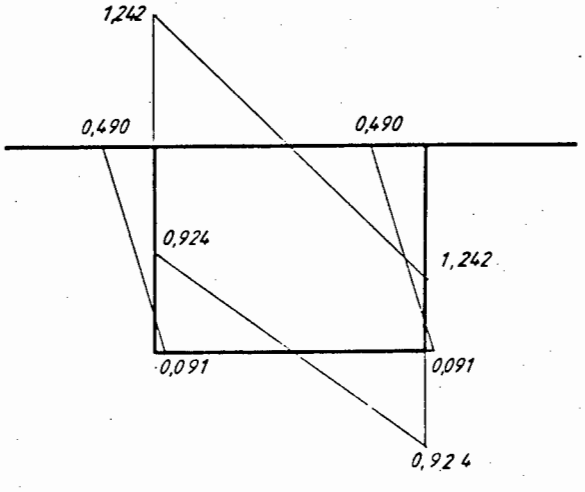

c) Transverse stresses at midspan

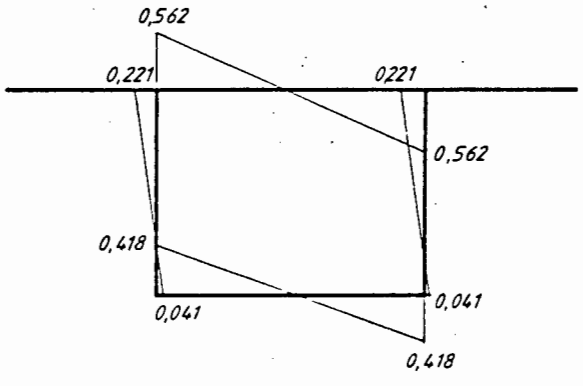

d) Transverse stresses at ¼ - span
(z = 300 mm)

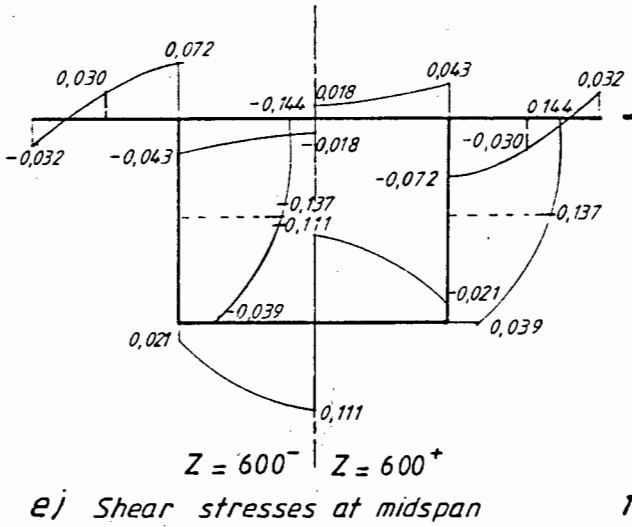

e) Shear stresses at midspan

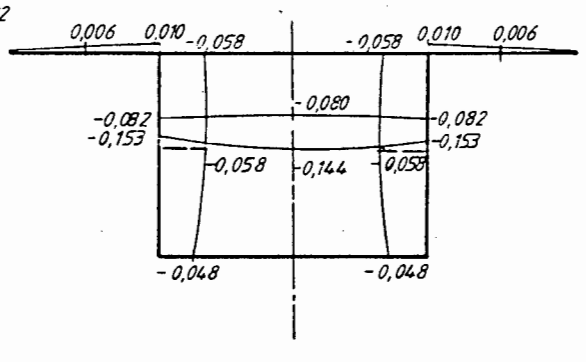

f) Shear stresses at ¼ - span

FIGURE 4.7: Model 2 Loadcase 2
Combined stresses from analysis MPa

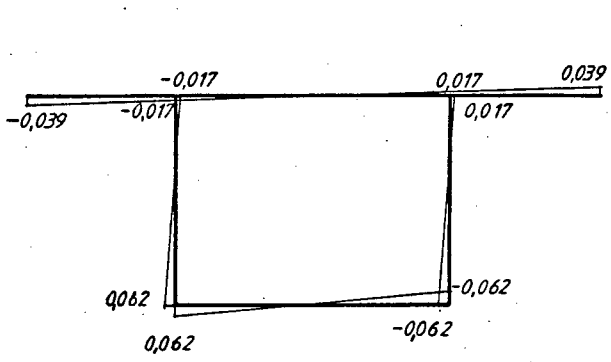

a) Longitudinal stresses at midspan

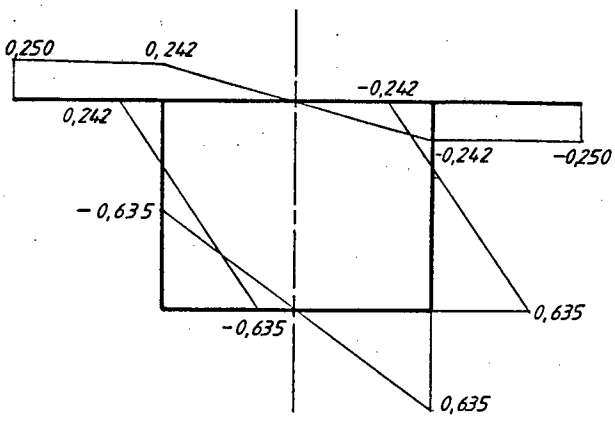

b) Longitudinal stresses at ¼-span

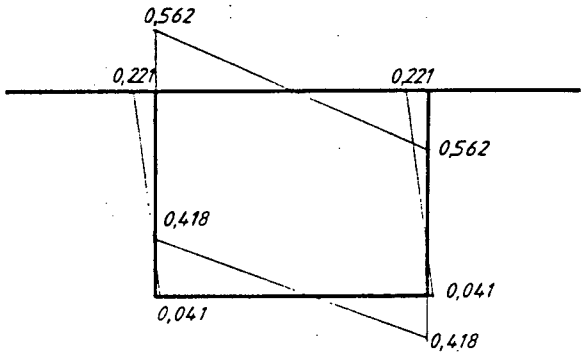

c) Transverse stresses at midspan

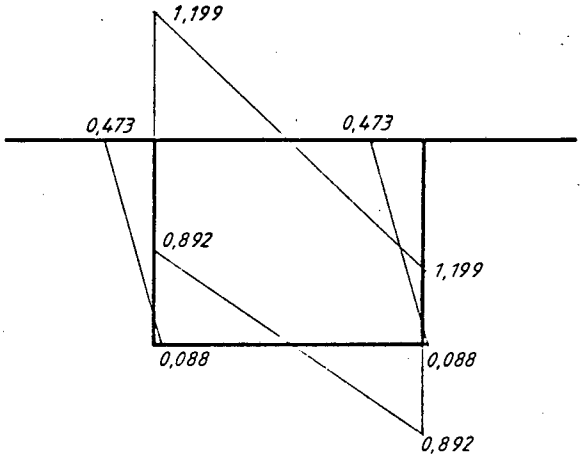

d) Transverse stresses at ¼-span
(z = 300 mm)

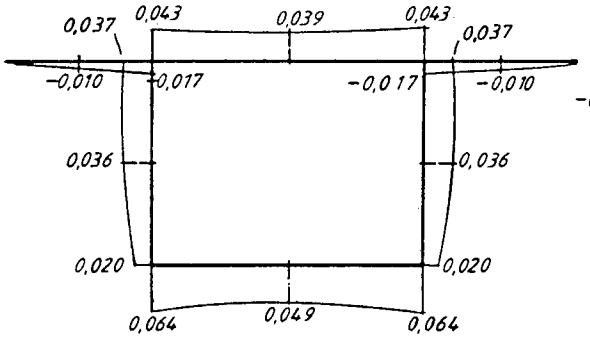

e) Shear stresses at midspan

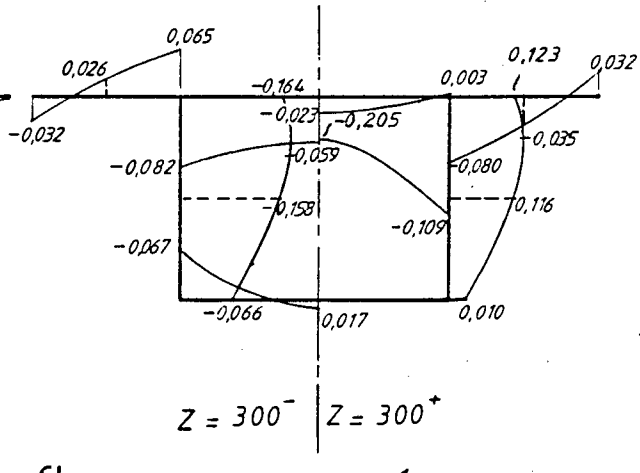

f) Shear stresses at ¼-span

FIGURE 4.8: Model 2 Loadcase 3
Combined stresses from analysis MPa

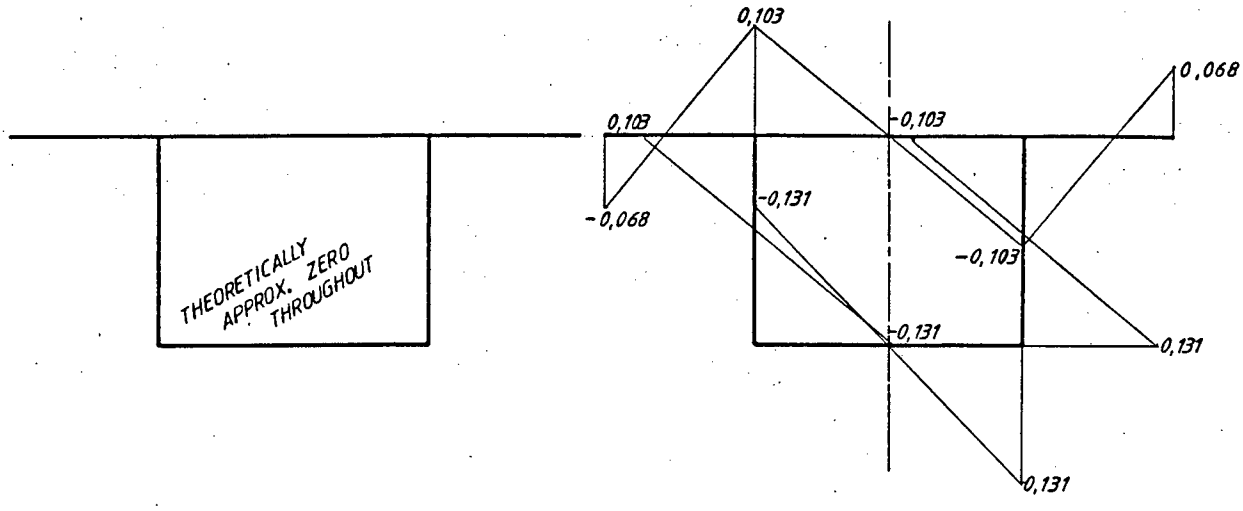

a) Longitudinal stresses at midspan

b) Longitudinal stresses at ¼-span

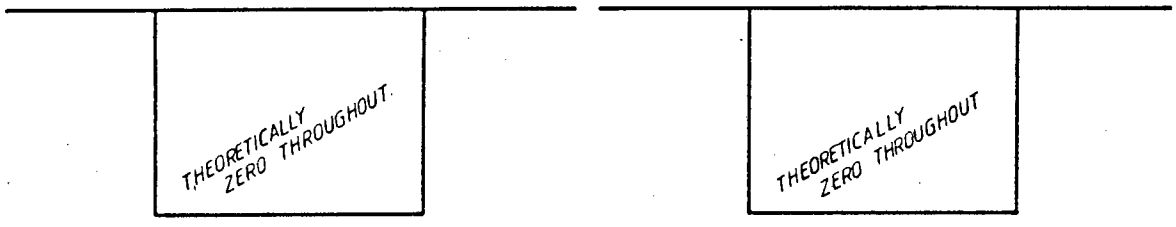

c) Transverse stresses at midspan

d) Transverse stresses at ¼-span
(z = 300 mm)

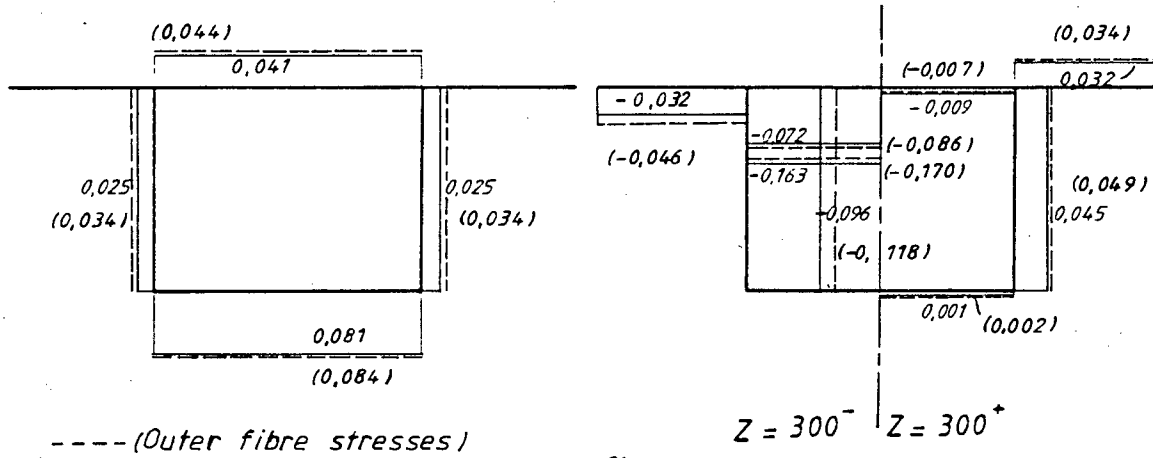

---- (Outer fibre stresses)

e) Shear stresses at midspan

f) Shear stresses at ¼-span

FIGURE 4.9: Model 2 Loadcase 4
Combined stresses from analysis MPa

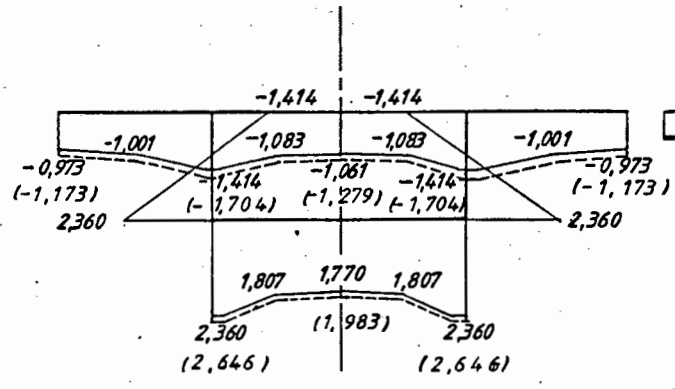

a) Longitudinal stresses at midspan

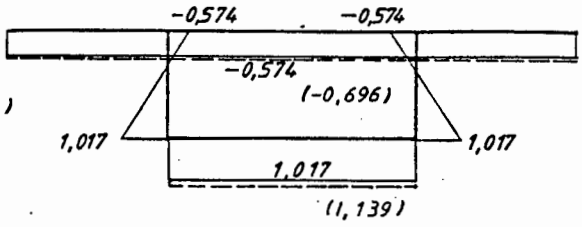

b) Longitudinal stresses at ¼ - span (z = 300 mm)

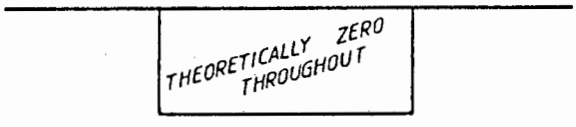

c) Transverse stresses at midspan

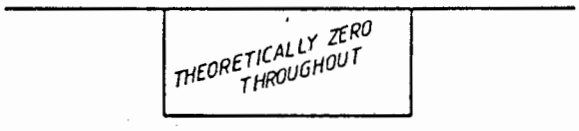

d) Transverse stresses at ¼ - span (z = 300 mm)

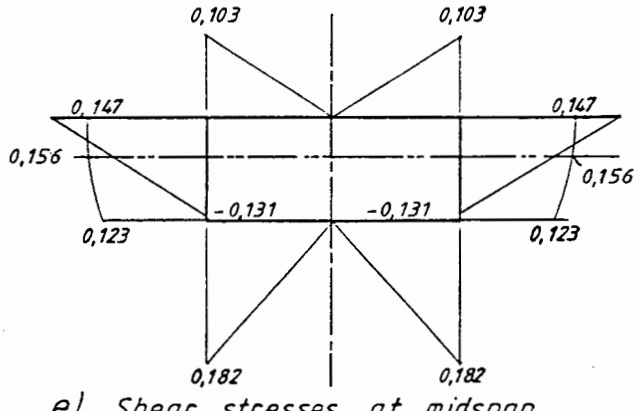

e) Shear stresses at midspan

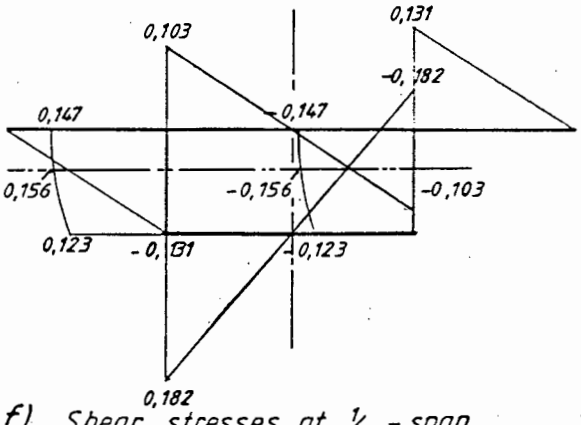

f) Shear stresses at ¼ - span (z = 300 mm)

$Z = 600^-$ | $Z = 600^+$

——— (Outer fibre stresses)

FIGURE 4.10: Model 3 Loadcase 1
Combined stresses from analysis MPa

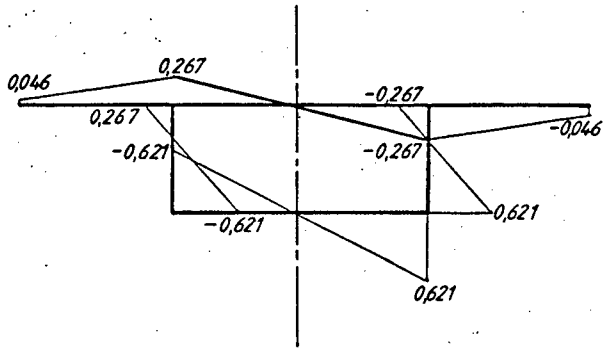

a) Longitudinal stresses at midspan

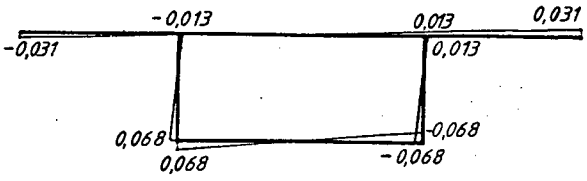

b) Longitudinal stresses at ¼ - span (z = 300 mm)

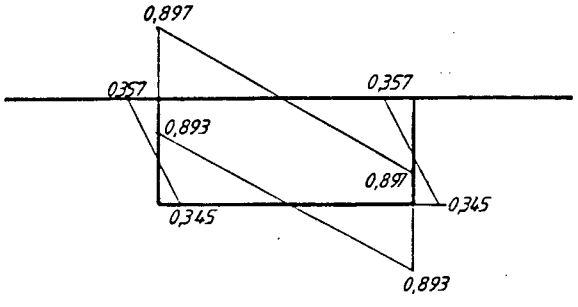

c) Transverse stresses at midspan

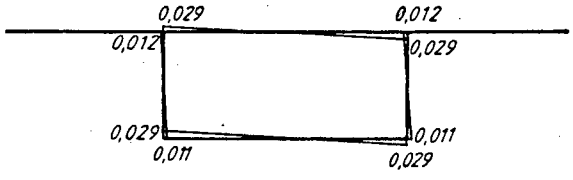

d) Transverse stresses at ¼ - span (z = 300 mm)

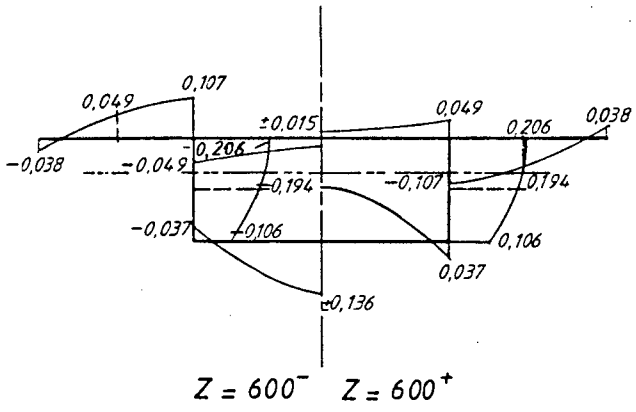

Z = 600⁻ Z = 600⁺

e) Shear stresses at midspan

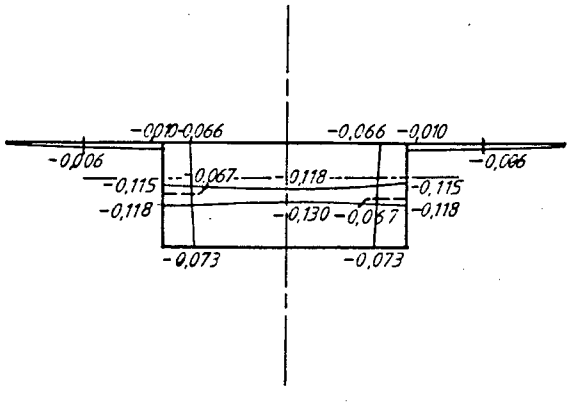

f) Shear stresses at ¼ - span (z = 300 mm)

FIGURE 4.11: Model 3 Loadcase 2
Combined stresses from analysis MPa

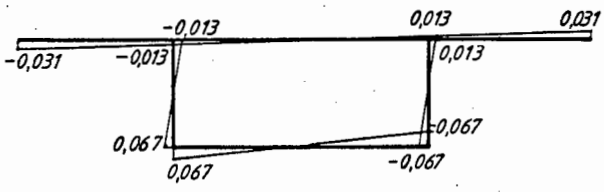

a) Longitudinal stresses at midspan

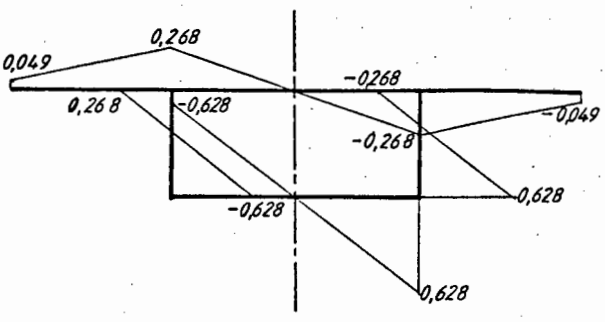

b) Longitudinal stresses at 1/4 - span (z = 300 mm)

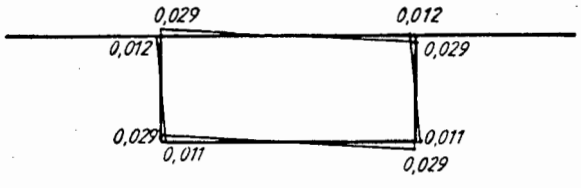

c) Transverse stresses at midspan

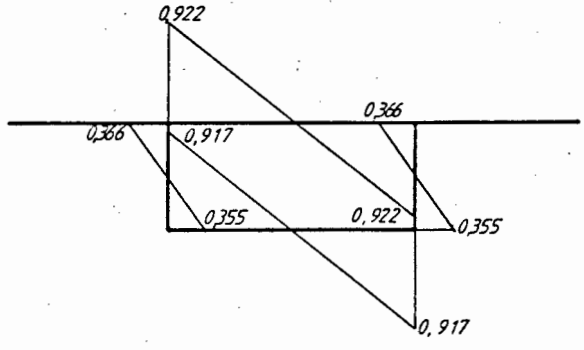

d) Transverse stresses at 1/4 - span (z = 300 mm)

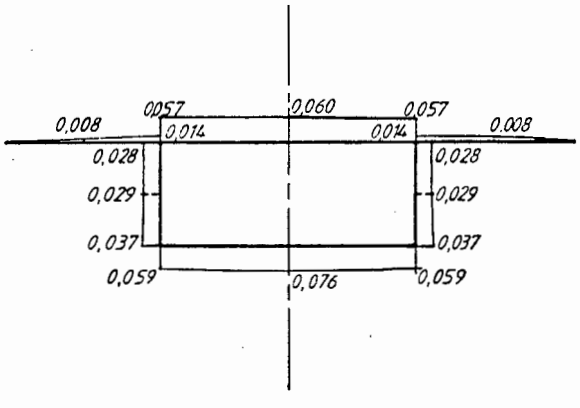

e) Shear stresses at midspan

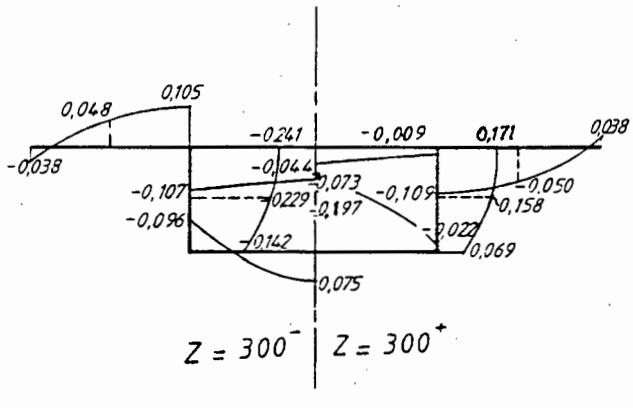

f) Shear stresses at 1/4 - span (z = 300 mm)

FIGURE 4.12: Model 3 Loadcase 3
Combined stresses from analysis MPa

a) Longitudinal stresses at midspan

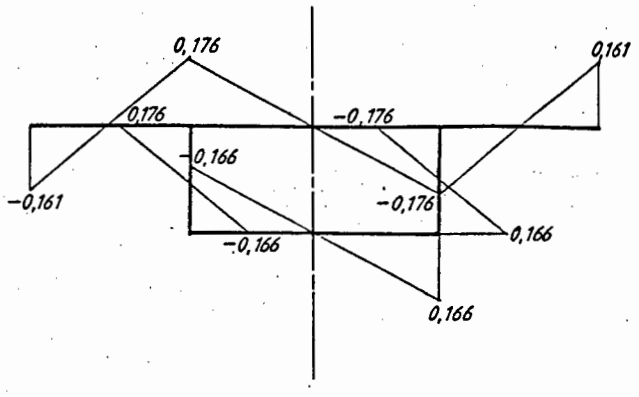

b) Longitudinal stresses at ¼ - span
(z = 300 mm)

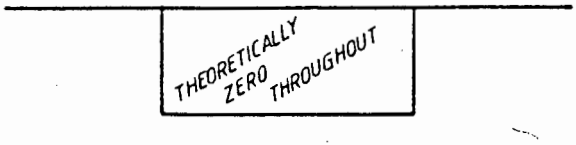

c) Transverse stresses
at midspan

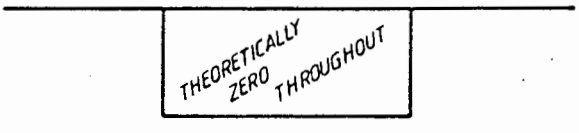

d) Transverse stresses
at ¼ - span
(z = 300 mm)

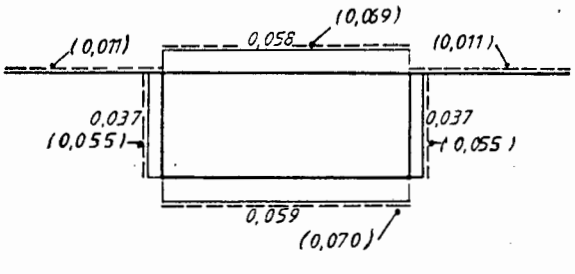

---- (Outer fibre stresses)

e) Shear stresses at midspan

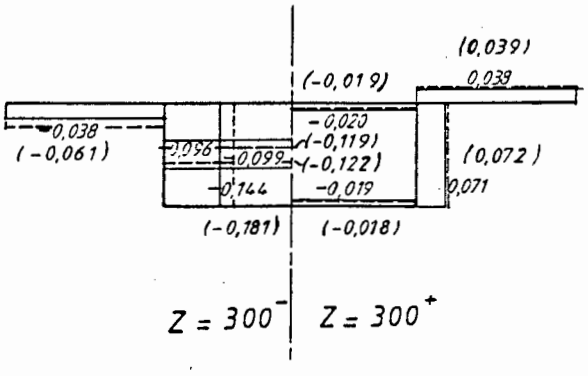

f) Shear stresses at ¼ - span
(z = 300 mm)

FIGURE 4.13: Model 3 Loadcase 4
Combined stresses from analysis MPa

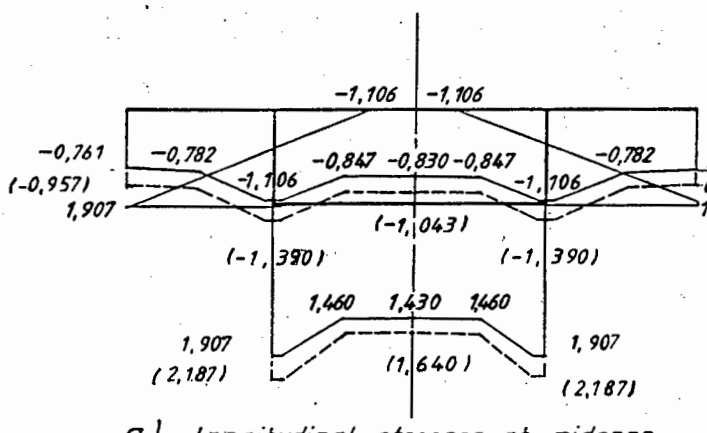

a) Longitudinal stresses at midspan

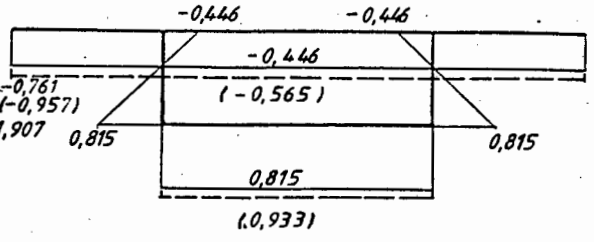

b) Longitudinal stresses at ¼ - span (z = 300 mm)

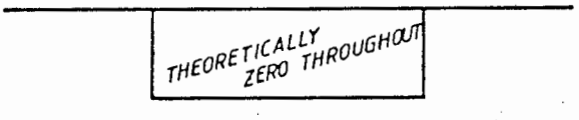

c) Transverse stresses at midspan

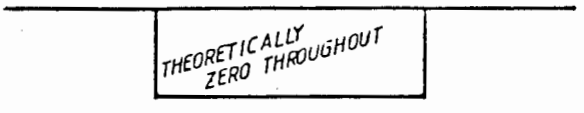

d) Transverse stresses at ¼ - span (z = 300 mm)

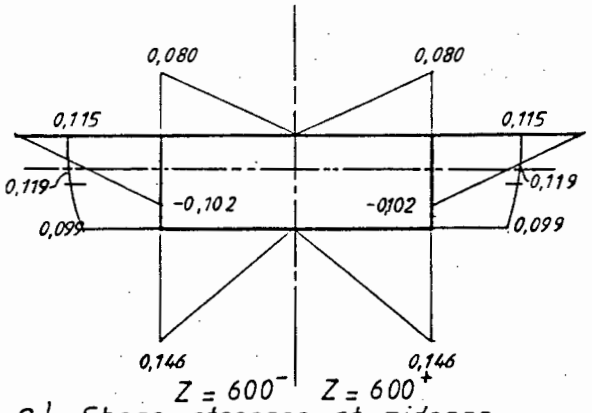

e) Shear stresses at midspan

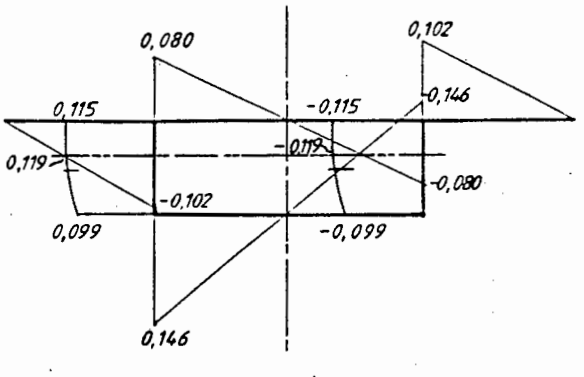

f) Shear stresses at ¼ - span (z = 300 mm)

----- (Outer fibre stresses)

FIGURE 4.14: Model 4 Loadcase 1
Combined stresses from analysis MPa

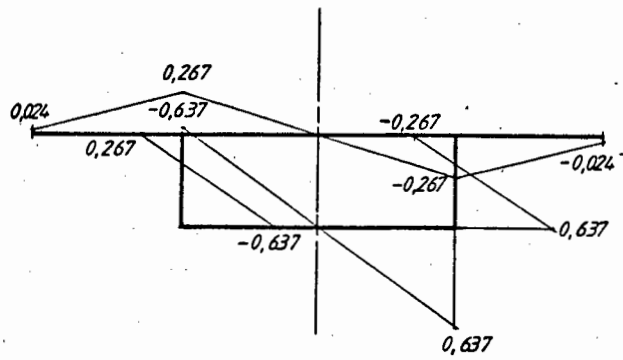

a) Longitudinal stresses at midspan

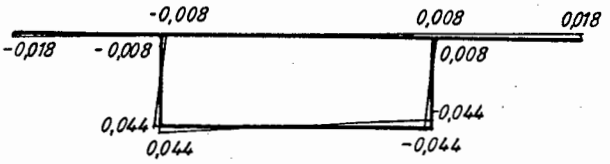

b) Longitudinal stresses at ¼ - span (z = 300 mm)

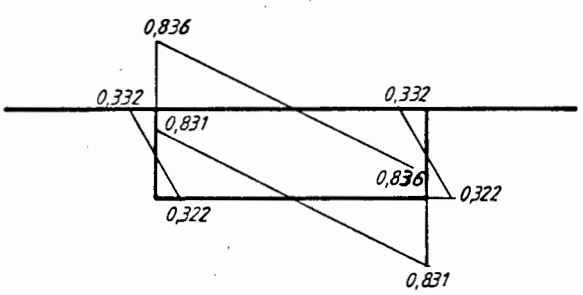

c) Transverse stresses at midspan

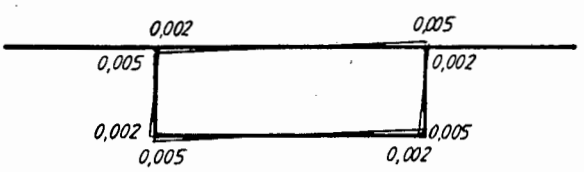

d) Transverse stresses at ¼ - span (z = 300 mm)

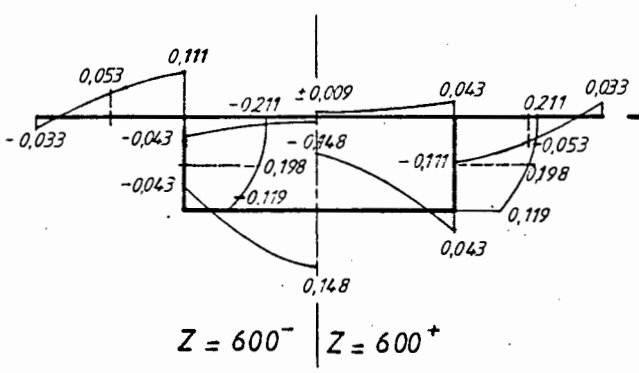

e) Shear stresses at midspan

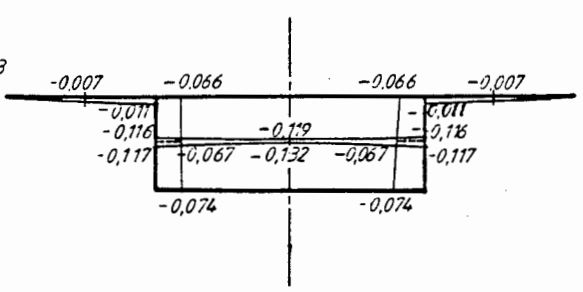

f) Shear stresses at ¼ - span (z = 300 mm)

FIGURE 4.15: Model 4 Loadcase 2
Combined stresses from analysis MPa

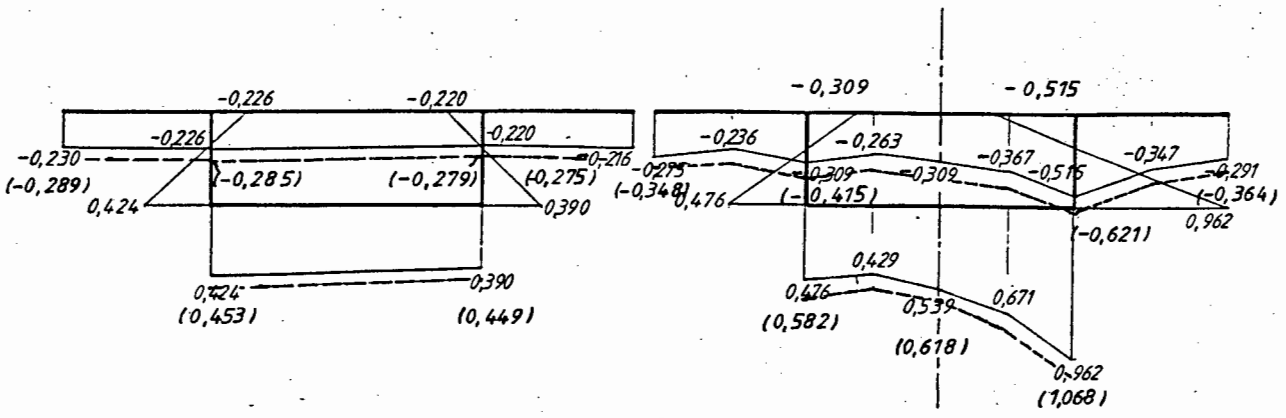

a) Longitudinal stresses at midspan

b) Longitudinal stresses at ¼ - span (z = 300 mm)

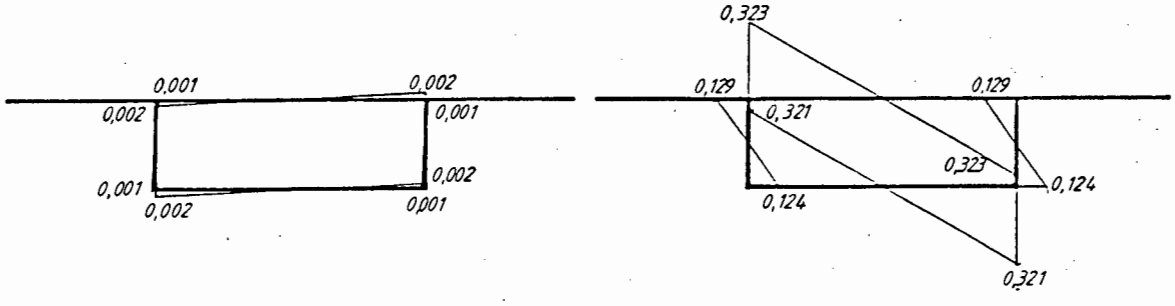

c) Transverse stresses at midspan

d) Transverse stresses at ¼ - span (z = 300 mm)

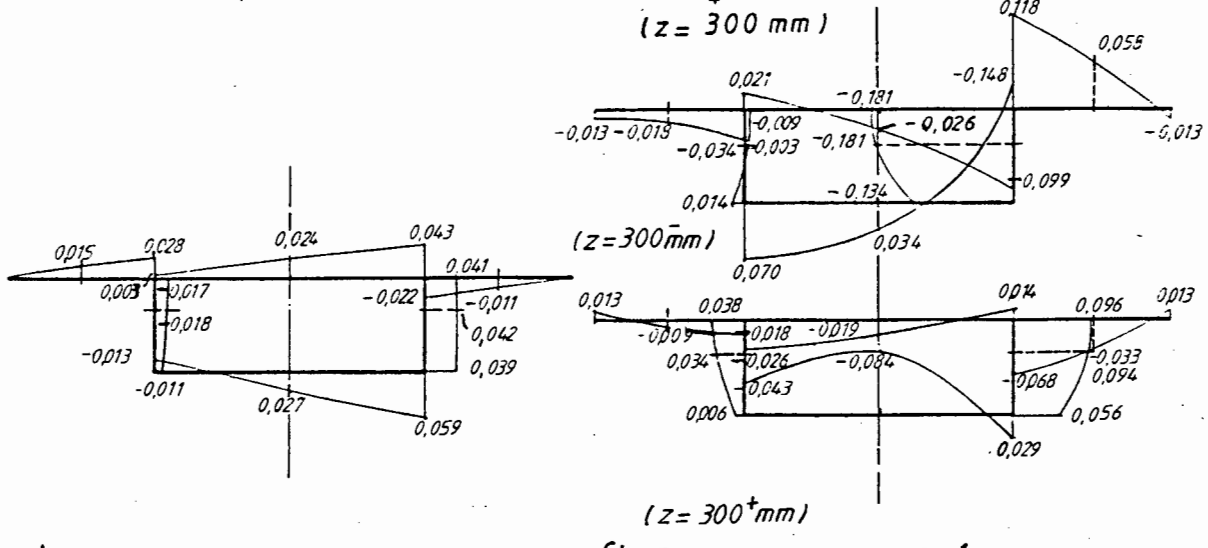

e) Shear stresses at midspan

f) Shear stresses at ¼ - span (z = 300⁺mm)

(- - - - - Outer fibre stresses)

FIGURE 4.16: Model 4 Loadcase 4
Combined stresses from analysis MPa

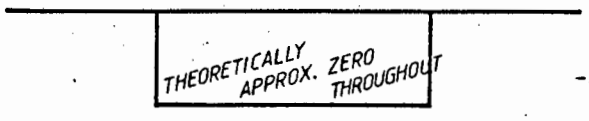

a) Longitudinal stresses at midspan

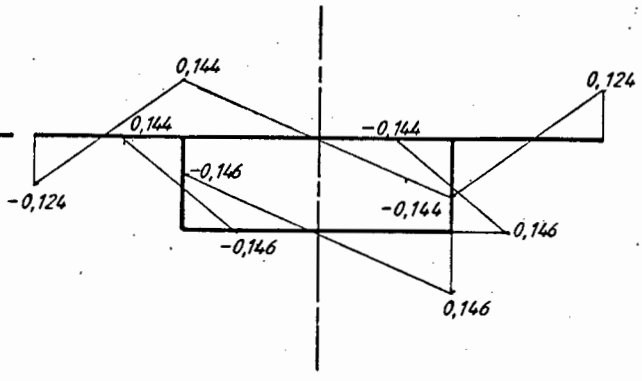

b) Longitudinal stresses at ¼ - span (z = 300 mm)

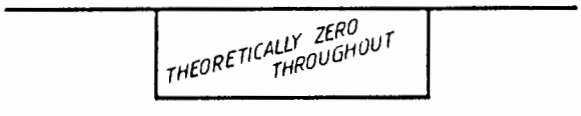

c) Transverse stresses at midspan

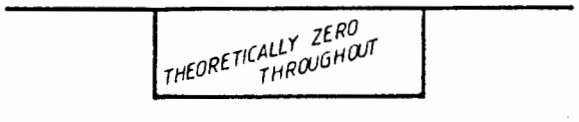

d) Transverse stresses at ¼ - span (z = 300 mm)

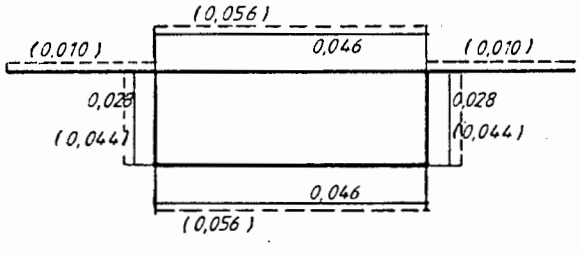

---- (Outer fibre stresses)

e) Shear stresses at midspan

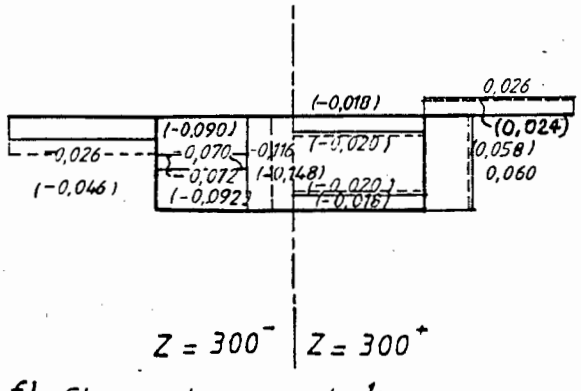

f) Shear stresses at ¼ - span (z = 300 mm)

FIGURE 4.17: Model 4 Loadcase 5
Combined stresses from analysis MPa

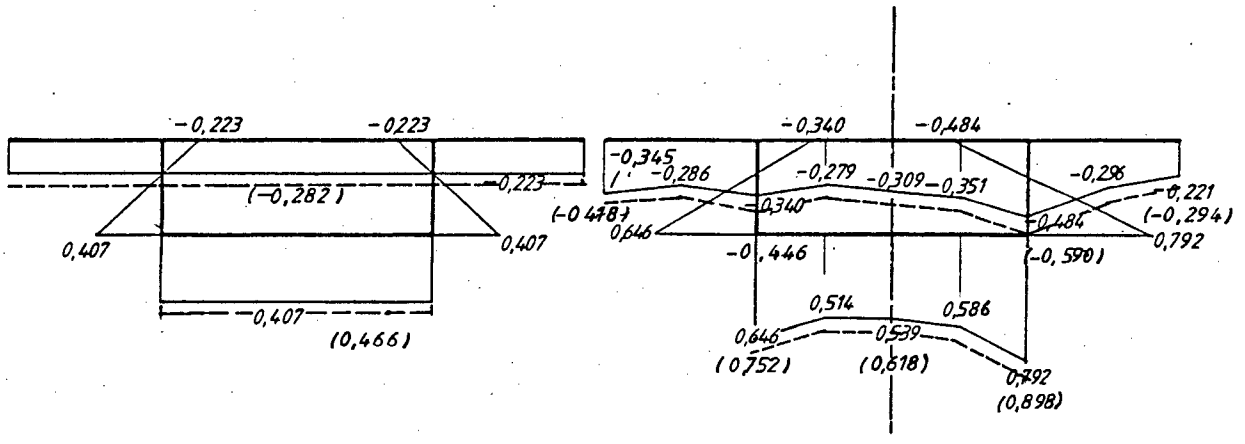

a) Longitudinal stresses at midspan

b) Longitudinal stresses at ¼ - span (z = 300 mm)

c) Transverse stresses at midspan

d) Transverse stresses at ¼ - span (z = 300 mm)

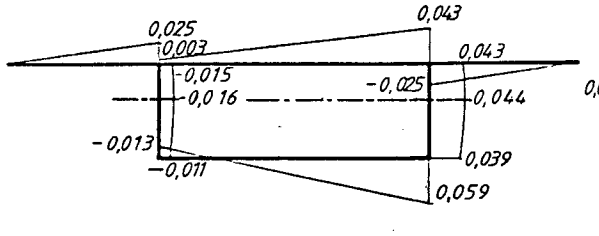

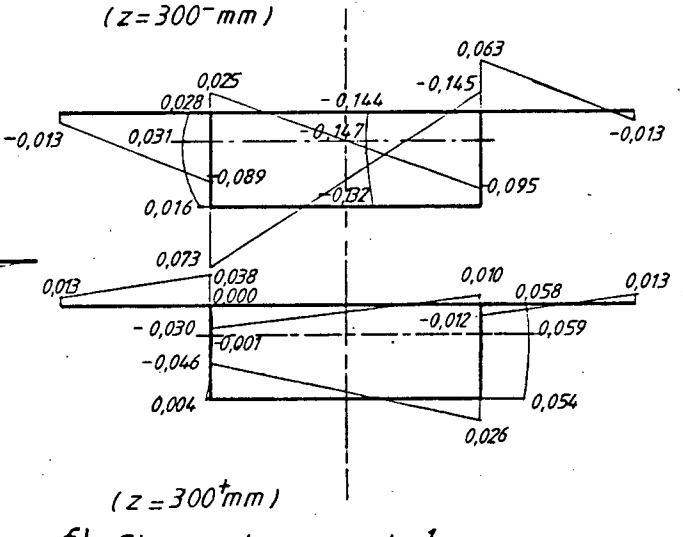

e) Shear stresses at midspan

f) Shear stresses at ¼ - span

--- Outer fibre stresses

FIGURE 4.18: Model 4 Loadcase 6
Combined stresses from analysis MPa

5 COMPARISON OF RESULTS AND DISCUSSION

5.1 GENERAL

The results from the model tests are used here to broadly assess the accuracy of the proposed method of analysis in finding the various internal stresses. The influence of the cross-sectional proportions and the distribution of stresses around cross-sections, as well as longitudinally along spans, are also investigated. Figures 5.1 to 5.8, 5.10 to 5.16 and 5.18 and 5.19 show the experimentally determined stresses superimposed onto the appropriate stress diagrams from Chapter 4 for the theory.

The correlation between actual stresses and those from the analyses are examined as far as possible in the context of the individual structural action types defined in the theory, namely: simple bending and shear lag in bending; torsional warping and St Venant torsion; and distortional warping and transverse bending. The following sections deal with different the action types and those loadcases which are relevant to each.

5.2 SIMPLE BENDING AND SHEAR LAG IN BENDING

Loadcases 1.1, 2.1, 3.1 and 4.1 are applicable to these aspects of the theory for Models 1 to 4 respectively, i.e having equal point loads applied to webs at midspan and thus with no torsion present.

Figures 5.1 to 5.4 show the various stress diagrams for experimental and theoretical values.

5.2.1 Longitudinal normal stresses

Midspan (z = 600)

Main points of note on the cross-sections are those on the flanges at the webs where peak stresses occur and on the centrelines of the flanges as well as on outer edges of the top flange where minimum stresses occur. Stresses found at the positions of the applied loads, i.e. top flanges over webs, are affected by local concentrated stress effects of the point loads and are therefore not reliable. Table 5.1 gives the ratio of stresses derived from the experiments to those from the theory for the outer fibres at various points.

MODEL.LOADCASE		1.1	2.1	3.1	4.1
Bottom Flange	left web	0.87	0.86	0.81	0.82
	right web	0.90	0.82	0.82	0.81
	centreline	1.07	1.01	0.98	0.97
Top Flange	right edge	1.03	1.02	0.95	0.93
	left edge	1.04	1.01	0.96	0.96
	centreline	1.07	1.00	0.97	0.96

Table 5.1 Ratio of experimental to theoretical longitudinal stresses at midspan using outer fibre stresses throughout.

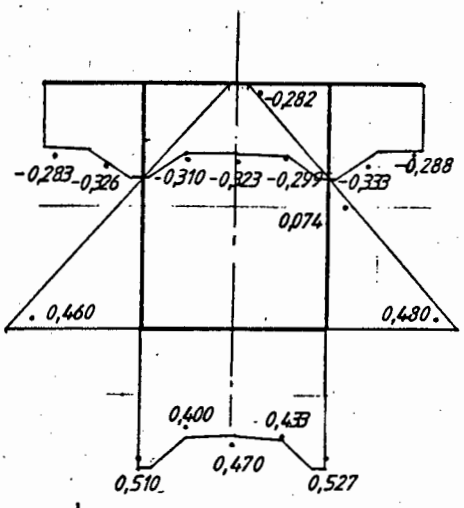

a) Longitudinal stresses at at midspan

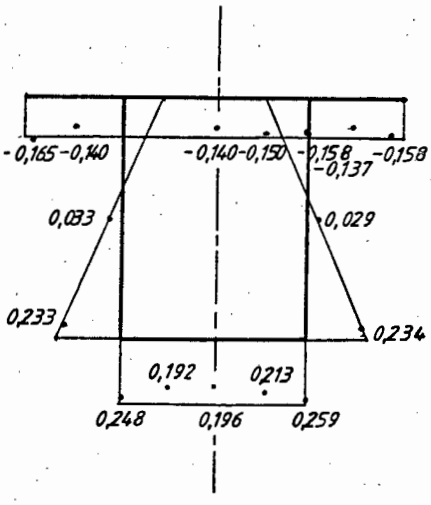

b) Longitudinal stresses at ¼ -span (z = 300 mm)

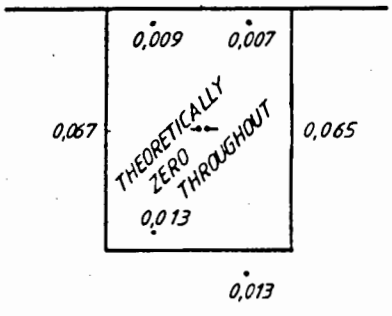

c) Transverse stresses at midspan

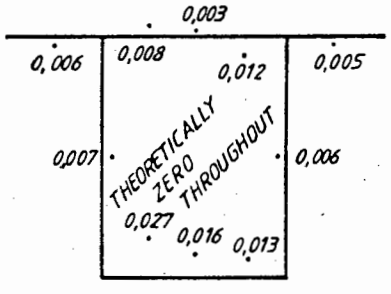

d) Transverse stresses at ¼ – span (z = 300 mm)

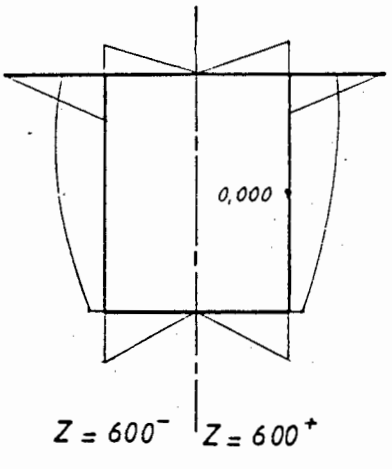

e) Shear stresses at midspan

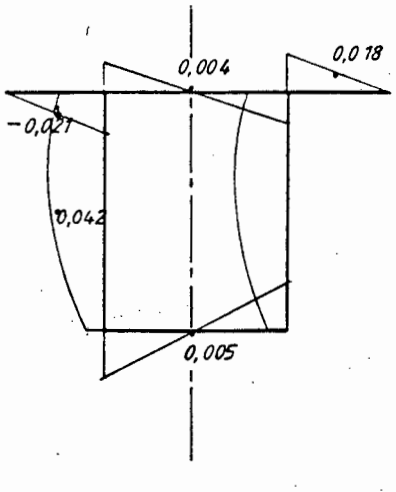

f) Shear stresses at ¼ -span (z = 300 mm)

FIGURE 5.1: Model 1 Loadcase 1B
Stress values from experiments MPa

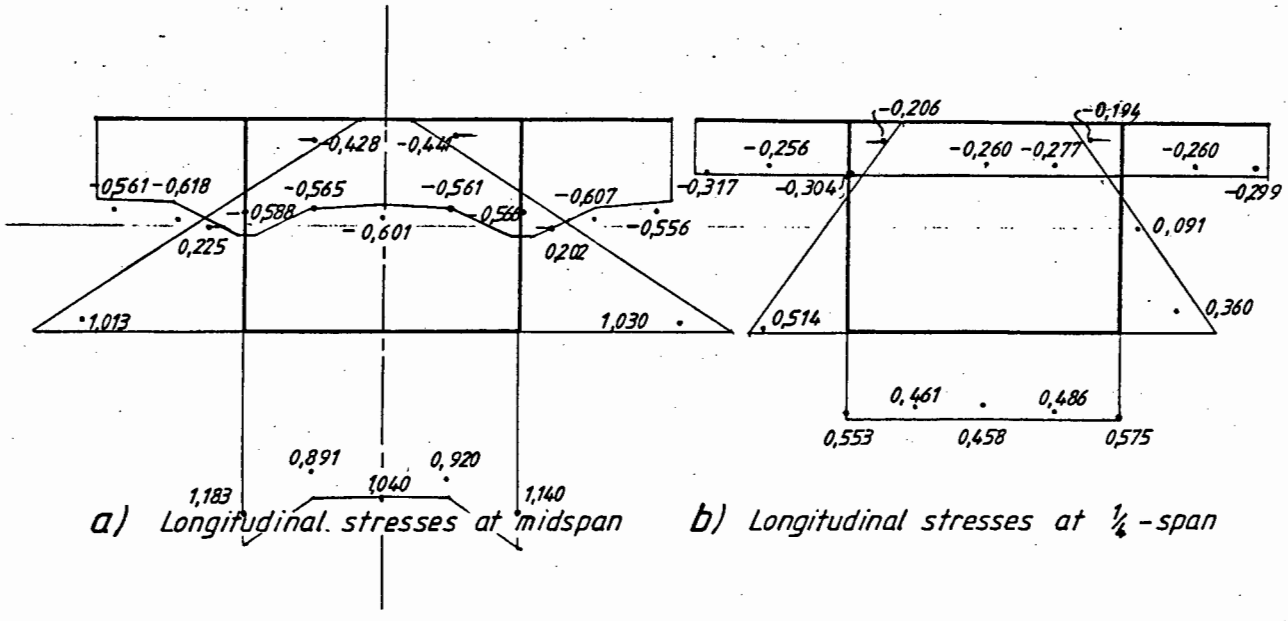

a) Longitudinal stresses at midspan

b) Longitudinal stresses at ¼-span

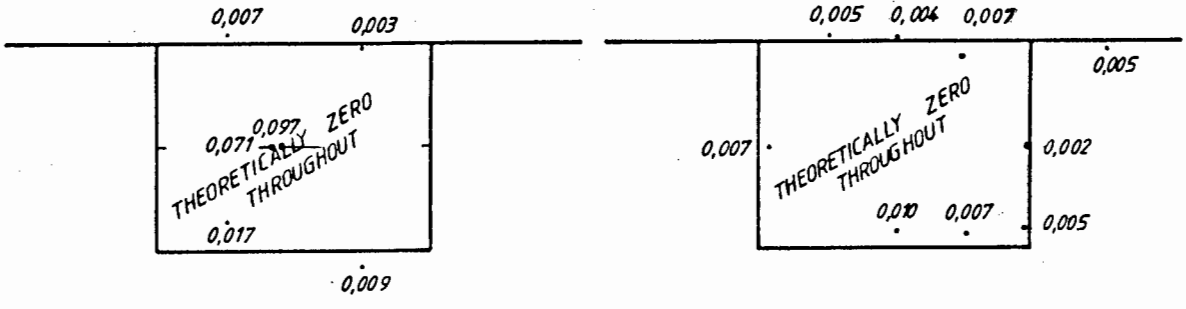

c) Transverse stresses at midspan

d) Transverse stresses at ¼-span (z = 300 mm)

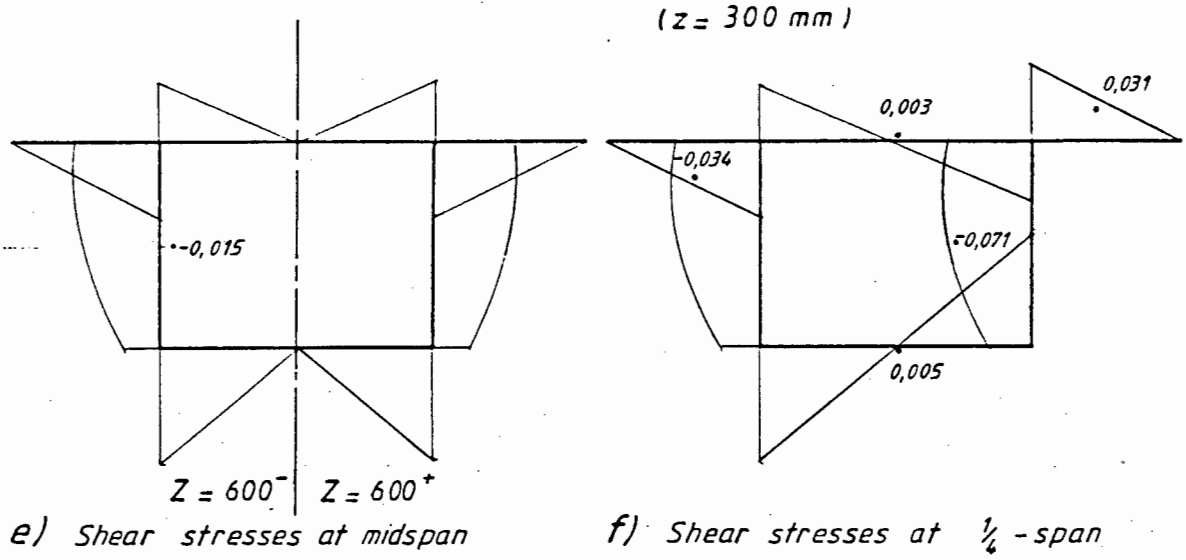

e) Shear stresses at midspan

f) Shear stresses at ¼-span

FIGURE 5.2: Model 2 Loadcase 1
Stress values from experiments MPa

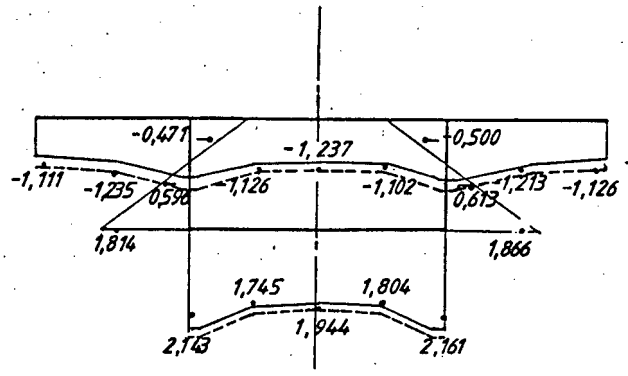

a) Longitudinal stresses at midspan

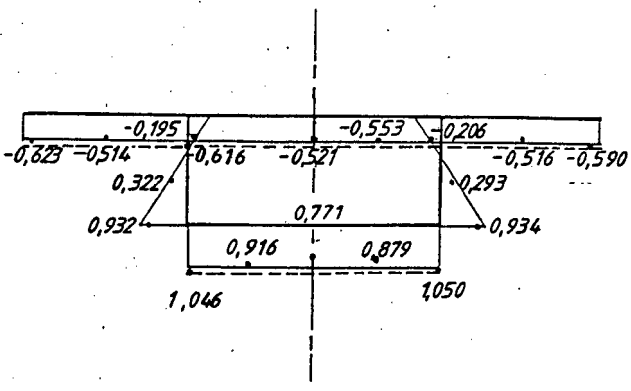

b) Longitudinal stresses at ¼ - span (z = 300 mm)

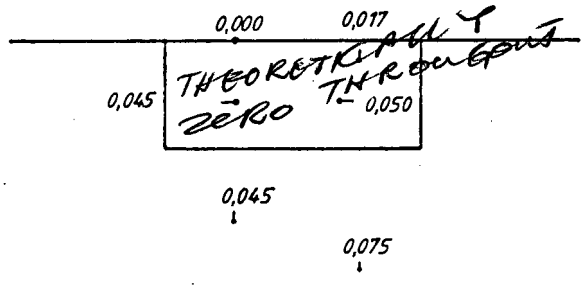

c) Transverse stresses at midspan

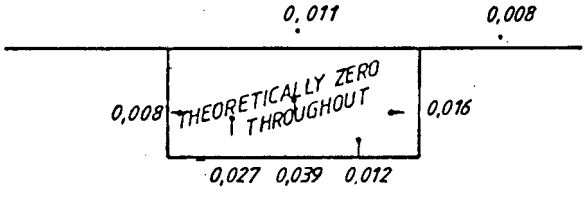

d) Transverse stresses at ¼ - span (z = 300 mm)

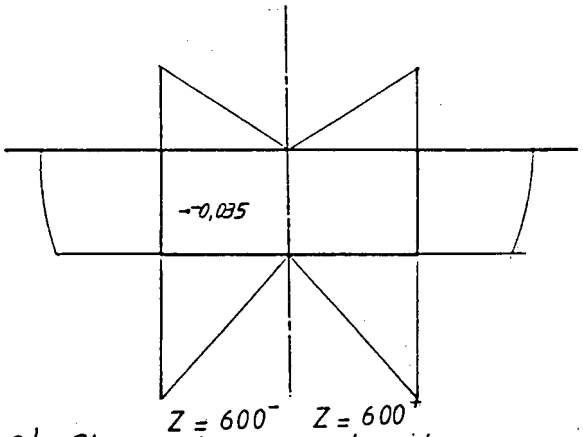

e) Shear stresses at midspan

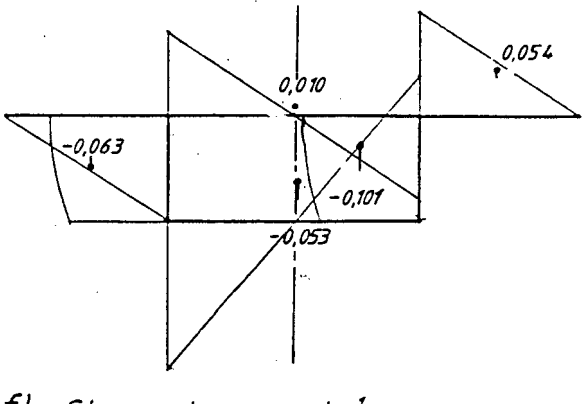

f) Shear stresses at ¼ - span (z = 300 mm)

-----Outer fibre stresses

FIGURE 5.3: Model 3 Loadcase 1
Stress values from experiments MPa

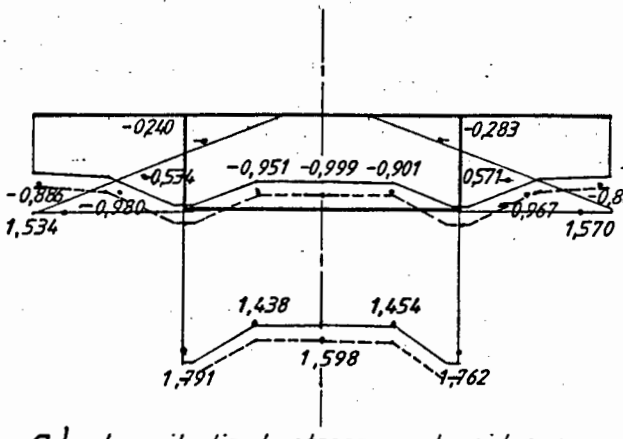

a) Longitudinal stresses at midspan

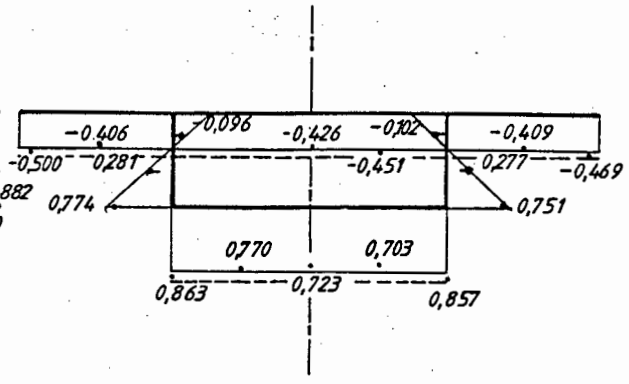

b) Longitudinal stresses at ¼ - span (z = 300 mm)

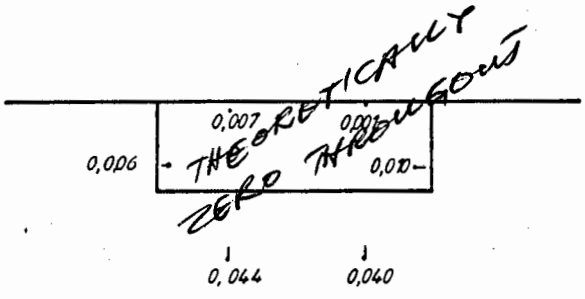

c) Transverse stresses at midspan

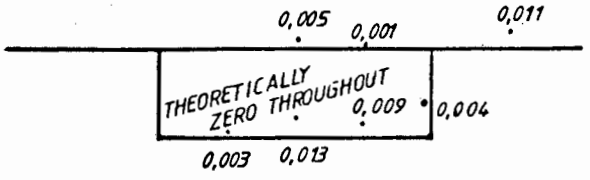

d) Transverse stresses at ¼ - span (z = 300 mm)

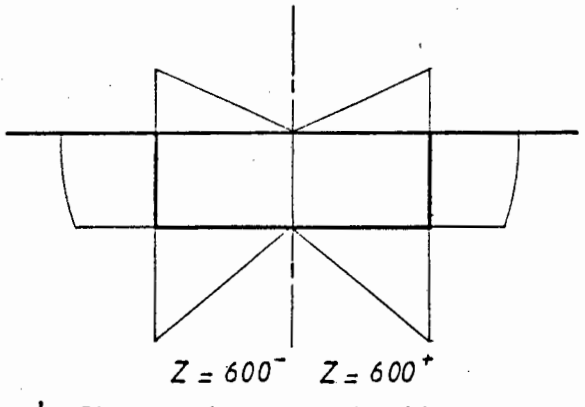

e) Shear stresses at midspan

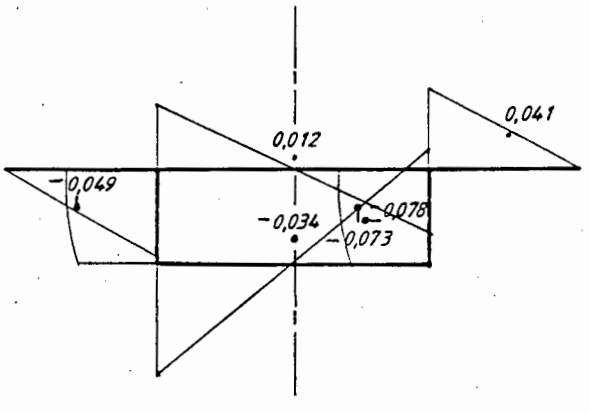

f) Shear stresses at ¼ - span (z = 300 mm)

---Outer fibre stresses

FIGURE 5.4. Model 4 Loadcase 1
Stress values from experiments MPa

From the longitudinal stress diagrams, it is apparent that the stresses found from the experiments are generally slightly lower than those predicted by the theory.

The ratios for loadcase 1.1 vary between 0.87 and 1.07 and decrease progressively through loadcases 2.1 and 3.1 to vary between 0.82 and 0.97 in the case of 4.1. The best correlation is for stresses on the centrelines of the flanges which lie between 1.07 and 0.97 for the bottom flange and lie between 1.07 and 0.96 for the top flange. Values on the edges of the top flange also agree well with these ratios being between 1.04 and 0.92. However, for the important peak stresses on the lower flange at webs, the theory overestimates the actual stresses by between 10 % and 23 %, i.e. from ratios of 0.91 and 0.81.

Anomalies occur in terms of the stresses measured on the top and bottom flanges between webs in that the values found at the centrelines are slightly higher than the values at the adjacent points, i.e. at the midpoints between centrelines and the webs. All the loadcases considered here reflect this trend.

Quarter-Span (z = 300)

The comparative diagrams show that as for the midspan section, the experimental stresses are consistently slightly lower than those predicted by theory. The distribution of stresses on the top flanges are fairly uniform whereas for the lower flanges there is a clear decrease in the measured stresses from webs to centreline. The above trends are present in all these loadcases. Table 5.2 gives the ratios for the experimental centreline stress values to average of the stresses at the webs, as well as the ratios for the average measured values to the theoretical outer fibre stresses for the bottom flange.

MODEL.LOADCASE	1.1	2.1	3.1	4.1
expt. cl./av. expt. @ webs	0.77	0.81	0.74	0.84
av. all expt./theory	0.82	0.81	0.82	0.84

Table 5.2 Ratios of longitudinal bottom flange stresses.

A convenient way to assess the average difference between theory and the actual stresses is to compare these values at a position where the readings are fairly uniform and no other influencing factors are apparent, such as for the top flange at the quarter-span section. Table 5.3 gives the ratios between average measured stress and the outer fibre stresses from the theory.

MODEL.LOADCASE	1.1	2.1	3.1	4.1
av. all expt./theory	0.87	0.82	0.81	0.79

Table 5.3 Ratios of longitudinal top flange stresses at quarter-span.

From this table, it is clear that the theory overestimates the stresses to a greater degree for the shallower sections. The average ratio for all loadcases given in the table is 0.82.

5.2.2 Transverse Stresses

For the symmetrical loading considered here, with point loads applied directly over webs, the theory gives the transverse stresses as zero for all sections.

Midspan (z = 600)

The experimental values show that small (i.e. if compared to the peak longitudinal bending stresses) transverse compressive stresses occur within webs below loading points for the deeper sections, i.e. loadcases 1.1 to 3.1 but that for the shallowest section (loadcase 4.1) these are negligible. Also apparent is the occurence of small tensile stresses within the lower flanges of the shallower sections, i.e. loadcases 3.1 and 4.1.

Quarter-span section.

Compressive stresses, again small if compared to the peak longitudinal bending stresses, occur within the lower flanges at these sections with those for loadcases 1.1 and 3.1 being the most prominent.

5.2.3 Shear stresses

Shear stresses measured at midspan sections are not relevant since these coincide with the step in the shear force diagram at the loaded section.

Quarter-span section

The measured shear stresses are generally slightly less than the values predicted by the theory and the difference is more marked in the case of the webs than the case of the flanges and decks. Table 5.4 gives the ratios of measured shear stresses to theoretical stresses for the webs as well as for the projecting top flanges.

MODEL.LOADCASE	1.1	2.1	3.1	4.1
expt. web/theory web	0.78	0.80	-	0.69
av. expt. cant./theory cant.	0.96	0.84	0.84	0.82

Table 5.4 **Ratios of measured and theoretical shear stresses for webs and cantilevers.**

5.2.4 Discussion

Longitudinally, the major trend is that the experimental values are consistently lower than those given by the theory throughout. This is illustrated in both Tables 5.1 and 5.3 which indicates the difference to be in the order of about 20%. This phenomenon can be attributed to a difference between the E-value used for converting the strain readings to stresses and the actual E-value. As was discussed in Chapter 2, Perspex is prone to considerable creep deformation and the extent of creep is dependant on the period for which the loading is applied as well as the magnitude of stress which affects the rate of creep. It was also explained in Chapter 2 that for the experimental strain readings, the creep component was largely eliminated by using the average of the readings taken at the start and at the end of a load cycle with the loads removed. The creep component is however not eliminated in the same way from the E-value determined by means of the tensile tests and this would result in reduced stress values. A rough assessment of the difference between the value used, i.e. 2918 MPa, and a value that largely excludes creep, is made by comparing the above to one obtained from the AECI brochure[9] for a faster rate of strain.

The tangent modulus for a high rate of 1 % per minute is 3357 MPa which is about 15 % higher than the one used for the models and is of the same order as the discrepencies experienced here.

The experiments show that shear lag does significantly affect the magnitude and distribution of the longitudinal bending stresses. For the lower flange at midspan, the ratio of the average longitudinal stresses at the webs to the stress at the centreline is 1.10 for loadcase 1.1 and 1.11 for each of 1.2, 1.3 and 1.4. Although the theory does not show shear lag effects occurring at the quarter-span section, there is a clear reduction in the longitudinal stresses in the lower flanges from the webs towards the centreline in all cases indicating that shear lag is present. These ratios are in the range from 1.35 to 1.19 which are even higher than the equivalent ratios at midspan. Also evident is the anomalous trend in the stress values on the flange and deck centrelines at midspan where these are higher than the adjacent stress values measured midway between the centrelines and the webs. This trend is not present at the quarter-span section. The influence of shear lag on the stresses within the top flanges is not as clear as in the case of the lower flanges and appears to be absent in the top flange at quarter-span altogether.

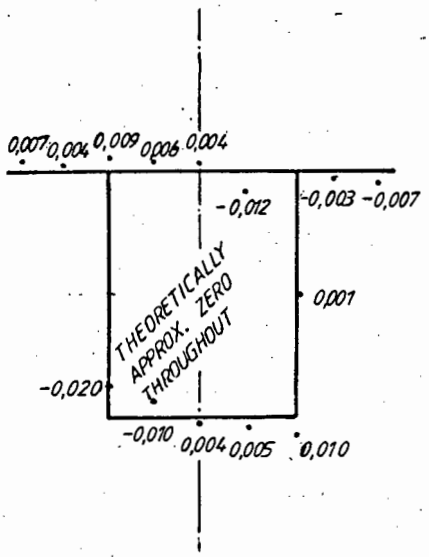

a) Longitudinal stresses at at midspan

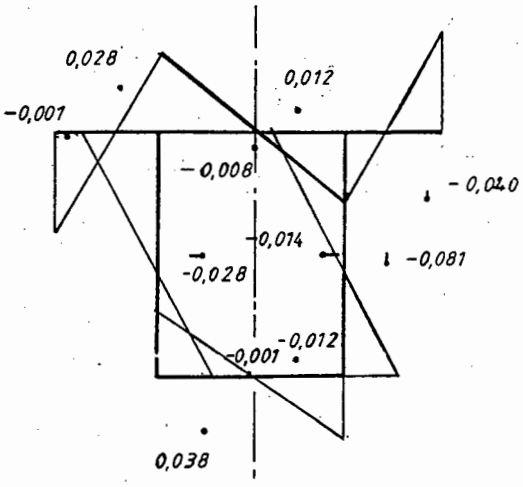

b) Longitudinal stresses at ¼ -span (z = 300 mm)

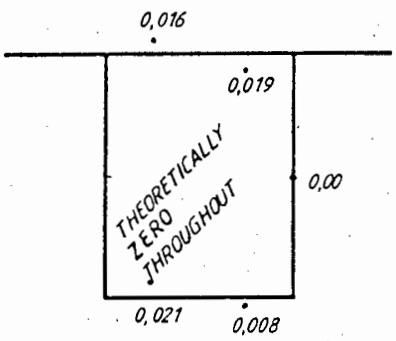

c) Transverse stresses at midspan

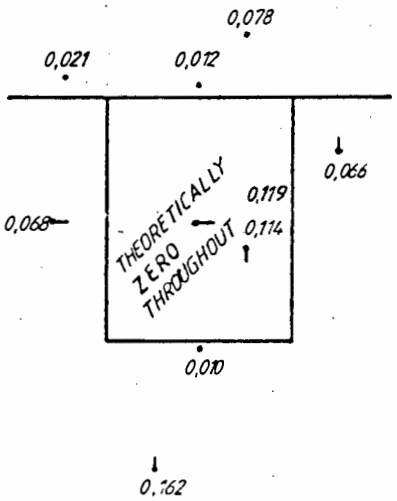

d) Transverse stresses at ¼ - span (z = 300 mm)

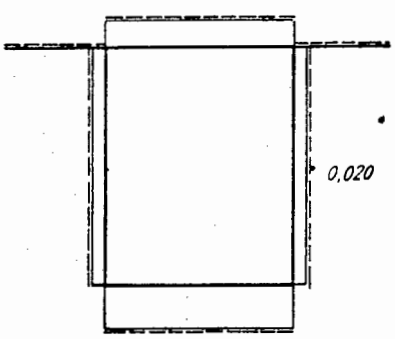

e) Shear stresses at midspan
---Outer fibre stresses

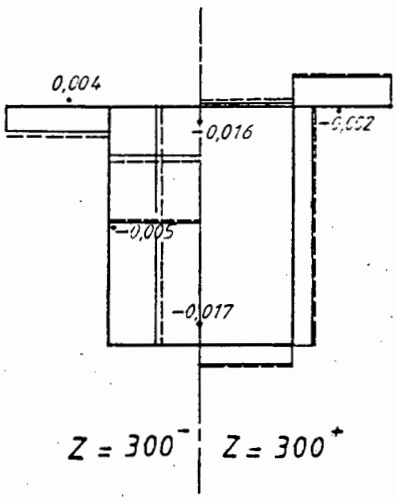

f) Shear stresses at ¼ - span (z = 300 mm)

FIGURE 5.5. Model 1 Loadcase 4
Stress values from experiments MPa

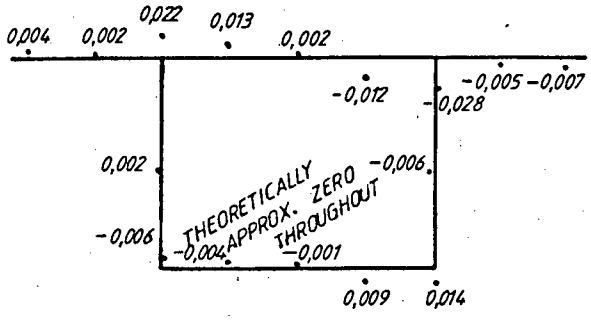

a) Longitudinal stresses at midspan

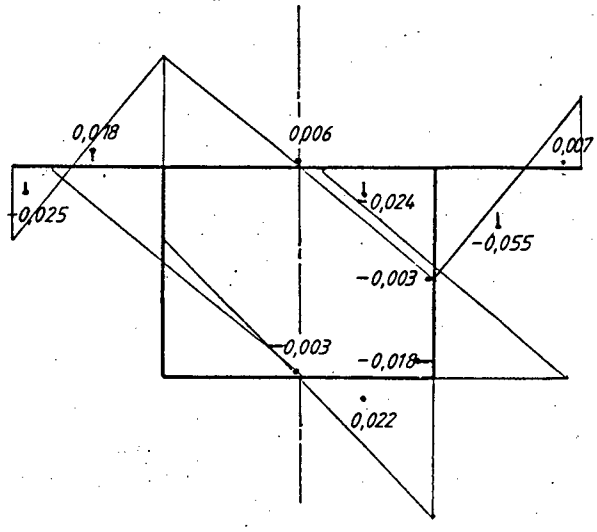

b) Longitudinal stresses at ¼-span

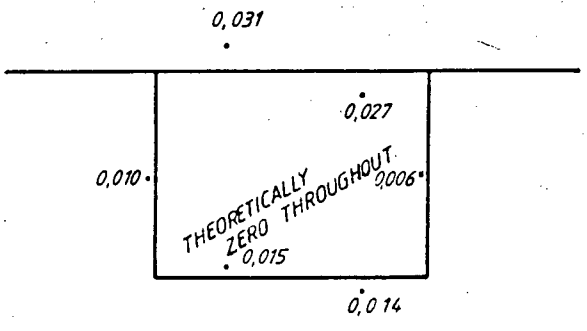

c) Transverse stresses at midspan

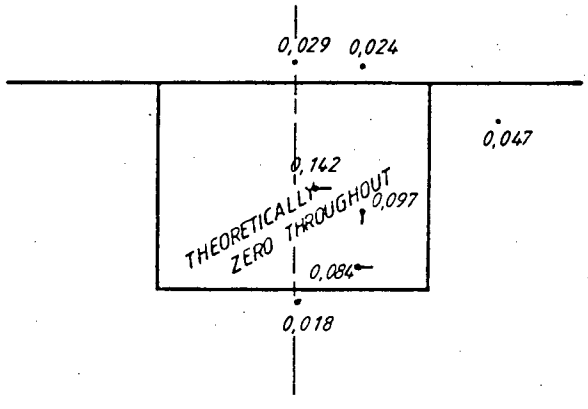

d) Transverse stresses at ¼-span
(z = 300 mm)

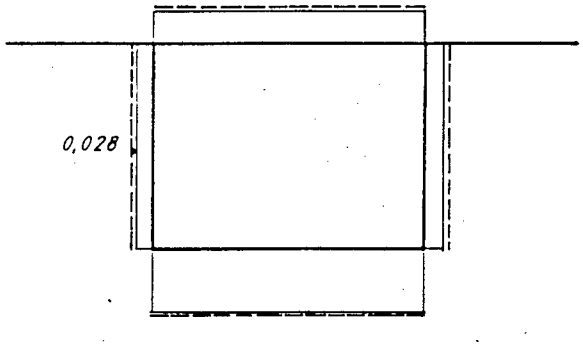

e) Shear stresses at midspan

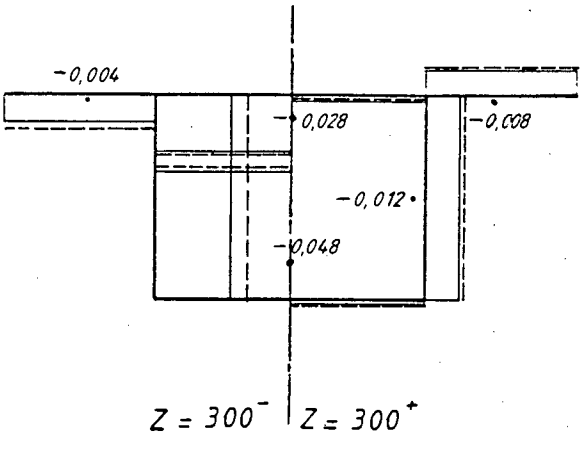

f) Shear stresses at ¼-span

------- Outer fibre stresses

FIGURE 5.6. Model 2 Loadcase 4
Stress values from experiments MPa

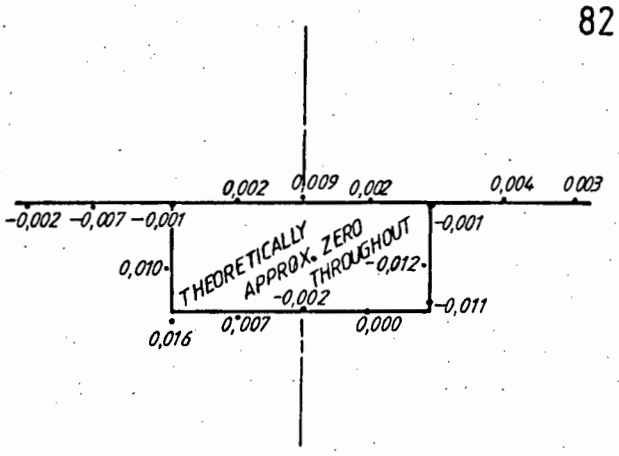

a) Longitudinal stresses at midspan

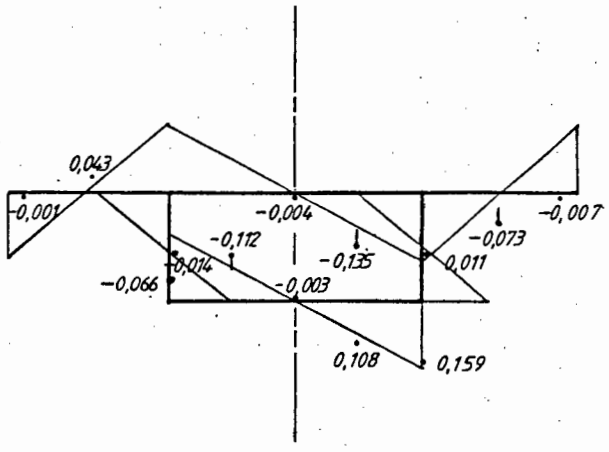

b) Longitudinal stresses at ¼ - span (z = 300 mm)

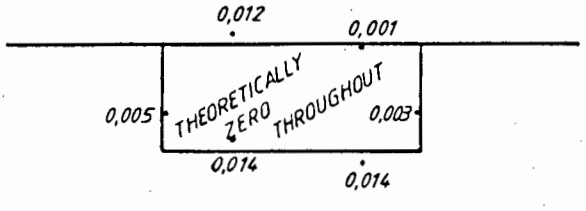

c) Transverse stresses at midspan

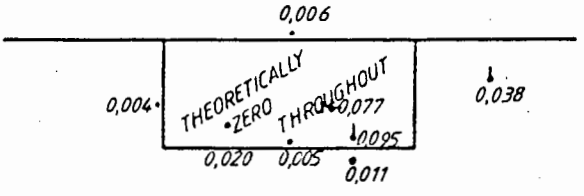

d) Transverse stresses at ¼ - span (z = 300 mm)

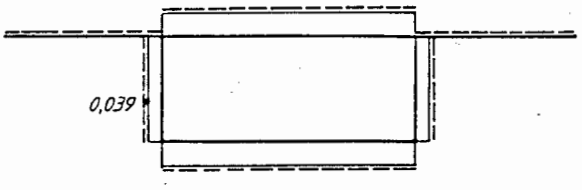

e) Shear stresses at midspan

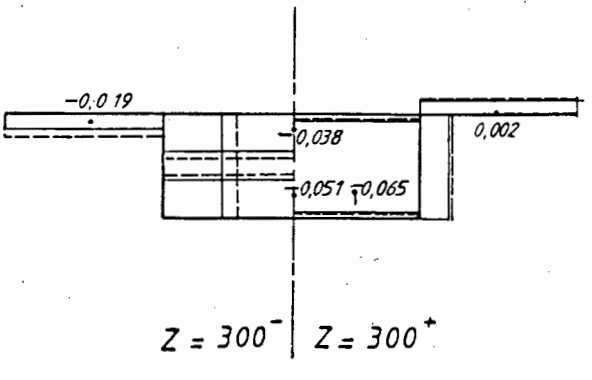

f) Shear stresses at ¼ - span (z = 300 mm)

----- Outer fibre stresses

FIGURE 5.7. Model 3 Loadcase 4
Stress values from experiments MPa

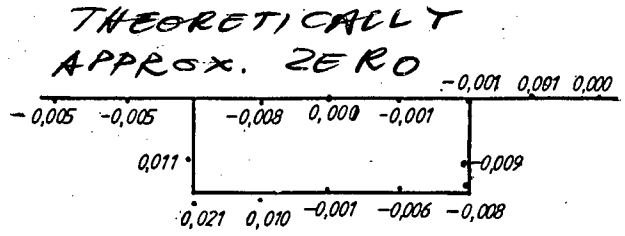

a) Longitudinal stresses at midspan

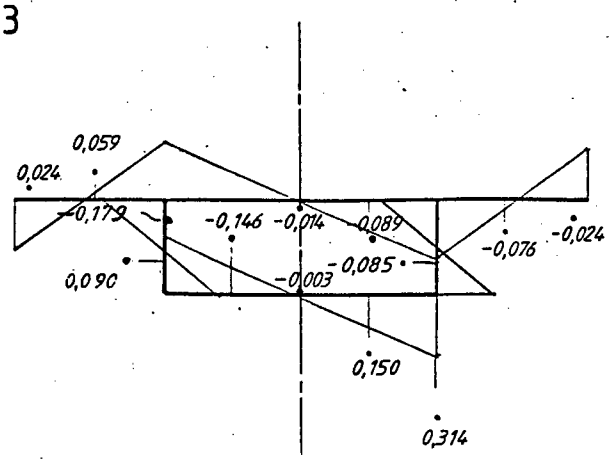

b) Longitudinal stresses at ¼ - span (z = 300 mm)

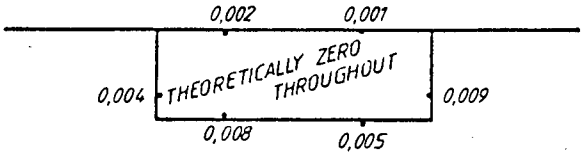

c) Transverse stresses at midspan

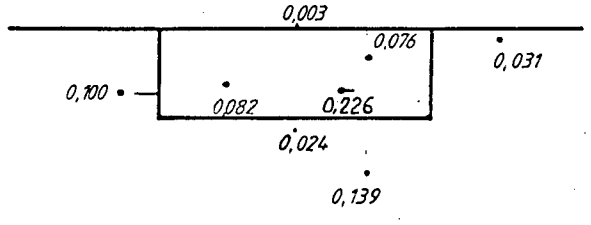

d) Transverse stresses at ¼ - span (z = 300 mm)

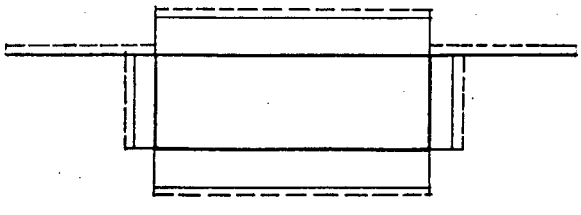

e) Shear stresses at midspan

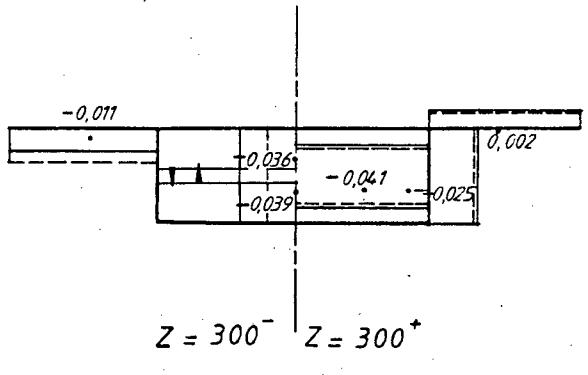

f) Shear stresses at ¼ - span (z = 300 mm)

------- Outer fibre stresses

FIGURE 5.8. Model 4 Loadcase 5
Stress values from experiments MPa

Figures 5.5, 5.6, 5.7 and 5.8 show the various stress diagrams for experimental and theoretical values.

5.3.1 Longitudinal stresses

Quarter-span section (z = 300)

Three broad trends are apparent. The first two are that for the same loading, the measured warping stresses increase with decreasing section depth and that the torsional warping stress pattern around the cross-sections become more discernable, also with decreasing section depth. For loadcase 1.4 the experimental stress values do not follow the predicted stress distribution at all, but in general the stresses are small and of the same order of magnitude as those from the theory. The best correlation between measured and calculated stresses is found with Loadcase 3.4 where the torsional warping pattern is clearly reflected by the measured values and the stress magnitudes are comparable. Table 5.5 gives the ratio of the extrapolated (from the average of the midpoint values since those at the webs are not reliable) experimental stresses to the theoretical stress values at the webs for both top and bottom flanges.

MODEL.LOADCASE	1.4	2.4	3.4	4.5
Top flg. av. expt./theory	-	0.52	1.51	1.14
Bot flg. av. expt./theory	-	0.36	1.33	2.01
av. ratio for top & bot. flanges	-	0.44	1.42	1.58

Table 5.5 Ratios of measured (extrapolated from centreline and flange midpoint values) and theoretical longitudinal stresses at the webs for top and bottom flanges.

The third trend is that the measured longitudinal stresses in the cantilever portions of the deck elements are about zero at the outer edges and appear to increase linearly to a peak value, either positive or negative, at the webs. This occurs for all four loadcases and is in contrast to the theory which gives stress values of approximately equal magnitude (slightly higher at the webs) but opposite signs at the edges and webs respectively. In all cases the rate of change of stress from edge of deck to webs follow the same sign. Table 5.6 gives the averaged ratios of the extrapolated (from cantilever midline) measured web stresses to the theoretical values.

MODEL.LOADCASE	1.4	2.4	3.4	4.5
av. expt./theory	1.95	0.86	0.64	0.77

Table 5.6 **Ratios of measured (extrapolated) and theoretical longitudinal stresses for the top flanges at the webs.**

Midspan (z = 600)

The longitudinal stresses measured at midspan are small throughout (compared to those at quarter-span) and as such agree well with the small stresses from the theory. Peak stresses were generally measured at the lower flanges on the line of the webs.

It is apparent that the lower flange stresses for all loadcases vary approximately linearly between webs with stresses of opposite signs at the respective webs. For loadcases 1.4 and 2.4 negative stress values occur at the webs under upward point loading and for 3.4 and 4.5 these stresses are positive.

5.3.2 Transverse stresses

As stated before, the transverse stresses at the quarter-span sections are affected by the axial forces within the struts forming the diaphragms and are therefore not reliable. This is reflected in the random nature of the measured values both with respect to distribution as well as magnitude.

Midspan (z = 600)

In all cases transverse stresses occur which follow a typical transverse bending pattern and if these are compared to the transverse bending stresses that occur at the loaded section with the diaphragms omitted (i.e. loadcases 1.3, 2.3 and 3.3), it can be seen that these negligibly small.

From these diagrams it is also evident that for loadcases 1.4 and 2.4 the presence of diaphragms at quarter-span cause a considerable reduction in the midspan transverse stresses but that in the case of loadcase 3.4 the difference is hardly noticable. Although the loading for loadcase 4.4 was not the same as for 4.5, it can be expected that transverse bending stresses at midspan would be more pronounced in the absence of a diaphragm at quarter-span but, as for 3.4, this appears not to affect the midspan stresses.

5.3.3 Shear stresses

Shear stresses measured at quarter-span sections are not reliable since these coincide with the step in the shear force diagram at the loaded section.

Midspan (z = 600)

The shear stresses were measured on the outside of the webs for loadcases 1.4, 2.4 and 3.4. These stresses are wholly St Venant shear stresses according to the theory and the correlation with the experimental readings are good as can be seen from Table 5.7.

MODEL.LOADCASE	1.4	2.4	3.4	4.5
experimental	0.020	0.028	0.039	-
theoretical	0.019	0.034	0.055	0.044

Table 5.7 **Measured and theoretical shear stresses at outside of webs. (MPa)**

5.3.4 Discussion

The aspect of the analysis examined by this series of model tests, i.e. torsional warping, is based on the theories of Vlasov which are applicable to thin walled box-girder members. Various criteria are given for the definition of thin walled members and the table below shows to which extent the different models meet these requirements.

MODEL.LOADCASE	1.4	2.4	3.4	4.5
Vlasov:				
h/b or h/d ($\leq$ 0.100)	0.082	0.104	0.212	0.300
b/l or d/l ($\leq$ 0.100)	0.127	0.097	0.097	0.097
Kollbrunner and Basler:				
A_{effect}/A_{enc} ($\leq$ 0.200)	0.239	0.281	0.481	0.552
A_{effect}/A_{enc} ($\leq$ 1.0)	0.239	0.281	0.481	0.352
$\delta v_{svt}/v_{svt}$ ($\leq$ 0.100)	0.244	0.352	0.478	0.568
$\delta T_{svt}/T_{svt}$ ($\leq$ 0.100)	0.008	0.012	0.024	0.031

Table 5.8 **Various criteria for thin-walled box-girder members applied to the models tested.**

It also follows that the observations made in the discussion relating to longitudinal bending and shear lag with respect to the applicable E-value and the shear modulus are also relevant here, i.e. that the actual E- and G-values are about 15 % higher than the values used for converting strains to stresses. This means that the measured stress values presented here should also be higher by the same margin.

The longitudinal stresses measured around the cross sections at the loaded sections do not follow pure torsional warping patterns and in the case of 1.4 no recognisable pattern at all. In all these loadcases small transverse stresses occur at midspan which are typical transverse bending stresses. This indicates that the diaphragms did not eliminate distortion of the cross-section entirely and that a small degree of distortional warping was present. The above observation is supported firstly by the anomalous stresses measured on the cantilevers at quarter-span which reflect the stress pattern that could be expected if distortional warping stresses are superimposed onto those for torsional warping, i.e. the stresses at the edge of the deck would for the two action types be subtractive and if the magnitudes are similar would be close to zero. See Figures 3.14 and 3.18.

The second phenomenon that supports the observation is that, although very small, the longitudinal stresses at midspan follow typical distortional warping patterns with those for the two shallower sections indicating a reversal in the sign of the stresses. According to the theory, and illustrated by Figures 3.15 and 3.19, the sign reversal only occurs with distortional warping and not for torsional warping .

The random nature of the warping stresses from loadcase 1.4 is likely as a result of the small stress values being overshadowed by local concentrated stress effects which for the other loadcases where larger warping stresses are generated, are not overriding.

It is difficult to make a good estimate of the portion of stresses at the loaded section which results from distortional warping. Using the proportion of the distortional warping stresses measured at midspan for 3.4 to the distortional warping stresses from the analysis for loadcase 3.3, a rough estimate can be made of the magnitude of the distortional warping stresses at quarter-span. Figure 5.9 gives the measured warping stresses together with the superimposed diagrams for the torsional and estimated distortional warping stresses.

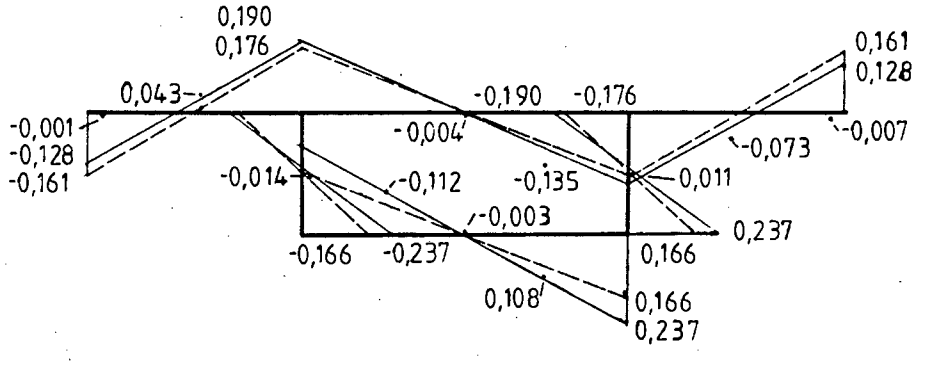

Figure 5.9 **Comparison of measured warping stresses at quarter-span to the theoretical stresses allowing for distortional warping (due to inefficiency of diaphragm). (MPa)**

From the above it is apparent that the addition of the estimated distortional warping stresses generally improves the correlation of the theory with the experimental readings. Also, it must be added that this procedure is not very reliable since the accuracy of such an adjustment is highly dependant on the location of the point along the span where the distortional warping stresses cross over from positive to negative and which occurs at approximately midspan in the case of the loading being applied at quarter-span. The above excercise was not repeated for the other loadcases in this series.

The main conclusions are as follows:

The torsional warping analysis, given that the E-value used for converting strain to stresses was about 15 % too low, generally slightly under-estimates the actual stresses.

The under estimation of torsional warping stresses by the torsional warping theory is not a serious source of error in terms of the total warping stresses seeing that these are mostly less than a quarter of the total warping stresses according to the parameter study[7] for a 30 m span under purely live loading and are also highly localised longitudinally.

The torsional warping theory gives best results for the shallower sections, as shown by loadcases 3.4 and 4.5.

The trend in the experimental results that the torsional warping stresses increase with a decrease in section depth for the same loading is confirmed in the parameter study[7].

The fact that the torsional warping theory was developed for thin walled sections and that all the models tested are thick-walled in terms of the Vlasov criteria, is the most likely source of the differences between theory and the measured stresses, together with the diaphragms not fully preventing distortion of the cross-sections.

5.4 COMBINED TORSIONAL AND DISTORTIONAL WARPING AND TRANSVERSE BENDING

Two loading formats are used to examine these aspects of the theory and are illustrated in Figure 4.1. The first comprises equal point loads, one acting vertically upwards and the other vertically downwards, applied to the top of the deck on the centrelines of the respective webs at midspan (z = 600). The relevant loadcases are 1.2, 2.2, 3.2 and 4.2.

The second format is like the first with the exception that the loads are applied at the quarter-span section (z = 300) and are represented by loadcases 1.3, 2.3, and 3.3. All these loadcases are purely torsional with no longitudinal bending present.

As was the case with the loadcases discussed previously, stress concentrations arise in the immediate vicinity of the loading points so that readings at or near these positions may be affected.

Figures 5.10, 5.11, 5.12 and 5.13 show the various stress diagrams from both the theory and the experiments for loadcases 1.2, 2.2, 3.2 and 4.2 and Figures 5.14, 5.15 and 5.16 the diagrams for loadcases 1.3, 2.3 and 3.3.

5.4.1 Longitudinal stresses

5.4.1.1 Loading at midspan (1.2, 2.2, 3.2 and 4.2)

Midspan (z = 600)

A number if trends manifest themselves throughout these loadcases.

Firstly, the theory and experimental values agree very well at the edges and midpoints of the cantilevers for all loadcases with most experimental values tending to be fractionally smaller than the theory.

Secondly, at the midpoints between centreline and webs on the deck, the experimental readings are considerably higher than the values from the theory, being on average about twice as high. The biggest differences occur with loadcases 1.2 and 2.2.

Another trend is noticeable with regard to the lower flange stresses. For loadcases 1.2 and 2.2 the experimental values are considerably higher than those given by the theory but for 3.2 and 4.2 the differences are negligible. Furthermore, whereas the theory predicts a linear variation in the lower flange stresses between webs, the measured stresses have a distinct non-linear tendency in all cases, with increased peak stresses at the webs.

In overall terms, almost complete agreement between theory and the experiments is obtained for loadcases 3.2 and 4.2; and for 1.2 and 2.2 the theory underestimates the actual stresses, especially at the midpoints between the girder centreline and webs on the top flanges and at the webs on the bottom flanges.

Finally, for the same applied loading, the measured longitudinal stresses show a clear increase with the decrease in the section depth from 1.2 to 4.2 as does the theory. A useful reference point for this observation is the peak stress values at the web centreline on the lower flange. Adjusting these on a pro rata basis to allow for different magnitudes of loading, the measured stresses (theoretical values in brackets) are, arranged from deep to shallow: 0.496(0.312); 0.712(0.564); 1.064(0.966) and 1.590(1.574) MPa for loadcases 1.2 to 4.2.

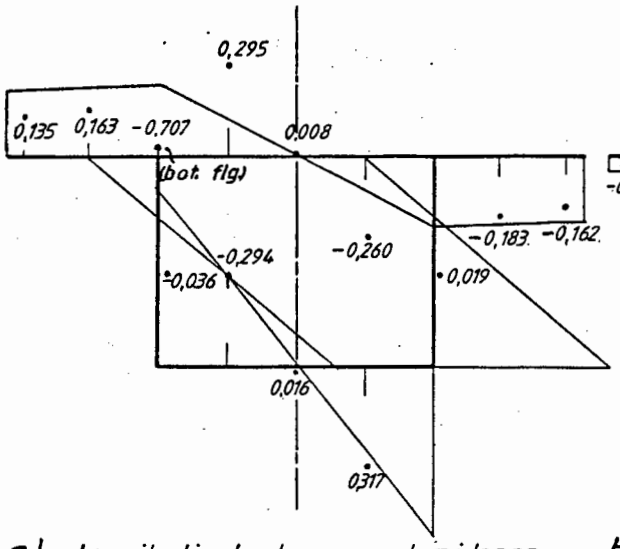

a) Longitudinal stresses at midspan

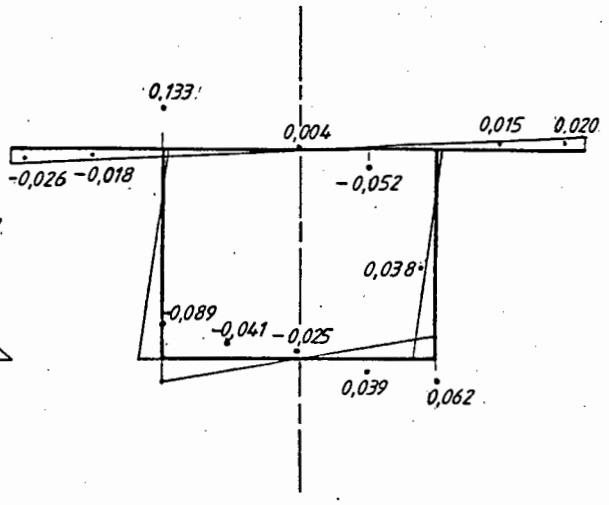

b) Longitudinal stresses at ¼ - span

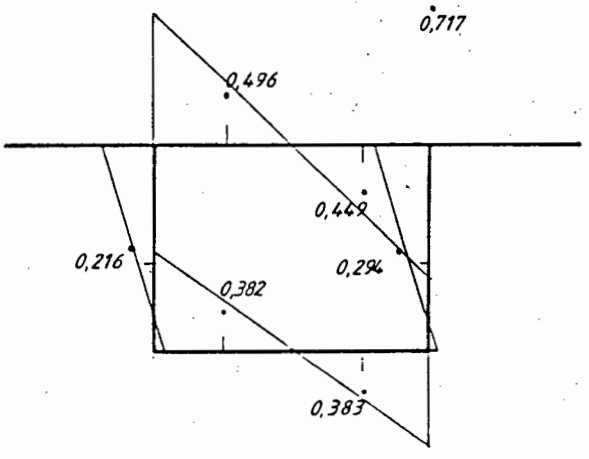

c) Transverse stresses at midspan

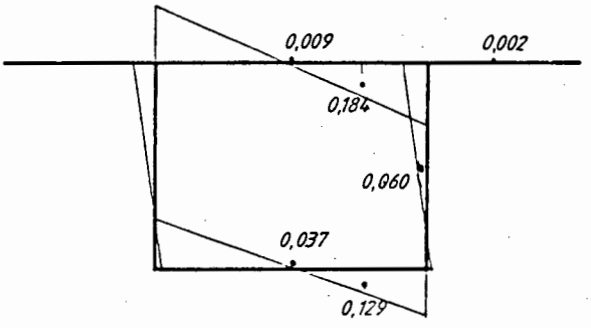

d) Transverse stresses at ¼ - span (z = 300 mm)

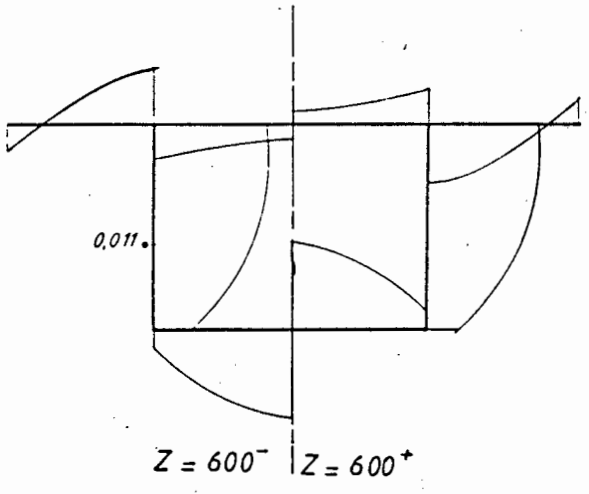

e) Shear stresses at midspan

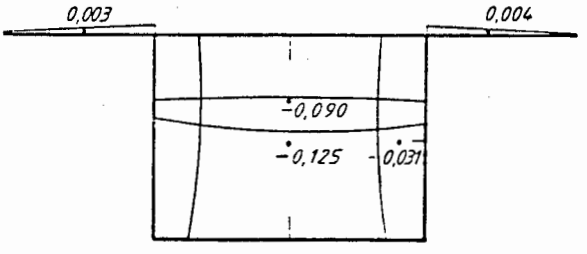

f) Shear stresses at ¼ - span

FIGURE 5.11. Model 2 Loadcase 2
Stress values from experiments MPa

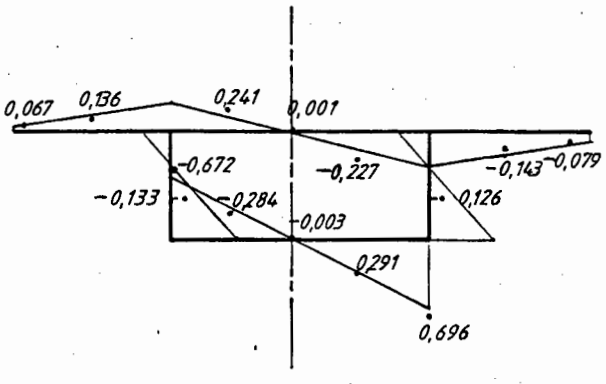

a) Longitudinal stresses at midspan

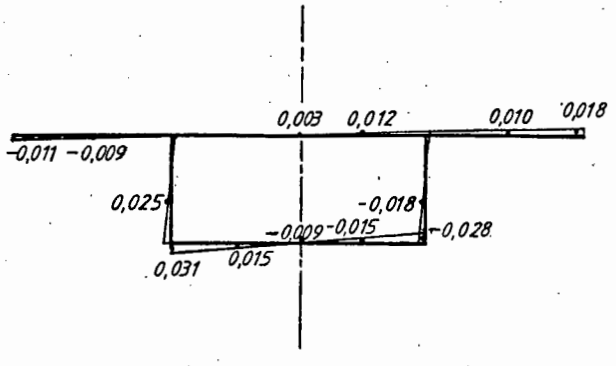

b) Longitudinal stresses at $\frac{1}{4}$ - span ($z = 300\,mm$)

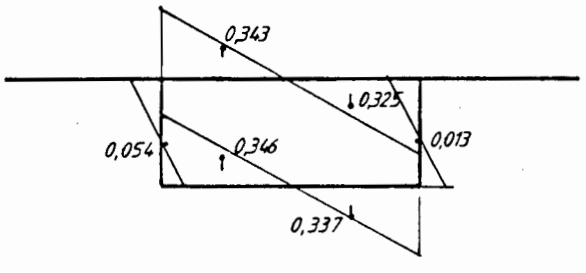

c) Transverse stresses at midspan

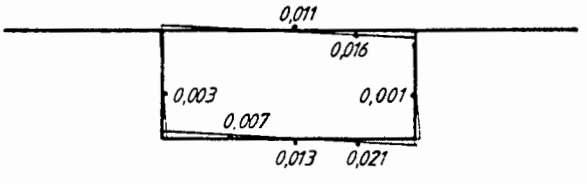

d) Transverse stresses at $\frac{1}{4}$ - span ($z = 300\,mm$)

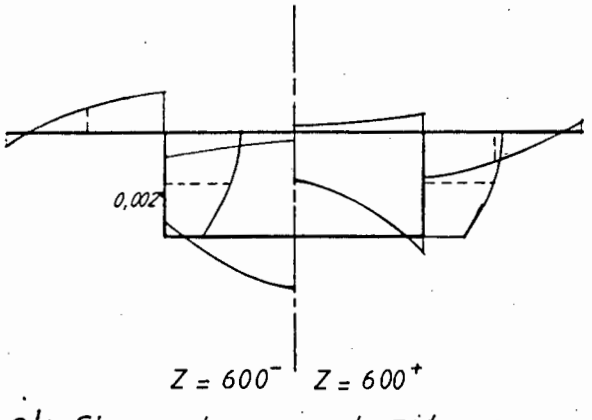

e) Shear stresses at midspan

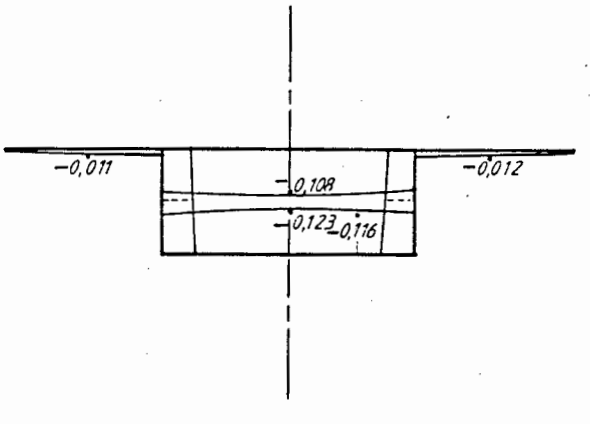

f) Shear stresses at $\frac{1}{4}$ - span ($z = 300\,mm$)

FIGURE 5.12. Model 3 Loadcase 2
Stress values from experiments MPa

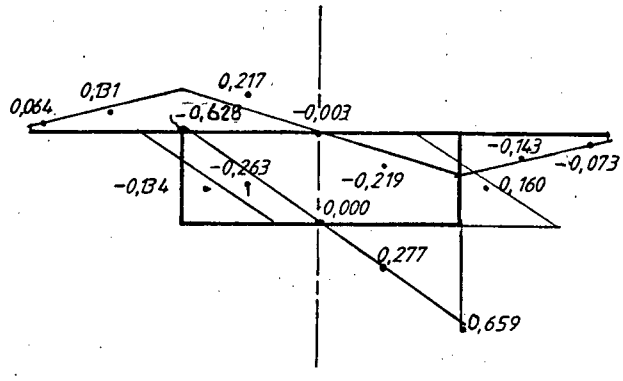

a) Longitudinal stresses at midspan

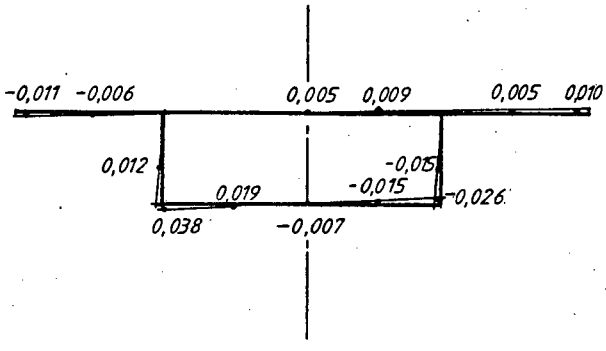

b) Longitudinal stresses at ¼ - span (z = 300 mm)

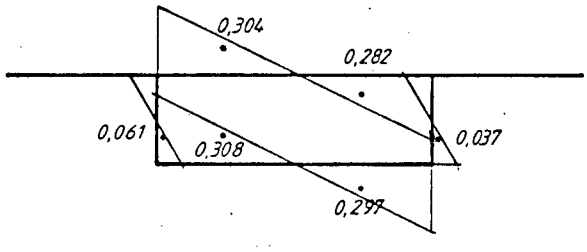

c) Transverse stresses at midspan

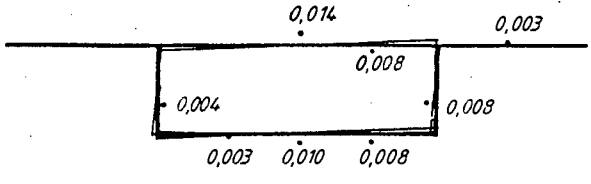

d) Transverse stresses at ¼ - span (z = 300 mm)

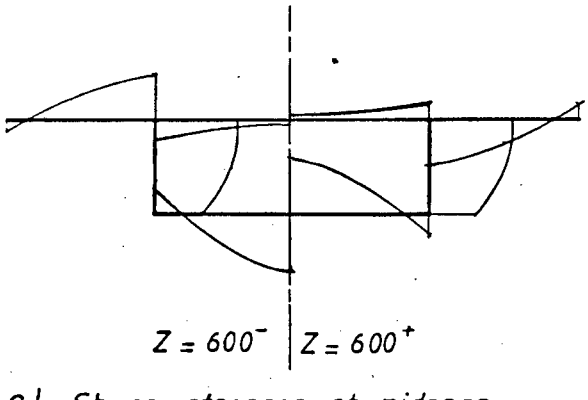

e) Shear stresses at midspan

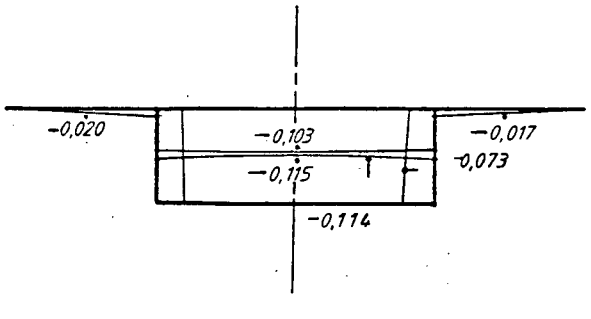

f) Shear stresses at ¼ - span (z = 300 mm)

FIGURE 5.13. Model 4 Loadcase 2
Stress values from experiment MPa

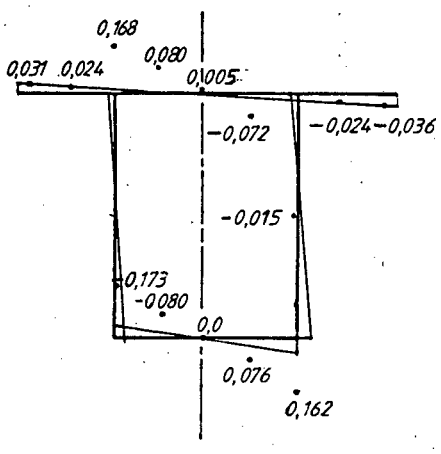

a) Longitudinal stresses at at midspan

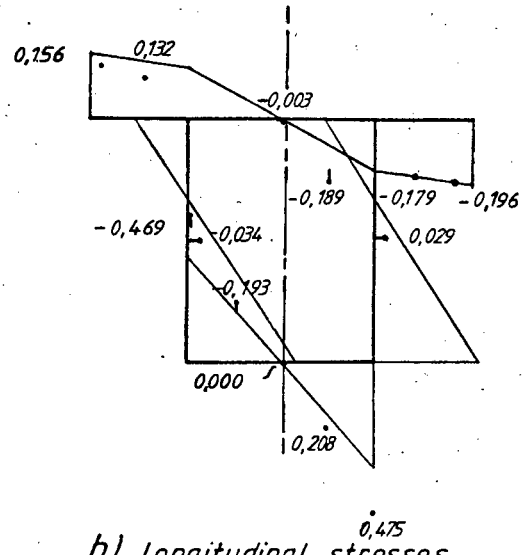

b) Longitudinal stresses at 1/4 -span (z = 300 mm)

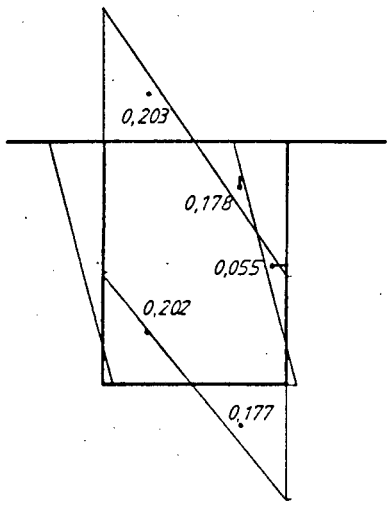

c) Transverse stresses at midspan

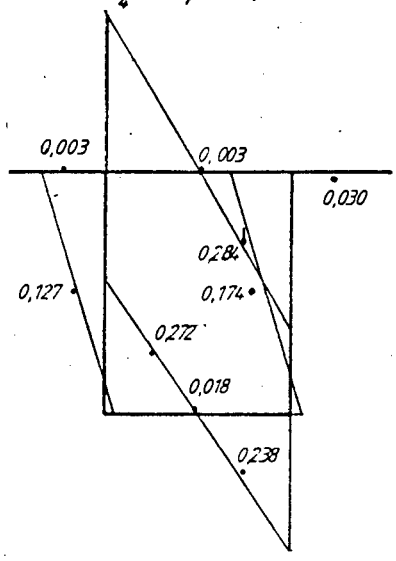

d) Transverse stresses at 1/4 - span (z = 300 mm)

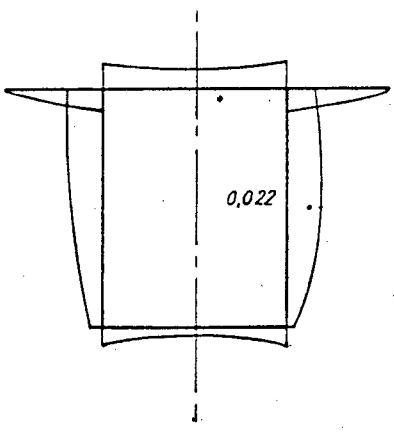

e) Shear stresses at midspan

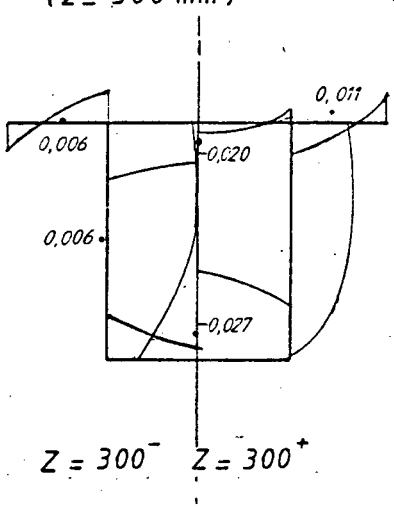

f) Shear stresses at 1/4 - span (z = 300 mm)

FIGURE 5.14. Model 1 Loadcase 3
Stress values from experiments MPa

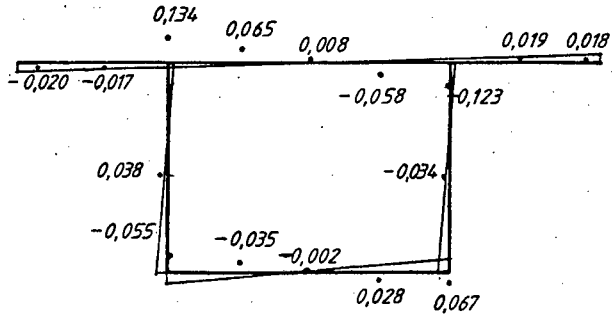

a) Longitudinal stresses at midspan

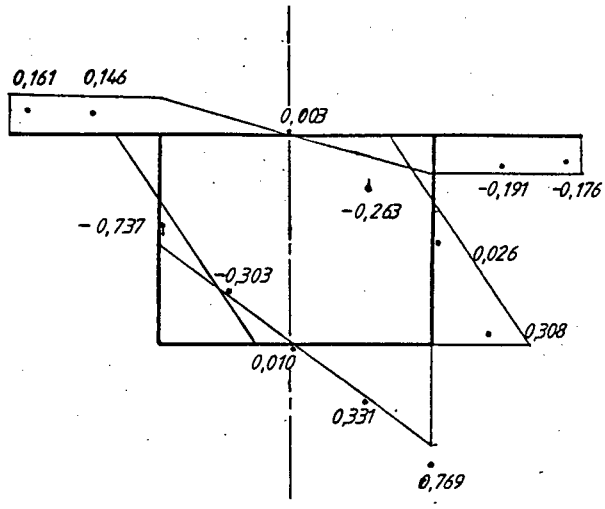

b) Longitudinal stresses at ¼ - span

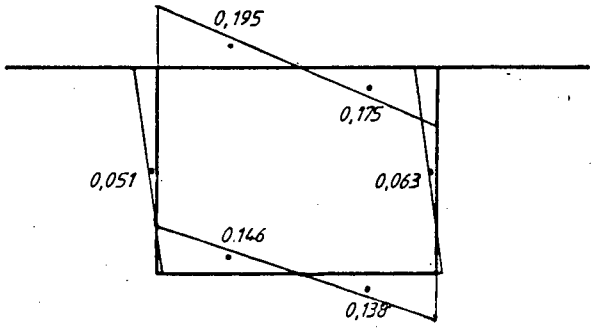

c) Transverse stresses at midspan

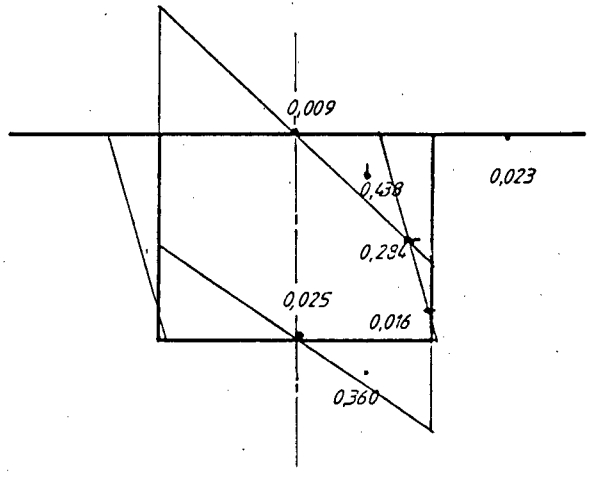

d) Transverse stresses at ¼ - span (z = 300 mm)

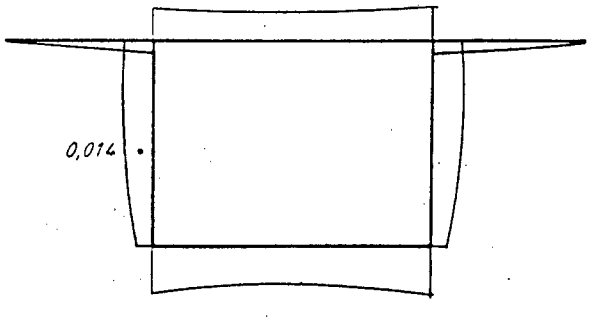

e) Shear stresses at midspan

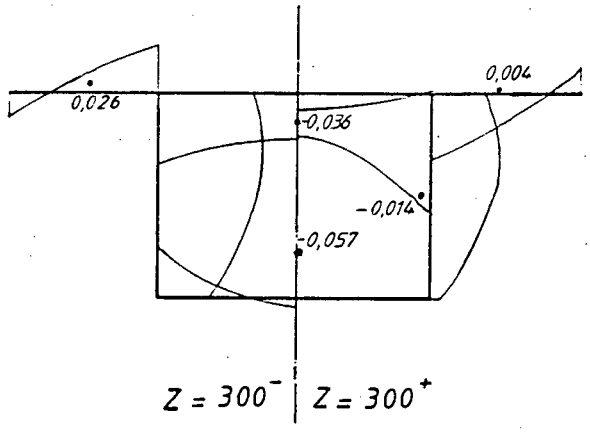

f) Shear stresses at ¼ - span

FIGURE 5.15. Model 2 Loadcase 3
Stress values from experiments MPa

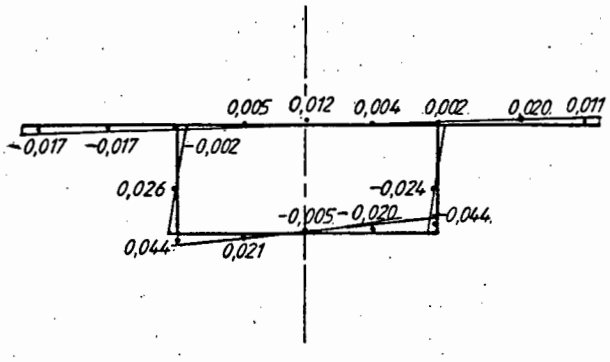

a) Longitudinal stresses at midspan

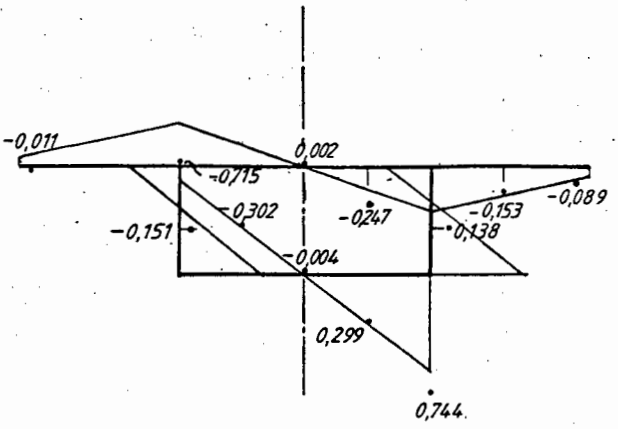

b) Longitudinal stresses at ¼ - span (z = 300 mm)

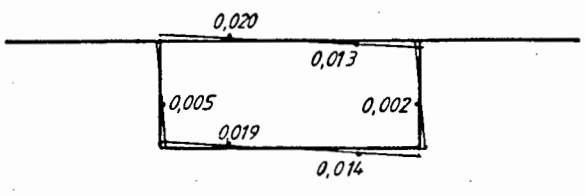

c) Transverse stresses at midspan

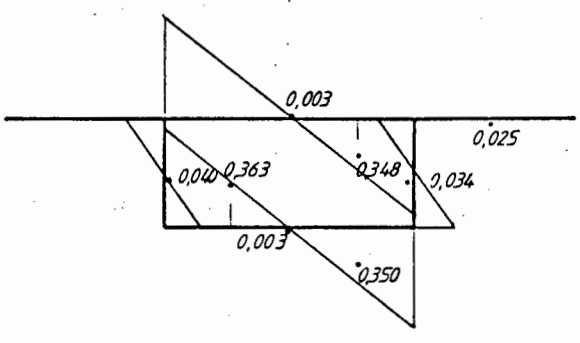

d) Transverse stresses at ¼ - span (z = 300 mm)

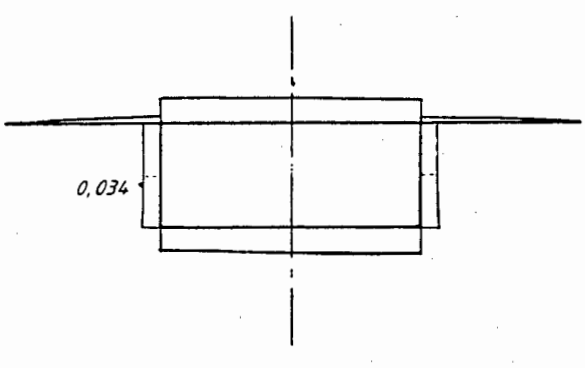

e) Shear stresses at midspan

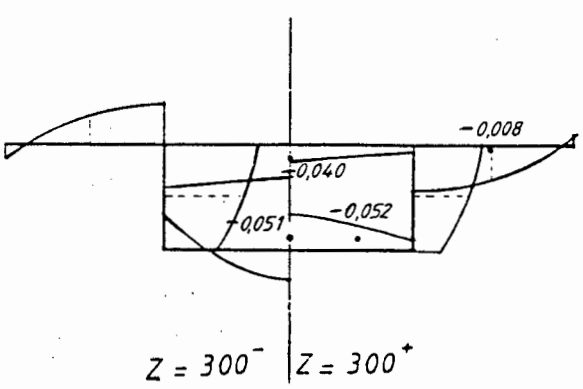

f) Shear stresses at ¼ - span (z = 300 mm)

FIGURE 5.16. Model 3 Loadcase 3
Stress values from experiments MPa

Table 5.9 gives the ratios of the measured longitudinal stresses to stresses from the theory for various points around the cross-section. Note that since the diagrams for longitudinal stresses are anti-symmetrical about the girder centreline, a single average ratio can be determined for equivalent points.

MODEL.LOADCASE		1.2	2.2	3.2	4.2
Top Flange	edges cants.	0.89	0.72	1.18	1.63
	midpts. cants.	0.99	0.81	0.85	0.89
	midpts. webs/cl.	2.68	2.50	1.75	1.63
Bot Flange	midpts. webs/cl.	1.39	1.08	0.93	0.87
	webs	1.59	1.26	1.10	1.01

Table 5.9 **Ratios of experimental to theoretical longitudinal stresses for various points on the midspan cross-section.**

Quarter-span (z = 300)

Both the measured and calculated stresses at these sections are substantially smaller than those at midspan and therefore follow a similar trend. Also, for loadcases 2.2, 3.2 and 4.2 the theory indicates a reversal of sign for the stresses from those at midspan which is also the case with the experimental readings from 3.2 and 4.2, but not 2.2. The readings for 1.2 have the same sign as for midspan as do the calculated values.

Best correlation is found with loadcase 4.2 where the stresses agree closely with respect to distribution and magnitude - the experimental values are marginally less. Loadcase 3.2 also shows good agreement as far as distribution around the cross-section is concerned but the experimental values are approximately only half those from the theory.

5.4.1.2 Loading at quarter-span (1.3, 2.3, and 3.3)

Quarter-span (z = 300 mm)

The overall trends are the following:

For the top flange, the tendency for the measured stresses in the cantilever portions is to follow the same pattern as that given by the analysis but only slightly smaller. In all three loadcases an anomalous reading occurs at the midpoint between the centreline and the lefthand web which is considerably higher than the theoretical stress.

At the lower flanges a good correlation is found at the centreline and midpoint values throughout. However, in all cases the stresses at the webs are markedly higher than those given by the theory.

For the same applied loading, the measured longitudinal stresses show a clear increase with the decrease in the section depth from 1.3 to 3.3 as does the theory. Using the peak stress values at the web centreline on the lower flange as a reference point, and adjusting these on a pro rata basis to allow for different magnitudes of loading, the measured stresses (theoretical values in brackets) are, arranged from deep to shallow, 0.472(0.339), 0.753(0.635) and 1.135(0.977) MPa for 1.3 to 3.3.

Table 5.10 gives the ratios of measured to calculated longitudinal stresses for the main points around the cross-section. As for Table 5.9 a single average stress ratio can be determined for points symmetrical about the girder centreline.

MODEL.LOADCASE		1.3	2.3	3.3
Top Flange	~~egdes~~ edges cantilevers	0.88	0.68	0.60
	midpts. cantilevers	0.86	0.67	0.92
	midpts. webs/cantilevers	2.33	2.17	1.84
Bot. Flange	midpts. webs/cantilevers	1.18	1.00	0.96
	webs	1.39	1.19	1.16

Table 5.10 **Ratios of experimental to theoretical longitudinal stresses for various points on the loaded quarter-span cross-section.**

Midspan (z = 600 mm)

The stress measurements and theory at midspan both show a large decrease from those at the loaded quarter-span sections for all loadcases. With regard to signs, the theory shows a reversal for loadcases 2.3 and 3.3 from those at quarter-span but the experimental values only shows this for loadcase 3.3. For loadcase 2.3 the stresses on the cantilever portions of the deck follow the sign reversal indicated by the theory whereas the stresses between webs on both top and bottom flanges do not.

The best agreement is found at loadcase 3.3 where the measured values are slightly smaller than those from the theory throughout. For loadcases 1.3 and 2.3 a poor correlation exists between the different stresses.

5.4.1.3 Comparison of 5.4.1.1 and 5.4.1.2

The loadcases for midspan and quarter-span loading show similar trends at the loaded sections as well as at the non-loaded sections of a model for the observed and the analytical stresses. Note that a matching loadcase with loading at quarter-span was not tested for Model 4 so that the results for 4.2 are not included here.

For each model, identical trends in the distribution of stresses around the cross-section occur at the loaded sections for both loadcases but with slight differences in the stress values.

Table 5.11 shows stress values at various points on the loaded sections for theory and measurements.

MODEL.LOADCASE		1.2	1.3	2.2	2.3	3.2	3.3
APPLIED LOADING		+168 N	+168 N	+168 N	+168 N	+108 N	+108 N
Top Flange:							
edge cant.	av. expt.	0.158	0.176	0.149	0.169	0.073	0.039
	theory	0.177	0.200	0.206	0.249	0.062	0.065
midpt.	av. expt.	0.164	0.156	0.173	0.169	0.140	0.153
	theory	0.165	0.181	0.214	0.246	0.165	0.107
midpt. web/cl.	av. expt	0.204	0.189	0.278	0.263	0.234	0.247
	theory	0.076	0.001	0.111	0.121	0.134	0.134
Bottom Flange:							
midpt. web/cl.	av. expt.	0.218	-0,201	-0.306	-0.317	-0.288	-0.301
	theory	-0.156	-0.170	-0.282	-0.318	-0.311	-0.314
webs	av. expt.	-0.496	-0.472	-0.712	-0.753	-0.684	-0.730
	theory	-0.312	-0.339	-0.564	-0.635	-0.621	-0.628

Table 5.11 Comparison of stress values at the loaded sections for various points on the cross-section for theoretical and measured values. (MPa)

As with the loaded sections, identical trends occur for the individual models at the non-loaded sections with the small differences being in the magnitudes of the measured stresses. The theoretical stresses at the non-loaded sections are identical for loading at midspan and at quarter-span.

5.4.2 Transverse stresses

Loaded sections

In all, the stresses from theory and the measured values compare well although the theory consistently presents with slightly higher values.

There is a trend for the transverse bending stresses to increase with decreasing depth of section, both for loading at midspan and at quarter-span.

Table 5.12 gives the average of stresses measured at the midpoints between the webs and the girder centreline for top and bottom flanges as well as theoretical values. Stress values in the table have been adjusted on a proportional basis to reflect the same magnitude of loading throughout.

MODEL.LOADCASE		1.2	1.3	2.2	2.3	3.2	3.3
Top Flange	av. expt.	0.337	0.284	0.473	0.438	0.320	0.541
	theory	0.438	0.321	0.621	0.600	0.698	0.717
Bot. Flange	av. expt.	0.324	0.255	0.383	0.360	0.532	0.555
	theory	0.391	0.287	0.462	0.446	0.605	0.712

Table 5.12 **Comparison of transverse stress values at the loaded sections for midpoints between girder centreline and the webs for top and bottom flanges. (MPa)**

Non-loaded sections

There is a very good agreement between the analysis and the tests for loadcases 3.2 and 3.2, but the theory clearly gives higher values for 1.2, 1.3, 2.2 and 2.3.

Table 5.13 gives the average of stresses measured at the midpoints between the webs and the girder centreline for top and bottom flanges for both theoretical and experimental values. Stress values in the table have been adjusted on a pro rata basis to represent the same applied loading throughout.

MODEL.LOADCASE		1.2	1.3	2.2	2.3	3.2	3.3
Top Flange	av. expt	0.178	0.191	0.184	0.185	0.025	0.026
	theory	0.271	0.272	0.281	0.281	0.023	0.023
Bot. Flange	av. expt.	0.187	0.198	0.129	0.142	0.022	0.026
	theory	0.243	0.243	0.209	0.209	0.023	0.023

Table 5.13 **Comparison of transverse stress values at the non-loaded sections for midpoints between girder centreline and the webs for top and bottom flanges. (MPa)**

The stresses at the non-loaded sections can be compared to those at the loaded sections by using the above table and Table 5.12.

5.4.3 Shear stresses

Loaded sections

The experimental values at the loaded sections are not suitable for making comparisons since the position of the strain gauges coincide with the step in the longitudinal torsional-moment function at the position of the applied loading.

Non-loaded sections

Loading at midspan (Loadcases 1.2, 2.2, 3.2, 4.2)

Loadcases 3.2 and 4.2 show close agreement between the readings and the theory throughout. Similarly, for Loadcases 1.2 and 2.2 there is also generally a good correlation between theory and the measured values with the exception being the web readings, where the measured stresses are significantly less than those from the analysis.

Loading at quarter-span (Loadcases 1.3, 2.3 and 3.3)

Here, at the midspan section, readings were only taken at the mid-height of the webs. Loadcases 1.3 and 2.3 give experimental values that are lower than the calculated values while 3.3 shows only a small difference.

Table 5.14 compares the different shear stress values for the above loadcases.

MODEL.LOADCASE		1.2	1.3	2.2	2.3	3.2	3.3	4.2
webs	expt.	-0.015	0.022	-0.031	0.014	-	0.034	-0.073
	theory	-0.041	0.030	-0.058	0.036	-	0.030	-0.069
midpt. cant.	expt.	0.008	-	0.004	-	-0.012	-	-0.019
	theory	0.009	-	0.006	-	-0.006	-	-0.007
cl. top flg.	expt	-0.052	-	-0.090	-	-0.108	-	-0.103
	theory	-0.044	-	-0.080	-	-0.118	-	-0.119
cl. bot. flg.	expt	0.077	-	-0.125	-	-0.123	-	-0.115
	theory	-0.066	-	-0.144	-	-0.130	-	-0.132

Table 5.14 **Shear stress values from the theory and the experiments at the non-loaded sections for various points on the cross-sections. (MPa)**

5.4.4 Discussion

As discussed previously, the measured stress values given in the diagrams should be approximately 15 % higher than shown due to the under-estimation of the elastic modullus.

Longitudinal and transverse stresses at the loaded sections

From the stress diagrams, a trend is clearly discernable at the loaded sections whereby the measured longitudinal stresses in the flanges between webs are consistently higher than the theoretical values. The largest differences occur at the deep section and reduce progressively with decreasing depth. At the same time the stresses observed at the edges and the midpoints of the cantilevers show a much closer agreement with the theory throughout. Tables 5.9 and 5.10 support these observations.

The transverse bending stresses are confined to the zone between and including the webs and from Table 5.12 it is clear that the theoretical values are higher than the experimental values throughout. The average difference, using the values from the table is about 28 % and varies by between 13 % and 37 % higher.

It can be seen that if an upward adjustment of 15 % is made to the measured stresses to allow for the higher actual E value, the longitudinal stresses excluding the cantilever stresses would be roughly 30 % higher than the theory on average (using the average of the ratios for the lower flanges for midspan and quarter-span loading). The experimental transverse stresses would still be slightly less than the theory by an average of roughly 1.28/1.15 which is about 11 %.

The high stresses measured longitudinally can be explained in terms of the the high transverse stresses, which are mostly higher than the longitudinal stresses themselves, and the Poisson's ratio effect. According to Maisel and Roll[7], in their conclusion, the Poisson's ratio effect becomes significant and must be allowed for where the transverse stresses are of the same order of magnitude as the longitudinal stresses.

An approximate assessment can be made of the contribution to the longitudinal stresses by the Poisson's ratio effect and this can then be compared with the effects observed above. Table 5.15 shows that if the Poisson's ratio effect is omitted, the measured longitudinal stresses become less than the theory with the difference increasing with decreasing section depth. Similarly the transverse stresses which are slightly less than the theory to start with, reduces even further if the Poisson's ratio effect is removed. Note that the experimental stresses in the table have all been increased by 15 % to offset the under-estimation of the E-value.

MODEL.LOADCASE	1.2	1.3	2.2	2.3	3.2	3.3	4.2
Longitudinal							
expt. with v	0.251	0.231	0.351	0.365	0.331	0.346	0.311
expt. without v	0.124	0.137	0.212	0.226	0.209	0.219	0.207
theory	0.156	0.170	0.282	0.318	0.311	0.314	0.319
Transverse							
expt. with v	0.373	0.293	0.440	0.414	0.393	0.410	0.348
expt. without v	0.324	0.240	0.357	0.314	0.311	0.324	0.267
theory	0.391	0.287	0.462	0.446	0.447	0.459	0.416

Table 5.15 Theoretical stresses and experimental stresses calculated both allowing for and ignoring Poisson's ratio for the midpoints on the bottom flange at the loaded cross-sections. (MPa)

Another less prominent trend, is the tendency for the measured longitudinal stresses on the lower flanges to increase exponentially towards the webs. This tendency is more pronounced for the deep sections and becomes less noticable for loadcases 3.2, 3.3 and 4.2. From this it appears as if a small shear lag effect in warping is present.

Longitudinal and transverse stresses at the non-loaded sections

The variations between the values from the analysis and the experimental work can be explained along similar lines to those for the loaded sections.

In the case of loadcases 1.2 and 1.3, the transverse stresses in the flanges between webs for experiments as well as theory, are more than twice the magnitude of the measured longitudinal stresses, which are in turn about two to three times bigger than the longitudinal stresses from the theory. This discrepancy in the values of the longitudinal stresses can only be ascribed to the Poisson's ratio effect.

Similarly, for loadcases 2.2 and 2.3, for both the top and bottom flanges between webs, the transverse stresses are considerably larger than the measured longitudinal stresses which are approximately equal in size to the longitudinal stresses from the theory but opposite in sign. The reversal of the sign of the longitudinal stresses are again due to the Poisson's ratio effect which overshadows the warping stresses.

For the other loadcases, i.e. 3.2, 3.3 and 4.2, both the transverse and longitudinal stresses are small and therefore the Poisson's ratio effect does not have a noticable influence.

The main conclusions are:

The analysis gives longitudinal stress values which lie between the measured values and the measured values adjusted to exclude the Poisson's ratio effect. Also, for the transverse stresses, the analysis gives values which are slightly higher than the measured values which allow for Poisson's ratio.

The Poisson's ratio effect, although it is seen to have major effect on the longitudinal stresses as far as the outside surfaces of the models are concerned, only is applicable to the outer surfaces and ceases to exist at the mid-lines of the flanges and webs, i.e. the neutral axes of transverse bending. Therefore from a design point of view these have local implications but are unlikely to influence the overall stability of the structure.

A sufficient degree of shear lag in warping appears to take place at the loaded sections to merit further consideration.

The longitudinal stresses at the loaded sections follow the trends set out in the parameter study[7] by increasing with decreasing depth, i.e increasing b/d for the same loading. The transverse stresses also follow these trends as can be seen from Figure 5.17 below, even though the h/d ratios are different for each model.

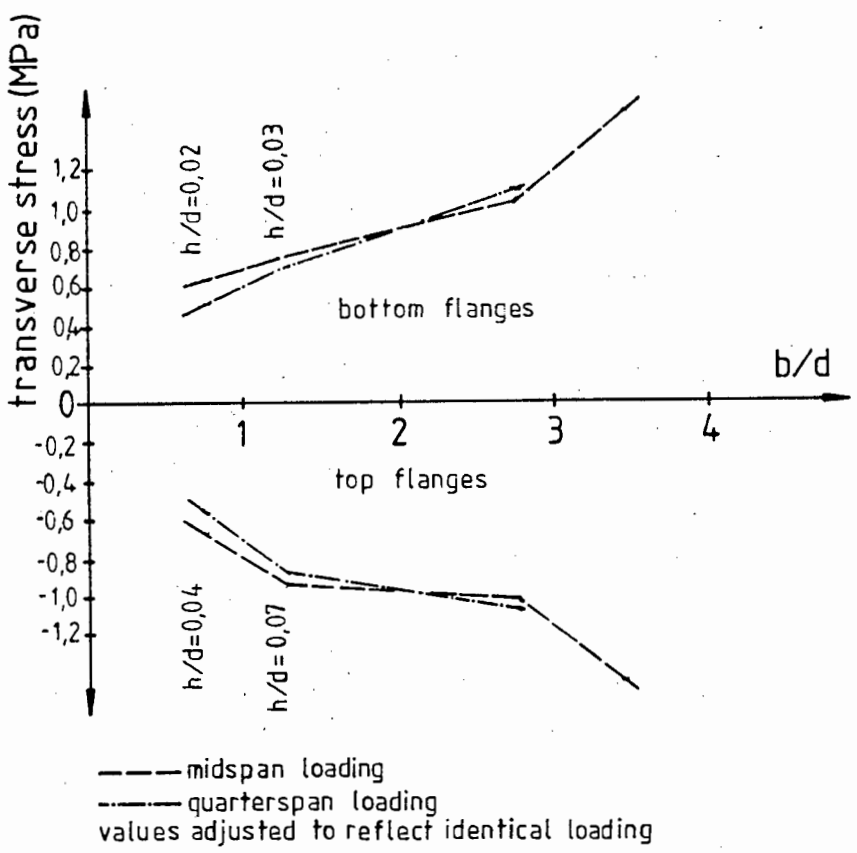

Figure 5.17 **Measured peak transverse bending stresses at the webs (extrapolated from mid-point) for top and bottom flanges versus b/d. (MPa)**

5.5 Combination of all action types

Loadcase 4.4 incorporates all action types namely, longitudinal bending and shear lag in bending, torsional warping and St Venant torsion, as well as distortional warping. Loadcase 4.6 is the same as 4.4 in all respects but with a diaphragm installed at the loaded quarter-span section and is a useful measure to assess the contribution of distortional warping and transverse bending.

As discussed before, stress concentrations arise in the immediately vicinity of the loading point so that readings at or near these positions may be affected. However in the instance of 4.4, only a single point load is applied to the model which leaves more of the readings unaffected by the stress concentrations than in the case of double loads being applied. The same local effects associated with diaphragms and discussed in 5.3 apply for Loadcase 4.6.

Figures 5.18 and 5.19 show the various stress diagrams from both the theory and the experiments for loadcases 4.4 and 4.6.

In overall terms, for Loadcase 4.4, the differences between theory and the stresses from the model tests readings are consistently very small at both midspan and quarter-span sections for longitudinal as well as transverse stresses. Shear stresses were not measured at the unloaded section, i.e. at midspan, so that these are not part of this assessment.

Good correlation between results are also found for Loadcase 4.6, notably for the longitudinal stresses and transverse stresses at midspan, i.e. the unloaded section. The transverse stresses at quarter-span are affected by the presence of the diaphragm and shear stresses were not recorded at the unloaded midspan section.

The main conclusion to be drawn from the results for 4.4 are: Since the transverse bending stresses are proportionally smaller than the longitudinal stresses than was the case for the loadcases discussed in Section 5.4, the Poisson's ratio effect on the stress values in both direction is smaller and consequently there is better agreement between the measured and the experimental values. Also the addition of longitudinal bending stresses which in previous loadcases showed good correlation between the theory and the experiments results, adds to the improvement in the agreement between the stresses.

On the basis of the good agreement of the theory with the observed values for a combination of all action types, the recommended analytical method gives results that are adequate for use in the design of concrete box-girders for the categories defined here.

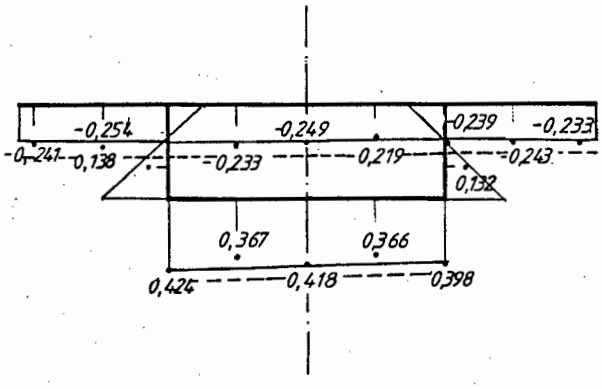

a) Longitudinal stresses at midspan

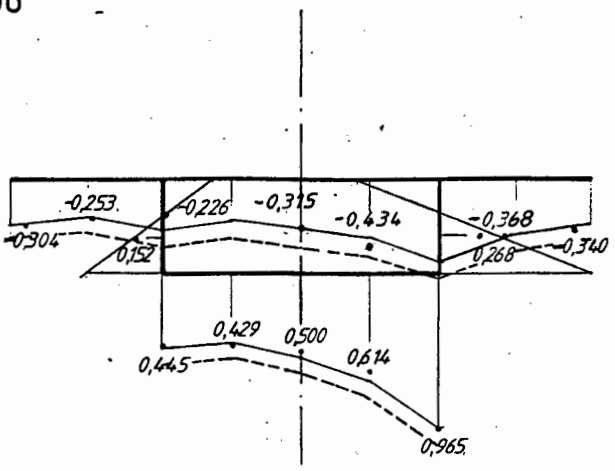

b) Longitudinal stresses at ¼ - span (z = 300 mm)

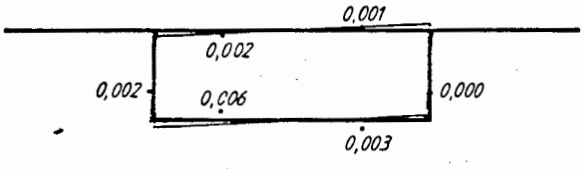

c) Transverse stresses at midspan

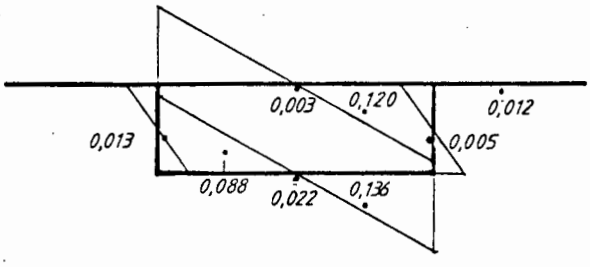

d) Transverse stresses at ¼ - span (z = 300 mm)

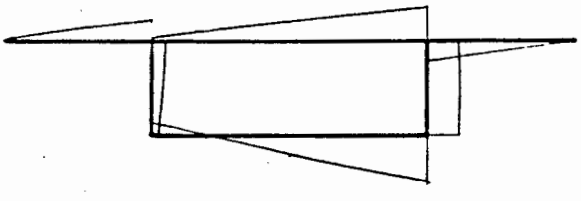

e) Shear stresses at midspan

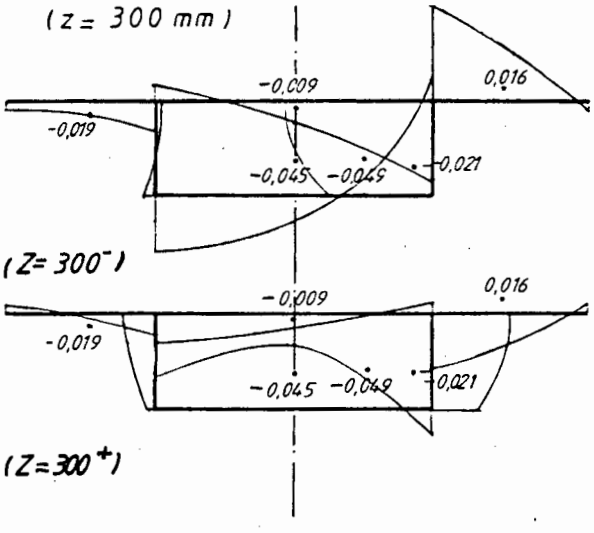

f) Shear stresses at ¼ - span

----- Outer fibre stresses

FIGURE 5.18. Model 4 Loadcase 4
Stress values from experiments MPa

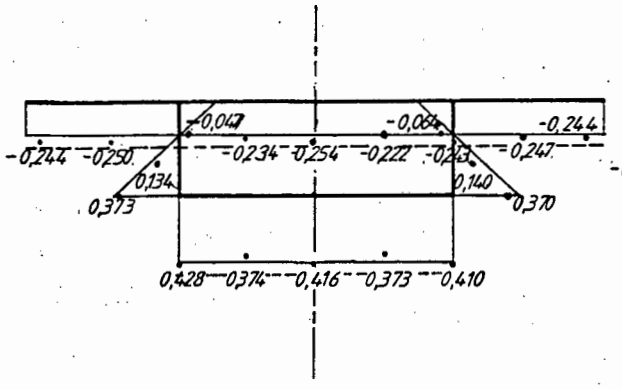

a) Longitudinal stresses at midspan

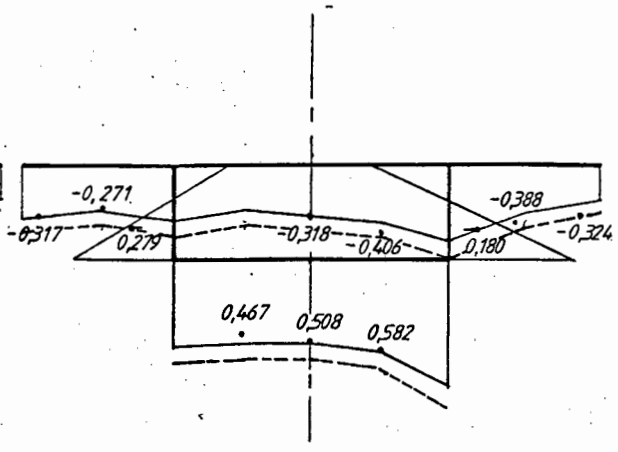

b) Longitudinal stresses at ¼ - span (z = 300 mm)

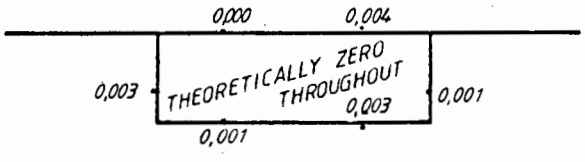

c) Transverse stresses at midspan

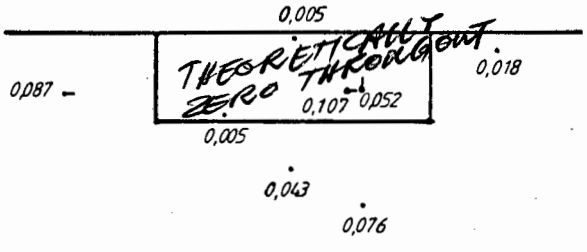

d) Transverse stresses at ¼ - span (z = 300 mm)

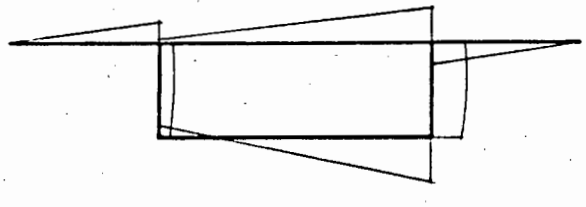

e) Shear stresses at midspan

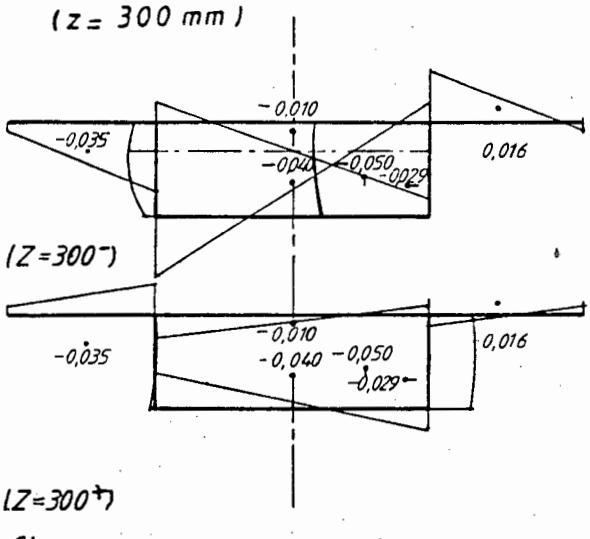

f) Shear stresses at ¼ - span

-----Outer fibre stresses

FIGURE 5.19 Model 4 Loadcase 6
Stress values from experiments MPa

6 CONCLUSION

General

The experimental results confirm the accuracy of the analysis method for the individual structural action types, as well as for combinations. No major discrepancies were found and the measured stresses also follow the trends set out in the parameter study.

Using a programmable hand calculator takes too long to produce results and for this to be a feasible method of analysis it should be available in program form.

Experimental work

For research involving multiple strain gauge readings on this scale, a data logging system should have been available to speed up and and to optimize taking readings and to process the results.

Analytical work

Shear lag and bending

Shear lag does significantly increase the longitudinal flange stresses over the webs in the vicinity of the loaded section and must be considered for the design of members.

The shear lag effect extends further away from the loaded section than predicted by the theory presented by Schmidt, Peil and Born[11].

Torsional warping

The torsional warping analysis under-estimates the actual stresses. However, this is not a serious source of error in terms of the total stresses since these are usually less than a quarter of the total warping stresses and are also highly localised longitudinally.

The torsional warping theory gives better results for shallower sections.

Combined torsional warping, St Venant torsion, distortional warping and transverse bending

The Poisson's ratio effect, although it has a major influence on the longitudinal stresses on the outside surfaces of the models, ceases to exist at the mid-lines of the flanges and webs, i.e. at the neutral axes of transverse bending. Therefore from a design point of view these have local implications only.

A sufficient degree of shear lag in warping takes place at the loaded sections to warrant further study.

Combination of all action types

The analytical method gives good results for a combination of all structural action types (as for 4.4) and on this basis is adequate for the design of concrete box-girder bridge decks.

REFERENCES

1 Case, John and Chilver, A.H. **Strength of Materials and Structures,** 2nd edition. Edward Arnold (Publishers) Ltd, 1976. pp.69-89.

2 Heilig, R. **A contribution to the theory of box-girders of arbitrary cross-sectional shape.** Cement and Concrete Association. 1971. Translation No 145.

3 Kollbrunner, C.F., and Basler, K. **Sektorielle Grossen und Spannungen bei offenen dunnwandigen Querschnitten.**(Sectorial quantities and stresses in open thin-walled cross-sections). Mitteilungen Schweizer Stahlbau-Vereinigung, Zurich. January 1964.

4 Kollbrunner, C.F., and Basler, K. **Torsion in structures. An engineering approach.**(Translated from German). Springer 1969.

5 Kolbrunner, C.F. and Hajdin, N. **Warping torsion of thin-walled beams of closed section.** Mitteilungen der Technischen Kommission, Heft 32. Schweizer Stahlbau-Vereiniging, Zurich. 1966.

6 Maisel, B.I. **Analysis of concrete box beams using small- computer capacity.** Cement and Concrete Association. December 1982. Development Report 5.

7 Maisel, B.I. and Roll, F. **Methods of analysis and design of concrete boxbeams with side cantilevers.** Cement and Concrete Association. November 1974. Technical Report 42.494.

8 Moffatt, K.R. and Dowling, P.J. **Steel box-girders. Parametric study on the shear lag phenomenon in steel box girder bridges.** CESLIC Report BG17. Civil Engineering Department, Imperial College, London. September 1972.

9 **Perspex properties.** Acrylic Products (Pty)Ltd under copywrite of Imperial Chemical Industries Limited. September 1975.

10 Reissner, E. **Analysis of shear lag in box beams by the principle of minimum potential energy.** Quarterly of Applied Mathematics. October 1946. pp. 268-278.

11 Schmidt, H., Peil, U., und Born, W. **Scheibenwirkung breiter Strassenbrückengurte - Verbesserungsvorschlag für Berechnungsvorschriften (mitwirkende Gurtbreite).** Bauingenieur 54, 1979. pp. 131-138.

12 Steinle, A. **Torsion and cross-sectional distortion of the single-cell box beam.** Beton- und Stahlbetonbau. September 1970. pp. 215-222.

13 Swann, R.A. **A feature survey of concrete box spine-beam bridges.** Cement and Concrete Association. June 1972. Technical Report 42.469.

APPENDIX A

Tables of Experimental Results

Strains given in millistrain units

Stresses given in MPa

TABLE 1
Strain gauge readings for Model 1 Loadcase 1

READ NO	GUAGE FACTOR	NO	NO LOAD	LOAD	NO LOAD	AV STRAIN	STRESS NOTE
1.	1/4 W:T	2,08	15,763	15,776	15,764	0,0123	0,033
			15,763	15,776	15,765		SY=-0,007
2.	1/4 W:B	2,10	14,848	14,929	14,851	0,080	0,133
			14,855	14,934	14,853		SY=0
3.	1/4 W:M	2,05	16,002	16,984	16,0015	-0,0175	-0,042
			16,002	15,9855	16,0035		SEE 1&4.
4.	1/4 W:M	2,05	17,195	17,1895	17,198	-0,0069	-0,007
			17,198	17,192	17,1995		SX=0,083
5.	1/4 F:W	2,08	14,758	14,725	14,754	-0,0329	-0,013
			14,7585	14,722	14,755		SX=0,013
6.	1/4 F:W	2,08	16,120	16,1945	16,1205	0,0746	0,215
			16,121	16,196	16,121		SY=-0,003
7.	1/4 F:W	2,08	16,394	16,462	16,3935	0,0693	0,182
			16,3915	16,461	16,390		SY=-0,007
8.	1/4 F:E	2,05	15,703	15,724	15,702	0,0214	0,005
			15,704	15,724	15,7015		SEE 11&12
9.	1/4 F:W	2,10	16,925	17,013	16,9215	0,0886	0,159
			16,821	17,008	16,920		SY=0
10.	1/4 F:W	2,10	15,659	15,742	15,657	0,0850	0,148
			15,660	15,744	15,656		SY=0
11.	1/4 F:E	2,05	15,5565	15,628	15,6585	0,0693	0,196
			15,5575	15,625	15,5665		SY=-0,016
12.	1/4 F:E	2,10	15,830	15,7989	15,830	-0,0316	-0,016
			15,834	15,801	15,8315		SX=0,196
13.	1/4 F:E	2,08	15,696	15,658	15,690	-0,0348	-0,027
			15,690	15,698	15,695		SX=0,192
14.	1/2 D:E	2,10	16,225	16,1115	16,225	-0,1108	-0,923
			16,228	16,1185	16,225		SY=0
15.	1/2 D:E	2,08	15,889	15,929	15,889	0,0423	-0,007
			15,890	15,9335	15,888		SX=0,299
16.	1/2 D:E	2,08	15,7835	15,676	15,7815	-0,1051	-0,310
			15,785	15,681	15,7849		SY=-0,003
17.	1/2 D:E	2,10	15,6565	15,468	15,656	-0,0571	-0,089
			15,661	15,4645	16,560		SY=0
18.	1/2 D:E	2,10	15,208	15,097	15,210	-0,1116	-0,326
			15,211	15,1015	15,2145		SY=0
19.	1/2 D:W	2,10	NON-FUNCTIONAL.			-	LOAD POINT
20.	1/2 D:W	2,10	15,178	15,082	15,171		LOAD POINT
			15,175	15,083	15,171		
21.	1/2 D:E	2,10	16,1635	16,0465	16,164	-0,1140	-0,333
			16,163	16,0495	16,164		SY=0
22.	1/2 D:E	2,08	15,399	15,295	15,396	-0,1035	-0,299
			15,401	15,295	15,398		SY=-0,007
23.	1/2 D:E	2,10	14,736	14,639	14,736	-0,0983	-0,288
			14,736	14,638	14,739		SY=0
24.	1/2 D:E	2,08	15,437	15,473	15,487	0,0385	-0,009
			15,437	15,479	15,489		SX=0,340
25.	1/2 W:B	2,10	15,009	15,167	15,0105	0,1578	0,460
			15,0105	15,1635	15,012		SY=0
26.	1/2 W:M	2,08	NON-FUNCTIONAL			-	-
							-
27.	1/2 W:T	2,10	NON-FUNCTIONAL			-	-
							-
28.	1/2 W:M	2,08	15,660	15,627	15,660	-0,0329	-0,067
			15,660	15,628	15,6615		SX=0,074
29.	1/4 W:M	2,08	14,884	14,879	14,8885	-0,0059	-0,008
			14,8855	14,8765	14,8835		SX=0,029
30.	1/4 W:M	2,10	14,650	14,661	14,6505	0,0108	0,029
			14,6495	14,660	14,649		SY=-0,006
31.	1/4 W:T	2,10	14,6415	14,596	14,6325	-0,0443	-0,128
			14,6385	14,5945	14,6385		SY=0

READ NO	GUAGE FACTOR	NO	NO LOAD	LOAD	NO LOAD	AV STRAIN	STRESS NOTE
32.	1/4 W:B	2,10	14,696	14,7765	14,6955	0,0801	0,234
			14,699	14,7775	14,697		SY=0
33.	1/4 D:E	2,08	15,532	15,4825	15,532	-0,0498	-0,150
			15,532	15,482	15,532		SY=-0,012
34.	1/4 D:E	2,08	NON-FUNCTIONAL.			-	-
							-
35.	1/4 D:E	2,10	15,365	15,3125	15,363	-0,0540	-0,158
			15,363	15,305	15,360		SY=0
36.	1/4 D:E	2,08	15,616	15,6385	15,616	0,0218	0,008
			16,6145	15,6345	15,6165		SEE 33.
37.	1/4 D:E	2,05	15,849	15,8445	15,850	-0,0055	0,021
			16,8505	15,8445	15,8505		SEE 35&45
38.	1/4 D:W	2,05	15,666	15,6195	15,6665	-0,0462	-0,137
			15,6665	15,6205	15,666		SY=-0,005
39.	1/4 D:E	2,05	15,3885	15,341	15,3885	-0,0471	-0,140
			16,390	15,343	15,3835		SY=-0,006
40.	1/4 D:E	2,05	15,8505	15,835	15,861	-0,0160	-0,004
			15,853	15,837	15,8535		SEE 41&47.
41.	1/4 D:E	2,05	16,220	16,2405	16,220	0,0196	0,003
			16,220	16,2395	16,2215		SX=-0,140
42.	1/4 D:W	2,05	15,6395	15,616	15,6395	-0,0236	-0,018
			15,6395	15,616	15,640		SEE 38&44.
43.	1/4 D:W	2,10	15,336	15,284	15,3365	-0,054	-0,158
			15,335	15,280	15,3365		SY=0
44.	1/4 D:W	2,08	15,726	15,741	15,7245	0,0159	-0,012
			15,722	15,739	15,724		SX=-0,150
45.	1/4 D:W	2,10	NON-FUNCTIONAL.			-	-
							-
46.	1/4 D:E	2,10	15,1145	15,060	15,117	-0,0566	-0,185
			15,1165	15,0585	15,1185		SY=0
47.	1/4 D:E	2,05	15,9525	15,903	15,960	-0,0413	-0,140
			15,955	15,905	15,9515		SY=0,003
48.	1/4 D:E	2,05	14,2945	14,3095	14,292	0,0166	-0,005
			14,295	14,3105	14,292		SX=-0,187
49.	1/4 D:E	2,05	14,8675	14,885	14,8695	0,0169	-0,006
			14,870	14,8865	14,8695		SX=-0,140
50.	1/2 F:W	2,08	14,948	15,086	14,949	0,1388	0,400
			14,948	15,088	14,948		SY=-0,013
51.	1/2 F:W	2,08	15,797	15,944	16,798	0,1469	0,433
			15,7975	15,9455	15,799		SY=0,013
52.	1/2 F:W	2,10	14,686	14,868	14,688	0,1808	0,527
			14,686	14,867	14,687		SY=0
53.	1/2 F:W	2,10	15,822	15,997	15,822	0,1748	0,510
			15,826	16,0005	15,826		SY=0
54.	1/2 F:E	2,10	16,360	16,521	16,361	0,1610	0,470
			16,360	16,522	16,361		SY=0
55.	1/2 F:W	2,08	15,389	15,334	15,386	-0,0536	0,013
			15,388	15,3335	15,3865		SX=0,433
56.	1/2 F:E	2,08	15,566	15,505	15,563	-0,0580	-0,013
			15,563	15,507	15,564		SX=0,400
57.	1/2 W:M	2,05	15,107	15,1435	15,1085	0,0343	0,074
			15,109	15,142	15,1095		SY=-0,065
58.	1/2 W:M	2,05	15,2435	15,2465	15,245	0,0011	0,000
			15,245	15,246	15,245		SEE 51&59
59.	1/2 W:M	2,05	15,5815	15,548	15,582	-0,0324	-0,065
			15,5815	15,5605	15,5815		SX=0,074
60.	1/2 W:T	2,10	15,1405	15,040	15,1395	-0,0965	-0,282
			15,1395	15,0465	15,1395		SY=0
61.	1/2 W:B	2,10	15,0315	15,134	15,034	0,1046	0,480
			15,034	15,132	15,032		SY=0
62.							

TABLE 2
Strain gauge readings for Model 1 Loadcase 2

READ NO	GUAGE FACTOR	NO	NO LOAD	LOAD	NO LOAD	AV STRAIN	STRESS NOTE	READ NO	GUAGE FACTOR	NO	NO LOAD	LOAD	NO LOAD	AV STRAIN	STRESS NOTE
1.	¼F:E	2,06	15,128	15,068	15,128	-0,0538	-0,204	32.	½F:E	2,10	16,629	16,632	16,630	0,0025	0,000
			15,128	15,068	15,127		SX=-0,075				16,629	16,632	16,630		SY=-0,017
2.	¼F:W	2,08	16,077	16,078	16,076	0,0015	-0,075	33.	½F:E	2,08	14,923	14,997	14,921	0,0760	0,907
			16,075	16,076	16,074		SY=-0,204				14,922	14,998	14,920		SX=0,827
3.	¼F:W	2,10	15,846	15,840	15,846	-0,0070	0,118	34.	½D:E	2,10	16,355	16,354	16,355	-0,0013	0,002
			15,845	15,839	15,846		SY=0,367				16,356	16,355	16,357		SY=0,018
4.	¼F:W	2,10	17,034	17,042	17,034	0,0078	-0,130	35.	½D:E	2,10	15,330	15,382	15,331	0,052	0,152
			17,035	17,042	17034		SY=-0,301				15,331	15,385	15,333		SY=0
5.	¼F:E	2,05	14,446	14,406	14,445	-0,0393	-0,077	36.	½D:E	2,08	15,255	16,170	15,261	-0,0839	-0,321
			14,445	14,406	14,445		SEE 6&8.				15,245	15,157	15,240		SX=-0,195
6.	¼F:E	2,05	14,365	14,365	14,365	-0,0005	-0,007	37.	½D:W	2,08	15,255	15,279	15,255	0,0255	0,212
			14,365	14,364	14,365		SY=-0,015				15,256	15,283	15,257		SY=0,353
7.	¼F:E	2,05	15,955	15,960	15,954	0,0059	SX=0,081	38.	½D:W	2,10	NON-FUNCTIONAL			—	LOADING POINT
			15,953	15,958	15,953		SY=0,170								
8.	¼F:E	2,05	14,645	14,641	14,646	-0,0043	-0,015	39.	½D:E	2,10	14,849	14,790	14,848	-0,0585	-0,171
			14,646	14,642	14,646		SX=-0,007				14,850	14,792	14,851		SY=0
9.	¼F:W	2,08	16,493	15,541	15,494	0,0473	SY=0,170	40.	½D:W	2,08	15,483	15,578	15,485	0,0928	0,353
			15,495	15,543	15,497		SX=0,081				15,484	15,576	15,485		SX=0,212
10.	½W:M	2,05	15,155	15,139	15,156	-0,0170	0,001	41.	½D:W	2,10	15,2635	15,269	15,263		LOADING POINT
			15,156	15,139	15,157		SEE 11&12				15,263	15,2695	16,263		
11.	½W:M	2,05	15,026	15,056	15,027	0,0288	0,014	42.	½D:E	2,10	15,669	15,718	15,668	0,0498	0,145
			15,027	15,055	15,027		SY=0,179				15,670	15,720	15,670		SY=0
12.	½W:M	2,05	15,516	15,452	15,516	-0,0633	-0,179	43.	½D:E	2,10	16,265	16,203	16,264	-0,0603	-0,178
			15,516	15,453	15,515		SX=0,014				16,265	16,206	16,263		SY=0
13.	½W:T	2,10	15,319	15,270	15,321			44.	½D:E	2,08	15,186	15,159	15,183	-0,0240	-0,195
			15,319	15,272	15,319						15,184	15,161	15,183		SY=-0,321
14.	½W:B	2,10	15,218	15,306	15,220			45.	¼D:E	2,08	15,462	15,463	15,463	0,0008	-0,067
			15,220	15,305	15,222						15,463	15,464	15,463		SY=-0,138
15.	¼W:T	2,10	14,939	14,934	14,939			46.	¼D:W	2,10	15,391	15,386	15,390	-0,0049	-0,156
			14,941	14,936	14,941						15,391	15,386	15,391		SY=-0,345
16.	¼W:M	2,08	15,463	15,446	15,464	-0,0115	-0,059	47.	¼D:E	2,05	14,618	14,644	14,618	0,0263	0,052
			15,462	15,445	15,463		SX=-0,019				14,618	14,645	14,619		SEE 61&66
17.	¼W:M	2,08	14,794	14,795	14,794	0,0013	-0,019	48.	¼D:E	2,10	15,541	15,530	15,541	-0,0108	-0,031
			14,793	14,794	14,792		SY=-0,059				15,542	15,531	15,541		SY=0
18.	¼W:B	2,10	14,948	14,959	14,949			49.	¼D:E	2,05	14,172	14,178	14,172	0,0058	0,016
			14,949	14,959	14,950						14,172	14,177	14,171		SX=-0,001
19.	¼W:B	2,10	15,150	15,142	15,150			50.	¼D:E	2,08	14,743	14,741	14,7435	-0,0025	-0,001
			15,150	15,142	15,149						14,7435	14,741	14,744		SX=0,018
20.	¼W:M	2,05	14,849	14,847	14,849	-0,0016	0,017	51.	¼D:E	2,05	14,639	14,637	14,639	-0,0023	-0,008
			14,849	14,848	14,850		SY=0,057				14,640	14,6375	14,640		SEE 49&50
21.	¼W:M	2,05	15,407	15,424	15,407	0,0173	0,057	52.	¼D:E	2,08	14,516	14,506	14,514	-0,0085	-0,026
			15,409	15,424	15,406		SX=0,067				14,514	14,506	14,513		SY=-0,088
22.	¼W:M	2,05	15,072	15,087	15,072	0,0148	0,015	53.	¼D:E	2,05	15,555	15,567	15,556	0,0023	-0,003
			15,073	15,087	15,072		SEE 20&21				15,5565	15,5585	15,5565		SX=-0,026
23.	½W:M	2,08	NON-FUNCTIONAL			—	—	54.	¼D:E	2,08	15,576	16,631	15,577		NO.55 NOT WORKING.
							—				15,577	15,632	15,578		
24.	½W:T	2,10	NON-FUNCTIONAL			—	—	55.	¼D:E	2,08	NON-FUNCTIONAL			—	—
							—								—
25.	½W:M	2,08	16,349	15,405	15,350		NO.23 NOT WORKING.	56.	¼D:E	2,05	15,976	15,979	15,976	0,0028	0,009
			15,350	15,406	15,351						15,977	15,9795	15,977		SX=0,004
26.	½W:B	2,10	15,239	15,165	15,239			57.	¼D:E	2,05	14,513	14,508	14,513	-0,0045	-0,003
			15,240	15,164	15,239						14,513	14,509	14,513		SEE 52&53
27.	½F:E	2,08	15,309	15,343	15,310	0,0335	0,117	58.	¼D:W	2,10	NON-FUNCTIONAL			—	—
			15,308	15,342	15,308		SY=0,307								—
28.	½F:W	2,08	14,986	14,896	14,983	-0,0878	-0,341	59.	¼D:E	2,10	15,229	15,238	15,228	0,0105	0,031
			14,985	14,897	14,984		SX=-0,278				15,228	15,230	15,227		SY=0
29.	½F:W	2,08	14,492	14,469	14,491	-0,0293	-0,218	60.	¼D:E	2,08	15,708	15,656	15,707	-0,0520	-0,178
			14,491	14,460	14,489		SY=-0,341				15,709	15,656	15,709		SX=-0,067
30.	½F:W	2,10	14,973	15,062	14,976	0,0870	0,501	61.	¼D:E	2,08	16,091	16,091	16,091	0,0000	0,004
			14,973	15,061	14,976		SY=0,631				16,093	16,093	16,093		SY=0,009
31.	½F:W	2,10	16,044	15,965	16,042	-0,079	-0,490	62.							
			16,044	15,963	16,042		SX=-0,665								

TABLE 3

Strain gauge readings for Model 1 Loadcase 3

READ NO	GUAGE FACTOR	NO	NO LOAD	LOAD	NO LOAD	AV STRAIN	STRESS NOTE	READ NO	GUAGE FACTOR	NO	NO LOAD	LOAD	NO LOAD	AV STRAIN	STRESS NOTE
1.	$\frac{1}{2}F^{L}:W$	2,10	14,817	14,826	14,8175	0,0004	0,168 SY=0,367	32.	$\frac{1}{4}F:E$	2,05	15,511	15,1955	15,511	-0,0145	-0,077 See 36&38
			14,817	14,825	14,817						16,512	15,4965	15,511		
2.	$\frac{1}{2}F^{R}:W$	2,10	15,958	15,951	15,958	-0,0071	-0,179 SY=-0,382	33.	$\frac{1}{4}F:E$	2,05	15,448	15,4505	15,448	0,0028	-0,00 SY=-0,08
			15,958	15,950	15,956						16,448	15,4500	15,448		
3.	$\frac{1}{2}F:E$	2,08	15,781	15,785	15,7825	0,0025	0,076 SY=0,177	34.	$\frac{1}{4}F:E$	2,08	16,234	16,204	16,234	-0,0236	-0,193 SY=-0,472
			15,784	15,7855	15,7835						16,234	16,2045	16,2335		
4.	$\frac{1}{2}F:E$	2,08	16,311	15,3625	15,311	0,0505	0,177 SY=0,076	35.	$\frac{1}{4}F:W$	2,10	15,751	15,660	15,750	-0,0304	-0,409 -0,527
			15,314	15,3625	15,312						15,754	15,661	15,750		
5.	$\frac{1}{2}F:E$	2,08	14,974	14,974	14,974	-0,0003	-0,080 SY=-0,202	36.	$\frac{1}{4}F:E$	2,05	15,851	15,845	15,851	-0,0060	-0,018 SY=-0,00
			14,974	14,973	14,972						15,868	15,847	15,853		
6.	$\frac{1}{2}F:E$	2,08	15,484	15,424	15,4815	-0,0586	-0,202 SY=0,080	37.	$\frac{1}{4}F:W$	2,08	15,271	15,203	15,270	-0,0675	-0,172 SY=-0,193
			15,481	15,422	15,480						15,271	15,2035	15,271		
7.	$\frac{1}{2}F:E$	2,10	16,491	16,492	16,491	0,0015	0,09 SY=-0,005	38.	$\frac{1}{4}D:E$	2,05	15,093	15,0905	15,0935	-0,0012	-0,003 SY=0,003
			16,491	16,493	16,491						15,095	15,0945	15,095		
8.	$\frac{1}{2}W:M$	2,05	15,0035	15,006	15,005	0,0021	-0,015 SY=0,055	39.	$\frac{1}{4}D:E$	2,08	16,209	16,284	16,209		No 44 not working
			15,005	15,007	15,005						16,209	16,283	16,209		
9	$\frac{1}{2}W:E$	2,10	15,079	15,087	15,080			40.	$\frac{1}{4}D:E$	2,05	14,856	14,8405	14,857	-0,0166	0,003 SX=0,192
			15,080	15,0875	15,081						14,857	14,840	14,8575		
10.	$\frac{1}{2}W:T$	2,10	15,189	15,185	15,1895			41.	$\frac{1}{4}D:W$	2,05	14,500	14,517	14,5005	0,0138	-0,030 SX=-0,179
			15,189	15,185	15,1895						14,503	14,517	14,504		
11.	$\frac{1}{2}W:M$	2,05	15,175	15,179	15,176	0,0030	0,022 SEE 12&8	42.	$\frac{1}{4}D:E$	2,05	15,137	15,1395	15,1365	0,0015	0,003 SX=-0,003
			15,176	15,1785	15,176						15,139	15,140	15,1385		
12.	$\frac{1}{2}W:M$	2,05	15,530	15,5135	15,531	-0,0168	-0,055 SX=-0,005	43.	$\frac{1}{4}D:E$	2,05	14,6325	14,575	14,6335	-0,0573	-0,179 SY=0,050
			15,530	15,5135	15,530						14,634	14,5785	14,636		
13.	$\frac{1}{2}D:E$	2,10	16,379	16,3765	16,379	0,0000	0,005 SY=0,013	44.	$\frac{1}{4}D:E$	2,08	NON FUNCTIONAL			—	—
			16,380	16,381	16,380										—
14.	$\frac{1}{2}D:W$	2,10	15,319	15,3235	15,319	0,0048	0,168 SY=0,364	45.	$\frac{1}{4}D:W$	2,10	15,4615	15,435	15,460		LOAD POINT.
			15,319	15,324	15,319						15,4615	15,438	15,466		
15.	$\frac{1}{2}D:E$	2,10	14,870	14,858	14,871	-0,0123	-0,036 SY=0	46.	$\frac{1}{4}D:W$	2,10	NON FUNCTIONAL			—	LOAD POINT.
			14,872	14,860	14,872										
16.	$\frac{1}{2}D:W$	2,10	NON-FUNCTIONAL			—	—	47.	$\frac{1}{4}D:E$	2,08	15,710	15,6345	15,708	-0,0780	-0,284 SX=-0,189
							—				15,709	15,639	15,708		
17.	$\frac{1}{2}D:E$	2,10	15,3585	15,367	15,359	0,0081	0,024 SY=0.	48.	$\frac{1}{4}D:W$	2,05	14,329	14,305	14,329	-0,0269	-0,011 SEE 43&41
			15,360	15,368	15,360						14,329	14,295	14,329		
18.	$\frac{1}{2}D:E$	2,08	15,991	16,050	15,991	0,0588	0,208 SX=0,080	49.	$\frac{1}{4}D:E$	2,05	14,221	14,266	14,223	0,0448	0,132 SY=0,008
			15,992	16,050	15,991						14,223	14,269	14,224		
19.	$\frac{1}{2}D:E$	2,10	15,694	15,705	15,6945	0,0105	-0,031 SY=0.	50.	$\frac{1}{4}D:E$	2,10	15,144	15,1965	15,1465	0,0533	-0,156 SY=0
			15,695	15,705	15,6945						15,145	15,204	15,151		
20.	$\frac{1}{2}D:E$	2,08	15,801	15,801	15,801	0,0003	0,080 SY=0,203	51.	$\frac{1}{4}D:E$	2,05	15,965	15,975	15,965	0,0097	0,020 See 38&42
			15,801	15,802	15,802						15,967	15,977	15,968		
21.	$\frac{1}{2}D:E$	2,10	16,291	16,283	16,291	-0,0083	-0,024 SY=0.	52.	$\frac{1}{4}W:M$	2,05	16,712	16,759	16,7115	0,0481	0,127 SX=-0,034
			16,2915	16,286	16,2915						16,712	16,761	16,712		
22.	$\frac{1}{2}D:E$	2,08	15,685	15,684	15,685	-0,0009	-0,072 SY=-0,178	53.	$\frac{1}{4}W:E$	2,05	15,844	15,850	15,843	0,0068	-0,006 SEE 53&52
			15,685	15,684	16,6845						15,841	15,847	15,839		
23.	$\frac{1}{2}D:E$	2,08	15,871	15,818	15,868	-0,0315	-0,178 SX=-0,092	54.	$\frac{1}{4}W:E$	2,10	14,938	14,854	14,938		
			15,869	15,816	15,866						14,935	14,849	14,9355		
24.	$\frac{1}{4}D:E$	2,08	16,134	16,1065	16,136	-0,0269	-0,189 SY=-0,284	55.	$\frac{1}{4}W:M$	2,05	14,707	14,679	14,7095	-0,0288	-0,034 SY=0,127
			16,137	16,112	16,139						14,7095	14,698	14,7095		
25.	$\frac{1}{2}W:M$	2,05	NON-FUNCTIONAL			—	—	56.	$\frac{1}{4}W:E$	2,10	14,806	14,805	14,808		
							—				14,806	14,900	14,8075		
26.	$\frac{1}{2}W:E$	2,10	15,156	15,150	15,156			57.	$\frac{1}{4}W:M$	2,08	15,196	15,230	15,197	0,0338	0,029 SY=-0,174
			15,156	15,149	15,155						15,194	15,228	15,196		
27.	$\frac{1}{2}W:T$	2,10	NON FUNCTIONAL			—	—	58.	$\frac{1}{4}W:M$	2,08	15,363	15,301	15,363	-0,0635	-0,174 SX=0,048
							—				15,363	15,2085	15,364		
28.	$\frac{1}{2}W:M$	2,08	15,985	16,004	15,986		No 28 not working	59.	$\frac{1}{4}W:T$	2,10	14,8005	14,754	14,806		
			15,985	16,003	15,986						14,805	14,759	14,812		
29.	$\frac{1}{4}F:E$	2,05	15,491	15,544	15,491	0,0539	0,228 SX=0,208	60.	$\frac{1}{4}D:E$	2,10	15,451	15,384	15,453	-0,0678	-0,196 SY=0
			15,491	15,546	15,4915						15,454	15,3685	15,456		
30.	$\frac{1}{4}F:E$	2,08	15,933	15,871	15,933	0,0895	0,208 SY=0,238	61.	$\frac{1}{4}D:E$	2,08	14,682	14,693	14,681	0,0110	-0,006 SEE 48&46
			15,932	16,0945	15,933						14,680	14,6925	14,684		
31.	$\frac{1}{4}F:W$	2,10	16,879	16,777	16,880	0,0870	0,416 SY=0,463	62.							
			16,8795	16,937	16,8775										

TABLE 4
Strain gauge readings for Model 1 Loadcase 4

READ NO	GUAGE FACTOR	NO	NO LOAD	LOAD	NO LOAD	AV STRAIN	STRESS NOTE
① 1.	½ W:M	2,08	NON-FUNCTIONAL			—	— —
① ● 2.	½ W:B	2,10	15,193 15,189	15,191 15,188	15,190 15,190		
① 3.	½ W:M	2,08	16,0085 16,007	16,0085 16,007	16,006 16,0065		No.1 NOT WORKING.
① 4.	½ W:T	2,10	NON-FUNCTIONAL			—	— —
① 5.	½ F:W/E	2,08	15,286 15,289	15,288 15,290	15,286 15,286	0,0023	0,008 SX=0,005
① 6.	½ F:E	2,10	16,485 16,485	16,489 16,485	16,4845 16,485	0,0021	0,004 SY=0,007
① 7.	½ F:W	2,10	16,038 16,041	16,087 16,038	16,039 16,041	-0,0023	-0,020 SY=-0,086
① 8.	½ F:W/E	2,08	15,617 15,616	15,6105 15,610	15,616 15,6155	-0,0059	-0,021 SX=-0,010
① 9.	½ F:W/E	2,08	14,982 14,981	14,9815 14,980	14,982 14,981	-0,0008	-0,010 SY=-0,021
① 10.	½ F:W/E	2,08	15,751 15,697	15,754 15,696	15,755 15,695	0,0005	0,005 SY=0,008
① ● 11.	½ F:W	2,10	14,965 14,972	14,965 14,971	14,966 14,972	0,0003	0,010 SY=0,023
② 12.	½ D:E	2,10	16,301 16,361	16,3045 16,361	16,304 16,359	0,0015	0,004 SY=-0,002
② 13.	½ D:W	2,10	15,098 15,0965	16,097 15,096	15,0985 15,098	-0,0013	0,009 SY=0,024
② 14.	½ D:W/E	2,08	15,274 15,276	15,274 15,276	15,274 15,276	0,000	0,006 SY=0,016
① 15.	½ D:W/E	2,08	15,411 15,409	15,406 15,403	15,410 15,407	-0,0048	-0,019 SX=-0,012
② 16.	½ D:E/W	2,10	15,338 15,339	15,338 15,3405	15,338 15,337	0,0013	0,004 SY=0.0
② 17.	½ D:W	2,10	NON-FUNCTIONAL			—	— —
② 18.	½ D:E	2,10	14,819 14,817	14,8165 14,8145	14,819 14,817	-0,0025	-0,007 SY=0.0
② 19.	½ D:W/E	2,08	15,416 15,415	15,421 15,4195	15,415 15,416	0,0048	0,018 SX=0,006
② 20.	½ D:E	2,10	15,700 15,701	15,700 15,703	15,6985 15,697	0,0024	0,007 SY=0.0
② 21.	½ D:W/E	2,10	16,301 16,3005	16,2985 16,3005	16,3005 16,3001	-0,0010	-0,003 SY=0.0
② ● 22.	½ D:W/E	2,08	15,624 15,621	15,622 15,621	15,624 15,623	-0,0016	-0,012 SY=-0,019
② ● 23.	¼ W:M	2,05	16,961 16,926	16,985 16,949	16,956 16,920	0,0271	0,088 SX=-0,028
① 24.	¼ F:W/E	2,08	15,654 15,652	15,665 15,614	15,654 15,651	-0,0375	-0,114 SX=-0,012
① 25.	¼ F:E	2,05	14,710 14,711	14,713 14,715	14,710 14,710	0,0038	0,010 SY=-0,001
① ● 26.	¼ F:W/E	2,08	15,671 15,661	15,680 15,676	15,669 15,666	0,0113	-0,013 SY=-0,114
① 27.	¼ F:E	2,05	14,397 14,398	14,395 14,3955	14,397 14,3965	-0,0019	-0,001 SY=0,010
① ● 28.	¼ F:W	2,10	16,279 16,275	16,379 16,3695	16,272 16,273	0,0951	0,395 SY=0,300
① 29.	¼ F:W/E	2,08	16,565 16,566	16,557 16,556	16,565 16,565	-0,0088	0,028 SY=0,162
① ● 30.	¼ F:E	2,05	14,675 14,673	14,669 14,663	14,675 14,671	-0,0073	-0,017 [illegible]
① 31.	¼ F:W	2,10	17,161 17,156	17,060 17,056	17,158 17,166	-0,0898	-0,388 SY=-0,252

READ NO	GUAGE FACTOR	NO	NO LOAD	LOAD	NO LOAD	AV STRAIN	STRESS NOTE
① 32.	¼ F:W/E	2,08	15,768 15,770	15,8235 15,8165	15,771 15,769	0,0505	0,162 SX=0,098
② 33.	¼ D:E/W	2,05	15,719 15,721	15,721 15,724	15,719 15,719	0,0030	-0,004 SEE 47&48
① 34.	¼ D:E	2,05	14,604 14,606	14,613 14,614	14,606 14,605	0,0083	0,018 SEE 61&59
② 35.	¼ D:E	2,10	15,560 15,560	15,646 15,546	15,560 15,5585	-0,0138	-0,040 SY=0,0
② 36.	¼ D:W/E	2,08	15,259 15,260	15,281 15,288	15,260 15,259	0,0250	0,078 SX=0,012
② 37.	¼ D:W	2,10	NON-FUNCTIONAL			—	LOAD POINT
② 38.	¼ D:E/W	2,05	15,805 15,807	15,8085 15,8105	15,806 15,806	0,0035	0,021 SX=0,028
② 39.	¼ D:W/E	2,08	NON-FUNCTIONAL			—	— —
② 40.	¼ D:W	2,10	15,7825 15,780	15,861 15,864	15,7765 15,7765		LOAD POINT.
② ● 41.	¼ D:W/E	2,08	15,496 15,492	15,489 15,490	15,494 15,496	-0,0081	0,012 SY=0,078
② 42.	¼ D:W/E	2,05	15,6975 15,701	15,6855 15,6855	15,6985 15,703	-0,0145	0,002 SEE 60&57
② 43.	¼ W:M	2,05	16,238 16,239	16,245 16,245	16,2385 16,239	0,0064	0,005 SEE 45&43
① 44.	¼ W:B	2,10	15,481 15,475	15,521 15,5165	15,4775 15,4795		
② ● 45.	¼ W:M	2,05	16,005 16,006	15,9855 15,987	16,0045 16,006	-0,0188	-0,028 SY=0,068
② ● 46.	¼ D:E	2,10	15,068 15,071	15,071 15,070	15,073 15,0705	-0,0004	-0,001 SY=0,0
② 47.	¼ D:E/W	2,05	15,435 15,436	15,441 15,445	15,436 15,438	0,0068	0,028 SY=0,024
① 48.	¼ W:M	2,08	15,440 15,440	15,4015 15,400	15,440 15,439	-0,0390	-0,119 SX=-0,014
① 49.	¼ W:B	2,10	14,679 14,681	14,660 14,661	14,680 14,681		
① 50.	¼ W:T	2,10	14,692 14,689	14,656 14,6555	14,690 14,691		
② 51.	¼ W:M	2,08	14,7295 14,729	14,7405 14,739	14,7285 14,727	0,0113	-0,014 SY=-0,119
① 52.	½ W:M	2,05	16,775 16,776	16,777 16,776	16,778 16,778	-0,0003	0,00 SX=0,001
① 53.	½ W:T	2,10	15,143 15,1385	15,140 15,1395	15,141 15,1415		
① 54.	½ W:B	2,10	15,0285 15,0265	15,0235 15,0275	15,021 15,0245		
② 55.	½ W:M	2,05	15,290 15,290	15,300 15,300	15,291 15,291	0,0095	0,020 SEE 52&56
① 56.	½ W:M	2,05	16,2985 16,2985	16,300 16,2985	16,2995 16,2985	0,0005	0,001 SY=0,00
② 57.	¼ D:W/E	2,05	15,649 15,649	15,687 15,637	15,649 15,649	-0,012	-0,066 SX=-0,081
② 58.	¼ D:W/E	2,08	15,712 15,7145	15,7005 15,700	15,7135 15,7155		No.59 NOT WORKING
② 59.	¼ D:E	2,05	16,490 16,489	16,4955 16,4935	16,4895 16,4885	0,0053	0,012 SX=-0,008
② 60.	¼ D:W/E	2,05	15,888 15,890	15,870 15,871	15,889 15,890	-0,0188	-0,081 SY=-0,066
② 61.	¼ D:E	2,05	16,354 16,3515	16,3455 16,350	16,3515 16,3515	-0,0044	-0,008 SY=-0,016
62.							

TABLE 5

Strain gauge readings for Model 2 Loadcase 1

READ NO	GUAGE FACTOR	NO	NO LOAD	LOAD	NO LOAD	AV STRAIN	STRESS NOTE
1.	1/4 W:T	2,10	13,7105	13,640	13,7105	-0,0706	-0,206
			13,7095	13,639	13,710		SY=0
2.	1/4 W:M	2,08	14,963	14,950	14,9645	-0,0149	-0,007
			14,965	14,951	14,9665		SX=0,089
3.	1/4 W:B	2,10	14,8295	15,0065	14,8315	0,1763	0,514
			14,8305	15,008	14,8325		SY=0
4.	1/4 F:W/E	2,08	15,690	15,620	15,687	-0,0674	-0,007
			15,686	15,619	15,687		SX=0,486
5.	1/4 F:℄	2,05	16,433	15,369	15,433	-0,0646	-0,010
			15,436	15,372	15,4385		SX=0,458
6.	1/4 F:W/E	2,08	NON-FUNCTIONAL				
7.	1/4 F:W/E	2,08	16,297	16,455	16,298	0,158	0,461
			16,296	16,465	16,297		SY=0
8.	1/4 F:℄	2,05	15,308	15,468	15,3095	0,1583	0,458
			15,308	15,466	15,3095		SY=-0,010
9.	1/4 F:W	2,10	14,878	15,0695	14,8785	0,1895	0,553
			14,876	15,065	14,8785		SY=0
10.	1/4 F:℄	2,05	15,566	15,616	15,566	0,0494	0,005
			15,5665	15,616	15,568		SEE 3&8
11.	1/4 F:W	2,10	14,749	14,945	14,7475	0,1971	0,575
			14,746	14,9435	14,746		SY=0
12.	1/4 F:W/E	2,08	15,975	16,143	15,976	0,1675	0,486
			15,975	16,143	15,976		SY=-0,007
13.	1/2 D:W/E	2,08	15,496	15,571	15,498	0,0739	-0,003
			15,4985	15,571	15,496		SX=-0,560
14.	1/2 D:E/W	2,10	15,018	14,8065	15,0165	-0,2119	-0,618
			15,0165	14,8045	15,0185		SY=0
15.	1/2 D:W/E	2,08	15,223	15,028	15,221	-0,1945	-0,565
			15,221	15,026	15,221		SY=0,007
16.	1/2 D:E	2,10	15,3335	15,139	15,330	-0,1924	-0,561
			15,331	15,138	15,329		SY=0
17.	1/2 D:E	2,10	14,608	14,415	14,602	-0,1905	-0,556
			14,602	14,410	14,600		SY=0
18.	1/2 D:W	2,10	14,610	14,8565	14,571	-0,1941	-0,586
			14,575	14,391	14,575		SY=0 (LOAD POINT)
19.	1/2 D:W	2,10	14,999	14,825	14,997	-0,1810	-0,528
			14,996	14,807	14,996		SY=0 (LOAD POINT)
20.	1/2 D:W/E	2,10	16,0555	15,846	16,0515	-0,2079	-0,607
			16,054	15,8455	16,0535		SY=0
21.	1/2 D:W/E	2,08	15,552	15,630	15,555	0,0778	0,007
			15,5545	15,634	15,5555		SX=-0,565
22.	1/2 D:W/E	2,08	15,1045	14,912	15,1045	-0,1916	-0,560
			15,1055	14,9155	15,107		SY=-0,003
23.	1/2 D:℄	2,10	16,068	15,859	16,0655	-0,206	-0,601
			16,066	15,861	16,0645		SY=0
24.	1/4 W:B	2,08	15,2885	15,289	15,288	-0,0496	-0,005
			15,287	15,2365	15,286		SX=-0,560
25.	1/4 W:T	2,10	14,476	14,408	14,4745	-0,0664	-0,194
			14,480	14,4135	14,478		SY=0
26.	1/4 W:M	2,08	15,049	15,0235	15,048	-0,0245	-0,071
			15,0455	15,022	15,0465		SEE 28&29
27.	1/4 W:B	2,08	15,230	15,3545	15,2305	0,1239	0,360
			15,230	15,354	15,231		SY=-0,005
28.	1/4 W:M	2,05	14,460	14,492	14,460	0,0314	0,091
			14,460	14,491	14,4605		SY=-0,002
29.	1/4 W:M	2,08	14,0195	14,0065	14,020	-0,0129	-0,002
			14,0195	14,007	14,0195		SX=0,091
30.	1/2 F:W/E	2,08	15,2155	15,5255	15,220	0,308	0,891
			15,217	15,5265	15,221		SY=-0,011
31.	1/2 F:W	2,10	15,422	15,829	15,425	0,406	1,185
			15,4205	15,8285	15,423		SY=0
32.	1/2 F:W/E	2,08	15,531	15,410	15,5295	-0,1198	0,009
			15,5305	15,4095	15,527		SX=0,920
33.	1/2 F:W	2,10	15,341	15,736	15,343	0,3805	1,140
			15,340	15,729	15,344		SY=0
34.	1/2 F:W/E	2,08	15,549	15,422	15,5465	-0,1249	-0,017
			15,548	15,4245	15,549		SX=0,89
35.	1/2 F:℄	2,10	14,962	15,320	14,965	0,356	1,040
			14,9635	15,321	14,966		SY=0
36.	1/2 F:W/E	2,08	15,992	16,308	15,994	0,314	0,920
			15,991	16,3055	15,994		SY=0,009
37.	1/4 D:E/W	2,05	15,2855	15,1965	15,285	-0,0876 (SL 0,0142)	-0,256
			15,287	15,201	15,288		SY=0
38.	1/4 D:W/E	2,05	15,719	15,709	15,720	-0,0105	0,034
			15,7215	15,711	15,7215		SEE 37&40
39.	1/4 D:W/E	2,05	15,497	15,4085	15,496	-0,0885	-0,260
			15,4965	15,407	15,4955		SY=-0,005
40.	1/4 D:E	2,10	15,0345	14,9245	15,032	-0,1086	-0,317
			15,033	14,923	15,030		SY=0
41.	1/4 D:℄	2,05	15,054	14,9645	15,0535	-0,0898	-0,260
			15,0545	14,964	15,054		SY=0,004
42.	1/4 D:W/E	2,08	16,224	16,263	16,223	0,0388	0,005
			16,223	16,2615	16,224		SX=-0,277
43.	1/4 D:W/E	2,08	NON-FUNCTIONAL				
44.	1/4 D:W	2,10	NON-FUNCTIONAL				
45.	1/4 D:W/E	2,08	15,574	15,480	15,574	-0,0840	-0,277
			15,5815	15,4865	15,5795		SY=-0,007
46.	1/4 D:W/E	2,08	15,3685	15,404	15,369	0,0345	-0,007
			15,369	15,403	15,3695		SX=-0,277
47.	1/4 D:E	2,10	15,2635	15,160	15,260	-0,1024	-0,299
			15,260	15,157	15,260		SY=0
48.	1/4 D:E/W	2,08	NON-FUNCTIONAL				
49.	1/4 D:E/W	2,05	15,4935	15,451	15,494	-0,0424	-0,081
			15,494	15,4515	15,493		SEE 38&50
50.	1/4 D:E/W	2,05	15,4985	15,5315	15,4975	0,0330	-0,005
			15,4985	15,531	15,4985		SX=-0,260
51.	1/4 D:℄	2,05	16,238	16,274	16,238	0,0363	0,004
			16,237	16,274	16,238		SX=-0,260
52.	1/4 D:℄	2,05	15,800	15,772	15,800	-0,0080	-0,003
			15,800	15,772	15,800		SEE 41&51
53.	1/4 D:W	2,10	14,6995	14,5945	14,6975	-0,1041	-0,304
			14,6985	14,594	14,698		SY=0
54.	1/2 W:M	2,05	14,9205	15,007	14,923	0,0866	0,225
			14,921	15,010	14,923		SY=-0,071
55.	1/2 W:B	2,10	14,616	14,969	14,621	0,34715	1,013
			14,615	14,965	14,619		SY=0
56.	1/2 W:M	2,08	15,515	15,461	15,515	-0,0545	-0,071
			15,514	15,4595	15,515		SX=0,225
57.	1/2 W:M	2,05	15,2335	15,2565	15,234	0,0231	0,015
			15,2335	15,2575	15,2345		SEE 54&56
58.	1/2 W:T	2,10	14,085	13,9365	14,081	-0,147	-0,428
			14,081	13,934	14,081		SY=0 (LOAD POINT)
59.	1/2 W:M	2,08	15,596	15,6805	15,5985	0,0821	0,202
			15,596	15,680	15,596		SY=-0,087
60.	1/2 W:B	2,10	14,2805	14,6335	14,281	0,353	1,031
			14,279	14,635	14,283		SY=0
61.	1/2 W:T	2,10	14,6435	14,4915	14,641	-0,1513	-0,441
			14,641	14,4905	14,6435		SY=0 (LOAD POINT)
62.	1/2 W:M	2,08	14,7665	14,7065	14,766	-0,0601	-0,087
			14,764	14,7045	14,766		SX=0,202

TABLE 6

Strain gauge readings for Model 2 Loadcase 2

READ NO	GUAGE FACTOR	NO	NO LOAD	LOAD	NO LOAD	AV STRAIN	STRESS NOTE	READ NO	GUAGE FACTOR	NO	NO LOAD	LOAD	NO LOAD	AV STRAIN	STRESS NOTE
1.	¼F:W	2,08	15,8105	15,849	15,810	0,0381	0,129	32.	¼W:M	2,05	14,986	14,9915	14,988	-0,0154	-0,060
			15,8095	15,849	15,8095		SX=0,039				14,987	14,973	14,9835		SX=-0,038
2.	¼F:E	2,08	15,912	15,9105	15,9135	-0,0041	0,039	33.	½W:M	2,08	15,560	15,6105	15,5645	0,0459	0,019
			15,913	15,9085	15,9135		SY=0,189				15,561	15,6055	15,5615		SY=-0,294
3.	¼F:E	2,05	16,287	16,2765	16,286	-0,009	-0,037	34.	¼D:E	2,05	15,439	15,4385	15,438	-0,0003	-0,004
			16,285	16,2765	16,2855		SX=-0,025				15,436	15,4365	15,438		SEE 38 & 26
4.	¼F:W	2,10	14,6655	14,651	14,6685	-0,0181	.0,062	35.	¼D:W	2,10	14,691	14,683	14,691	-0,0071	.0,133
			14,665	14,646	14,665		SY=0,295				14,6905	14,685	14,692		SY=0,395
5.	¼F:E	2,05	16,024	15,959	16,0245	-0,0661	-0,125	36.	¼D:E	2,05	14,465	14,4655	14,466	-0,0013	0,002
			16,0265	15,960	16,026		SEE 3 & 7				14,4645	14,4615	14,4635		SX=0,015
6.	¼F:W	2,10	14,8385	14,859	14,839	0,0189	-0,089	37.	¼D:E	2,05	15,2385	15,240	15,2375	0,0027	0,009
			14,8375	14,8555	14,8385		SY=0,369				15,236	15,238	15,235		SY=0,004
7.	¼F:E	2,05	15,7745	15,7715	15,7735	-0,0038	-0,025	38.	¼D:E	2,05	14,551	14,5555	14,5505	0,0048	0,015
			15,7735	15,769	15,7745		SY=-0,037				14,549	14,5535	14,5485		SY=0,002
8.	¼F:W	2,08	16,432	16,447	16,4335	0,0131	-0,041	39.	¼D:E	2,10	15,2355	15,242	15,235	0,0068	-0,020
			16,4345	16,4465	16,4335		SY=-0,203				15,234	15,241	15,2345		SY=0
9.	¼F:W	2,08	NON-FUNCTIONAL					40.	¼D:W	2,08	15,9255	15,869	15,924	-0,0561	-0,184
											15,920	15,8635	15,920		SX=-0,052
10.	½W:M	2,08	14,776	14,6755	14,774	-0,1034	-0,294	41.	¼D:E	2,10	15,008	14,998	15,0065	-0,0089	-0,026
			14,772	14,6605	14,7755		SX=0,019				15,007	14,9985	15,007		SY=0
11.	½W:B	2,10	14,251	14,390	14,2555			42.	¼D:E	2,05	14,607	14,650	14,6065	0,0441	0,090
			14,2528	14,385	14,2545						14,606	14,652	14,608		SEE 50 & 57
12.	½W:T	2,10	14,624	14,568	14,6235			43.	¼D:E	2,05	15,798	15,7955	15,7985	-0,0033	-0,003
			14,6215	14,573	14,6235						15,7985	15,794	15,797		SEE 45 & 46
13.	½D:W	2,10	14,9935	15,004	14,9915		LOADING POINT.	44.	¼D:W	2,10	NON-FUNCTIONAL				
			14,990	15,005	14,9915										
14.	½D:E	2,10	16,064	16,061	16,0645	-0,0005	0,008	45.	¼D:E	2,08	16,101	16,1065	16,1015	0,0069	-0,052
			16,065	16,0665	16,066		SY=0,024				16,101	16,111	16,104		SY=-0,184
15.	½D:W	2,08	16,0355	15,919	16,035	-0,1101	-0,449	46.	¼D:E	2,08	NON-FUNCTIONAL				
			16,034	15,916	16,0345		SX=-0,260								
16.	½D:E	2,10	14,990	15,044	14,990	0,056	.0,168	47.	¼D:E	2,08	16,298	16,354	16,2985		NO 46 NOT WORKING
			14,990	15,049	14,991		SY=0				16,2985	16,354	16,298		
17.	½D:E	2,10	14,6035	14,5465	14,6045	-0,0555	-0,102	48.	¼D:E	2,05	NON-FUNCTIONAL				
			14,604	14,5515	14,608		SY=0								
18.	½D:W	2,10	14,530	14,4765	14,5305		LOADING POINT	49.	¼D:E	2,05	15,164	15,1565	15,1635	-0,0063	-0,018
			14,530	14,503	14,5315						15,1635	15,158	15,1645		SY=0
19.	½D:E	2,08	15,7515	15,7845	15,7515	0,0346	0,295	50.	¼D:E	2,05	14,880	14,8795	14,8805	0,0001	0,004
			15,749	15,786	15,751		SY=0,486				14,8785	14,880	14,8805		SY=0,009
20.	½D:W	2,08	16,189	16,320	16,190	0,1307	0,498	51.	½F:W	2,08	15,556	15,463	15,5545	-0,0915	-0,382
			16,187	16,319	16,189		SX=0,295				15,554	15,463	15,5535		SX=-0,294
21.	½D:W	2,08	15,6335	15,599	15,6335	-0,0292	-0,260	52.	½F:W	2,08	15,089	15,1485	15,0885	0,0576	0,317
			15,6215	15,5965	15,6235		SY=-0,449				15,089	15,1445	15,089		SY=0,383
22.	½D:W	2,10	16,0325	15,9695	16,0325	-0,0677	-0,183	53.	½F:W	2,10	15,365	15,5145	15,3715	0,1433	.0,117
			16,0335	15,974	16,0325		SY=0				15,3685	15,510	15,369		SY=0,766
23.	½D:E	2,10	15,3595	15,4015	15,357	0,0461	.0,135	54.	½F:E	2,10	14,940	14,9465	14,940	0,0053	.0,016
			15,355	15,403	15,356		SY=0				14,940	14,9435	14,9385		SY=0,001
24.	¼W:B	2,10	14,8085	14,827	14,8085			55.	½F:W	2,08	15,2815	15,234	15,282	-0,0496	-0,294
			14,8075	14,8245	14,809						15,281	15,229	15,280		SY=-0,382
25.	¼W:T	2,10	13,726	13,722	13,726			56.	½F:W	2,10	15,4655	15,3275	15,463	-0,1400	-0,707
			13,7215	13,7205	13,725						15,466	15,320	15,4615		SY=-0,766
26.	¼W:M	2,08	15,364	15,3515	15,365		LONG GAUGE NOT WORKING	57.	½F:W	2,08	15,1335	15,2195	15,131	0,0888	0,383
			15,363	15,3495	15,3625						15,1315	15,2215	15,131		SX=0,317
27.	¼W:M	2,05	15,4285	15,424	15,429	-0,0051	-0,038	58.	½W:M	2,05	14,441	14,4565	14,445	0,0138	-0,011
			15,4295	15,424	15,4295		SY=-0,060				14,446	14,460	14,4455		SEE 59 & 60
28.	¼W:B	2,08	15,346	15,354	15,346	0,0081	0,008	59.	½W:M	2,05	14,075	14,0345	14,074	-0,0411	-0,036
			15,343	15,3515	15,3435		SX=-0,040				14,074	14,0315	14,0735		SY=0,216
29.	¼W:T	2,10	14,5215	14,5265	14,526			60.	½W:M	2,05	14,673	14,7515	14,6735	0,0789	0,216
			14,5235	14,5285	14,525						14,6715	14,751	14,672		SX=-0,036
30.	¼W:M	2,08	16,128	16,100	16,1285	-0,0278	-0,037	61.	½W:T	2,10	14,3785	14,428	14,3785		
			16,1285	16,102	16,130		SEE 7 & 32				14,3765	14,429	14,378		
31.	¼W:B	2,10	14,3345	14,320	14,334	-0,0149	-0,040	62.	½W:B	2,10	14,7605	14,637	14,7585		
			14,333	14,3165	14,331		SY=0,008				14,7565	14,6295	14,7555		

TABLE 7

Strain gauge readings for Model 2 Loadcase 3

READ NO	GUAGE FACTOR	NO	NO LOAD	LOAD	NO LOAD	AV STRAIN	STRESS NOTE	READ NO	GUAGE FACTOR	NO	NO LOAD	LOAD	NO LOAD	AV STRAIN	STRESS NOTE
1.	$\frac{1}{4}$F:W	2,08	15,765	15,8435	15,765	0,0793	0,360	32.	$\frac{1}{2}$W:M	2,08	14,7315	14,714	14,7331	-0,0171	-0,063
			15,764	15,844	15,764		SX=0,331				14,7265	14,7125	14,7325		SX=-0,084
2.	$\frac{1}{4}$F:W	2,08	15,977	16,0435	15,978	0,0658	0,831	33.	$\frac{1}{4}$D:W	2,10	NON-FUNCTIONAL				LOADING
			15,977	16,041	15,976		SY=0,360								POINT.
3.	$\frac{1}{4}$F:W	2,10	14,8235	14,678	14,821	-0,1464	-0,787	34.	$\frac{1}{4}$D:E	2,05	16,2665	16,269	16,2665	0,0026	0,009
			14,8215	14,671	14,8175		SY=0,795				16,266	16,2685	16,2655		SX=0,003
4.	$\frac{1}{4}$F:W	2,10	14,6635	14,834	14,668	0,1638	0,769	35.	$\frac{1}{4}$D:W	2,08	15,9275	15,812	15,925	-0,1149	-0,488
			14,666	14,8285	14,6645		SY=0,745				15,924	15,8065	15,920		SX=-0,263
5.	$\frac{1}{4}$F:E	2,08	16,418	16,3705	16,417	-0,0489	0,303	36.	$\frac{1}{4}$D:E	2,10	15,217	15,1545	15,215	-0,0603	-0,176
			16,416	16,364	16,4135		SY=0,410				15,2135	15,1545	15,2135		SY=0
6.	$\frac{1}{4}$F:E	2,05	14,6095	14,581	14,6095	-0,0289	-0,057	37.	$\frac{1}{4}$D:E	2,05	14,3335	14,269	14,3315	-0,0625	-0,101
			14,611	14,581	14,6095		SEE T69				14,3305	14,270	14,3325		SY=-0,003
7.	$\frac{1}{4}$F:E	2,05	14,344	14,351	14,3445	0,0068	0,010	38.	$\frac{1}{4}$D:E	2,08	16,0835	16,0495	16,0815	-0,0318	-0,263
			14,3435	14,348	14,3415		SY=-0,025				16,0815	16,050	16,081		SX=0,438
8.	$\frac{1}{4}$F:E	2,08	NON-FUNCTIONAL					39.	$\frac{1}{4}$D:E	2,10	15,000	15,0535	14,997	0,0550	0,101
											14,996	15,051	14,996		SY=0
9.	$\frac{1}{4}$F:E	2,05	14,882	14,872	14,8825	-0,0099	-0,025	40.	$\frac{1}{4}$D:W	2,05	14,775	14,7865	14,7745	0,0124	-0,006
			14,883	14,8735	14,883		SX=0,010				14,7735	14,7865	14,7785		SEE 49&47
10.	$\frac{1}{2}$W:D	2,10	14,213	14,196	14,2085			41.	$\frac{1}{4}$D:E	2,05	14,819	14,836	14,818	0,0184	0,038
			14,206	14,186	14,203						14,818	14,8365	14,8165		SEE 48&84
11.	$\frac{1}{2}$W:M	2,08	15,578	15,5765	15,5785	-0,0033	-0,084	42.	$\frac{1}{4}$D:W	2,05	14,4685	14,4875	14,471	0,0176	-0,023
			15,5765	15,573	15,577		SY=-0,063				14,470	14,4885	14,472		SX=-0,191
12.	$\frac{1}{2}$D:E	2,10	16,058	16,0585	16,058	0,0015	0,008	43.	$\frac{1}{4}$D:E	2,05	14,519	14,494	14,5215	-0,0243	-0,004
			16,056	16,0585	16,056		SY=0,010				14,516	14,494	14,518		SEE 31&42
13.	$\frac{1}{2}$D:W	2,10	14,966	14,961	14,966	-0,0049	0,134	44.	$\frac{1}{4}$D:W	2,08	16,285	16,421	16,2865		NO 45 WIT
			14,9635	14,9595	14,9635		SY=0,380				16,287	16,4235	16,2885		WORKING
14.	$\frac{1}{2}$D:E	2,10	15,0035	14,996	15,001	-0,0058	-0,017	45.	$\frac{1}{4}$D:E	2,08	NON-FUNCTIONAL				
			15,000	14,9955	15,0015		SY=0								
15.	$\frac{1}{2}$D:W	2,08	16,0265	15,9735	16,0255	-0,0524	-0,175	46.	$\frac{1}{4}$D:W	2,10	14,6025	14,631	14,600		LOADING
			16,0235	15,9705	16,022		SX=-0,058				14,600	14,6335	14,600		POINT.
16.	$\frac{1}{2}$D:E	2,10	14,588	14,594	14,588	0,0063	0,018	47.	$\frac{1}{4}$D:E	2,05	NON-FUNCTIONAL				
			14,585	14,5915	14,585		SY=0								
17.	$\frac{1}{2}$D:E	2,10	15,7255	15,7215	15,725	-0,0038	0,065	48.	$\frac{1}{4}$D:E	2,05	14,8685	14,8685	14,8715	-0,0001	0,003
			15,7235	15,7205	15,7235		SY=0,195				14,871	14,873	14,8725		SY=0,009
18.	$\frac{1}{2}$D:W	2,10	14,5435	14,548	14,5415	0,0061	-0,123	49.	$\frac{1}{4}$D:E	2,05	14,1165	14,1465	14,116	0,0501	0,148
			14,5385	14,5455	14,536		SY=-0,360				14,1185	14,1685	14,1185		SY=0
19.	$\frac{1}{2}$D:E	2,10	15,3255	15,3185	15,325	-0,0068	-0,020	50.	$\frac{1}{4}$W:B	2,08	15,1545	15,108	15,155	-0,0466	-0,010
			15,3245	15,3185	15,326		SY=0				15,1545	15,108	15,1545		SX=0,308
20.	$\frac{1}{2}$D:E	2,08	16,069	16,128	16,068	0,0581	0,195	51.	$\frac{1}{4}$W:M	2,05	15,4785	15,525	15,4765	0,0468	0,026
			16,066	16,1235	16,066		SX=0,065				15,476	15,5215	15,475		SY=-0,284
21.	$\frac{1}{2}$D:E	2,08	15,6065	15,6095	15,6065	0,0037	-0,058	52.	$\frac{1}{4}$W:M	2,05	15,0665	14,966	15,0665	-0,1006	-0,284
			15,607	15,6115	15,6075		SY=-0,175				15,0665	14,966	15,0665		SX=0,026
22.	$\frac{1}{2}$D:E	2,10	16,071	16,078	16,072	0,0065	0,019	53.	$\frac{1}{4}$W:B	2,08	15,2935	15,404	15,296	0,1076	0,308
			16,071	16,078	16,072		SY=0				15,2945	15,401	15,2955		SY=-0,096
23.	$\frac{1}{2}$W:T	2,10	14,517	14,5185	14,517			54.	$\frac{1}{4}$W:M	2,08	16,1235	16,091	16,1235	-0,0335	-0,014
			14,517	14,5205	14,5185						16,1215	16,087	16,1215		SEE 52&51
24.	$\frac{1}{4}$W:M	2,08	14,9985	15,0655	14,999		NO READ FOR GAUGE	55.	$\frac{1}{4}$W:T	2,10	14,504	14,448	14,5035		
			14,9985	15,0665	14,9986						14,5015	14,4465	14,5015		
25.	$\frac{1}{4}$W:T	2,10	13,7515	13,8025	13,752			56.	$\frac{1}{2}$F:W	2,08	15,8895	15,8815	15,8895	-0,0088	0,028
			13,7535	13,8075	13,7555						15,8895	15,880	15,8895		SY=0,138
26.	$\frac{1}{4}$W:B	2,10	14,807	14,6655	14,805			57.	$\frac{1}{2}$F:W	2,08	14,927	14,8815	14,927	-0,0454	-0,146
			14,8046	14,656	14,8005						14,9275	14,882	14,927		SX=-0,035
27.	$\frac{1}{2}$W:B	2,10	14,6285	14,6485	14,628			58.	$\frac{1}{2}$F:W	2,10	15,475	15,494	15,4725	0,0196	0,055
			14,6255	14,6435	14,625						15,4715	15,490	15,4705		SY=0,288
28.	$\frac{1}{2}$W:M	2,05	14,812	14,8185	14,8135	0,0061	0,038	59.	$\frac{1}{2}$F:W	2,08	14,8565	14,8645	14,856	0,0076	-0,025
			14,814	14,821	14,815		SY=0,051				14,8555	14,862	14,8545		SY=-0,146
29.	$\frac{1}{2}$W:M	2,05	15,213	15,2155	15,213	0,0026	-0,014	60.	$\frac{1}{2}$F:W	2,08	14,859	14,902	14,8595	0,0434	0,138
			15,211	15,2135	15,2105		SEE 28&81				14,8595	14,9035	14,8925		SX=0,028
30.	$\frac{1}{2}$W:T	2,10	14,287	14,286	14,287			61.	$\frac{1}{2}$F:W	2,10	15,412	15,3985	15,412	0,0144	0,067
			14,292	14,292	14,294						15,411	15,3935	15,409		SY=0,280
31.	$\frac{1}{2}$W:M	2,08	15,4835	15,496	15,4835	0,0125	0,051	62.	$\frac{1}{2}$F:E	2,10	14,8665	14,9565	14,968	0,000	-0,0024
			15,4835	15,496	15,4835		SX=0,038				14,969	14,968	14,9695		SY=-0,004

TABLE 8

Strain gauge readings for Model 2 Loadcase 4

READ NO	GUAGE FACTOR	NO	NO LOAD	LOAD	NO LOAD	AV STRAIN	STRESS NOTE
1.	1/4 W:B	2,10	15,2115	15,1845	15,211	-0,0163	-0,084 Sx=-0,018
			15,206	15,181	15,2085		
2.	1/4 W:M	2,08	14,413	14,482	14,4135	0,0180	-0,003 SY=-0,142
			14,4185	14,481	14,414		
3.	1/4 W:M	2,05	14,097	14,049	14,0985	-0,0483	-0,142 Sx=-0,003
			14,0965	14,0495	14,098		
4.	1/4 W:B	2,08	15,1935	15,1935	15,194	0,0051	-0,018 SY=-0,084
			15,189	15,1935	15,189		
5.	1/4 W:M	2,05	15,125	15,104	15,124	-0,0208	-0,012 SEE 3&12
			15,1245	15,1035	15,1245		
6.	1/4 W:T	2,10	14,589	14,6065	14,5895		
			14,586	14,606	14,5865		
7.	1/2 F:W	2,08	15,8815	15,884	15,8825	0,0013	0,009 SY=0,0144
			15,882	15,8825	15,882		
8.	1/2 F:W	2,08	14,9035	14,898	14,9015	-0,0046	-0,015 Sx=-0,004
			14,9015	14,896	14,900		
9.	1/2 F:W	2,10	15,4935	15,496	15,4935	0,0021	-0,006 SY=-0,030
			15,494	15,494	15,492		
10.	1/2 F:W	2,08	14,6145	14,6165	14,615	0,0006	-0,004 SY=-0,015
			14,6145	14,614	14,6145		
11.	1/2 F:W	2,08	14,8895	14,8915	14,8895	0,0037	0,014 Sx=0,009
			14,890	14,8945	14,8905		
12.	1/2 F:W	2,10	15,424	15,4265	15,424	0,0008	0,0014 SY=0,009
			15,423	15,4215	15,422		
13.	1/2 F:E	2,10	14,9695	14,969	14,968	-0,0001	-0,001 SY=0,001
			14,9675	14,966	14,9655		
14.	1/2 W:B	2,10	14,610	14,6135	14,610		
			14,6095	14,610	14,607		
15.	1/2 W:M	2,05	14,9045	14,908	14,905	0,0031	0,010 Sx=0,002
			14,904	14,907	14,904		
16.	1/2 W:M	2,05	15,5235	15,5215	15,523	-0,0006	0,002 Sx=0,010
			15,5235	15,523	15,5235		
17.	1/2 W:T	2,10	14,494	14,493	14,4945		
			14,4915	14,492	14,4925		
18.	1/2 W:M	2,05	15,3155	15,303	15,3155	-0,0173	-0,028 SEE 16&15
			15,315	15,303	15,315		
19.	1/2 W:T	2,10	14,340	14,3415	14,339		
			14,338	14,3405	14,3385		
20.	1/2 W:M	2,08	15,059	15,0585	15,0595	-0,0011	-0,006 Sx=-0,006
			15,0595	15,058	15,0595		
21.	1/4 W:B	2,10	14,890	14,978	14,891		
			14,890	14,9745	14,8865		
22.	1/2 W:M	2,08	14,2465	14,246	14,2465	-0,0013	-0,006 Sx=-0,006
			14,2475	14,246	14,2465		
23.	1/2 D:E	2,10	16,0435	16,0435	16,0435	0,0005	0,002 SY=0,002
			16,044	16,045	16,044		
24.	1/2 D:M	2,08	15,544	15,5365	15,544	-0,0078	-0,027 Sx=-0,012
			15,5435	15,5355	15,5435		
25.	1/2 D:M	2,10	14,931	14,9315	14,931	0,0008	0,002 SY=0
			14,9305	14,9315	14,9305		
26.	1/2 D:M	2,08	15,261	15,260	15,261	0,0003	0,013 Sy=0,031
			15,2615	15,2635	15,2625		
27.	1/2 D:E	2,10	14,5465	14,5445	14,5465	-0,0023	-0,007 SY=0
			14,546	14,543	14,545		
28.	1/2 D:W	2,10	14,5285	14,5245	14,5275	-0,0023	-0,028 SY=-0,056
			14,528	14,5265	14,527		
29.	1/2 D:M	2,08	15,625	15,634	15,625	0,0080	0,031 Sx=0,013
			15,6255	15,6345	15,6255		
30.	1/2 D:W	2,10	14,9765	14,976	14,976	0,0006	0,002 SY=0,060
			14,973	14,978	14,973		
31.	1/2 D:E	2,10	15,3165	15,319	15,3185	0,0014	0,004 SY=0
			15,3235	15,324	15,3215		

READ NO	GUAGE FACTOR	NO	NO LOAD	LOAD	NO LOAD	AV STRAIN	STRESS NOTE
32.	1/2 D:E	2,10	16,041	16,0395	16,041	-0,0016	-0,005 SY=0
			16,038	16,0365	16,0385		
33.	1/2 D:E	2,05	15,1295	15,1285	15,1265	-0,0005	-0,012 SY=-0,027
			15,1285	15,128	15,1285		
34.	1/2 W:B	2,10	14,144	14,145	14,144		
			14,1425	14,1415	14,144		
35.	1/4 W:M	2,08	15,2035	15,239	15,204		NO READING BECAUSE GAUGE FAULTY
			15,2045	15,238	15,2045		
36.	1/4 W:T	2,10	13,7985	13,7885	13,797		
			13,794	13,779	13,7945		
37.	1/4 D:E	2,05	15,965	15,963	15,9655	-0,0019	0,006 SY=0,029
			15,9655	15,964	15,9655		
38.	1/4 D:W	2,10	14,633	14,5765	14,6315		LOAD POINT.
			14,6305	14,575	14,6315		
39.	1/4 D:M	2,05	NON-FUNCTIONAL				
40.	1/4 D:E	2,10	15,234	15,235	15,233	0,0025	0,007 SY=0
			15,230	15,234	15,231		
41.	1/4 F:W	2,08	15,562	15,5295	15,562	-0,0061	-0,057 Sx=-0,022
			15,562	15,5255	15,5605		
42.	1/4 F:E	2,05	15,9805	15,9865	15,9795	0,0068	0,018 Sx=-0,008
			15,9785	15,9855	15,9785		
43.	1/4 F:E	2,05	15,395	15,3955	15,3955	-0,0036	-0,003 SY=-0,018
			15,3965	15,390	15,3955		
44.	1/4 F:E	2,05	15,756	15,7355	15,7565	-0,0214	-0,048 SEE 43&42
			15,7565	15,7345	15,7565		
45.	1/4 F:E	2,05	15,5925	15,6145	15,593	0,0204	0,022 SY=-0,097
			15,5925	15,611	15,5915		
46.	1/4 F:W	2,10	15,028	15,087	15,026		SY=?
			15,0256	15,0825	15,024		
47.	1/4 F:W	2,10	14,8915	14,8565	14,8925		SY=?
			14,891	14,8535	14,8905		
48.	1/4 F:W	2,08	16,096	16,091	16,0965		SY=?
			16,0965	16,068	16,0955		
49.	1/4 F:W	2,08	NON-FUNCTIONAL				
50.	1/4 D:E	2,05	15,6795	15,683	15,6795	0,0089	0,004 SEE SY=39
			15,6795	15,6835	15,679		
51.	1/4 D:E	2,08	16,3135	16,325	16,313		NO GI NOT WORKING
			16,3115	16,3235	16,3115		
52.	1/4 D:E	2,05	15,4685	15,455	15,4665	-0,0126	-0,055 SY=-0,047
			15,468	15,4555	15,467		
53.	1/4 D:E	2,08	15,3585	15,350	15,3605	-0,0088	-0,047 SX=-0,056
			15,3605	15,3515	15,361		
54.	1/4 D:E	2,05	15,7305	15,7465	15,7305	0,0109	0,028 SEE 8&56
			15,731	15,749	15,7315		
55.	1/4 D:M	2,08	15,963	15,9735	15,962	0,0115	0,024 SX=-0,024
			15,964	15,9765	15,965		
56.	1/4 D:E	2,05	16,187	16,1965	16,188	0,0091	0,029 SX=0,008
			16,189	16,198	16,1885		
57.	1/4 D:M	2,05	15,1895	15,189	15,182	0,0061	0,018 SY=0
			15,1835	15,1895	15,1835	$\varepsilon_{yield}=0.0046$	
58.	1/4 D:E	2,05	14,3435	14,342	14,3485	-0,0070	0,008 SEE 52&53
			14,3465	14,3395	14,3465		
59.	1/4 D:E	2,10	15,0695	15,0535	15,0605	-0,0086	-0,005 SY=0
			15,0695	15,0515	15,059		
60.	1/4 D:W	2,10	NON-FUNCTIONAL				LOAD POINT
61.	1/4 D:M	2,08	NON-FUNCTIONAL				
62.	1/4 D:E	2,08	16,141	16,129	16,141	-0,0116	-0,024 SY=0,024
			16,141	16,132	16,1445		

TABLE 9
Strain gauge readings for Model 3 Loadcase 1

READ NO	GUAGE: FACTOR/No.	NO LOAD	LOAD	NO LOAD	M. STRAIN	STRESS NOTE:
1.	$\frac{1}{4}$F:W 2,05	15,393	16,297	15,398	0,8029	0,879
		15,996	16,3015	15,9965		SY=-0,012
2.	$\frac{1}{4}$F:E 2,05	13,853	13,7305	13,851	-0,1216	-0,012
		13,8515	13,729	13,850		SX=0,879
3.	$\frac{1}{4}$F:E 2,08	15,5715	15,4385	15,5705	-0,1318	-0,027
		15,5715	15,439	15,5685		SX=0,916
4.	$\frac{1}{4}$F:E 2,05	15,3265	15,209	15,325	-0,1163	-0,039
		15,325	15,208	15,3235		SX=0,771
5.	$\frac{1}{4}$F:E 2,05	15,250	15,351	15,2485	0,1016	0,053
		15,249	15,349	15,246		SEE 10 & 4
6.	$\frac{1}{4}$F:E 2,02	15,055	15,3755	15,061	0,3176	0,916
		15,059	15,378	15,0615		SY=-0,027
7.	$\frac{1}{4}$F:W 2,10	12,160	12,526	12,165	0,3600	1,051
		12,160	12,519	12,1615		SY≈0
8.	$\frac{1}{4}$F:E 2,05	14,914	15,052	14,915	0,1385	0,101
		14,911	15,0525	14,915		SEE 1 & 2
9.	$\frac{1}{4}$F:W 2,10	11,3965	11,760	11,4005	0,3584	1,046
		11,396	11,753	11,399		SY≈0
10.	$\frac{1}{4}$F:E 2,05	15,4345	15,7015	15,4315	0,2694	0,771
		15,433	15,7015	15,4295		SY=-0,039
11.	$\frac{1}{2}$F:W 2,10	12,2385	12,994	12,249	0,7405	2,161
		12,2405	12,976	12,250		SY≈0
12.	$\frac{1}{2}$D:E 2,08	14,806	14,430	14,805	-0,3755	-1,102
		14,809	14,4335	14,809		SY=-0,017
13.	$\frac{1}{2}$D:E 2,10	16,009	15,590	16,015	-0,4240	-1,237
		16,017	15,5895	16,014		SY≈0
14.	$\frac{1}{2}$D:E 2,08	15,546	15,6685	15,549	0,1415	-0,017
		15,5485	15,691	15,5495		SX=-1,102
15.	$\frac{1}{2}$D:W 2,10	14,971	14,561	14,971		LOAD POINT
		14,9695	14,5915	14,965		
16.	$\frac{1}{2}$D:E 2,08	15,212	14,8185	15,2105	-0,3860	-1,126
		15,215	14,832	15,2165		SY=0,0001
17.	$\frac{1}{2}$D:E 2,10	14,970	14,540	14,962	-0,4233	-1,235
		14,965	14,5435	14,963		SY≈0
18.	$\frac{1}{2}$D:E 2,10	14,503	14,1135	14,495	-0,3859	-1,126
		14,496	14,108	14,4905		SY≈0
19.	$\frac{1}{2}$D:W 2,10	14,490	14,055	14,484		LOAD POINT
		14,486	14,067	14,472		
20.	$\frac{1}{2}$D:E 2,10	15,314	14,9305	15,310	-0,3809	-1,111
		15,3115	14,934	15,317		SY≈0
21.	$\frac{1}{2}$D:E 2,08	15,604	15,7565	15,6075	0,1505	0,000
		15,605	15,756	15,6066		SX=-1,126
22.	$\frac{1}{2}$D:E 2,10	15,351	15,5355	15,3515	-0,4158	-1,213
		15,3535	15,5415	15,361		SY≈0
23.	$\frac{1}{4}$W:M 2,05	13,4185	13,5215	13,4185	0,1025	0,293
		13,4165	13,5195	13,4185		SY=-0,016
24.	$\frac{1}{4}$W:T 2,10	14,4685	14,3965	14,4665	-0,0705	-0,206
		14,465	14,395	14,465		SY≈0
25.	$\frac{1}{4}$W:M 2,05	12,351	12,306	12,3505	-0,0446	-0,016
		12,349	12,3045	12,349		SX=0,292
26.	$\frac{1}{4}$W:B 2,10	14,481	14,805	14,485	0,3201	0,934
		14,463	14,802	14,4645		SY≈0
27.	$\frac{1}{2}$F:E 2,08	15,360	15,9565	15,368	0,5919	1,745
		15,365	15,9585	15,3695		SX=-0,045
28.	$\frac{1}{2}$F:E 2,10	14,988	15,671	14,998	0,6662	1,944
		14,9935	15,6565	14,999		SY≈0
29.	$\frac{1}{2}$F:W 2,10	12,442	13,191	12,455	0,7343	2,143
		12,446	13,181	12,456		SY≈0
30.	$\frac{1}{2}$F:W 2,10	15,625	16,440	15,636	0,6083	1,804
		15,632	16,443	15,633		SY=0,015
31.	$\frac{1}{2}$F:E 2,10	15,663	16,434	15,676	-0,2176	0,045
		15,671	16,426	15,681		SX=1,145

READ NO	GUAGE: FACTOR/No.	NO LOAD	LOAD	NO LOAD	M. STRAIN	STRESS NOTE:
32.	$\frac{1}{2}$F:W 2,05	15,708	15,490	15,7045	-0,2155	0,075
		15,7055	16,4885	15,701		SX=1,804
33.	$\frac{1}{4}$D:E 2,10	14,9415	14,725	14,9375	-0,2136	-0,623
		14,939	14,725	14,9365		SY≈0
34.	$\frac{1}{4}$D:W 2,10	14,570	14,356	14,5655	-0,2110	-0,616
		14,568	14,3565	14,5655		SY≈0
35.	$\frac{1}{4}$D:E 2,05	15,0565	14,8795	15,055	-0,1761	-0,514
		15,0585	14,8815	15,0565		SY≈0.
36.	$\frac{1}{4}$D:E 2,05	15,2595	15,081	15,2595	-0,1778	-0,516
		15,2595	15,0815	15,2575		SY=0,008
37.	$\frac{1}{4}$D:E 2,05	15,755	15,9295	15,752	-0,0239	0,063
		15,754	15,7295	15,7515		SEE 35 & 61
38.	$\frac{1}{4}$D:E 2,05	16,2095	16,2845	16,211	0,0734	0,011
		16,211	16,284	16,212		SX=-0,521
39.	$\frac{1}{4}$D:E 2,05	15,7605	15,722	15,781	-0,0580	-0,010
		15,7825	15,725	15,782		SEE 41 & 38
40.	$\frac{1}{4}$D:E 2,08	NON-FUNCTIONAL				
41.	$\frac{1}{4}$D:E 2,08	15,381	15,4555	15,383	0,0741	0,001
		15,383	15,458	15,3835		SX=-0,553
42.	$\frac{1}{4}$D:E 2,05	15,4035	15,4765	15,4055	0,0716	0,008
		15,4055	15,477	15,406		SX=-0,516
43.	$\frac{1}{4}$D:E 2,05	15,4725	15,393	15,4715	-0,0789	-0,054
		15,4725	15,393	15,4725		SEE 36 & 42
44.	$\frac{1}{4}$D:E 2,10	15,569	15,3785	15,5675	-0,1896	-0,653
		15,570	15,380	15,569		SY=0,001
45.	$\frac{1}{4}$D:E 2,08	15,8045	15,8835	15,806		NO 40 NOT WORKING
		15,8055	15,8815	15,806		
46.	$\frac{1}{4}$D:E 2,10	15,204	15,000	15,200	-0,2023	-0,590
		15,200	14,996	15,197		SY≈0
47.	$\frac{1}{4}$D:E 2,05	15,0515	14,8715	15,051	-0,1799	-0,521
		15,0545	14,8735	15,053		SY=0,0111
48.	$\frac{1}{4}$W:M 2,08	15,400	15,512	15,4015	0,1114	0,322
		15,400	15,5115	15,4000		SY=-0,008
49.	$\frac{1}{4}$W:B 2,10	14,5095	14,830	14,511	0,3195	0,932
		14,5085	14,8285	14,510		SY≈0
50.	$\frac{1}{4}$W:M 2,08	15,259	15,212	15,2575	-0,0456	-0,008
		15,2585	15,2135	15,257		SX=0,322
51.	$\frac{1}{4}$W:T 2,10	13,8215	13,7545	13,821	-0,0668	-0,195
		13,820	13,7535	13,8205		SY≈0
52.	$\frac{1}{2}$W:M 2,08	15,569	15,789	15,5735	0,2165	0,613
		15,5715	15,7885	15,575		SY=-0,050
53.	$\frac{1}{2}$W:T 2,10	14,538	14,363	14,5365	-0,1713	-0,500
		14,5365	14,3665	14,536		SY≈0
54.	$\frac{1}{2}$W:M 2,08	12,1115	12,0085	12,104	-0,0988	-0,050
		12,1045	12,004	12,0975		SX=0,613
55.	$\frac{1}{2}$W:B 2,10	15,296	15,0485	15,308	0,6395	1,866
		15,3015	15,0335	15,3035		SY≈0
56.	$\frac{1}{2}$W:M 2,08	14,2985	14,3745	14,3005	0,0741	0,035
		14,3005	14,3744	14,301		SEE 60 & 58
57.	$\frac{1}{2}$W:T 2,10	14,356	14,194	14,355	-0,1610	-0,471
		14,3565	14,194	14,355		SY≈0
58.	$\frac{1}{2}$W:M 2,05	13,1444	13,055	13,1455	-0,0951	-0,045
		13,145	13,0455	13,1455		SX=0,596
59.	$\frac{1}{2}$W:B 2,10	13,5855	14,2135	13,593	0,6215	1,814
		13,5846	14,207	13,592		SY≈0
60.	$\frac{1}{2}$W:M 2,05	13,1155	13,3255	13,118	0,2104	0,596
		13,1165	13,3255	13,120		SY=-0,049
61.	$\frac{1}{4}$D:E 2,05	NON-FUNCTIONAL				
62.	$\frac{1}{4}$D:W 2,10	NON-FUNCTIONAL				

TABLE 10
Strain gauge readings for Model 3 Loadcase 2

READ ING	GUAGE LOCATION	GUAGE FACTOR	NO LOAD	LOAD	NO LOAD	AV. STRAIN	STRESS NOTE
1.	1/4 W:O	2.10	14,564	14,5785	14,564		
			14,5635	14,5784	14,5595		
2.	1/4 W:M	2.08	14,9145	14,924	14,9145	0,0089	0,025
			14,9145	14,922	14,913		SY=-0,003
3.	1/4 W:T	2.10	13,809	13,8105	13,809		
			13,809	13,8105	13,809		
4.	1/4 W:M	2.08	14,7845	14,780	14,7845	-0,0044	-0,003
			14,7845	14,7805	14,785		SX=0,025
5.	1/2 F:W	2.08	15,409	15,3635	15,4105	-0,0509	-0,284
			15,410	15,362	15,4045		SY=-0,346
6.	1/2 F:W	2.10	12,136	12,291	12,1415	0,1476	0,696
			12,136	12,2765	12,135		SY≈0,679
7.	1/2 F:W	2.10	12,4365	12,3025	12,4365	-0,1384	-0,672
			12,436	12,267	12,428		SY≈-0,688
8.	1/2 F:W	2.08	15,064	14,981	15,062	-0,0806	-0,346
			15,064	14,9845	15,0635		SX=-0,284
9.	1/2 F:W	2.08	15,362	15,422	15,3655	0,0546	0,291
			15,364	15,414	15,362		SY=0,337
10.	1/2 F:W	2.08	15,759	15,833	15,757	0,0766	0,397
			15,758	15,836	15,759		SX=0,291
11.	1/2 F:W	2.10	15,0205	15,085	15,025	-0,0004	-0,003
			15,023	15,017	15,017		SY≈0,005
12.	1/2 D:W	2.10	15,0365	15,0865	15,0375		LOAD
			15,037	15,094	15,041		POINT
13.	1/2 D:W	2.10	14,524	14,4460	14,5215		LOAD
			14,524	14,4464	14,524		POINT
14.	1/2 D:W	2.08	15,359	15,320	15,3565	-0,0345	-0,227
			15,360	15,330	15,3615		SY=-0,325
15.	1/2 D:E	2.10	15,3334	15,3355	15,3335	0,0231	-0,067
			15,3335	15,3615	15,3365		SY≈0
16.	1/2 D:E	2.08	15,4425	15,5285	15,482	0,0369	0,241
			15,493	15,533	15,438		SY=0,343
17.	1/2 D:E	2.10	14,513	14,4486	14,5115	-0,0270	-0,079
			14,515	14,491	14,5185		SY≈0
18.	1/2 D:E	2.10	16,0315	16,0265	16,0225	-0,0009	-0,001
			16,0305	16,0335	16,034		SY≈0,008
19.	1/2 D:E	2.08	16,0355	15,9945	16,0355	-0,0810	-0,325
			16,076	15,9945	16,0755		SX=0,227
20.	1/2 D:E	2.10	14,9835	15,027	14,9815	0,0468	0,136
			14,9815	15,0315	14,9835		SY≈0
21.	1/2 D:E	2.08	16,1185	16,2035	16,120	0,0853	0,343
			16,119	16,206	16,1205		SX=0,241
22.	1/2 D:W	2.10	15,9865	15,9355	15,985	-0,0491	-0,143
			15,986	15,939	15,986		SY≈0
23.	1/2 W:B	2.10	13,6275	13,500	13,626		
			13,6275	13,491	13,613		
24.	1/2 W:M	2.05	14,1155	14,115	14,1155	-0,0006	-0,054
			14,1155	14,115	14,116		SX=-0,133
25.	1/2 W:M	2.05	13,9605	13,924	13,961	-0,0385	-0,133
			13,961	13,9265	13,9605		SY=-0,054
26.	1/2 W:M	2.05	15,2915	15,271	15,2915	-0,0205	-0,002
			15,2915	15,271	15,2915		SEE 25&24
27.	1/2 W:T	2.10	14,309	14,3345	14,3065		
			14,309	14,338	14,311		
28.	1/2 W:T	2.10	14,573	14,5365	14,573		
			14,5735	14,5444	14,5755		
29.	1/2 W:M	2.08	14,978	15,026	14,981	0,0450	0,126
			14,981	15,0245	14,981		SY=-0,013
30.	1/2 W:M	2.05	11,436	11,4335	11,4325	-0,0214	-0,013
			[illegible]	[illegible]	[illegible]		SX=0,126
31.	1/2 W:T	2.10	[illegible]	[illegible]	[illegible]		

READ ING	GUAGE FACTOR	GUAGE LOCATION	NO LOAD	LOAD	NO LOAD	AV. STRAIN	STRESS NOTE
32.	1/4 W:M	2.08	13,399	13,3935	13,3985	-0,0060	-0,018
			13,3985	13,3915	13,398		SY=-0,001
33.	1/4 W:T	2.10	14,4665	14,466	14,468		
			14,468	14,468	14,470		
34.	1/4 W:M	2.05	12,3365	12,3365	12,3365	0,0020	-0,001
			12,3365	12,3395	12,3365		SX=-0,018
35.	1/4 W:C	2.10	14,4815	14,4205	14,4315		
			14,4335	14,4145	14,4865		
36.	1/4 F:W	2.08	14,356	14,343	14,3535	0,0090	0,021
			14,3535	14,3535	14,3541		SX=-0,015
37.	1/4 F:C	2.05	14,4365	14,4441	14,435	0,0058	0,013
			14,4355	14,4442	14,436		SX=-0,009
38.	1/4 F:W	2.05	13,9444	14,001	13,945	0,0559	0,116
			13,944	13,999	13,9435		SEE44&36
39.	1/4 F:C	2.05	14,416	14,4765	14,4185	0,0589	0,123
			14,417	14,476	14,418		SEE43&37
40.	1/4 F:W	2.08	15,347	15,3555	15,348	0,0062	0,015
			15,348	15,3515	15,3455		SY=-0,007
41.	1/4 F:W	2.10	11,296	11,311	11,296	0,0134	0,031
			11,2945	11,305	11,292		SY≈-0,021
42.	1/4 F:W	2.10	12,161	12,1485	12,1615	-0,0142	-0,028
			12,161	12,143	12,1565		SY≈0,085
43.	1/4 F:C	2.05	14,639	14,6365	14,641	-0,0049	-0,009
			14,6395	14,6355	14,638		SY=0,013
44.	1/4 F:C	2.08	16,584	16,5785	16,586	-0,0078	-0,015
			16,5845	16,574	16,5815		SY=0,021
45.	1/4 F:W	2.08	15,752	15,747	15,7515	-0,0045	-0,007
			15,7515	15,746	15,753		SX=0,015
46.	1/4 D:E	2.10	14,999	14,9935	14,9965	-0,0036	-0,011
			14,9985	14,9955	14,9985		SY≈0
47.	1/4 D:W	2.10	14,6285	14,624	14,627		DO. 62 NOT
			14,6275	14,6245	14,6305		WORKING
48.	1/4 D:C	2.05	15,4215	15,421	15,4215	-0,0009	0,001
			15,4215	15,420	15,421		SX=0,010
49.	1/4 D:C	2.05	16,2215	16,2255	16,2215	0,0034	0,011
			16,2215	16,2214	16,221		SX=0,003
50.	1/4 D:C	2.05	15,790	15,8435	15,791	0,0529	0,108
			15,791	15,844	15,791		SEE57&49
51.	1/4 D:E	2.10	15,240	15,2445	15,2375	0,0063	0,018
			15,239	15,246	15,2395		SY≈0
52.	1/4 D:E	2.08	15,4665	15,470	15,468	0,0038	0,010
			15,4685	15,473	15,470		SY=0,001
53.	1/4 D:C	2.08	15,606	15,6105	15,605	0,0062	0,012
			15,6065	15,6145	15,6085		SY=-0,016
54.	1/4 D:C	2.05	15,7545	15,759	15,7545	0,0044	0,011
			15,7555	15,7595	15,755		SEE56&60
55.	1/4 D:E	2.05	15,306	15,314	15,308	0,0069	0,012
			15,308	15,315	15,3085		SEE 52&48
56.	1/4 D:E	2.05	15,0885	15,084	15,0865	-0,0083	-0,009
			15,088	15,086	15,090	SY=-0,0013	SY≈0
57.	1/4 D:C	2.05	16,081	16,0735	16,0795	-0,0004	0,003
			16,081	16,0815	16,082		SY≈0,011
58.	1/4 D:E	2.08	15,8385	16,8465	15,8385		NO.42 NOT
			15,8385	16,845	15,8375		WORKING
59.	1/4 D:C	2.08	15,3815	15,375	15,382	0,0070	-0,016
			15,382	15,374	15,3805		SX=0,012
60.	1/4 D:W	2.05	NON-FUNCTIONAL.				
61.	1/4 D:W	2.10	NON-FUNCTIONAL.				
62.	1/4 D:C	2.08	NON-FUNCTIONAL.				

TABLE 11
Strain gauge readings for Model 3 Loadcase 3

READ NO	GUAGE FACTOR	NO	NO LOAD	LOAD	NO LOAD	AV STRAIN	STRESS NOTE
1.	1/4 W:M	2,08	15,3835	15,3365	15,381	-0,0465	-0,154
			15,360	15,3315	15,3775		SY=-0,040
2.	1/4 W:B	2,10	14,466	14,330	14,4645		
			14,4645	14,3205	14,4585		
3.	1/4 W:M	2,08	14,764	14,772	14,7645	0,0066	-0,040
			14,765	14,7705	14,765		SX=-0,151
4.	1/4 W:T	2,10	13,803	13,8355	13,8045		
			13,8045	13,838	13,8045		
5.	1/4 F:W/E	2,05	12,905	12,9845	12,906	0,0800	0,350
			12,905	12,986	12,906		SX=0,299
6.	1/4 F:℄	2,05	14,376	14,396	14,376	0,0016	0,003
			14,3715	14,375	14,3715		SX=-0,004
7.	1/4 F:℄	2,05	14,344	14,368	14,3435	0,0248	0,051
			14,343	14,3665	14,3425		SEE 8&6
8.	1/4 F:℄	2,05	14,5185	14,5175	14,517	-0,0018	-0,004
			14,5155	14,511	14,514		SY=0,003
9.	1/4 F:W/E	2,08	14,8045	14,751	14,8045	-0,0550	-0,302
			14,803	14,7455	14,801		SY=-0,363
10.	1/4 F:W/E	2,05	13,9515	14,0405	13,948	0,0926	0,052
			13,9465	14,0415	13,951		SEE 12&5
11.	1/4 F:W	2,10	11,2665	11,129	11,2655	-0,1478	-0,715
			11,2635	11,1095	11,260		SY=-0,727
12.	1/4 F:W/E	2,05	15,141	15,1985	15,1415	0,0558	0,299
			15,141	15,1945	15,1395		SY=0,350
13.	1/4 F:W/E	2,08	15,1935	15,1085	15,193	-0,0689	-0,368
			15,193	15,1095	15,192		SX=-0,302
14.	1/2 W:M	2,08	12,093	12,0955	12,0825	0,0025	-0,002
			12,0935	12,095	12,0935		SX=-0,024
15.	1/2 W:B	2,10	15,281	15,263	15,282		
			15,2835	15,260	15,2835		
16.	1/2 W:T	2,10	14,549	14,5475	14,5495		
			14,549	14,5485	14,5505		
17.	1/2 W:M	2,08	15,1165	15,1085	15,1165	-0,0080	-0,024
			15,1165	15,1085	15,1165		SY=-0,002
18.	1/2 W:M	2,05	14,285	14,271	14,285	-0,0143	-0,034
			14,285	14,270	14,284		SEE 22&20
19.	1/2 W:T	2,10	14,336	14,340	14,3355		
			14,333	14,3385	14,333		
20.	1/2 W:M	2,05	13,1145	13,1085	13,112	-0,0053	-0,005
			13,112	13,1055	13,1105		SX=0,026
21.	1/2 W:B	2,10	13,6165	13,637	13,6165		
			13,6145	13,6315	13,611		
22.	1/2 W:M	2,05	13,029	13,0385	13,0285	0,0096	0,026
			13,0265	13,036	13,025		SY=-0,005
23.	1/4 F:W	2,10	12,1735	12,3445	12,175	0,1603	0,744
			12,1725	12,336	12,178		SY=0,709
24.	1/2 F:W/E	2,08	14,596	14,586	14,595	-0,0093	-0,019
			14,5955	14,5865	14,5955		SX=0,021
25.	1/2 F:W/E	2,08	15,3895	15,3835	15,391	-0,0087	-0,020
			15,390	15,380	15,3895		SY=0,014
26.	1/2 F:W/E	2,08	15,274	15,2805	15,2735	0,0074	0,014
			15,2735	15,2815	15,2735		SX=-0,020
27.	1/2 F:W	2,10	12,529	12,550	12,5295	0,0200	0,044
			12,527	12,546	12,5265		SY=-0,086
28.	1/2 F:W	2,10	12,2655	12,2465	12,265	-0,0194	-0,044
			12,264	12,244	12,264		SY=0,081
29.	1/2 F:℄	2,10	15,0715	15,0735	15,0715	-0,0012	-0,005
			15,071	15,0665	15,0695		SY=-0,008
30.	1/2 F:W/E	2,08	14,9855	14,899	14,9865	0,0096	0,024
			14,986	14,994	[illegible]		SY=-0,019
31.	1/4 W:B	2,10	[illegible]	[illegible]	[illegible]		
			14,5625	14,712	14,5715		

READ NO	GUAGE FACTOR	NO	NO LOAD	LOAD	NO LOAD	AV STRAIN	STRESS NOTE
32.	1/4 W:M	2,05	12,6295	12,595	12,6265	-0,0301	-0,034
			12,626	12,5965	12,625		SX=0,138
33.	1/4 W:M	2,05	14,4595	14,5155	14,4615	0,0519	0,138
			14,461	14,511	14,4615		SY=-0,034
34.	1/4 W:T	2,10	14,440	14,4055	14,4405		
			14,438	14,4085	14,4415		
35.	1/4 D:W/E	2,08	15,461	15,4205	15,4595	-0,0381	-0,247
			15,4595	15,4235	15,4605		SY=-0,348
36.	1/4 D:W	2,10	NON-FUNCTIONAL				LOADING
							POINT
37.	1/4 D:℄	2,05	15,8745	15,874	15,875	0,0001	0,002
			15,8745	15,8765	15,8765		SY=0,003
38.	1/4 D:℄	2,05	15,659	15,678	15,659	0,0194	0,040
			15,6595	15,6795	15,660		SEE 37&43
39.	1/4 D:W/E	2,05	15,634	15,648	15,6355		NO. 62 NOT
			15,6365	15,6515	15,635		WORKING
40.	1/4 D:E	2,10	15,151	15,1195	15,151	-0,0304	-0,089
			15,145	15,1165	15,1465		SY=0
41.	1/4 D:W	2,10	14,526	14,573	14,526		LOADING
			14,522	14,571	14,5245		POINT
42.	1/4 D:W/E	2,08	15,7395	15,833	15,740		NO. 61 NOT
			15,7395	15,8325	15,740		WORKING
43.	1/4 D:E	2,05	16,1765	16,1785	16,176	0,0009	0,005
			16,175	16,174	16,174		SX=0,002
44.	1/4 D:W/E	2,05	15,5495	15,498	15,5485	-0,0490	-0,153
			15,5465	15,501	15,5475		SY=-0,025
45.	1/4 D:W/E	2,05	15,405	15,3905	15,4065	-0,0150	0,008
			15,406	15,3915	15,4065		SEE 44&46
46.	1/4 D:W/E	2,05	15,499	15,5105	15,4985	0,0118	-0,025
			15,4985	15,510	15,498		SX=0,153
47.	1/2 D:W/E	2,10	14,984	14,9765	14,982	-0,0058	-0,017
			14,9815	14,9765	14,9815		SY=0
48.	1/2 D:E	2,10	14,5055	14,5085	14,5055	0,0039	0,011
			14,5055	14,5095	14,504		SY=0
49.	1/2 D:W/E	2,08	15,575	15,570	15,575	-0,0050	-0,013
			15,5735	15,5685	15,5735		SX=0,004
50.	1/2 D:℄	2,10	16,0085	16,011	16,008	0,0035	0,012
			16,008	16,013	16,0095		SY=0,004
51.	1/2 D:W	2,10	14,9845	14,9785	14,984	-0,0041	0,002
			14,981	14,980	14,984		SY=0,037
52.	1/2 D:W/E	2,08	15,0955	15,098	15,096	0,0030	0,004
			15,0935	15,098	15,095		SY=-0,013
53.	1/2 D:W/E	2,08	15,6145	15,6205	15,614	0,0061	0,020
			15,6135	15,6195	15,6135		SX=0,005
54.	1/2 D:W/E	2,10	15,988	15,9985	15,989	0,0069	0,020
			15,989	15,9965	15,9905		SY≈0
55.	1/2 D:W/E	2,08	15,236	15,2345	15,2365	-0,0009	0,006
			15,2335	15,2335	15,2335		SY=0,020
56.	1/4 D:E	2,10	14,922	14,9485	14,9215	0,0271	-0,011
			14,9805	14,9435	14,9235		SY=0
57.	1/2 D:W	2,10	14,511	14,515	14,5105	0,0048	0,002
			14,5075	14,514	14,510		SY=-0,030
58.	1/2 D:E	2,10	15,316	15,309	15,3155	-0,0058	-0,017
			15,3145	15,3105	15,316		SY=0
59.	1/4 D:E/W	2,05	14,0945	14,131	14,094		NO. 62 NOT
			14,0935	14,1345	14,0935		WORKING
60.	1/4 D:W/E	2,08	15,8635	15,7765	15,862	-0,0864	-0,348
			15,8615	15,7745	15,8605		SX=-0,247
61.	1/4 D:W/E	2,08	NON-FUNCTIONAL				
62.	1/4 D:W/E	2,05	NON-FUNCTIONAL				

TABLE 12

Strain gauge readings for Model 3 Loadcase 4

READ NO	GUAGE FACTOR	NO	NO LOAD	LOAD	NO LOAD	AV STRAIN	STRESS NOTE	READ NO	GUAGE FACTOR	NO	NO LOAD	LOAD	NO LOAD	AV STRAIN	STRESS NOTE
1.	1/4W:M	2.08	15,4805	15,481	15,477	0,0034	0,004 Sx=-0,014	32.	1/4F:E	2.08	14,496	14,491	14,4915	-0,0018	-0,005 Sx=-0,003
		2.08	15,475	15,4785	15,472					2.10	14,492	14,494	14,4945		
2.	1/4W:M	2.08	15,505	15,4935	15,504	-0,0054	-0,014 SY=0,004	33.	1/4F:W	2.10	12,183	12,2345	12,185	0,0507	0,159 SY=0,027
		2.08	15,502	15,4955	15,5005					2.10	12,184	12,241	12,190		
3.	1/4W:B	2.10	14,8085	14,8305	14,805			34.	1/4F:W	2.08	14,053	14,0975	14,054	0,0431	0,065 SEE 38&40
		2.10	14,8035	14,8245	14,8035					2.08	14,0535	14,0955	14,053		
4.	1/4W:T	2.10	13,975	13,944	13,974			35.	1/4F:E	2.05	14,4435	14,471	14,4465	0,0234	0,051 SEE 37&39
		2.10	13,9745	13,940	13,971					2.05	14,4455	14,4685	14,4414		
5.	1/4W:B	2.10	14,7205	14,721	14,7205			36.	1/4F:W	2.10	11,334	11,318	11,3295	-0,0179	-0,066 SY=0,036
		2.10	14,7185	14,716	14,7185					2.10	11,326	11,3025	11,321		
6.	1/4W:M	2.05	14,5405	14,553	14,5395	0,0140	0,011 SY=-0,077	37.	1/4F:E	2.05	14,5865	14,588	14,5865	-0,0003	-0,003 SY=-0,005
		2.05	14,539	14,555	14,541					2.05	14,5865	14,5845	14,584		
7.	1/4W:M	2.08	13,410	13,379	13,409	-0,0278	-0,077 SX=0,011	38.	1/4F:W	2.08	16,0555	16,0895	16,051	0,0355	0,108 SY=0,011
		2.08	13,4085	13,384	13,409					2.08	16,0495	16,084	16,049		
8.	1/4W:T	2.10	14,693	14,7255	14,694			39.	1/4F:W	2.08	15,161	15,128	15,1615	0,0358	-0,112 SX=-0,020
		2.10	14,6945	14,727	14,6935					2.08	15,1595	15,1145	15,154		
9.	1/4D:W	2.05	14,4815	14,468	14,4795	-0,0123	-0,007 SEE 13&18	40.	1/4F:W	2.05	14,6165	14,6035	14,614	0,0108	0,011 SX=0,108
		2.05	14,479	14,4635	14,475					2.05	14,614	14,6045	14,6145		
10.	1/4D:W	2.08	15,868	15,8555	15,868	0,0144	-0,095 SX=0,135	41.	1/4F:W	2.08	15,657	15,6635	15,654	0,0083	-0,020 SX=-0,112
		2.08	15,868	15,8505	15,8655					2.08	15,655	15,664	15,656		
11.	1/4D:E	2.10	15,0035	15,0015	15,001	-0,0004	0,001 SY=0	42.	1/2F:W	2.08	14,147	14,151	14,1465	0,0048	0,014 SX=0,000
		2.10	15,001	15,001	15,0005					2.08	14,1445	14,152	14,147		
12.	1/4D:E	2.08	15,066	15,064	15,068	-0,0023	-0,004 SY=0,006	43.	1/2F:W	2.08	14,446	14,4335	14,4455	-0,0056	-0,014 SX=0,007
		2.08	15,069	15,069	15,072					2.08	14,4455	14,441	14,4465		
13.	1/4D:W	2.08	14,569	14,5455	14,5655	-0,0199	-0,073 SX=0,038	44.	1/2F:W	2.10	12,5135	12,526	12,515	0,0093	0,016 SY=-0,028
		2.08	14,5665	14,548	14,566					2.10	12,515	12,5215	12,5135		
14.	1/4D:W	2.05	14,8145	14,8285	14,8155	0,0135	0,019 SEE 26&29	45.	1/2F:W	2.08	15,190	15,1905	15,191	-0,0018	0,000 SY=0,014
		2.05	14,8135	14,829	14,8155					2.08	15,1905	15,186	15,1885		
15.	1/4D:E	2.08	15,335	15,3385	15,335	0,0026	0,006 SX=0,004	46.	1/2F:W	2.10	12,2705	12,2445	12,2705	-0,0075	-0,011 SY=0,028
		2.08	15,335	15,336	15,3335					2.10	12,271	12,2605	12,268		
16.	1/4D:W	2.10	14,6505	14,6335	14,6495		LOADING POINT.	47.	1/2F:E	2.10	15,0935	15,0745	15,0745	-0,0008	-0,002 SY=0,000
		2.10	14,6485	14,6335	14,649					2.10	15,0935	15,091	15,0915		
17.	1/4D:E	2.10	15,2165	15,2135	15,2165	-0,0024	0,007 SY=0	48.	1/2F:E	2.08	14,7695	14,7785	14,7705	0,0041	0,007 SX=-0,014
		2.10	15,2155	15,2145	15,216					2.08	14,770	14,772	14,7715		
18.	1/4D:E	2.05	14,468	14,466	14,4635	-0,0031	-0,038 SX=0,013	49.	1/2D:E	2.10	14,5155	14,5145	14,515	0,0010	0,003 SY=0
		2.05	14,467	14,4645	14,469					2.10	14,5155	14,5185	14,516		
19.	1/4D:E	2.05	14,654	14,673	14,655	0,0189	0,039 SEE 12&15	50.	1/2D:E	2.10	15,357	15,3545	15,355	-0,0008	0,002 SY=0
		2.05	14,654	14,674	14,6555					2.10	15,355	15,356	15,357		
20.	1/4D:W	2.08	15,6165	15,6345	15,6185		NO 30 NOT WORKING	51.	1/2D:W	2.10	14,3935	14,3895	14,3935	-0,0023	-0,007 SY=0
		2.08	15,6165	15,632	15,6155					2.10	14,3935	14,3835	14,3945		
21.	1/4D:E	2.05	14,135	14,1435	14,1365	0,0146	0,043 SY=0	52.	1/2D:W	2.10	14,5335	14,5335	14,5335	0,0006	-0,001 SY=-0,008
		2.05	14,1385	14,153	14,1365					2.10	14,5335	14,536	14,536		
22.	1/4D:W	2.08	15,947	15,9085	15,947	-0,0038	-0,135 SX=-0,095	53.	1/2D:W	2.10	15,021	15,0165	15,021	-0,0029	-0,001 SY=0,019
		2.08	15,947	15,9165	15,950					2.10	15,021	15,021	15,0235		
23.	1/2W:M	2.08	15,6145	15,6115	15,615	-0,0038	-0,012 SY=-0,003	54.	1/2D:W	2.08	15,606	15,604	15,6055	-0,0008	0,002 SY=0,012
		2.08	15,615	15,6105	15,6145					2.08	15,606	15,6065	15,6065		
24.	1/2W:M	2.08	12,108	12,1065	12,106	0,0006	-0,003 SX=-0,012	55.	1/2D:W	2.08	16,0985	16,100	16,1015	-0,0008	-0,001 SX=0,002
		2.08	12,107	12,108	12,1035					2.08	16,102	16,101	16,103		
25.	1/2W:B	2.10	15,2905	15,2835	15,291			56.	1/2D:E	2.05	16,1985	16,164	16,160	0,0038	0,012 SX=0,007
		2.10	15,291	15,280	15,2885					2.05	16,159	16,162	16,1595		
26.	2W:T	2.10	14,560	14,559	14,5605			57.	1/2W:M	2.08	14,313	14,3555	14,3735	-0,0183	-0,039 SEE 6&59
		2.10	14,561	14,561	14,563					2.08	14,313	14,354	14,3725		
27.	1/2D:E	2.10	16,041	16,0425	16,0415	0,0023	0,009 SY=0,006	58.	1/2W:T	2.10	12,8085	12,813	12,808		
		2.10	16,0415	16,048	16,046					2.10	12,808	12,8115	12,8165		
28.	1/2D:W	2.10	15,9835	15,9845	15,9835	0,0013	0,004 SY=0	59.	1/2W:M	2.05	12,978	12,975	12,977	-0,0029	-0,005 SX=0,010
		2.10	15,984	15,9865	15,986					2.05	12,977	12,9745	12,9785		
29.	1/4D:W	2.05	NON-FUNCTIONAL.					60.	1/2W:B	2.10	13,5795	13,591	13,5795		
										2.10	13,5795	13,5865	13,577		
30.	1/4D:W	2.08	NON-FUNCTIONAL.					61.	1/2W:M	2.08	14,4165	14,4285	14,417	0,0039	0,010 SX=-0,005
										2.08	14,4165	14,421	14,4175		
31.	1/2D:W	2.10	NON-FUNCTIONAL.				LOADING POINT	62.	1/2D:W	2.10	15,5935	15,596	15,5935	0,0009	0,007 SY=-0,001
										2.10	15,5985	15,600	15,5995		

TABLE 13.
Strain gauge reading for Model 4 Loadcase 1

READ NO	GUAGE FACTOR	NO	NO LOAD	LOAD	NO LOAD	AV STRAIN	STRESS NOTE
(1) 1.	1/4 W:T L (L)	2,10	14,4265	14,392	14,4265	-0,0350	-0,102
			14,427	14,392	14,428		SY≈0
(1) 2.	1/4 W M L (L)	2,08	14,8005	14,8865	14,801	0,0956	0,277
			14,801	14,8865	14,801		SY=-0,004
(1) 3.	1/4 W:B L (L)	2,10	14,833	15,095	14,8415	0,2574	-0,751
			14,835	15,0935	14,838		SY≈0
(1) 4.	1/4 W:M L (L)	2,05	15,3055	15,2965	15,3045	-0,0085	-0,078
			15,3055	15,2965	15,3046		SEE 2&5
(1) 5.	1/4 W:M L	2,05	15,190	15,1505	15,1885	-0,0385	-0,004
			15,189	15,151	15,1895		SX=0,277
(1) 6.	1/2 W:T L (L)	2,10	14,406	14,3085	14,4035	-0,0969	-0,283
			14,405	14,3095	14,405		SY≈0
(1)(9) 7.	1/2 W:B L (L)	2,10	14,855	15,405	14,869	0,5379	-1,570
			14,858	15,397	14,863		SY≈0
(1) 8.	1/2 W:M L (L)	2,08	15,368	15,568	15,373	0,1071	0,571
			15,3665	15,5665	15,371		SY=-0,010
(1) 9.	1/2 W:M L	2,08	15,421	15,340	15,420	-0,0798	-0,010
			15,421	15,3415	15,420		SX=0,511
(1) 10.	1/4 F:℄	2,05	15,479	15,3755	15,475	-0,1009	-0,019
			15,477	15,376	15,4755		SX=-0,723
(1)(9) 11.	1/4 F:W L (L)	2,10	12,2385	12,544	12,248	0,2954	-0,857
			12,241	12,537	12,246		SY≈0,012
(1) 12.	1/4 D: W/E L (L)	2,08	15,9885	15,8315	15,9845	-0,1548	-0,451
			15,9875	15,831	15,9835		SY=0,001
(1) 13.	1/4 F:℄ (45)	2,05	15,538	15,629	15,5385	0,0906	0,034
			15,538	15,6285	15,538		SEE 13&10
(1) 14.	1/4 F:W R (L)	2,10	11,344	11,643	11,3485	0,2959	-0,863
			11,345	11,642	11,349		SY≈0,000
(1) 15.	1/4 F: W/E R (L)	2,08	15,393	15,660	15,397	0,2641	0,770
			15,394	15,6595	15,3985		SY=-0,003
(3) 16.	1/4 D:E L (L)	2,10	15,2145	15,049	15,209	-0,1608	-0,469
			15,213	15,0585	15,2115		SY≈0
(1) 17.	1/4 D: W/E L	2,05	15,531	15,589	15,5315	0,0583	0,011
			15,5315	15,590	15,531		SX=-0,409
(1) 18.	1/4 F:℄ (L)	2,05	15,701	15,9555	15,7065	0,2494	0,723
			15,704	15,952	15,706		SY=-0,015
(3) 19.	1/4 F: W/E L (45)	2,05	15,013	15,122	15,016	0,1073	0,073
			15,014	15,122	15,016		SEE 20&22
(3) 20.	1/4 F: W/E L (L)	2,05	16,1505	16,396	16,155	0,2423	0,703
			16,1505	16,394	16,155		SY=-0,009
(1) 21.	1/4 F: W/E R (T)	2,08	15,728	15,6215	15,7235	-0,1039	-0,003
			15,7265	15,6215	15,7235		SX=0,110
(3) 22.	1/4 F: W/E L (T)	2,05	14,024	13,925	14,021	-0,0970	-0,009
			14,0235	13,926	14,0215		SX=-0,703
(3) 23.	1/4 D:W R (L)	2,10	14,4745	14,306	14,471		No. 36&58
			14,4745	14,3065	14,472		NOT WORKING
(3) 24.	1/4 D:E R (L)	2,10	14,3615	14,788	14,358	-0,1714	-0,500
			14,3615	14,788	14,3565		SY≈0
(3)(8) 25.	1/4 D:℄ (L)	2,05	16,063	15,912	16,058	-0,1466	-0,426
			16,061	15,914	16,059		SY=-0,005
(2) 26.	1/4 D:℄ (45)	2,08	15,8315	15,782	15,8315	-0,0496	-0,012
			15,832	15,782	15,8315		SEE 25&29
(3) 27.	1/4 D: W/E L (L)	2,05	15,514	15,371	15,511	-0,1415	-0,409
			15,514	15,3715	15,512		SY=-0,011
(3) 28.	1/4 D: W/E (45)	2,05	15,518	15,456	15,5165	-0,0613	-0,041
			15,518	15,456	15,5165		SEE 27&17
(3) 29.	1/4 D:℄ (T)	2,05	16,2995	16,359	16,301	0,0586	0,005
			16,300	16,3585	16,300		SX=-0,426
(3) 30.	1/4 D: E/W	2,08	15,7565	15,737	15,7565	-0,0193	0,049
			15,758	15,7385	15,757		SEE 31&28
(3) 31.	1/4 D:E	2,10	15,2745	15,133	15,271	-0,1390	-0,406
			15,2745	15,134	15,2715		SY≈0

READ NO	GUAGE FACTOR	NO	NO LOAD	LOAD	NO LOAD	AV STRAIN	STRESS NOTE
(3) 32.	1/4 D: W/E L (L)	2,08	15,9185	15,979	15,919	0,0605	0,001
			15,919	15,981	15,9215		SX=-0,451
(3) 33.	1/4 D: W/E R (L)	2,08	16,276	16,3386	16,277		NO. 38 NOT
			16,276	16,3375	16,2765		WORKING
(3) 34.	1/2 F:W R (L)	2,10	12,2365	12,8495	12,249	0,6076	-1,781
			12,239	12,8525	12,249		SY≈0,0046
(8) 35.	1/2 F:W L (L)	2,10	12,258	12,866	12,275	0,5988	-1,762
			12,261	12,8685	12,270		SY≈0,0038
36.	1/4 D: E/W R (L)	2,08	NON-FUNCTIONAL.				
37.	1/4 D:W L (L)	2,10	NON-FUNCTIONAL.				
38.	1/4 D: W/E R (L)	2,08	NON-FUNCTIONAL.				
(3) 39.	1/2 F:℄ (L)	2,10	15,0815	15,645	15,109	0,5420	-1,598
			15,0935	15,639	15,106		SY≈0,0042
(3) 40.	1/2 F: W/E R (T)	2,08	15,112	14,932	15,106	-0,1771	0,044
			15,111	14,9325	15,1085		SX=-1,438
(3) 41.	1/2 F: W/E R (L)	2,08	15,474	15,9665	15,483	0,4870	1,439
			15,479	15,968	15,483		SY=-0,044
(3) 42.	1/2 F: W/E L (L)	2,08	15,9146	16,4115	15,9215	0,4930	1,454
			15,9165	16,4115	15,9215		SY=-0,040
(1) 43.	1/2 F: W/E L (T)	2,08	16,524	16,339	16,518	-0,1808	0,040
			16,522	16,3405	16,518		SX=-1,454
(1) 44.	1/4 W:B R (L)	2,10	14,2865	14,555	14,2915	0,2651	-0,774
			14,289	14,556	14,2945		SY≈0
(1) 45.	1/4 W:T R (L)	2,10	13,7966	13,7635	13,7965	-0,0328	-0,096
			13,796	13,7635	13,796		SY≈0
(1) 46.	1/4 W:M R (T)	2,08	16,3015	16,2635	16,300	-0,0365	0,003
			16,303	16,266	16,3005		SX=-0,081
(1) 47.	1/4 W:M R (L)	2,08	16,9015	16,997	16,9015	0,0959	0,281
			16,9015	16,9975	16,901		SY=-0,003
(1) 48.	1/2 W:M R (L)	2,08	16,399	16,585	16,4025	0,1839	0,534
			16,401	16,585	16,402		SY=-0,006
(1) 49.	1/2 W:T R (L)	2,10	14,354	14,270	14,352	-0,0823	-0,240
			14,353	14,271	14,352		SY≈0
(1) 50.	1/2 W:M R (T)	2,08	16,7285	16,654	16,7255	-0,0734	-0,006
			16,727	16,6515	16,7235		SX=-0,534
(1) 51.	1/2 W:B R (L)	2,10	14,898	15,431	14,9065	0,5258	-1,534
			14,898	15,425	14,9065		SY≈0
(3) 52.	1/2 D: W/E L (L)	2,08	16,441	16,129	16,4345	-0,3086	-0,901
			16,440	16,129	16,435		SY=-0,001
(1) 53.	1/2 D:℄ (L)	2,10	16,0135	15,667	16,0065	-0,3418	-0,999
			16,0115	15,6695	16,0085		SY≈0,004
(3) 54.	1/2 D:E L (L)	2,10	14,496	14,1915	14,4815	-0,3023	-0,882
			14,499	14,194	14,4935		SY≈0
(3) 55.	1/2 D:E R (L)	2,10	15,265	14,958	15,258	-0,3085	-0,886
			15,264	14,9585	15,260		SY≈0
(3) 56.	1/2 D: W/E L (L)	2,10	15,951	15,6175	15,946	-0,3315	-0,967
			15,9515	15,617	15,9465		SY≈0
(3) 57.	1/2 D:W L (L)	2,10	14,5015	14,1585	14,4955		LOADING
			14,501	14,1465	14,4935		POINT
(3) 58.	1/2 D:W R (L)	2,10	NON-FUNCTIONAL.				LOADING
							POINT
(1)(8) 59.	1/2 D: W/E L (45)	2,08	17,1395	17,2615	17,1415	0,1201	-0,001
			17,132	17,2515	17,1335		SX=-0,901
(1) 60.	1/2 D: W/E R (L)	2,08	16,6775	16,344	16,6665	-0,3249	-0,951
			16,6715	16,346	16,664		SY=-0,007
(3) 61.	1/2 D: E/W R	2,08	16,061	16,188	16,064	0,1248	-0,007
			16,063	16,1865	16,062		SX=-0,351
(3) 62.	1/2 D:E R	2,10	14,935	14,5945	14,9265	-0,3358	-0,980
			14,933	14,594	14,9255		SY≈0

TABLE 14
Strain gauge reading for Model 4 Loadcase 2

READ NO	GUAGE FACTOR	NO	NO LOAD	LOAD	NO LOAD	AV STRAIN	STRESS NOTE
1.	1/4 W:B	2,10	14,3114	14,326	14,3114		
			14,3135	14,323	14,3105		
2.	1/4 W:M	2,08	14,976	14,9735	14,9765	-0,0029	-0,004 SX=0,012
			14,978	14,974	14,976		
3.	1/4 W:T	2,10	13,794	13,796	13,7935		
			13,7925	13,795	13,7935		
4.	1/4 W:M	2,08	15,3285	15,3335	15,328	0,0048	0,012 SY=0,004
			15,3285	15,3315	15,326		
5.	1/2 F:€	2,08	15,819	15,881	15,826	0,0553	0,277 SY=0,297
			15,821	15,872	15,819		
6.	1/2 F:€	2,08	17,260	17,3235	17,2585	0,0648	0,297 SX=0,277
			17,261	17,3265	17,2615		
7.	1/2 F:W	2,10	12,146	12,016	12,146	-0,1335	-0,628 SY=0,611
			12,146	12,004	12,136		
8.	1/2 F:€	2,08	15,094	15,020	15,030	-0,0103	-0,308 SX=0,263
			15,093	15,025	15,094		
9.	1/2 F:W	2,10	12,1735	12,3235	12,180	0,1456	0,659 SY=0,600
			12,176	12,3135	12,174		
10.	1/2 F:W	2,08	15,470	15,4255	15,4715	-0,0491	-0,263 SY=-0,308
			15,470	15,415	15,466		
11.	1/2 F:€	2,10	15,025	15,0305	15,028	0,0009	0,000 SY=-0,006
			15,026	15,0215	15,0205		
12.	1/2 D:€	2,08	16,099	16,176	16,103	0,0151	0,804 SX=0,217
			16,0985	16,176	16,101		
13.	1/2 D:€	2,10	14,9085	14,9515	14,908	0,0449	0,181 SY=0
			14,909	14,958	14,912		
14.	1/2 D:€	2,08	16,084	16,0165	16,0835	-0,0674	-0,282 SX=-0,219
			16,084	16,015	16,081		
15.	1/2 D:€	2,08	15,4715	15,506	15,4735	0,0336	0,217 SY=0,304
			15,474	15,511	15,477		
16.	1/2 D:€	2,10	15,979	15,925	15,9765	-0,0481	-0,143 SY=0
			15,979	15,935	15,982		
17.	1/2 D:E	2,10	14,523	14,494	14,5195	-0,0249	-0,073 SY=0
			14,523	14,503	14,5265		
18.	1/2 D:W	2,10	14,5315	14,454	14,5285		LOADING POINT
			14,531	14,4485	14,534		
19.	1/2 D:E	2,10	15,2935	15,313	15,291	0,0219	0,064 SY=0
			15,2915	15,3165	15,2955		
20.	1/2 D:€	2,08	15,562	15,521	15,560	0,0373	-0,219 SX=-0,282
			15,562	15,529	15,565		
21.	1/2 D:€	2,10	16,0085	16,004	16,0065	-0,0024	-0,003 SY=0,011
			16,008	16,009	16,011		
22.	1/2 D:W	2,10	NON-FUNCTIONAL.				LOADING POINT.
23.	1/2 W:B	2,10	15,046	14,931	15,047		
			15,0485	14,9225	15,041		
24.	1/2 W:M	2,08	17,0815	17,040	17,0735	-0,0578	-0,184 SY=-0,061
			17,0715	17,031	17,0665		
25.	1/2 W:M	2,08	17,5145	17,511	17,5115	-0,0029	-0,061 SX=-0,134
			17,5155	17,511	17,5114		
26.	1/2 W:T	2,10	14,3685	14,380	14,369		
			14,3685	14,382	14,371		
27.	1/4 D:€	2,08	17,735	17,7315	17,735	-0,0040	-0,008 SX=-0,009
			17,7365	17,7305	17,7345		
28.	1/4 D:€	2,08	17,859	17,8625	17,8565		NO.62 NOT WORKING
			17,851	17,8535	17,848		
29.	1/4 D:E	2,10	15,0095	15,0015	15,005	-0,0036	0,011 SY=0
			15,007	15,005	15,007		
30.	1/4 D:E	2,08	15,1415	15,151	15,1425	0,0089	0,020 SEE 52&61
			15,144	15,153	15,1445		
31.	1/4 F:W	2,10	12,339	12,3315	12,3415	-0,0105	-0,026 SY=0,011
			12,341	12,3265	12,3345		
32.	1/4 D:E	2,05	15,2235	15,2205	15,222	-0,0020	-0,006 SY=0
			15,2235	15,222	15,224		
33.	1/4 D:W	2,10	NON-FUNCTIONAL.				
34.	1/4 W:T	2,10	14,443	14,4405	14,443		
			14,4415	14,439	14,4415		
35.	1/4 W:M	2,08	13,628	13,625	13,6285	0,0040	-0,015 SY=-0,008
			13,6285	13,623	13,627		
36.	1/4 W:B	2,10	14,8345	14,826	14,834		
			14,833	14,818	14,826		
37.	1/4 W:M	2,08	14,153	14,116	14,1535	0,0373	-0,079 SEE 36&38
			14,154	14,1165	14,1535		
38.	1/4 W:M	2,08	14,056	14,0555	14,056	0,0006	-0,008 SX=-0,015
			14,054	14,054	14,0555		
39.	1/2 W:T	2,10	14,4185	14,388	14,4165		
			14,417	14,396	14,419		
40.	1/2 W:B	2,10	14,8665	15,011	14,8744		
			14,868	14,8965	14,866		
41.	1/2 W:M	2,08	15,378	15,4315	15,3815	0,0499	0,160 SY=0,051
			15,379	15,427	15,379		
42.	1/2 W:M	2,08	15,4515	15,440	15,452	-0,0086	0,037 SY=0,160
			15,452	15,448	15,455		
43.	1/4 D:€	2,05	15,537	15,588	15,5375	0,0510	0,103 SEE 58&50
			15,539	15,5915	15,5415		
44.	1/4 D:W	2,10	15,2465	15,2555	15,2465	0,0089	0,017 SEE 56&57
			15,2465	15,256	15,248		
45.	1/4 F:€	2,10	15,4845	15,488	15,483	0,0045	0,010 SX=-0,007
			15,4835	15,4885	15,484		
46.	1/4 F:€	2,05	15,533	15,589	15,534	0,0553	0,115 SEE 61&45
			15,538	15,588	15,533		
47.	1/4 F:W	2,10	11,4835	11,5085	11,486	0,0128	0,038 SY=0,001
			11,4335	11,5035	11,490		
48.	1/4 F:€	2,08	15,469	15,4785	15,472	0,0060	0,019 SY=-0,003
			15,4715	15,4735	15,4675		
49.	1/4 D:E	2,10	15,1785	15,181	15,178	0,0085	0,010 SY=0
			15,1785	15,184	15,181		
50.	1/4 D:€	2,10	16,265	16,270	16,266	0,0041	0,014 SX=0,005
			16,2655	16,269	16,265		
51.	1/4 F:€	2,08	15,6935	15,6915	15,694	-0,0038	-0,007 SY=0,010
			15,6915	15,686	15,689		
52.	1/4 F:€	2,08	15,100	15,155	15,1015	0,0536	0,114 SEE 53&55
			15,101	15,154	15,101		
53.	1/4 F:€	2,08	16,194	16,190	16,1965	-0,0063	-0,015 SY=0,008
			16,195	16,186	16,1915		
54.	1/4 F:€	2,08	15,7135	15,7105	15,713	-0,0015	0,003 SX=0,019
			15,7135	15,714	15,7155		
55.	1/4 F:W	2,08	14,096	14,0385	14,094	0,0048	0,008 SX=-0,015
			14,0945	14,101	14,0385		
56.	1/4 D:W	2,05	15,2815	15,281	15,2805	0,0014	0,005 SY=0,003
			15,277	15,2815	15,280		
57.	1/4 D:W	2,05	14,3655	14,3665	14,367	0,0003	0,008 SX=0,005
			14,3665	14,3675	14,368		
58.	1/4 D:€	2,05	15,812	15,8115	15,812	-0,0001	0,005 SY=0,014
			15,814	15,8155	15,816		
59.	1/4 D:€	2,08	15,984	15,987	15,9835	0,0041	0,009 SX=-0,008
			15,9855	15,991	15,9865		
60.	1/4 D:W	2,10	14,478	14,4715	14,476		NO.62 NOT WORKING
			14,478	14,4735	14,479		
61.	1/4 D:E	2,05	NON-FUNCTIONAL.				
62.	1/4 D:E	2,08	NON-FUNCTIONAL.				

TABLE 15
Strain gauge reading for Model 4 Loadcase 4

READ NO	GUAGE FACTOR	NO	NO LOAD	LOAD	NO LOAD	AV STRAIN	STRESS NOTE
1.	1/4 W:T	2,10	14,428	14,986	14,428		
		2,7	14,428	14,3855	14,428		
2.	1/4 W:M	2,10	14,8005	14,8335	14,801	0,0926	0,268 SY=-0,005
		2,7	14,800	14,893	14,801		
3.	1/4 W:B	2,10	14,838	15,096	14,841		
		2,7	14,8385	15,0965	14,8435		
4.	1/4 W:M	2,10	15,304	15,3235	15,3065	0,0114	-0,021 SEE 7&5.
		2,7	15,3065	15,3235	15,3075		
5.	1/4 W:M	2,10	15,1865	15,1515	15,189	-0,0375	-0,005 SX=0,268
		2,7	15,1895	15,152	15,190		
6.	1/2 W:T	2,10	14,4065	14,384	14,4065		
		2,7	14,4065	14,384	14,406		
7.	1/2 W:B	2,10	14,857	14,981	14,858		
		2,7	14,853	14,975	14,856		
8.	1/2 W:M	2,10	15,3585	15,404	15,359	0,0453	0,182 SY=0,000
		2,7	15,3585	15,404	15,359		
9.	1/2 W:M	2,8	15,421	15,4036	15,4215	-0,0176	0,000 SX=0,132
		2,7	15,421	15,4035	15,421		
10.	1/4 F:E	2,10	15,4705	15,4145	15,4735	-0,0594	0,092 SX=0,500
		2,7	15,476	15,416	15,4745		
11.	1/4 F:W	2,10	12,2415	12,540	12,246	0,2976	0,965 SY=0,248
		2,7	12,242	12,543	12,246		
12.	1/4 D:W	2,10	15,9865	15,6565	15,9865	-0,1326	-0,434 SY=-0,120
		2,7	15,2905	15,854	15,986		
13.	1/4 F:E	2,10	15,5385	15,615	15,539	0,0761	0,045 SEE 12&10
		2,7	15,539	15,6155	15,540		
14.	1/4 F:W	2,10	11,3415	11,523	11,345	0,1793	0,445 SY=-0,200
		2,7	11,3425	11,522	11,344		
15.	1/4 F:W	2,8	15,3935	15,5615	15,3955	0,1661	0,451 SX=-0,088
		2,7	15,3935	15,560	15,396		
16.	1/4 D:E	2,10	15,2215	15,1035	15,219	-0,1164	-0,340 SY=0
		2,7	15,2225	15,106	5,2215		
17.	1/4 D:E	2,8	15,538	15,581	15,536	0,0438	-0,012 SX=-0,358
		2,7	15,534	15,578	15,535		
18.	1/4 F:E	2,10	15,702	15,871	15,7045	0,1684	0,500 SX=0,022
		2,7	15,6985	15,869	15,7015		
19.	1/4 F:E	2,10	15,0165	15,119	15,019	0,1018	0,049 SEE 20&22
		2,7	15,0185	15,121	15,019		
20.	1/4 F:E	2,10	16,153	16,346	16,154	0,1921	0,614 SX=0,136
		2,7	16,1515	16,345	16,155		
21.	1/4 F:W	2,10	15,724	15,633	15,722	-0,0903	-0,068 SX=-0,451
		2,7	15,7235	15,632	15,7215		
22.	1/4 F:E	2,10	14,022	13,986	14,021	-0,0354	0,136 SX=-0,614
		2,7	14,0225	13,9865	14,021		
23.	1/4 D:W	2,10	14,4765	14,368	14,4765	-0,1084	-0,226 SY=0,231
		2,7	14,477	14,367	14,4745		
24.	1/4 D:E	2,10	14,9605	14,854	14,957	-0,1061	-0,307 SY=0
		2,7	14,961	14,854	14,958		
25.	1/4 D:E	2,10	16,066	15,9565	16,062	-0,1016	-0,315 SY=-0,003
		2,7	16,065	15,9565	16,0635		
26.	1/4 D:E	2,10	15,8365	15,8075	15,836	0,0290	0,009 SEE 25&29
		2,7	15,836	15,806	15,8345		
27.	1/4 D:W	2,10	15,519	15,398	15,518	-0,1210	-0,368 SY=-0,012
		2,7	15,519	15,3966	15,517		
28.	1/4 D:W	2,10	15,5205	15,4735	15,5185	-0,0460	-0,016 SEE 27&17
		2,7	15,5195	15,473	15,5185		
29.	1/4 D:E	2,10	16,299	16,3415	16,3005	0,0411	-0,003 SX=-0,316
		2,7	16,300	16,341.	16,301		
30.	1/4 D:W	2,8	15,761	15,7425	15,7595	-0,0174	0,019 SEE 31&26
		2,7	15,761	15,7435	15,766		
31.	1/4 D:W	2,8	15,2765	15,1885	15,214	-0,0866	-0,298 SY=0
		2,7	15,276	15,1885	15,214		

READ NO	GUAGE FACTOR	NO	NO LOAD	LOAD	NO LOAD	AV STRAIN	STRESS NOTE
32.	1/4 D:W	2,8	15,9268	15,9383	15,921	0,0168	-0,120 SX=-0,438
		2,7	15,9205	15,937	15,9215		
33.	1/4 D:E	2,8	16,278	16,3535	16,279		NO.33 NOT WORKING
		2,7	16,278	16,3535	16,279		
34.	1/2 F:W	2,10	12,2355	12,382	12,2365	0,1466	0,424 SY=-0,011
		2,7	12,235	12,384	12,2385		
35.	1/2 F:W	2,10	12,2585	12,3855	12,2615	0,1365	0,388 SY=0,008
		2,7	12,2605	12,389	12,2635		
36.	1/4 D:E	2,8	NON-FUNCTIONAL.				
37.	1/4 D:W	2,10	NON-FUNCTIONAL.				LOADING POINT.
38.	1/4 D:E	2,8	NON-FUNCTIONAL.				
39.	1/2 F:E	2,10	15,084	15,239	15,0865	0,1484	0,418 SY=-0,002
		2,7	15,0835	15,238	15,0865		
40.	1/2 F:E	2,8	15,1135	15,061	15,1115	-0,0511	-0,006 SX=0,367
		2,7	15,113	15,0615	15,1115		
41.	1/2 F:E	2,8	15,475	15,6015	15,476	0,1266	0,869 SY=-0,006
		2,7	15,475	15,603	15,4765		
42.	1/2 F:E	2,8	15,9055	16,0315	15,9075	0,1251	0,366 SY=0,008
		2,7	15,906	16,0325	15,9085		
43.	1/2 F:E	2,8	16,5224	16,475	16,522	-0,0460	0,003 SX=0,366
		2,7	16,524	16,476	16,524		
44.	1/4 W:B	2,10	14,2865	14,445	14,288		
		2,7	14,286	14,445	14,288		
45.	1/4 W:T	2,10	13,799	13,772	13,797		
		2,7	13,7965	13,772	13,7965		
46.	1/4 W:M	2,8	16,302	16,297	16,3015	-0,0249	-0,013 SX=0,152
		2,7	16,302	16,297	16,302		
47.	1/4 W:M	2,8	16,899	16,953	16,899	0,0539	0,152 SY=-0,013
		2,7	16,8985	16,9525	16,899		
48.	1/2 W:M	2,8	16,3965	16,4444	16,397	-0,0471	0,138 SY=0,002
		2,7	16,3965	16,4444	16,3975		
49.	1/2 W:T	2,10	14,3555	14,339	14,355		
		2,7	14,3555	14,339	14,355		
50.	1/2 W:M	2,8	16,7195	16,702	16,720	-0,0179	0,076 SX=0,158
		2,7	16,7195	16,7015	16,7195		
51.	1/2 W:B	2,10	14,8965	15,026	14,8985		
		2,7	14,8965	15,026	14,899		
52.	1/2 D:W	2,8	16,4435	16,3795	16,442	-0,0750	-0,219 SY=0,001
		2,7	16,442	16,3665	16,4405		
53.	1/2 D:E	2,10	16,0145	15,929	16,014	-0,0851	0,149 SY=-0,001
		2,7	16,016	15,930	16,014		
54.	1/2 D:E	2,10	14,504	14,4235	14,503	-0,0799	-0,233 SY=0
		2,7	14,506	14,425	14,5035		
55.	1/2 D:E	2,10	15,2675	15,184	15,2665	-0,0825	0,241 SY=0
		2,7	15,268	15,185	15,266		
56.	1/2 D:W	2,10	15,953	15,868	15,951	-0,0833	0,243 SY=0
		2,7	15,952	15,8686	15,950		
57.	1/2 D:W	2,10	14,506	14,4235	14,5053	-0,0824	-0,239 SY=0,003
		2,7	14,5065	14,424	14,5065		
58.	1/2 D:W	2,10	NON-FUNCTIONAL.				
59.	1/2 D:W	2,8	17,119	17,148	17,1185	0,0295	0,001 SX=-0,219
		2,7	17,117.	17,1465	17,1165		
60.	1/2 D:W	2,8	16,6615	16,582	16,661	0,0196	-0,238 SY=-0,002
		2,7	16,6615	16,5815	16,6615		
61.	1/2 D:W	2,8	16,0615	16,0315	16,0615	0,0305	0,088 SX=-0,253
		2,7	16,0615	16,0325	16,0615		
62.	1/2 D:E	2,10	14,331	14,449	14,3355	-0,0871	-0,254 SY=0
		2,7	14,3365	14,449	14,3355		

TABLE 16

Strain gauge reading for Model 4 Loadcase 5

READ NO	GUAGE FACTOR	NO	NO LOAD	LOAD	NO LOAD	AV STRAIN	STRESS NOTE
1.	1/4W:D	2	14,3735	14,384	14,375		
		2	14,373	14,38	14,3695		
2.	1/4W:T	2	13,9165	13,917	13,917		
		2	13,9165	13,9165	13,912		
3.	1/4W:M	2	16,3615	16,383	16,3605	0,0221	0,100 SY=0,090
		2	16,3615	16,3835	16,361		
4.	1/4W:M	2	17,0485	17,0685	17,0510	0,0176	0,090 SY=0,100
		2	17,0495	17,065	17,0485		
5.	1/2W:M	2	16,3715	16,3765	16,372	0,0044	0,011 SY=-0,004
		2	16,3735	16,3765	16,3715		
6.	1/2W:T	2	14,4635	14,4715	14,469		
		2	14,469	14,473	14,4685		
7.	1/2W:M	2	16,7735	16,769	16,772	-0,0028	-0,004 SE=0,011
		2	16,7735	16,771	16,772		
8.	1/2W:D	2	14,820	14,832	14,822		
		2	14,820	14,827	14,8185		
9.	1/2W:D	2	14,8845	14,880	14,885		
		2	14,8815	14,874	14,8795		
10.	1/2W:T	2	14,458	14,453	14,457		
		2	14,4585	14,455	14,4566		
11.	1/2W:M	2	16,2265	16,224	16,2265	-0,0030	-0,009 SY=-0,002
		2	16,226	16,222	16,225		
12.	1/2W:M	2	16,2085	16,210	16,210	0,0006	-0,002 SE=-0,002
		2	16,2105	16,211	16,2085		
13.	1/2D:E	2	16,2445	16,240	16,241	-0,0001	-0,001 SY=-0,001
		2	16,2445	16,2435	16,2435		
14.	2D:€	2	15,992	15,991	15,991	0,0004	0,000 SY=-0,002
		2	15,9915	15,9935	15,993		
15.	2D:W	2	14,492	14,491	14,4915	-0,0003	-0,001 SY=-0,001
		2	14,4915	14,4925	14,493		
16.	2D:E	2	14,4735	14,472	14,473	-0,0001	0,000 SY=0
		2	14,473	14,4745	14,474		
17.	2D:€	2	16,941	16,936	16,939	-0,0026	-0,008 SY=-0,002
		2	16,9465	16,945	16,9465		
18.	2D:€	2	16,9715	16,970	16,970	-0,0002	-0,001 SE=-0,001
		2	16,9685	16,969	16,969		
19.	2D:E	2	15,257	15,254	15,2565	-0,0018	-0,005 SY=0
		2	15,257	15,257	15,2555		
20.	2D:E	2	14,8915	14,8865	14,891	-0,0019	-0,005 SY=0
		2	14,8915	14,8915	14,8835		
21.	2D:W/E	2	15,910	15,9085	15,9085	0,0003	0,001 SY=0
		2	15,910	15,912	15,9115		
22.	2D:W	2	NON-FUNCTIONAL				
		2					
23.	2D:W/E	2	16,023	16,023	16,023	0,0004	-0,002 SE=-0,008
		2	16,0225	16,0235	16,023		
24.	4W:T	2	14,626	14,650	14,6265		
		2	14,6225	14,6497	14,6223		
25.	4W:M	2	14,081	14,086	14,081	0,0011	-0,085 SY=-0,226
		2	14,081	14,0785	14,080		
26.	4W:D	2	14,881	14,9385	14,886		
		2	14,8775	14,988	14,8765		
27.	4W:M	2	14,6395	14,601	14,6405	0,0442	-0,025 SE=5,62
		2	14,6415	14,5996	14,6414		
28.	2F:€	2	16,201	16,2065	16,2015	0,0044	0,010 SE=-0,008
		2	16,201	16,2035	16,199		
29.	2F:€	2	14,925	14,9265	14,9265	-0,0001	0,001 SY=0,002
		2	14,924	14,9285	14,921		
30.	2F:€	2	16,445	16,449	16,4465	0,0025	0,005 SE=-0,006
		2	16,4435	16,441	16,4435		
31.	2F:€	2	16,6535	16,6585	16,661	-0,0027	-0,006 SY=0,005
		2	16,660	16,655	16,6595		

READ NO	GUAGE FACTOR	NO	NO LOAD	LOAD	NO LOAD	AV STRAIN	STRESS NOTE
32.	2F:W	2	12,004	12,0155	12,0065	0,0093	0,021 SY=-0,05
		2	12,006	12,013	12,0035		
33.	2F:€	2	15,711	15,706	15,710	0,0040	-0,008 SE=0,010
		2	15,711	15,708	15,712		
34.	2F:W	2	12,1715	12,1685	12,1735	0,0043	0,008 SY=0,02
		2	12,172	12,1665	12,172		
35.	4D:E	2	NON-FUNCTIONAL				
		2					
36.	4D:E	2	16,756	16,772	16,756		No.42 NOT WORKING
		2	16,756	16,7715	16,7555		
37.	4D:W	2	16,334	16,3215	16,336	0,0141	-0,076 SE=0,089
		2	16,3355	16,3205	16,335		
38.	4D:E	2	15,1765	15,1665	15,1765	0,0083	-0,024 SE=0
		2	15,1765	15,171	15,160		
39.	4D:€	2	15,2885	15,293	15,290	0,0029	0,003 SE=-0,014
		2	15,290	15,2915	15,289		
40.	4D:€	2	15,026	15,0185	15,0235	0,0053	-0,014 SE=0,003
		2	15,025	15,0215	15,0265		
41.	4D:E	2	14,5085	14,496	14,5065	0,0104	0,002 SE=97548
		2	14,506	14,4965	14,5065		
42.	4D:W	2	NON-FUNCTIONAL.				
		2					
43.	4D:E	2	14,2965	14,316	14,2965	0,0204	0,059 SY=0
		2	14,2965	14,319	14,299		
44.	4D:E	2	14,7745	14,7865	14,776	0,0113	0,011 SE=43455
		2	14,775	14,7865	14,7755		
45.	4D:€	2	16,382	16,399	16,3995	0,0204	-0,089 SY=-0,078
		2	16,383	16,365	16,385		
46.	4D:€	2	14,806	14,8215	14,8085	0,0159	0,036 SE=40439
		2	14,806	14,822	14,806		
47.	4D:E	2	14,534	14,511	14,533	0,0220	-0,076 SY=-0,051
		2	14,534	14,5125	14,534		
48.	4D:W	2	14,489	14,4825	14,490	0,0004	-0,081 SE=-0,076
		2	14,4825	14,4885	14,489		
49.	4D:W	2	14,589	14,598	14,5885		LOADING POINT.
		2	14,589	14,594	14,591		
50.	4D:W	2	NON-FUNCTIONAL.				LOADING POINT.
		2					
51.	4D:E	2	14,946	14,9525	14,9465	0,0088	0,024 SY=0
		2	14,946	14,956	14,9465		
52.	4F:W	2	16,084	16,047	16,086	0,0391	-0,146 SY=-0,092
		2	16,086	16,0435	16,0815		
53.	4F:€	2	14,7265	14,724	14,728	0,0043	-0,003 SY=0,024
		2	14,7265	14,7205	14,725		
54.	4F:€	2	14,547	14,569	14,548	0,0209	0,089 SE=5,61
		2	14,548	14,5675	14,5465		
55.	4F:W	2	11,574	11,542	11,576	-0,0357	-0,179 SY=-0,133
		2	11,594	11,554	11,591		
56.	4F:€	2	13,1215	13,148	13,120	0,0276	0,139 SE=0,150
		2	13,121	13,1485	13,120		
57.	4F:W	2	12,396	12,4855	12,3805	0,0148	0,314 SY=0,250
		2	12,3965	12,4475	12,376		
58.	4F:€	2	16,403	16,392	16,401	0,0086	-0,082 SE=-0,146
		2	16,400	16,394	16,4025		
59.	4F:€	2	15,1015	15,154	15,1045	0,0496	0,041 SE=60856
		2	15,104	15,152	15,1035		
60.	4F:€	2	15,106	15,142	15,109	0,0328	0,150 SY=0,189
		2	15,1085	15,1385	15,1066		
61.	4F:€	2	15,399	15,406	15,397	0,0085	0,024 SE=-0,002
		2	15,3985	15,4085	15,4005		
62.	4W:M	2	14,5285	14,461	14,5275	0,0661	-0,276 SY=0,035
		2	14,5285	14,4464	14,530		

TABLE 17
Strain gauge reading for Model 4 Loadcase 6

READ NO	GUAGE FACTOR	NO	NO LOAD	LOAD	NO LOAD	AV STRAIN	STRESS NOTE
(1) 1.	1/4 W:B	2.10	14,369 14,3685	14,589 14,587	14,371 14,3705		
(1) 2.	1/4 W:T	2.10	13,9105 13,911	13,8865 13,8835	13,3115 13,312		
(1) 3.	1/4 W:M	2.08	16,3605 16,360	16,352 16,3515	16,359 16,358	-0,0076	0,0865 SX=0,278
(1) 4.	1/4 W:M	2.08	17,047 17,0465	17,1335 17,129	17,0485 17,047	0,0840	0,279 SY=0,087
(1) 5.	1/2 W:M	2.08	16,3715 16,393	16,485 16,449	16,3735 16,394	0,0458	0,184 SY=0,002
(3) 6.	1/2 W:T	2.10	14,466 14,4665	14,450 14,4505	14,466 14,4665	-0,0160	-0,047 SY≈0
(1) 7.	1/2 W:M	2.08	16,7725 16,7725	16,7545 16,755	16,772 16,7715	-0,0174	0,002 SX=0,134
(1) 8.	1/2 W:B	2.10	14,819 14,820	14,9485 14,9485	14,8215 14,8225	0,1278	0,373 SY≈0
(1) 9.	1/2 W:B	2.10	14,875 14,877	15,003 15,005	14,877 14,8795	0,1269	0,370 SY≈0
(1) 10.	1/2 W:T	2.10	14,4545 14,454	14,4325 14,432	14,454 14,4535	-0,0218	-0,064 SY≈0
(1) 11.	1/2 W:M	2.08	16,220 16,218	16,2685 16,266	16,220 16,2185	0,0481	0,140 SY=0,001
(1) 12.	1/2 W:M	2.08	16,2085 16,206	16,189 16,1865	16,207 16,206	-0,0191	-0,001 SX=0,140
(3) 13.	1/2 D:W/E	2.08	16,2415 16,2415	16,1645 16,1685	16,240 16,239	-0,0765	-0,222 SY=0,004
(3) 14.	1/2 D:E	2.10	15,9885 15,989	15,9015 15,901	15,9885 15,987	-0,0870	-0,254 SY≈0
(3) 15.	1/2 D:W	2.10	14,490 14,4905	14,4055 14,408	14,489 14,491	-0,0834	-0,243 SY≈0
(3) 16.	1/2 D:E	2.10	14,4705 14,4705	14,386 14,3865	14,4685 14,469	-0,0836	-0,244 SY≈0
(1) 17.	1/2 D:W/E	2.08	16,944 16,9445	16,863 16,8635	16,943 16,942	-0,0801	-0,234 SY=0,000
(1) 18.	1/2 D:W/E	2.08	16,9635 16,9625	16,9335 16,9935	16,9625 16,962	0,0808	0,004 SX=0,222
(3) 19.	1/2 D:E	2.10	15,256 15,2555	15,1715 15,171	15,2545 15,2535	-0,0886	-0,244 SY≈0
(3) 20.	1/2 D:E/W	2.10	14,8945 14,895	14,8085 14,8085	14,8935 14,8985	-0,0856	-0,250 SY≈0
(3) 21.	1/2 D:W/E	2.10	15,9075 15,9065	15,8215 15,8215	15,9055 15,9055	-0,0848	-0,247 SY≈0
(3) 22.	1/2 D:W	2.10	NON-FUNCTIONAL.				
(3) 23.	1/2 D:W/E	2.08	16,0235 16,024	16,055 16,055	16,024 16,023	0,0314	0,000 SX=0,234
(1) 24.	1/4 W:T	2.10	14,620 14,621	14,6015 14,600	14,6215 14,6195		
(1) 25.	1/4 W:M	2.05	14,0795 14,0785	14,1545 14,1555	14,0795 14,079	0,0759	0,180 SX=0,107
(1) 26.	1/4 W:B	2.10	14,8785 14,877	15,1115 15,114	14,880 14,879		
(1) 27.	1/4 W:M	2.05	14,641 14,6385	14,634 14,6315	14,638 14,6385	-0,0063	-0,029 SEE 62 & 25
(1) 28.	1/2 F:W/E	2.08	16,199 16,200	16,329 16,3285	16,202 16,2005	0,1284	0,374 SY=0,001
(1) 29.	1/2 F:E	2.10	14,919 14,920	15,062 15,0635	14,920 14,9215	0,1426	0,416 SY≈0
(1) 30.	1/2 F:W/E	2.08	16,469 16,4685	16,419 16,419	16,467 16,4665	-0,0488	0,005 SX=0,373
(1) 31.	1/2 F:W/E	2.08	16,656 16,659	16,786 16,786	16,6605 16,6605	0,1275	0,373 SY=0,008
(1) 32.	1/2 F:W	2.10	12,000 11,9985	12,1485 12,1465	12,0035 12,002	0,1465	0,428 SY≈0
(1) 33.	1/2 F:W/E	2.08	15,712 15,712	15,662 15,661	15,7145 15,7115	-0,0503	-0,001 SX=0,174
(1) 34.	1/2 F:W	2.10	12,1685 12,1685	12,311 12,309	12,170 12,171	0,1405	0,410 SY≈0
(3) 35.	1/4 D:W/E	2.05	NON-FUNCTIONAL				
(3) 36.	1/4 D:W/E	2.08	16,7615 16,7605	16,8065 16,8065	16,7615 16,7605		No. 42 NOT WORKING
(3) 37.	1/4 D:W/E	2.08	16,3385 16,3385	16,376 16,376	16,340 16,3385	0,0366	-0,052 SX=0,406
(3) 38.	1/4 D:E	2.10	15,177 15,1775	15,066 15,066	15,1765 15,1765	-0,1109	-0,324 SY≈0
(3) 39.	1/4 D:E	2.08	15,289 15,290	15,330 15,332	15,2905 15,2915	0,0408	-0,005 SX=0,318
(3) 40.	1/4 D:E	2.05	15,024 15,0235	14,915 14,9135	15,021 15,0215	-0,1088	-0,318 SY=0,005
(3) 41.	1/4 D:W/E	2.05	14,5065 14,506	14,461 14,461	14,505 14,505	-0,0446	-0,016 [illegible]
(3) 42.	1/4 D:W/E	2.08	NON-FUNCTIONAL				
(3) 43.	1/4 D:E/W	2.05	14,2965 14,2965	14,202 14,2035	14,295 14,295	-0,0930	-0,271 SY≈0
(3) 44.	1/4 D:W/E	2.05	14,7735 14,7735	14,756 14,756	14,7715 14,7715	-0,0168	0,025 SEE 43
(3) 45.	1/4 D:W/E	2.08	16,3835 16,3865	16,256 16,2485	16,3825 16,3815	-0,1323	-0,406 SY=0,058
(3) 46.	1/4 D:E	2.05	14,806 14,8055	14,7765 14,776	14,8055 14,8045	-0,0291	0,010 SEE 40 & 39
(3) 47.	1/4 D:W/E	2.05	14,535 14,535	14,421 14,4215	14,534 14,535	-0,1135	-0,338 SY=0,018
(3) 48.	1/4 D:W/E	2.05	14,4895 14,489	14,529 14,529	14,481 14,4805	0,0390	-0,018 SX=0,338
(3) 49.	1/4 D:W	2.10	14,588 14,587	14,4585 14,4565	14,586 14,585		
(3) 50.	1/4 D:W	2.10	NON-FUNCTIONAL				LOADING POINT
(3) 51.	1/4 D:E	2.10	14,945 14,9445	14,835 14,8345	14,943 14,9415	-0,1088	-0,317 SY≈0
(3) 52.	1/4 F:W/E	2.08	16,088 16,0885	16,2495 16,250	16,0895 16,0905	0,1606	0,467 SY=0,005
(1) 53.	1/4 F:E	2.05	14,7245 14,726	14,8845 14,8865	14,727 14,731	0,1604	0,508 SY=0,043
(1) 54.	1/4 F:E	2.05	14,547 14,5465	14,624 14,624	14,548 14,5485	0,0765	0,040 SEE 53 & 61
(3) 55.	1/4 F:W	2.10	11,5935 11,5835	11,8075 11,798	11,594 11,587		
(1) 56.	1/4 F:W/E	2.05	13,119 13,118	13,0655 13,0665	13,1165 13,117	-0,0516	0,076 SX=0,582
(3) 57.	1/4 F:W	2.10	12,376 12,379	12,6435 12,648	12,381 12,381		
(3) 58.	1/4 F:W/E	2.08	16,4005 16,401	16,336 16,3365	16,3385 16,3385	-0,0641	-0,005 SX=0,467
(3) 59.	1/4 F:W/E	2.05	15,1035 15,1035	15,196 15,197	15,104 15,1055	0,0924	0,060 SEE 60 & 56
(1) 60.	1/4 F:W/E	2.05	15,1085 15,111	15,2995 15,3015	15,112 15,114	0,1891	0,582 SY=0,076
(3) 61.	1/4 F:E	2.05	15,3995 15,4005	15,3465 15,346	15,399 15,3985	-0,0531	0,048 SX=0,508
(1) 62.	1/4 W:M	2.05	14,524 14,5215	14,461 14,461	14,521 14,520	-0,0606	-0,107 SX=0,180

APPENDIX B

TABLE 9 of the Technical Report - ie giving longitudinal torsional warping functions for concentrated torsional moments applied to box girders without warping restraints at the supports

TABLE 9 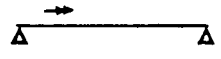

	$0 \leq z \leq a_1$
$B_{twr}(z)$	$\frac{T_{ext}}{K_{18} K_{19}} \frac{\sinh K_{18} a_2}{\sinh K_{18} \iota} \sinh K_{18} z$
$T_{svt}(z)$	$\frac{T_{ext}}{K_{19}} (\frac{a_2}{\iota} K_{19} - \frac{\sinh K_{18} a_2}{\sinh K_{18} \iota} \cosh K_{18} z)$
$T_{twr}(z)$	$\frac{T_{ext}}{K_{19}} \frac{\sinh K_{18} a_2}{\sinh K_{18} \iota} \cosh K_{18} z$
$\theta_z(z)$	$\frac{T_{ext}}{GC_{svt} K_{18} K_{19}} (\frac{a_2}{\iota} K_{18} K_{19} z - \frac{\sinh K_{18} a_2}{\sinh K_{18} \iota} \sinh K_{18} z)$
	$a_1 \leq z \leq \iota$
$B_{twr}(z)$	$\frac{T_{ext}}{K_{18} K_{19}} \frac{\sinh K_{18} a_1}{\sinh K_{18} \iota} \sinh K_{18} (\iota - z)$
$T_{svt}(z)$	$\frac{T_{ext}}{K_{19}} [-\frac{a_1}{\iota} K_{19} + \frac{\sinh K_{18} a_1}{\sinh K_{18} \iota} \cosh K_{18} (\iota - z)]$
$T_{twr}(z)$	$-\frac{T_{ext}}{K_{19}} \frac{\sinh K_{18} a_1}{\sinh K_{18} \iota} \cosh K_{18} (\iota - z)$
$\theta_z(z)$	$\frac{T_{ext}}{GC_{svt} K_{18} K_{19}} [\frac{a_1}{\iota} K_{18} K_{19} (\iota - z) - \frac{\sinh K_{18} a_1}{\sinh K_{18} \iota} \sinh K_{18} (\iota - z)]$

APPENDIX C

TABLE 16 of the Technical Report - ie giving longitudinal distortional warping functions for concentrated torsional moments applied to box girders without warping restraints at the supports

TABLE 16

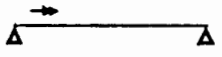

$B_{dwr}(z)$	$B_{dwr,o}(z) - \frac{T_{ext}\,\iota}{\pi^2} \sum_{n=1}^{\infty} \frac{\sin\frac{n\pi a_1}{\iota}\sin\frac{n\pi z}{\iota}}{n^2\left[1 + n^4\left(\frac{\pi^4 C_{dwr}}{I_{fra}\,\iota^4}\right)\right]}$
$B_{dwr,o}(z)$	$\frac{T_{ext}(\iota - a_1)}{2\iota} z \quad$ for $0 \leq z \leq a_1$
	$\frac{T_{ext}\,a_1}{2\iota}(\iota - z) \quad$ for $a_1 \leq z \leq \iota$
$\frac{d}{dz} B_{dwr}(z)$	$\frac{d}{dz} B_{dwr,o}(z) - \frac{T_{ext}}{\pi} \sum_{n=1}^{\infty} \frac{\sin\frac{n\pi a_1}{\iota}\cos\frac{n\pi z}{\iota}}{n\left[1 + n^4\left(\frac{\pi^4 C_{dwr}}{I_{fra}\,\iota^4}\right)\right]}$
$\frac{d}{dz} B_{dwr,o}(z)$	$\frac{T_{ext}(\iota - a_1)}{2\iota} \quad$ for $0 \leq z \leq a_1$
	$-\frac{T_{ext}\,a_1}{2\iota} \quad$ for $a_1 \leq z \leq \iota$
$\beta_{trb}(z)$	$\beta_{trb,o}(z) - \frac{T_{ext}\,\iota^3}{\pi^4 EC_{dwr}} \sum_{n=1}^{\infty} \frac{\sin\frac{n\pi a_1}{\iota}\sin\frac{n\pi z}{\iota}}{n^4\left[1 + n^4\left(\frac{\pi^4 C_{dwr}}{I_{fra}\,\iota^4}\right)\right]}$
$\beta_{trb,o}(z)$	$\frac{T_{ext}}{12\,EC_{dwr}}\left[(\iota - a_1)\, z\,(2a_1 - \frac{a_1^2}{\iota} - \frac{z^2}{\iota})\right] \quad$ for $0 \leq z \leq a_1$
	$\frac{T_{ext}}{12\,EC_{dwr}}\left[(\iota - a_1)\, z\,(2a_1 - \frac{a_1^2}{\iota} - \frac{z^2}{\iota}) + (z - a_1)^3\right] \quad$ for $a_1 \leq z \leq \iota$

APPENDIX D

TABLE 2 of the Technical Report - K_{28} values

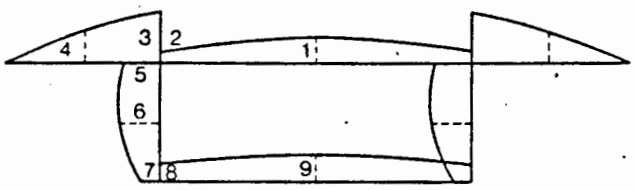

Figure 51: Points on cross-section at which K_{28} is defined in Table 2.

TABLE 2

Point on cross-section (Figure 51)	K_{28}
1	$\frac{K_{29}(A_{top} + 2A_{cant})}{4} + (5 - 4K_{25})\frac{A_{web}}{12} - K_{25}\frac{A_{bot}}{12}$
2	$\frac{(K^2_{29} - 1)}{4K_{29}}(A_{top} + 2A_{cant}) + (5 - 4K_{25})\frac{A_{web}}{12} - K_{25}\frac{A_{bot}}{12}$
3	$\frac{(K^2_{29} - 1)}{4K_{29}}(A_{top} + 2A_{cant})$
4	$\frac{(K_{29} - 1)(3K_{29} + 1)}{16K_{29}}(A_{top} + 2A_{cant})$
5	$(5 - 4K_{25})\frac{A_{web}}{12} - K_{25}\frac{A_{bot}}{12}$
6	$(1 - 5K_{25})\frac{A_{web}}{24} - K_{25}\frac{A_{bot}}{12}$
7	$-(1 - 2K_{25})\frac{A_{web}}{12} - K_{25}\frac{A_{bot}}{12}$
8	$-(1 - 2K_{25})\frac{A_{web}}{12} - K_{25}\frac{A_{bot}}{12}$
9	$\frac{K_{25}A_{bot}}{4} - (1 - 2K_{25})\frac{A_{web}}{12} - K_{25}\frac{A_{bot}}{12}$

APPENDIX E

Examples of typical analysis using the recommended method of analysis

ANALYSIS: MODEL NO1 LOADCASE 1B

1.1.1. SECTION PROPERTIES

I_x = 13254 001,25 mm⁴

y_c = 93,30 mm.

A = 1553,74 mm²

I_y = 15 541 630,38 mm⁴

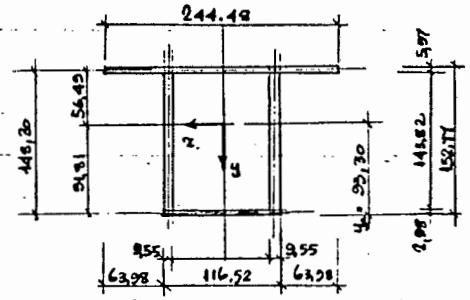

figure 1.1.1: cross-sectional dimensions

1.1.2. MATERIAL PROPERTIES

E = 2018 MPa.

V = 0,39

$G = \frac{E}{2(1+V)}$ = 1050 MPa.

1.1.3. LOADING AND INTERNAL FORCES.

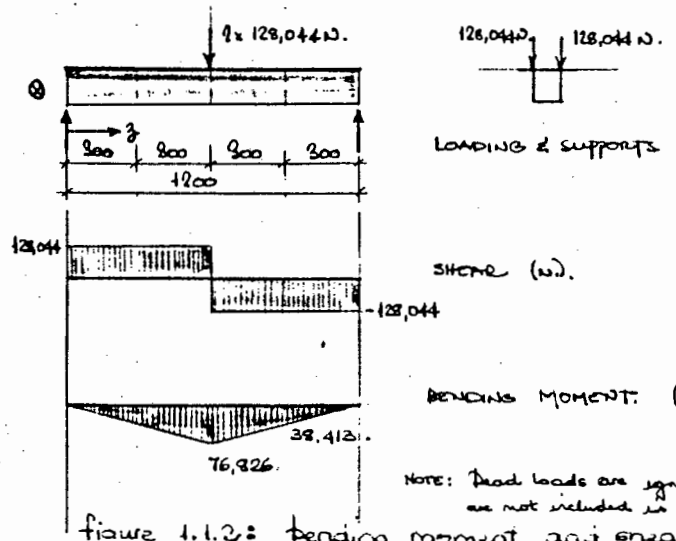

NOTE: Dead loads are ignored since they are not included in experimental readings

figure 1.1.2: bending moment and shear

ANALYSIS: MODEL NO1 LOADCASE 1B CONTD.

1.1.4. ANALYSIS OF STRUCTURAL EFFECTS.

Structural effects to be considered are longitudinal bending and shear as well as shear lag.

1.1.4.1. Longitudinal bending and shear.

Using engineer's theory of bending

$f_{lbg} = \frac{M_x \cdot y}{I_x}$ = longitudinal normal stress

at midline of top flange on midspan

f_{lbg} (top flange, midspan) = $\frac{76,826 \cdot 10^3 \cdot -56,49}{13254\,001,25}$ = -0,327 MPa.

on midline of bottom flange at midspan

f_{lbg} (bot. flange, midspan) = $\frac{76,826 \cdot 10^3 \cdot 91,81}{13254\,001,25}$ = 0,532 MPa.

at midline of top flange on ¼-span

f_{lbg} (top flange, ¼ span) = $\frac{38,413 \cdot 10^3 \cdot -56,49}{13\,254\,001,25}$ = -0,164 MPa.

at midline of bottom flange on ¼-span

f_{lbg} (bot. flange, ¼ span) = $\frac{38,413 \cdot 10^3 \cdot 91,81}{13\,254\,001,25}$ = 0,266 MPa.

Note that f_{lbg} values at topmost and bottom-most fibres of the respective flanges will be marginally higher than the midline values.

for the top flange

f_{lbg} (topmost fibre) $= \frac{56,49 + \frac{5,07}{2}}{56,49} \cdot f_{lbg}$ (midline)

$= 1,053\ f_{lbg}$ (midline).

similarly for the bottom flange

f_{lbg} (bottommost fibre) $= \frac{91,81 + \frac{2,08}{2}}{91,81} f_{lbg}$ (midline)

$= 1,016\ f_{lbg}$ (midline).

(Gauge readings taken at outermost fibres).

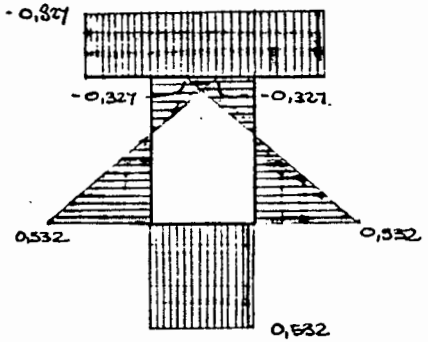

fig. 1.1.3: f_{lbg} on midlines at midspan (N/mm^2)

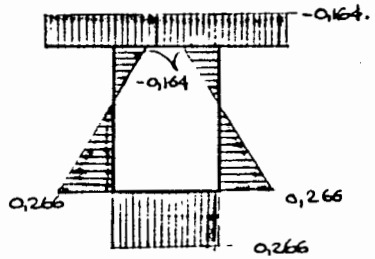

fig 1.1.4 : f_{lbg} on midlines at ¼-span (N/mm^2).

Calculate shear stresses as follows :

$v_{lbg} = -\frac{V_y (\bar{Ay})_{½}}{I_x \cdot h}$ = shear stress in longitudinal bending

note that by the symmetry about the vertical axis of cross-section (y), the longitudinal shear stress is zero at this axis (i.e. at $x=0$) and hence also the complementary shear stress in the plane of cross-section. (need therefore only analyse half the section as an open section)

$(\bar{Ay})_{½}$ = first moment of area of the partial half-cross section about the centroidal x-axis

The $(\bar{Ay})_{½}$ and v_{lbg} values can be calculated at the following sections:

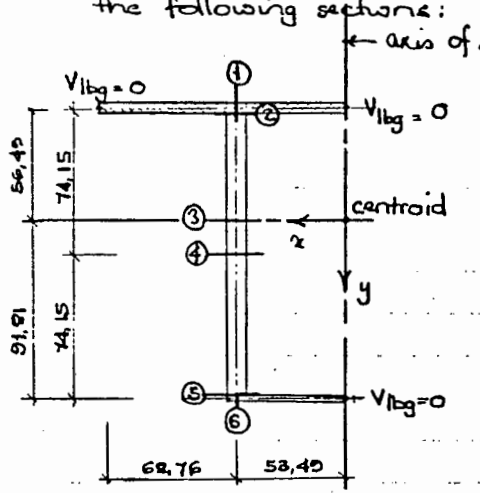

figure 1.1.5: sections for calculating v_{lbg}.

$(\bar{Ay})_{½}$ values are :

i) Top flange to right of midline of web (section ①)

$(\bar{Ay})_{½} = 5,07 \cdot 53,49 \cdot -56,49$

$= -18039,25\ mm^3$

(hatched ///)

ii) Top flange to left of midline of web (section ①)

$(\bar{Ay})_{½} = 5,07 \cdot 68,76 \cdot -56,49$

$= -13\,188,99\ mm^3$

(hatched \\\).

further $(\bar{A}y)_{\frac{1}{2}}$ values are as follows:

iii) Top of web, just below top flange (section ②):

$(\bar{A}y)_{\frac{1}{2}}$ = sum of i) and ii) above

i.e. $= -(18039,25 + 23\,188,99) = -41\,228,24\ mm^3$ ✓

iv) At level of centroid (section ③):

$(\bar{A}y)_{\frac{1}{2}}$ = iii) above + $(56,49 - 5,91/2)^2 . 9,55 . -\frac{1}{2}$

= $-41\,228,24 + (-13\,669,80)$

= $-54\,898,04\ mm^3$ ✓

v) At mid-depth of web (section ④):

$(\bar{A}y)_{\frac{1}{2}}$ = iv) above + $9,55 \times 17,66^2 . \frac{1}{2}$

= $-54\,898,04 + 1\,489,21$

= $-53\,408,83\ mm^3$ ✓

vi) At bottom of web (section ⑤), just above bottom fl.

$(\bar{A}y)_{\frac{1}{2}}$ = iv) above + $90,32^2 . \frac{1}{2} . 9,55$

= $-54\,898,04 + 38\,953,03$

= $-15\,945,01\ mm^3$ ✓

vii) Bottom flange, to right of midline of web (section ⑥)

$(\bar{A}y)_{\frac{1}{2}}$ = vi) above + $\frac{2,00}{2} . 9,55 . 81,81$

= $-15\,945,01 + 1206,41$

= $-14\,638,60\ mm^3$ ✓

As a check calculate $(\bar{A}y)_{\frac{1}{2}}$ value at centreline ($x = 0$) of the bottom flange

$(\bar{A}y)_{\frac{1}{2}}$ = vii) above + $53,49 . 2,98 . 81,81$

= $-14\,638,60 + 14\,634,53$

= $-4,07 \approx 0$

Using the above $(\bar{A}y)_{\frac{1}{2}}$ values calculate the shear stresses at the various sections at ¼ span (shear is zero at midspan.).

i) Top flange, to right of ①:

$$\tau_{1bg} = -\frac{V_y . (\bar{A}y)_{\frac{1}{2}}}{I_x . t} = -\frac{128,044 * -18039,25}{13254\,091,25 . 5,91}$$

$= 0,020\ N/mm^2$

ii) Top flange, to left of ①:

$$\tau_{1bg} = \frac{-128,044 . -23188,99}{13254\,091,25 . 5,91} = 0,038\ N/mm^2.$$

iii) Top of web, just below top flange - section ②:

$$\tau_{1bg} = \frac{-128,044 . -41\,228,24}{13\,254\,091,25 . 9,55} = 0,042\ N/mm^2$$

(approx. also flange midline value)

iv) At level of centroid - section ③:

$$\tau_{1bg} = \frac{-128,044 . -54\,898,04}{13\,254\,091,25 . 9,55} = 0,056\ N/mm^2$$

v) At mid-depth of web (section ④):

$$\tau_{1bg} = \frac{-128,044 . -53\,408,83}{13\,254\,091,25 . 9,55} = 0,054\ N/mm^2$$

vi) At bottom of web, just above bottom flange - section ⑤

$$\tau_{1bg} = \frac{-128,044 . -15\,945,01}{13\,254\,091,25 . 9,55} = 0,016\ N/mm^2$$

(approx. also flange midline value)

(vii) Bottom flange, to right of midline of web (section ⑥).

$$\sigma_{lbg} = \frac{-128,044 \cdot -14\,632,60}{13\,254\,091,25 \cdot 2,98} = -0,041 \ N/mm^2$$

The shear stresses can now be plotted as follows;

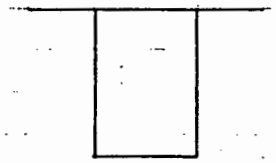

figure 1.1.6 : shear stresses (v_{lbg}) at midspan - all zero.

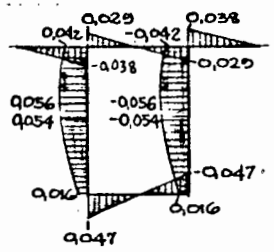

figure 1.1.4 : shear stresses at ¼ span (v_{lbg}). N/mm^2

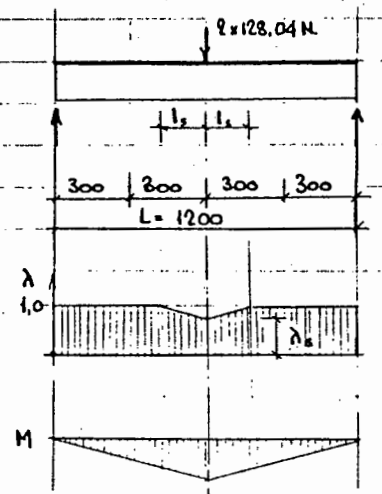

figure 1.1.8 : variation of λ_s over span.

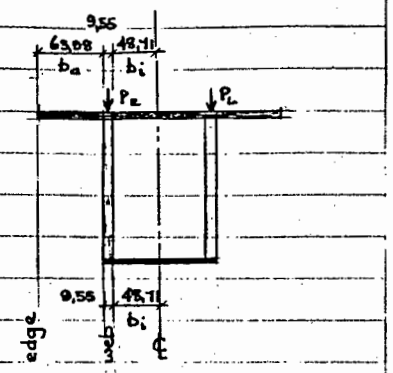

basic equation :

$$\frac{f_{lbg(edge\ or\ ℄)}}{f_{lbg(web)}} = 1,25\,(\lambda - 0,2)$$

Bending moments defined as type S due to the linear shape of the diagram (M above). Also $\psi = 0$.

Shear lag effect is a maximum at midspan and disappears at distance l_s on either side of midspan. i.e. λ becomes equal to unity and if entered into the basic equation :

$$\frac{f_{lbg(edge\ or\ ℄)}}{f_{lbg(web)}} = 1,25\,(1 - 0,2) = 1,0. \quad \text{i.e } f_{lbg(edge\ or\ ℄)} = f_{lbg(web)}$$

At midspan :

$$\frac{L}{b_a} = \frac{1200}{63,98} = 18,8 \Rightarrow \lambda_{sa} \doteq 0,75$$

$$\frac{L}{b_i} = \frac{1200}{48,71} = 24,6 \Rightarrow \lambda_{si} \doteq 0,8 \quad \text{(same for top and bottom flanges.)}$$

Note that for $\frac{L}{b} \geq 100$ $\lambda_s = 1,0$ and there is no shear lag effect.

Evaluate l_s where $l_s = 1,05\,(1 - \lambda_s)(2 - \psi) \cdot b$.

1.1.4.2 Shear Lag

Information given in the Maisel and Roll report is not adequate for the analysis of shear lag in box girders that are not symmetrical about both the horizontal and vertical centroidal axes.

A paper by Schmidt, Peil and Born published in Bauingenieur 54 (1979) deals with the shear lag effect in a practical way which is suitable for hand methods of analysis. Therefore this method will be used in place of the above for the following analyses.

therefore $l_{sa} = 1.05\,(2-\psi)\,[1-\lambda_s]\,b_a = 1,05 \cdot 2 \cdot [1-0,15] \cdot 63,98$

$= 33,6$ mm. (<300 mm)

and $l_{si} = 1.05\,(2-0)\,[1-0,8]\,48,71$

$= 10,5$ mm. (<300 mm) (top and bottom flanges).

From the above it can be seen that λ_s will be unity at the ¼-span points for both the edge and ℄ flanges and that consequently there will be no shear lag effect at these sections.

$$\alpha = 1 - 0,5\,\lambda_{si}\left(1-\frac{b_a}{b_i}\right)\left[1-0,64\,\frac{P_1}{P_2}-0,36\,\frac{P_1^2}{P_2^2}\right]$$

- factor for adjusting λ_{si} in order to allow for non-symmetrical loads ($P_2 \neq P_1$). (same for top and bottom flanges).

Since $P_1 = P_2$, $\alpha = 1,0$. Therefore use $\lambda_{si} = 0,8$ as before.

$$\frac{f'_{lbg\,(edge)}}{f'_{lbg\,(web)}} = 1,25\,(\lambda_{sa}-0,2)\left[1+0,5\,\frac{b_a}{b_i}\left(1-\frac{P_1}{P_2}\right)\right] \leq 1,5 \geq 0$$

$$= 1,25\,(0,15-0,2)\,[1+0] = 0,688$$

$$\frac{f'_{lbg\,(\text{℄})}}{f'_{lbg\,(web)}} = 1,25\,(\lambda_{si}-0,2)\left[1+0,5\,\frac{b_a}{b_i}\left(1-\frac{P_1}{P_2}\right)\right] \geq 0.$$

$$= 1,25\,(0,8-0,2)\,[1+0] = 0,75 \text{ (top \& bot flanges)}$$

where

$f'_{lbg}(\,)$ = longitudinal bending stress on the midlines of the top and bottom flanges taking shear lag effects into account by the Schmidt, Born and Peil method.

From the above, the stress diagram for the longitudinal normal stresses at midspan can be constructed in terms of the stress values over the webs for the top ($f'_{lbg\,(top)}$) and bottom flanges ($f'_{lbg\,(bot)}$). See figure 1.1.9 below.

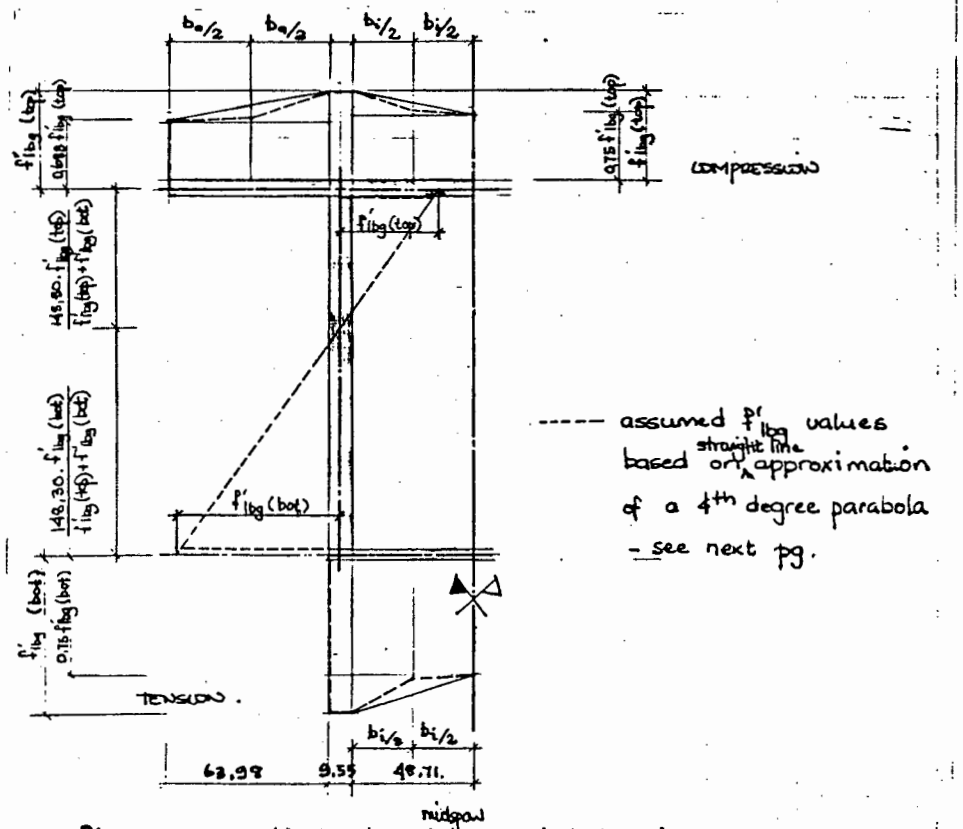

Figure 1.1.9 : distribution of longitudinal bending stress taking shear lag into account (f'_{lbg}).

The Schmidt, Peil and Born papers shows that the variation of longitudinal bending stress from edge of flange towards the web can be approximated with a fourth degree parabola. i.e. $f(x) = y = ax^4 + c$

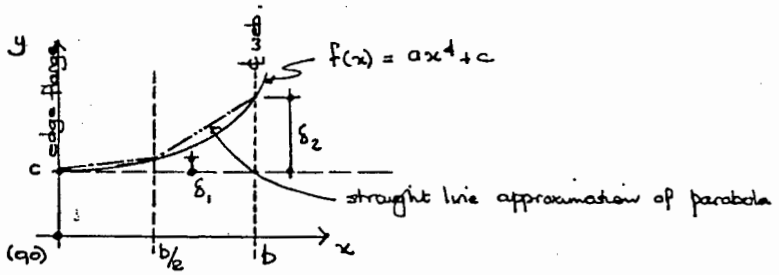

figure 1.1.10: Distribution function for longitudinal bending stresses over flange elements.

At $x = b/2$; $f(x) = a\frac{b^4}{2^4} + c$ and $\delta_1 = \frac{1}{16}ab^4$

$x = b$; $f(x) = ab^4 + c$ and $\delta_2 = ab^4$

The longitudinal bending stresses at the mid-points of the flange elements can therefore easily be determined in terms of f'_{lbg} at the webs. ($x = b$). A simplification would be to approximate the curve representing the longitudinal stresses with straight lines (—···—) as shown above.

Using figure 1.1.9, $f'_{lbg}(top)$ and $f'_{lbg}(bot)$ can be found as follows:

For equilibrium, the compressive and tensile forces making up the couple resisting the applied bending moment must be equal and furthermore, the resisting moment must equal the applied moment. The equilibrium equations are then:

$$-C_{\text{TOP FLANGE}} - C_{\text{WEBS}} = T_{\text{BOTTOM FLANGE}} + T_{\text{WEBS}} \quad \ldots\ldots (1)$$

where C and T are the compressive and tensile forces due to the resisting bending moment.

and the second equilibrium equation is

$$M_{APPLIED} = -\left[M^{C\ TOP\ FLG}_{RESIST} + M^{C\ WEBS}_{RESIST} + M^{T\ BOT\ FLG.}_{RESIST} + M^{T\ WEBS}_{RESIST}\right] \ldots\ldots (2)$$

The above equations can be re-written in terms of $f'_{lbg}(top)$ and $f'_{lbg}(bot)$ as follows:

Equation (1):

$$C_{\text{TOP FLG}} = 5{,}97 \cdot f'_{lbg}(top)\left[0{,}688 \cdot 63{,}08 + 975 \cdot 48{,}71 + 0{,}312 \cdot \tfrac{1}{16} \cdot 0{,}75 \cdot 63{,}08 + \ldots\right.$$
$$\left. \ldots + \tfrac{15}{16} \cdot 0{,}312 \cdot \tfrac{63{,}08}{4} + 0{,}25 \cdot \tfrac{1}{16} \cdot 0{,}75 \cdot 48{,}71 + \tfrac{15}{16} \cdot 0{,}25 \cdot \tfrac{48{,}71}{4}\right]$$

$$= 534{,}957\ f'_{lbg}(top) \leftarrow \quad \text{(for half section)}$$

$$C_{\text{WEBS}} = \frac{\left(\frac{f'_{lbg}(top) \cdot 148{,}30}{f'_{lbg}(top) + f'_{lbg}(bot)} + \frac{5{,}97}{2}\right)^2}{\left(\frac{f'_{lbg}(top) \cdot 148{,}30}{f'_{lbg}(top) + f'_{lbg}(bot)}\right)} \cdot f'_{lbg}(top) \cdot 9{,}55 \cdot \tfrac{1}{2} \leftarrow \text{(for half section)}$$

$$T_{\text{BOT FLG}} = 2{,}98 \cdot f'_{lbg}(bot)\left[0{,}75 \cdot 48{,}71 + 0{,}25 \cdot \tfrac{1}{16} \cdot 0{,}75 \cdot 48{,}71 + 0{,}25^2 \cdot \tfrac{15}{16} \cdot 48{,}71\right]$$

$$= 119{,}071\ f'_{lbg}(bot) \rightarrow \quad \text{(for half-section)}$$

$$T_{\text{WEBS}} = \frac{\left(\frac{f'_{lbg}(bot) \cdot 148{,}30}{f'_{lbg}(top) + f'_{lbg}(bot)} + \frac{2{,}98}{2}\right)^2}{\left(\frac{f'_{lbg}(bot) \cdot 148{,}30}{f'_{lbg}(top) + f'_{lbg}(bot)}\right)} \cdot f'_{lbg}(bot) \cdot 9{,}55 \cdot \tfrac{1}{2} \rightarrow$$
(for half section)

Replace $\frac{f'_{lbg}(top)}{f'_{lbg}(top) + f'_{lbg}(bot)}$ by ϕ and $\frac{f'_{lbg}(bot)}{f'_{lbg}(top) + f'_{lbg}(bot)}$ by μ.

Note: $\phi = 1 - \mu$

Equation (1) then becomes

$$-534,857\, f'_{lbg}(top) - \frac{(148,30\phi + \frac{5,07}{2})^2}{148,30\phi} \cdot f'_{lbg}(top) \cdot 9,55 \cdot \tfrac{1}{2} = \ldots$$

$$\ldots = 119,071\, f'_{lbg}(bot) + \frac{(148,30\mu + \frac{2,98}{2})^2}{148,30\,\mu} \cdot f'_{lbg}(bot) \cdot 9,55 \cdot \tfrac{1}{2} \quad \ldots\ldots (3)$$ ✓

and Equation (2) becomes

$$* \quad \tfrac{1}{2} M_{APPLIED} \overset{N}{=} -534,857\, f'_{lbg}(top) \cdot 148,30 \cdot \phi + 119,071\, f'_{lbg}(bot) \cdot 148,30\,\mu \ldots$$

$$\ldots - \frac{(148,30\phi + \frac{5,07}{2})^3}{148,30\phi} \cdot f'_{lbg}(top) \cdot 9,55 \cdot \tfrac{1}{2} \cdot \tfrac{2}{3} + \frac{(148,30\mu + \frac{2,98}{2})^3}{148,30\mu} \cdot f'_{lbg}(bot) \cdot 9,55 \cdot \tfrac{1}{2} \cdot \tfrac{2}{3}$$

$$\ldots\ldots\ldots\ldots\ldots\ldots (4)$$ ✓

Equations (3) and (4) can be solved for $f'_{lbg}(top)$ and $f'_{lbg}(bot)$ using a process of trial and error as follows:

As a first approximation use the stress values obtained from the simple bending analysis (see pg. 3 fig 1.1.3).

i.e $f'_{lbg}(top) = -0,327\ N/mm^2$ and $f'_{lbg}(bot) = 0,532\ N/mm^2$

p.t.o. →

✓

* Equation (4) assumes that the axial forces due to bending stresses acting in the top and bottom flanges do so at the level of the flange-midlines. This is not exactly so - i.e the axial forces act at points slightly above the midline of the top flange and slightly below the midline of the bottom flange respectively. The error due to this simplifying assumption would obviously be greater for shallower sections - e.g. Model no. 4. The error in the calculated moment of resistance of the top flange only for Model no. 4 is approximately 2,5 % — very small.

Equation (3) becomes: LHS $-C = 272,62\ N \leftarrow$

RHS $T = 304,29\ N \rightarrow$ $\therefore C$ ✓

As a next approximation (trial), increase the compressive force by increasing $f'_{lbg}(top)$ in order to balance the tensile and compressive forces and in so doing, also find the position of the neutral axis.

Try $f'_{lbg}(top) = \frac{304,29}{272,62} \cdot -0,327 = -0,365\ N/mm^2$

Then from equation (3): LHS $-C = 311,06\ N \leftarrow$

RHS $T = 294,41\ N \rightarrow < C$ ✓

The $f'_{lbg}(top)$ value for the next trial can be found by plotting the previously found values for C and T and then interpolating:

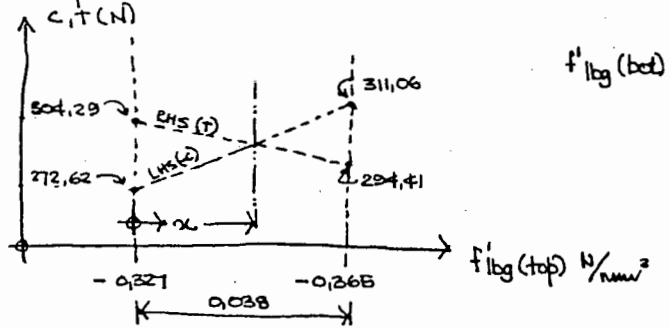

$f'_{lbg}(bot) = 0,532 = \text{CONSTANT}.$

Determine the value of x for which $-C = T$.

$$-\frac{x}{0,038}(311,06 - 272,62) + 272,62 = -\frac{x}{0,038}(294,41 - 304,29) + 304,29$$

$\therefore x = -0,025\ N/mm^2$ and $f'_{lbg}(top) = -0,352\ N/mm^2$

$-C = T \overset{\sim}{=} \frac{0,025}{0,038} \cdot (311,06 - 272,62) + 272,62 = 297,9\ N \rightarrow$

As a check, substitute $f'_{lbg}(top) = 0{,}352$ and $f'_{lbg}(bot) = 0{,}532$ N/mm² into equation (3) again :

LHS : $-C = 207{,}31$ N ← ✓
RHS : $T = 207{,}70$ N → ✓
} $-C \simeq T$ ✓

The position of the neutral axis is then

$$y'_c = \left(\frac{0{,}532}{0{,}532 + 0{,}357}\right) \cdot 148{,}80 + \frac{8{,}98}{2} = 90{,}74 \text{ mm} \quad ✓$$

= distance from bottom of bottom flange to neutral axis taking shear lag into account (as per Schmidt et al).

Using the above values for $f'_{lbg}(top)$ and $f'_{lbg}(bot)$, calculate the resisting moment by using equation (4) :

RHS : $-\frac{1}{2} M_{resist} = 35{,}478$ N-m < $\frac{1}{2} M_{applied} = 38{,}413$ N-m. ✓ ✓

Increase both $f'_{lbg}(top)$ and $f'_{lbg}(bot)$ by the ratio $\frac{38{,}413}{35{,}478}$ – i.e neutral axis remains in same position.

Therefore $f'_{lbg}(top) = -0{,}352 \cdot \frac{38{,}413}{35{,}478} = -0{,}381$ N/mm²

$f'_{lbg}(bot) = 0{,}532 \cdot \frac{38{,}413}{35{,}478} = 0{,}576$ N/mm²

Finally, re-substitute the above values into equations (3) and (4) to check whether equilibrium is satisfied :

Equation (3) LHS $-C = 322{,}33$ N ←
RHS $T = 322{,}35$ N →
} $\Rightarrow -C \simeq T$

Equation (4) LHS $\frac{1}{2} M_{applied} = 38{,}413$ N-m
RHS $-\frac{1}{2} M_{resist} = 38{,}408$ N-m.
} $\Rightarrow M_{applied} \simeq -M_{resist}$

The diagram for longitudinal bending stresses at midspan ($f'_{lbg}(\,)$) can now be plotted using figure 1.1.9 and the values of $f'_{lbg}(top)$ and $f'_{lbg}(bot)$ found above.

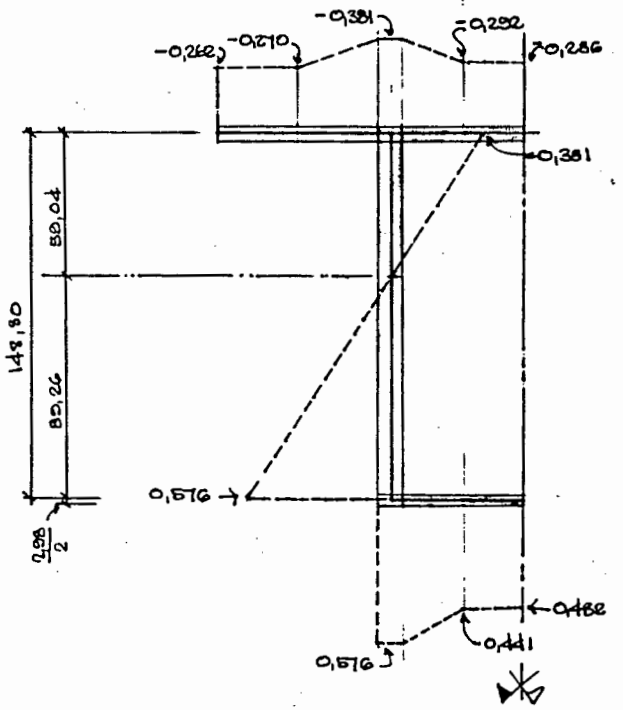

figure 1.1.11 : f'_{lbg} at midspan (final values). N/mm²

1.1.5 PLOTTING RESULTS

A summary of the results from the above analysis can be made by plotting the diagrams for longitudinal, transverse and shear stresses for both midspan and ¼-span sections. These diagrams would also be suitable for the comparison of analytical and experimental results. See figures 1.1.12 to 1.1.17 given on the next page.

The diagrams for the various stress-types are derived from the following figures in the preceding calculations:

¼-span:	longitudinal normal stress	fig. 1.1.4.
	transverse normal stress	not applicable
	shear stress	fig. 1.1.7
midspan:	longitudinal normal stress	figure 1.1.11
	transverse normal stress	not applicable
	shear stress	figure 1.1.7.

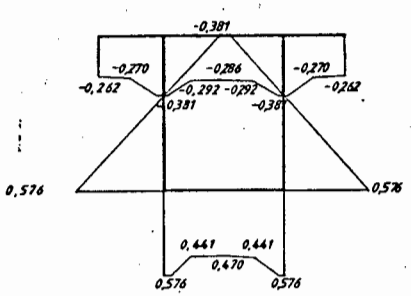

a) Longitudinal stresses at midspan

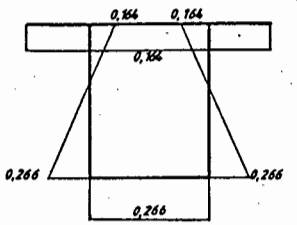

b) Longitudinal stresses at ¼ -span (z = 300 mm)

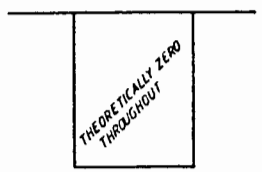

c) Transverse bending stresses at midspan

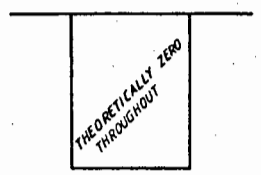

d) Transverse bending stresses at ¼ -span (z = 300 mm)

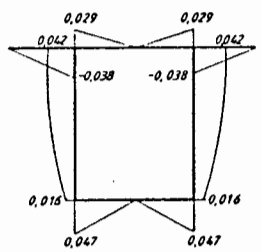

e) Shear stresses at midspan

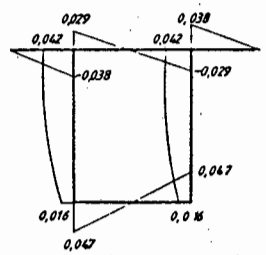

f) Shear stresses at ¼ -span (z = 300 mm)

FIGURE 4.2: Model 1 Loadcase 1B
Combined stresses from analysis

3.2.1 SECTION PROPERTIES

See 3.1.1 for cross-sectional dimension and I_x, y_c, A and I_y values.

Check cross-section i.t.o Vlasov's (torsional warping) thin-wall criterion :

$$\frac{\text{shell thickness}}{\text{width or depth of section}} = \frac{9,47}{44,77} = 0,212 \gg 0,10 \quad \checkmark$$

∴ criterion not met which is often the case with concrete box-girders.

and

$$\frac{\text{width or depth of section}}{\text{length of shell}} = \frac{116,70}{1200,0} = 0,097 < 0,10$$

∴ criterion satisfied ✓

Check cross-section i.t.o. Kollbrunner & Basler (St. Venant shear stress) criteria for thin-walled sections - assuming a constant wall thickness around the perimeter :
i.e 'there is less than 10% error in calculating the St. Venant shear stress if the effective area of cross-section is less than 1/5 th of the area enclosed by the wall centre-lines.

$$A_{effective} = 116,70\,(5,07 + 5,89) + 2.9,47.32,91 = 2008,4 \text{ mm}^2 \quad \checkmark$$

$$A_{enc} = (116,70 - 9,47).38,84 = 4168,3 \text{ mm}^2 \quad \checkmark$$ (9,47 → 107,32)

$$\therefore \frac{A_{effective}}{A_{enc}} = 0,481 \gg 0,2 \quad \checkmark \quad \therefore \text{criterion not met.}$$

This criterion is not usually satisfied by concrete box girders. ✓

The second criterion is : 'There is less than 10% error in the calculated internal torsional moment if the effective area of cross-section does not exceed the area enclosed by the wall centre-lines'. Since A_{enc} is much greater than $A_{effective}$, this criterion is met by MODEL 3. Note that concrete box-girders usually do satisfy this geometrical condition ✓

A more general form of the Kollbrunner and Basler criteria (than applied above) in which allowance is made for a variation in wall thickness around the perimeter can be used as follows :-

$$\frac{\Delta v_{svt}}{v_{svt}} = \frac{9,47^2}{2.4168,3}\left(\frac{107,32}{5,07} + \frac{107,32}{5,89} + \frac{2.38,84}{9,47}\right) = 0,478 \quad \checkmark$$ (44,4000)

$$\frac{\Delta T_{svt}}{T_{svt}} = \frac{1}{3\,C_{svt}}\left[b\,(h^3_{top} + h^3_{bot}) + 2d\,h^3_{web}\right] = 0,024 \text{ or } 2,4\% \quad \checkmark$$

∴ section is thin walled

where $C_{svt} = \dfrac{4.38,84^2.107,32^2}{\frac{107,32}{5,07} + \frac{107,32}{5,89} + \frac{2.38,84}{9,47}} = 1565,30.10^3 \text{ mm}^4$ (1565 287) ✓

Since the error in the torsional moment (T_{svt}) is less than 10% (due to Δv_{svt} 'effect'), the section can be considered to be thin-walled. i.e use C_{svt} value as calculated by equation 5 in the technical report.

However, allowance must be made for a variation in St. Venant shear stress (Δv_{svt}) through the wall thickness by using equation 4. ✓

3.2.2. MATERIAL PROPERTIES

See 3.1.2 for material properties.

3.2.3. LOADING AND INTERNAL FORCES.

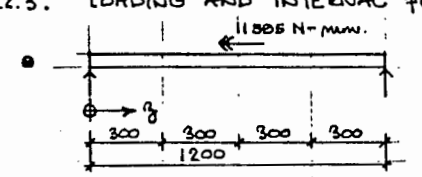

LOADING AND SUPPORTS

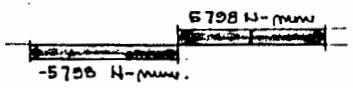

TORSIONAL MOMENT (N-mm)

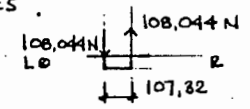

Supports provide full torsional and distortional restraint but not a warping restraint.
Dead load effects are ignored i.e. not reflected in expt. results. ✓

FIGURE 3.2.1 TORSIONAL LOADING.

3.2.4. ANALYSIS OF STRUCTURAL EFFECTS.

Structural effects to be considered are Torsional warping and St. Venant torsion, Distortional warping and Transverse bending. These effects must be determined for both the midspan and ¼-span (z = 300 mm) sections.

3.2.4.1 TORSIONAL WARPING AND ST. VENANT TORSION. (KOLLBRUNNER, HAJDIN AND HETLIG)

Position of shear centre :-

The following dimensions are to be used :

b = 107,32 mm
b_{cant} = 68,58 mm.
d = 38,84 mm
h_{top} = 5,07 mm.
h_{web} = 9,47 mm.
h_{bot} = 5,80 mm.
I_y = 9 851,14 * 10^3 mm^4 ✓

$K_{13} = \frac{1}{4}.107,32.5,80.9,47\left(\frac{1}{3}.107,32.5,80+3.38,87.9,47\right) = 1966\,666\ mm^5$ ✓

$K_{14} = 107,32.38,84.5,07.\left(\frac{1}{6}.5,80^2 - \frac{1}{4}.9,47^2\right) = -414\,039\ mm^5$ ✓

$K_{15} = \frac{1}{2}.5,07.5,80.9,47.\left(\frac{1}{6}.107,32^2 + 38,84^2\right) = 570\,780\ mm^5$ ✓

$K_{16} = 68,58.5,07.5,80.9,47\ (68,58 + 107,32) = 1\,017\,010\ mm^5$ ✓

$K_{17} = 107,32.9,47.(5,07+5,80) + 2.38,84.5,07.5,80 = 14\,785\ mm^3$ ✓

d_{shc} = depth of shear centre below mid-line of top slab.

$$= \frac{b^2 d}{I_y}\left(\frac{K_{13}+K_{14}+K_{15}+K_{16}}{K_{17}}\right) \quad \text{(15,3.)}$$

= 18,86 mm. ✓

Evaluation of w_{tor} :

$$C_{svt} = \frac{4.A_{enc}^2}{\frac{b}{h_{top}} + \frac{b}{h_{bot}} + \frac{2d}{h_{web}}} = 1\,565,30 * 10^3\ mm^4 \quad (1565\,297.)$$

✓ (see calculation on pg. 2.)

$\omega_{tor} = \int_0^{S_{per}} (a_s - \frac{C_{svt}}{2.A_{enc}.h}) ds_{per}$ = sectorial coordinate

where a_s = perpendicular dist. from shear centre to tangent to mid-line of wall at the point considered.

= 18,86 mm (top flange)

= $\frac{107,32}{2}$ = 53,66 mm (webs)

= 38,84 − 18,86 = 19,98 mm (bottom flange) ✓

At A and E, ω_{tor} = 0 (by anti-symmetry)

At B, $\omega_{tor} = \int_0^{53,66} (18,86 - \frac{1565,30.10^3}{2.107,32.38,84.5,97}) ds_{per}$ = − 675,6 mm² ✓

At C, $\omega_{tor} = \int_{53,66}^{122,24} (18,86) ds_{per} - 675,6$ = 617,8 mm² ✓

At D, $\omega_{tor} = \int_{53,66}^{92,50} (53,66 - \frac{187,76}{9,47}) ds_{per} - 675,6$ = 638,4 mm² ✓

As a check :

At E, $\omega_{tor} = \int_{92,50}^{146,16} (19,98 - \frac{187,76}{5,89}) ds_{per} + 638,4$ = 0,00

(i.e. should be zero)

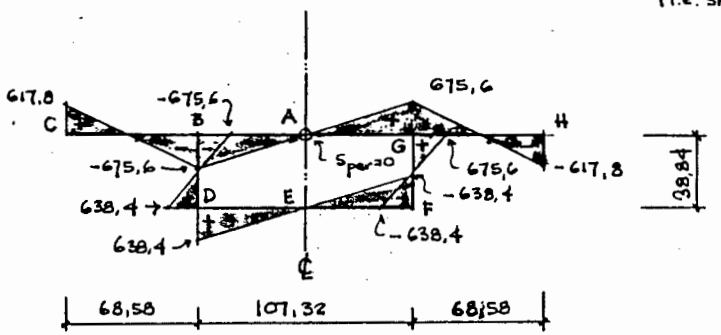

FIGURE 3.2.2 : ω_{tor} diagram (mm²)

✓

Revised 23.3.77

Evaluation of C_{tor} :

$C_{tor} = \int_A \omega_{tor}^2 dA$ = torsional warping moment of inertia of cross-section.

$= \frac{107,32.5,97}{6}(2.-675,6^2) + \frac{2.68,58.5,97}{6}(617,8^2+4.-28,5^2+-675,6^2) +$

$... + \frac{2.38,84.9,47}{6}(-675,6^2+4.-18,6^2+638,4^2) + \frac{107,32.5,89}{6}(2.638,4^2)$

= 404 288 518 = 404,29 * 10⁶ mm⁶ ✓

$C_{can} = \int_A a_s^2 dA$ = central torsional moment of inertia of cross-section.

= 244.46.5,97.18,86² + 2.38,84.9,47.53,66² + 107,32.5,89.19,98²

= 2 889 669 = 2,890 * 10⁶ mm⁴ ✓

$K_{19} = \frac{C_{can}}{C_{can} - C_{svt}} = \frac{2,890 * 10^6}{2,890.10^6 - 1,565.10^6} = 2,182^{216}$ ✓

$\bar{C}_{tor} = K_{19} . C_{tor} = 2,182 . 404,29 * 10^6 = 882,12 * 10^6$ mm⁴ (882 124 450)

$K_{18} = \sqrt{\frac{G . C_{svt}}{E \bar{C}_{tor}}} = \left(\frac{1050 . 1,565.10^6}{2918 . 882,12.10^6}\right)^{1/2} = 25,269 * 10^{-3}$ mm⁻¹ ✓

Evaluate ϕ_{tor}, τ_{svt} and τ_{tor} at the midspan and 1/4-span (z = 300 mm) sections using TABLE NO. 9 in APPENDIX 2 (pg. 104) of the technical report as follows :

T_{ext} = − 11 595 N-mm.

$a_1 = a_2$ = 600 mm.

Revised 03.10.78

K_{18} STO A ✓
K_{10} STO B ✓
$\sinh K_8 . 600$ STO C
$\sinh K_8 . 1200$ STO D
$\sinh K_{18} . 300$ STO E
$\sinh K_{18} . 300$ STO F
$\cosh K_{18} . 600$ STO G
$\cosh K_{18} . 300$ STO H
$\cosh K_{18} . 1200$ STO I ✓

At midspan ($\xi = 600$ mm) ;

$$B_{tor}(600) = \frac{-11\,595}{25{,}269.10^{-3} \cdot 2{,}182} \cdot \frac{(1920{,}6.10^3)^2}{7{,}378 \cdot 10^{12}}$$

$$= -105\,182 \quad N-mm^2 \qquad \checkmark$$

Note that $B_{tor}(600^-) = B_{tor}(600^+)$ i.e there is no step in the function at $\xi = 600$ mm. ✓

$$T_{svt}(600^-) = \frac{-11\,595}{2{,}182} \cdot \left(\frac{600}{1200} \cdot 2{,}182 - \frac{(1920{,}6.10^3)^2}{7{,}378 \cdot 10^{12}} \right)$$

$$= -3\,140{,}4 \quad N-mm. \qquad \checkmark$$

$$T_{svt}(600^+) = \frac{-11\,595}{2{,}182} \cdot \left(-\frac{600}{1200} \cdot 2{,}182 + \frac{(1920{,}6.10^3)^2}{7{,}378 \cdot 10^{12}} \right)$$

$$= +3\,140{,}4 \quad N-mm. \qquad \checkmark$$

$$T_{tor}(600^-) = \frac{-11\,595}{2{,}182} \cdot \frac{(1920{,}6.10^3)^2}{7{,}378 \cdot 10^{12}}$$

$$= -2\,657{,}1 \quad N-mm. \qquad \checkmark$$

$$T_{tor}(600^+) = -\frac{-11\,595}{2{,}182} \cdot \frac{(1920{,}6.10^3)^2}{7{,}378 \cdot 10^{12}}$$

$$= 2\,657{,}1 \quad N-mm. \qquad \checkmark$$

Check :- $T_{svt}(600^-) + T_{tor}(600^-) = -3140{,}4 - 2657{,}1 = -5797{,}5$

$$\simeq T_{ext} \cdot \frac{a_2}{l} = -5797{,}5 \quad N-mm. \qquad \checkmark$$

Published 03.10.77

$$T_{svt}(600^+) + T_{tor}(600^+) = 3140{,}4 + 2657{,}1 = 5797{,}5 \text{ N-mm.}$$

$$\simeq -T_{ext} \cdot \frac{a_1}{l} = 5797{,}5 \quad N-mm. \qquad \checkmark$$

At ¼-span ($\xi = 300$ mm) ;

$$B_{tor}(300) = \frac{-11\,595}{25{,}269.10^{-3} \cdot 2{,}182} \cdot \frac{1920{,}6.10^3}{7{,}378 \cdot 10^{12}} \cdot 979{,}96$$

$$= -58{,}68 \quad N-mm^2 \qquad \checkmark$$

$$T_{svt}(300) = \frac{-11\,595}{2{,}182} \cdot \left(\frac{600}{1200} \cdot 2{,}182 - \frac{1920{,}6.10^3}{7{,}378 \cdot 10^{12}} \cdot 979{,}96 \right)$$

$$= -5796{,}1 \quad N-mm. \qquad \checkmark$$

$$T_{tor}(300) = \frac{-11\,595}{2{,}182} \cdot \frac{1920{,}6.10^3}{7378 \cdot 10^{12}} \cdot 979{,}96$$

$$= -1{,}4 \quad N-mm. \qquad \checkmark$$

Check : $T_{svt}(300) + T_{tor}(300) = -5796{,}1 - 1{,}4 = -5797{,}5$ N-mm

$$\simeq T_{ext} \cdot \frac{a_2}{l} = -5797{,}5 \quad N-mm. \qquad \checkmark$$

Evaluation of torsional warping stresses (f_{tor}) :-

At midspan ($\xi = 600$) -

$$f_{tor}(600) = \frac{B_{tor}(600) \cdot \omega_{tor}}{C_{tor}} = \frac{-105\,182}{404{,}29.10^6} \omega_{tor} = -260{,}09.10^{-6} \cdot \omega_{tor}$$

See figure 3.2.2 for ω_{tor} values. ✓

Published 03.10.77

At A and E ; $f_{twr}(600) = 0$ by anti-symmetry.

At B ; $f_{twr}(600) = -260,09 . 10^{-6} . -675,6 = 0,176 \ N/mm^2$ ✓

At C ; $f_{twr}(600) = -260,09 . 10^{-6} . 617,8 = -0,161 \ N/mm^2$ ✓

At D ; $f_{twr}(600) = -260,09 . 10^{-6} . 638,4 = -0,166 \ N/mm^2$ ✓

See figure 3.2.3 for a diagram of the above stresses.

At ¼-span ($z = 300$) :-

$$f_{twr}(300) = \frac{B_{twr}(300) . w_{twr}}{C_{twr}} = \frac{-53,65}{404,29 . 10^6} . w_{twr} = -1,327 . 10^{-7} . w_{twr}$$ ✓

See figure 3.2.2 for w_{twr} values.

At A and E ; $f_{twr}(300) = 0$ by anti-symmetry

At B ; $f_{twr}(300) = -1,327 . 10^{-7} . -675,6 = 0,000090 \simeq 0$ ✓

At C ; $f_{twr}(300) = -1,327 . 10^{-7} . 617,8 = -0,000082 \simeq 0$ ✓

At D ; $f_{twr}(300) = -1,327 . 10^{-7} . 638,4 = -0,000085 \simeq 0$ ✓

See figure 3.2.6 for a diagram of the above stresses - ie. stresses are approximately zero throughout. ✓

Revised 03.10.89

Evaluation of torsional warping shear stresses (τ_{twr}) :-

At midspan ($z = 600^-$) ;

$$\tau_{twr}(600^-) = \frac{T_{twr}(600^-)}{C_{cen} - C_{svt}} . \frac{dw_{twr}}{ds_{per}} = \frac{-2657,1}{(2,890 - 1,565) . 10^6} . \frac{dw_{twr}}{ds_{per}}$$

$$= -2006,31 . 10^{-6} . \frac{dw_{twr}}{ds_{per}} \ N/mm^2$$ ✓

Use figure 3.2.2 (w_{twr}) to find $\frac{dw_{twr}}{ds_{per}}$ values.

Segment AB ; $\tau_{twr}(600^-) = -2006,31 . 10^{-6} . \frac{-675,6 - 0}{53,66} = 0,025 \ N/mm^2$ ✓

Segment BC ; $\tau_{twr}(600^-) = -2006,31 . 10^{-6} . \frac{617,8 - (-675,6)}{68,58} = -0,038 \ N/mm^2$ ✓

Segment BD ; $\tau_{twr}(600^-) = -2006,31 . 10^{-6} . \frac{638,4 - (-675,6)}{88,84} = -0,068 \ N/mm^2$ ✓

Segment DE ; $\tau_{twr}(600^-) = -2006,31 . 10^{-6} . \frac{0 - 638,4}{53,66} = 0,024 \ N/mm^2$ ✓

See figure 3.2.4 for a diagram of the above stresses. ✓

At midspan ($z = 600^+$) ;

$T_{twr}(600^+) = -T_{twr}(600^-)$ and therefore the torsional warping shear stresses at these sections (on either side of midspan) are equal in magnitude but opposite in sign. ✓

See figure 3.2.4 for a diagram of the above stresses. ✓

Revised 03.10.89

At ¼-span ($z = 300$) ;

$$\sigma_{tor}(300) = \frac{T_{tor}(300)}{C_{cen} - C_{svt}} \cdot \frac{d\omega_{tor}}{ds_{per}} = \frac{-1,4 \cdot 10^{-6}}{(2,890 - 1,565)} \cdot \frac{d\omega_{tor}}{ds_{per}}$$

$$= -1,024 * 10^{-6} \cdot \frac{d\omega_{tor}}{ds_{per}} \quad N/mm^2$$

Use figure 3.2.2 to find the $\frac{d\omega_{tor}}{ds_{per}}$ values.

Segment AB ; $\sigma_{tor}(300) = -1,024 \cdot 10^{-6} \cdot \frac{-675,6 - 0}{53,66} = 0,000013 \; N/mm^2 \simeq 0$

Segment BC ; $\sigma_{tor}(300) = -1,024 \cdot 10^{-6} \cdot \frac{617,8 - (-675,6)}{68,58} = -0,000019 \; N/mm^2 \simeq 0$

Segment BD ; $\sigma_{tor}(300) = -1,024 \cdot 10^{-6} \cdot \frac{638,4 - (-675,6)}{38,84} = -0,000035 \; N/mm^2 \simeq 0$

Segment DE ; $\sigma_{tor}(300) = -1,024 \cdot 10^{-6} \cdot \frac{0 - 638,4}{58,66} = 0,000012 \; N/mm^2 \simeq 0$

See figure 3.2.7 for a diagram of the above stresses - i.e stresses are approximately zero throughout. ✓

Evaluation of St. Venant shear stresses (σ_{svt}) ;

At midspan ($z = 600^-$) :-

$$\sigma_{svt_A}^{(600^-)} = \frac{T_{svt}(600^-)}{2 A_{enc} \cdot h} = \frac{-3140,4}{2.107,32 \cdot 38,84 \cdot h} = -\frac{0,377}{h} \quad N/mm^2$$

$$\Delta\sigma_{svt}(600^-) = \frac{h \cdot T_{svt}(600^-)}{C_{svt}} = \frac{h \cdot -3140,4}{1,565 \cdot 10^6} = -0,002006 \cdot h \; N/mm^2$$ ✓

Segment AB ; $\sigma_{svt}(600^-) = -\frac{0,377}{5,97} = -0,063 \; N/mm^2$ ✓

$$\Delta\sigma_{svt}(600^-) = -0,002006 \cdot 5,97 = -0,012 \; N/mm^2$$ ✓

Segment BC ; $\sigma_{svt}(600^-) = 0$

$$\Delta\sigma_{svt}(600^-) = -0,002006 \cdot 5,97 = -0,012 \; N/mm^2$$ ✓

Segment BD ; $\sigma_{svt}(600^-) = -\frac{0,377}{9,47} = -0,040 \; N/mm^2$ ✓

$$\Delta\sigma_{svt}(600^-) = -0,002006 \cdot 9,47 = -0,019 \; N/mm^2$$ ✓

Segment DE ; $\sigma_{svt}(600^-) = -\frac{0,377}{5,89} = -0,064 \; N/mm^2$ ✓

$$\Delta\sigma_{svt}(600^-) = -0,002006 \cdot 5,89 = -0,012 \; N/mm^2$$ ✓

See figure 3.2.5 for a diagram of the above stresses. ✓

At midspan ($z = 600^+$) :-

Since $T_{svt}(600^+) = -T_{svt}(600^-)$, the St. Venant shear stresses at these sections (on either side of midspan) will be equal in magnitude but opposite in sign.

See figure 3.2.3 for a diagram of the above stresses. ✓

At ¼-span ($z = 300$) ;

$$\sigma_{svt}\ (300) = \frac{T_{svt}\ (300)}{2\,A_{enc}\,.\,h} = \frac{-5706,1}{2.107,32.38,84.h} = -0,695 \cdot \frac{1}{h}\ N/mm^2$$ ✓

$$\Delta\sigma_{svt}\ (300) = \frac{h\,T_{svt}\ (300)}{C_{svt}} = \frac{h.\,-5706,1}{1565,3.10^3} = -0,003703.h\ N/mm^2$$ ✓

Segment AB ; $\sigma_{svt}\ (300) = -\frac{0,695}{5,97} = -0,116\ N/mm^2$ ✓

$\Delta\sigma_{svt}\ (300) = -0,003703.5,97 = -0,022\ N/mm^2$ ✓

Segment BC ; $\sigma_{svt}\ (300) = 0$

$\Delta\sigma_{svt}\ (300) = -0,003703.5,97 = -0,022\ N/mm^2$ ✓

Segment BD ; $\sigma^{(300)}_{svt_A} = -\frac{0,695}{9,47} = -0,073\ N/mm^2$ ✓

$\Delta\sigma^{(300)}_{svt_A} = -0,003703.9,47 = -0,035\ N/mm^2$ ✓

Segment DE ; $\sigma^{(300)}_{svt_A} = -\frac{0,695}{5,89} = -0,118\ N/mm^2$ ✓

$\Delta\sigma_{svt}\ (300) = -0,003703.5,89 = -0,022\ N/mm^2$ ✓

See figure 3.2.8 for a diagram of the above stresses. ✓

CHECKING FOR STRESS VALUES CALCULATED ABOVE :

Equilibrium check on values of $\sigma_{tor}\ (600^-)$:-

See figure 3.2.4

Anti-clockwise moment about the shear centre is :-

$18,86.\ 0,025.\ 5,97.\ 107,32 - 107,32.\ 9,47.\ 0,068.\ 38,84 + \ldots$
$\ldots + -18,86.\ 68,58.\ 2.5,97.\ 0,038 + 0,024.5,89.107,32.19,98$

$= -2\,665,9\ N\text{-}mm \cong 2\,657,1\ N\text{-}mm\ (= T_{tor}\ (600^-))$ ∴ O.K.

Vertical forces (in webs) are in equilibrium - i.e sum to zero.

Horizontal forces :

$-2.\ 0,038.\ 5,97.\ 68,58 + 0,025.\ 107,32.5,97 - 0,024.5,89.107,32$

$= -30,27\ N \rightarrow$ i.e large when compared to the applied loads.

∴ $\sigma_{tor}\ (600^-)$ stress system is approximately in equilibrium (i.t.o moment and the vertical forces) with the applied loading with the exception of the forces in the horizontal direction.

Equilibrium check on values of $\sigma_{tor}\ (600^+)$:-

Since the stresses for this section are equal in magnitude but opposite in sign to those above, i.e at $z = 600^-$, it follows that the anti-clockwise moment about the shear centre is + 2665,9 N-mm which in turn is approximately equal to the calculated internal torsional moment due to the torsional warping shear stresses i.e $T_{tor}\ (600^+) = 2657,1$ N-mm. (see pg. 7)

Similarly, the horizontal out-of-balance force would be 30,27 N← and again, also, the vertical forces (in the webs) would be in equilibrium.

∴ The σ_{thor} (600⁺) stress system is approximately in equilibrium in terms of the moment and the vertical forces but not horizontally.

Equilibrium check on values of σ_{thor} (300) :-
See figure 3.2.7 and calculations on page no. 11.
The stress values at this section are approximately zero since τ_{thor} (300) = -1,4 N-mm which is negligible when compared to the applied torsional moment of 11595 N-mm. Therefore equilibrium conditions are satisfied.

Equilibrium check on values of σ_{svt} (600⁻) :-

See figure 3.2.5.

Anti-clockwise moment about the shear centre is (ignoring the $\Delta\sigma_{svt}$ effect)

$-18,86 . 0,063 . 5,97 . 107,32 - 107,32 . 9,47 . 38,84 . 0,040 + \ldots$
$\ldots - 0,064 . 19,98 . 5,89 . 107,32$

$= -3148,5$ N-mm $\simeq -3140,4$ N-mm $(= \tau_{svt}(600^-))$

Vertical forces (in webs) are in equilibrium - i.e sum to zero.

Horizontal forces:

$-107,32 . 5,97 . 0,063 + 0,064 . 107,32 . 5,89 = 0,09$ N← ≃ zero.

∴ The σ_{svt} (600⁻) stress system is in equilibrium with the applied loading.

Equilibrium check on values of σ_{svt} (600⁺):-
See figure 3.2.5
$\sigma_{svt}(600^+)$
Since the values are equal in magnitude but opposite in sign to those for the section at $z = 600^-$ (i.e above), it follows that the anti-clockwise moment about the shear centre is equal to + 3148,5 N-mm which is approximately equal to the calculated internal torsional moment in St. Venant torsion. i.e $\tau_{svt}(600^+) = +3140,4$ N-mm - see pg 7. Similarly, the horizontal forces and the vertical forces would also sum to zero and would thus be in equilibrium. Hence, the $\sigma_{svt}(600^+)$ stress system is in equilibrium with the applied loading.

Equilibrium check on values of σ_{svt} (300) :-

See figure 3.2.8.

Anti-clockwise moment about the shear centre - ignoring the $\Delta\sigma_{svt}$ effect :

$-18,86 \cdot 107,32 \cdot 5,97 \cdot 0,116 - 107,32 \cdot 38,84 \cdot 9,47 \cdot 0,073 + \ldots$
$\ldots - 19,98 \cdot 107,32 \cdot 5,89 \cdot 0,118$

$= -5773,6$ N-mm $\simeq -5706,1$ N-mm ($= T_{svt}(300)$ - pg 8.)

Vertical forces (in webs) are in equilibrium - i.e sum to zero.

Horizontal forces :

$-0,116 \cdot 5,97 \cdot 107,32 + 0,118 \cdot 5,89 \cdot 107,32 = 0,27$ N $\leftarrow \simeq$ zero.

∴ The σ_{svt} (300) stress system is approximately in equilibrium with the applied loading.

Check on value of B_{twr} (600) using the f_{twr} (600) values calculated on page 9 and plotted in figure 3.2.3 together with the w_{twr} diagram - i.e. figure 3.2.2.

$$B_{twr}(600) = \int_A f_{twr}(600) \cdot w_{twr} \cdot dA$$

∴ Using Simpson's Rule for integration :

$$B_{twr}(600) = \frac{107,32 \cdot 5,97}{6}(2. -675,6 . 0,176) + \frac{107,32 \cdot 5,89}{6}(2 . 638,4 . -0,166) + \ldots$$

$$\ldots + \frac{2 . 68,58 . 5,97}{6}(-675,6 . 0,176 + 4 . -28,9 . 0,0075 + 617,8 . -0,161) + \ldots .$$

$$\ldots + \frac{2 . 38,84 . 9,47}{6}(-675,6 . 0,176 + 4 . -18,6 . 0,005 + 638,4 . -0,166)$$

$= -105\,261$ N-mm^2 $\simeq -105\,152$ N-mm^2 - see pg.7 for calculation of B_{twr} (600)

By anti-symmetry about the $\mathcal{L}$, the resultant axial force on the cross-section due to torsional warping stresses, is zero.

Therefore, the f_{twr} (600) values were correctly derived from the B_{twr} (600) value and the stresses are self-equilibrating.

Check on values of B_{twr} (300) using the f_{twr} (300) values calculated on page 9 together with the w_{twr} diagram (fig. 3.2.2.)

$$B_{twr}(300) = \frac{107,32 \cdot 5,97}{6}(2 . -675,6 . 9 \cdot 10^{-5}) + \frac{107,32 \cdot 5,89}{6}(2 . 638,4 . -8,5 \cdot 10^{-5}) + \ldots$$

$$\ldots + \frac{2 . 68,58 . 5,97 \cdot 10^{-5}}{6}(-675,6 . 9 + 4 . -28,9 . 0,4 + 617,8 . -8,2) + \ldots .$$

$$\ldots + \frac{2 . 38,84 . 9,47 \cdot 10^{-5}}{6}(-675,6 . 9 + 4 . -18,6 . 0,25 + 638,4 . -8,5)$$

$= -53,78$ N-mm^2 $\simeq -53,65$ N-mm^2 - see pg.8 for calculation of B_{twr} (300).

By anti-symmetry about the $\mathcal{L}$, the resultant axial force on the cross-section due to torsional warping stresses, is zero.

Therefore, the f_{twr} (600) values were correctly derived from the B_{twr} (300) value and the stresses are self-equilibrating.

ANALYSIS : MODEL NO. 3 LOADCASE 2

Units for the following diagrams are all N/mm^2 (MPa.)

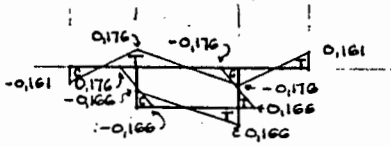

FIGURE 3.2.3 : f_{bur} at midspan ($z = 600$)

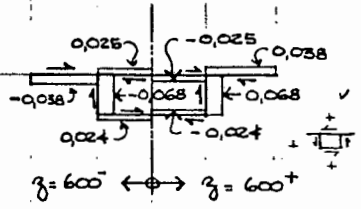

FIGURE 3.2.4 : σ_{bur} at midspan ($z = 600^-$ and 600^+)

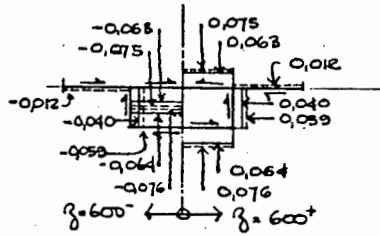

FIGURE 3.2.5 : σ_{svt} at midspan ($z = 600^-$ and 600^+)

NOTE : Dotted lines show $\sigma_{svt} + \Delta\sigma_{svt}$ values.

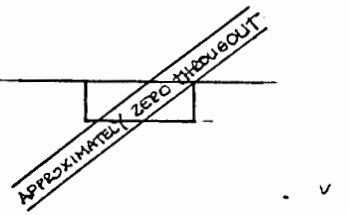

FIGURE 3.2.6 : f_{bur} at 1/4-span ($z = 300$)

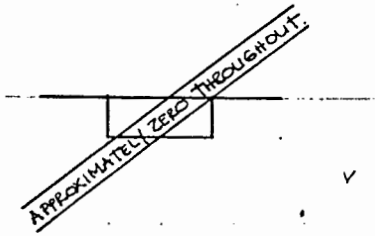

FIGURE 3.2.7 : σ_{bur} at 1/4-span ($z = 300$)

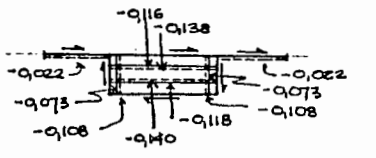

FIGURE 3.2.8 : σ_{svt} at 1/4-span ($z = 300$)

NOTE : Dotted lines show $\sigma_{svt} + \Delta\sigma_{svt}$ values.

ANALYSIS : MODEL NO. 3 LOADCASE 2

3.2.4.2 DISTORTIONAL WARPING AND TRANSVERSE BENDING (BEAM ON ELASTIC FOUNDATION ANALOGY.)

Evaluation of w_{dwr} as follows

$$K_c = \frac{bh_{top}}{dh_{web}} \left(\frac{b + 2b_{cant}}{b}\right)^3 = 10,593^{2,725}$$

$$K_T = \frac{bh_{bot}}{dh_{web}} = 1,719^{8,568}$$

where $b = 107,32$ mm

$b_{cant} = 68,58$ mm

$d = 38,84$ mm

$h_{top} = 5,97$ mm

$h_{web} = 8,47$ mm

$h_{bot} = 5,85$ mm

$$K_{2S} = \frac{3 + K_c}{3 + K_T} = 1,333\,975 = 5,000.$$

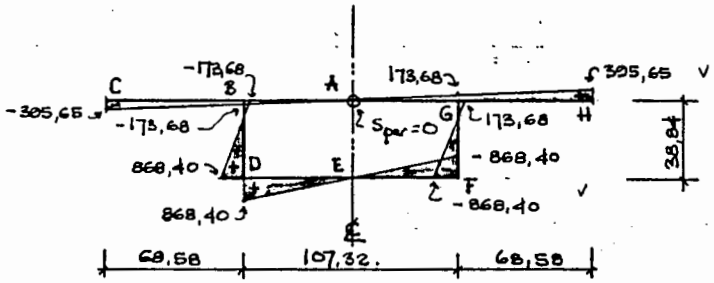

FIGURE 3.2.9 : w_{dwr} diagram (mm^2)

At F : $$w_{dwr} = -\frac{K_{2S} \cdot b \cdot d}{4(1 + K_{2S})} = -\frac{5,0 \cdot 107,32 \cdot 38,84}{4(1 + 5,0)} = -868,40 \text{ mm}^2$$

At G : $$w_{dwr} = \frac{b \cdot d}{4(1 + K_{2S})} = \frac{107,32 \cdot 38,84}{4(1 + 5,0)} = 173,68 \text{ mm}^2$$

3.2.4.2 DISTORTIONAL WARPING AND TRANSVERSE BENDING (BEAM ON ELASTIC FOUNDATION ANALOGY.)

Evaluation of w_{dwr} :

$$K_6 = \frac{bh_{top}}{dh_{web}} \left(\frac{b + 2b_{cant}}{b}\right)^3 = 20,593^{2725} \quad \checkmark$$

$$K_7 = \frac{bh_{bot}}{dh_{web}} = 1,719^{8568} \quad \checkmark$$

where $b = 107,32$ mm ✓
$b_{cant} = 68,58$ mm ✓
$d = 38,84$ mm ✓
$h_{top} = 5,97$ mm ✓
$h_{web} = 9,47$ mm ✓
$h_{bot} = 5,85$ mm ✓

$$K_{25} = \frac{3 + K_6}{3 + K_7} = \frac{4.390\,975}{} = 5,000. \quad \checkmark$$

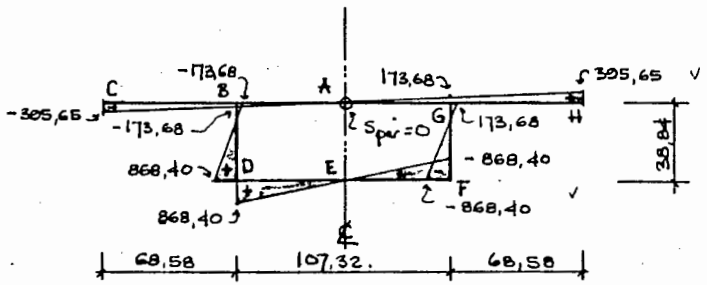

FIGURE 3.2.9 : w'_{dwr} diagram (mm^2) ✓

At F : $$w_{dwr} = -\frac{K_{25} \cdot b.d}{4(1+K_{25})} = -\frac{5,0 \cdot 107,32 \cdot 38,84}{4(1+5,0)} = -868,40 \text{ mm}^2$$ ✓

At G : $$w_{dwr} = \frac{b.d}{4(1+K_{25})} = \frac{107,32 \cdot 38,84}{4(1+5,0)} = 173,68 \text{ mm}^2$$

At H : $$w_{dwr} = \left(\frac{b + 2b_{cant}}{b}\right) \cdot \frac{bd}{4(1+K_{25})} = \frac{244,48}{107,32} \cdot 173,68 = 395,65 \text{ mm}^2$$ ✓

Calculate the distortional warping moment of inertia of the cross-section, C_{dwr}, as follows.

$$C_{dwr} = \frac{b^2 . d^3 . h_{web}}{48} \cdot K_4 = \frac{107,32^2 . 38,84^3 . 9,47}{48} \cdot 2,932 = 390,38 * 10^6 \text{ mm}^6$$ ✓ (390 383 970)

where $$K_4 = \frac{3 + 2(K_6 + K_7) + K_6 . K_7}{6 + K_6 + K_7} = 2,932^{137}$$ ✓

Evaluate I_{FEA} as follows :

$$I_{top} = \frac{h_{top}^3}{12(1-\nu^2)} = \frac{5,97^3}{12(1-0,30^2)} = 20,912 \text{ mm}^3/\text{mm}.$$ ✓

$$I_{bot} = \frac{h_{bot}^3}{12(1-\nu^2)} = \frac{5,85^3}{12(1-0,30^2)} = 20,083 \text{ mm}^3/\text{mm}.$$ ✓

$$I_{web} = \frac{h_{web}^3}{12(1-\nu^2)} = \frac{9,47^3}{12(1-0,39^2)} = 83,469 \text{ mm}^3/\text{mm}.$$ ✓

$$K_{26} = 1 + \frac{2\frac{b}{d} + 3\frac{I_{top} + I_{bot}}{I_{web}}}{\frac{I_{top}+I_{bot}}{I_{web}} + 6\frac{d}{b} \cdot \frac{I_{top} . I_{bot}}{I_{web}^2}} = 12,253^{2926}$$ ✓

$$I_{FEA} = \frac{24 . I_{web}}{K_{26} . d} = \frac{24 . 83,469}{12,253 . 38,84} = 4,209^{362} \text{ mm}^2$$ ✓

Evaluate $B_{dwr}(z)$, $dB_{dwr}(z)$ and $\beta_{brb}(z)$ at the midspan and 1/4-span ($z = 300$) sections using the equations given in TABLE 16, APPENDIX 3 (pg. 111). Use 'DISTORT' program for the HP 41-C desk-top calculator to evaluate the summation portions of the equations. ✓

At midspan : $T_{ext} = -11595$ N-mm.

$z = 600$ mm

$a_1 = a_2 = 600$ mm

$$B_{dwr}(600) = \frac{-11595(1200-600)}{2.1200}\cdot 600 - \frac{-11595.1200}{\pi^2}\cdot \left(\sum_{n=1}^{9} 1,088536\right)$$

$$= -204,651 * 10^3 \text{ N-mm}^2$$

NOTE : $B_{dwr}(600^+) = B_{dwr}(600^-)$ i.e. no step in function

$$\frac{d}{dz} B_{dwr}(600^-) = \frac{-11595(1200-600)}{2.1200} - \frac{-11595}{\pi}\left(\sum_{n=1}^{9} 1,1422.10^{-10}\right)$$

$$= -2898,75 \text{ N-mm}.$$

$$\frac{d}{dz} B_{dwr}(600^+) = -\frac{-11595.600}{2.1200} - \frac{-11595}{\pi}\left(\sum_{n=1}^{9}\right)$$

$$= 2898,75 \text{ N-mm} = -\frac{d}{dz} B_{dwr}(600^-)$$

$$\beta_{trb}(600) = \frac{-11595.10^{-6}}{2918.390,38}\left[\frac{600^2}{12}(1200-300-300) - \frac{1200^3}{\pi^4}\cdot\left(\sum_{n=1}^{9} 1,005217\right)\right]$$

$$= -1708,26 * 10^{-6} \quad \text{(dimensionless)}$$

NOTE : $\beta_{trb}(600^-) = \beta_{trb}(600^+)$ i.e no step in function.

At 1/4-span : $T_{ext} = -11595$ N-mm.

$z = 300$ mm

$a_1 = a_2 = 600$ mm.

$$B_{dwr}(300) = \frac{-11595(1200-600)}{2.1200}\cdot 300 - \frac{-11595.1200}{\pi^2}\left(\sum_{n=1}^{9}\right)$$

$$= 30,335 * 10^3 \text{ N-mm}^2$$

NOTE : $B_{dwr}(300^+) = B_{dwr}(300^-)$ i.e no step in function.

$$\frac{d}{dz} B_{dwr}(300) = \frac{-11595.600}{2400} - \frac{-11595}{\pi}\cdot\left(\sum_{n=1}^{9}\right)$$

$$= 202,54 \text{ N-mm}.$$

$$\beta_{trb}(300) = \frac{-11595.10^{-6}}{2918.390,38}\left[\frac{600.300}{12}(1200-300-75) - \frac{1200^3}{\pi^4}\cdot(0,697283)\right]$$

$$= -55,64 * 10^{-6} \quad \text{(dimensionless)}$$

Evaluation of distortional warping stresses f_{dwr} :-

At midspan ($z = 600$):

$$f_{dwr}(600) = \frac{B_{dwr}(600).w_{dwr}}{C_{dwr}} = \frac{-204,65.10^3}{390,38.10^6}\cdot w_{dwr} = -524,23.10^{-6}.w_{dwr}\ \frac{N}{mm^2}$$

See figure 3.2.9 for w_{dwr} values.

At A and E, $f_{dwr}(600) = 0$

At B, $f_{dwr}(600) = -524,23.10^{-6}.-173,68 = 0,091\ N/mm^2$

At C, $f_{dwr}(600) = -524,23.10^{-6}.-395,65 = 0,207\ N/mm^2$

At D, $f_{dwr}(600) = -524,23.10^{-6}.\ 868,40 = -0,455\ N/mm^2$ ✓

See figure 3.2.11 for a diagram of the above stresses. ✓

Similarly, at 1/4-span ($z = 300$) :-

$f_{dwr}(300) = \frac{30,385.10^3}{390,38.10^6} \cdot \omega_{dwr} = 77,707 \cdot 10^{-6} \cdot \omega_{dwr}\ N/mm^2$ ✓

At A and E, $f_{dwr}(300) = 0$

At B, $f_{dwr}(300) = 77,71.10^{-6}.\ -173,68 = -0,013\ N/mm^2$ ✓

At C, $f_{dwr}(300) = 77,71.10^{-6}.\ -395,65 = -0,031\ N/mm^2$ ✓

At D, $f_{dwr}(300) = 77,71.10^{-6}.\ 868,40 = 0,068\ N/mm^2$ ✓

See figure 3.2.14 for a diagram of the above stresses ✓

Evaluation of distortional warping shear stresses, τ_{dwr} :-

At midspan ($z = 600$) : ✓

$$\tau_{dwr}(600) = -\frac{d}{dz}B_{dwr}^{(600)} \cdot K_{28} \cdot \frac{bd}{4(1+K_{26})} = -\frac{-2038,75.107,32.38,84}{390,38.10^6.4\,(1+5,0)} \cdot \frac{K_{28}}{h}$$

$$= 1289,63 \cdot \frac{K_{28}}{h} \cdot 10^{-6}\ N/mm^2$$ ✓

K_{28} in the above equation can be found at various points on the cross-section (figure 3.2.10) using the equations given in TABLE 2 (pg. 44) of the technical report. ✓

$K_{26} = \frac{b + 2b_{cant}}{b} = \frac{244,48}{107,32} = 2,278$ ✓ *

$A_{top} = b h_{top} = 107,32 . 5,97 = 640,70\ mm^2$ ✓ B

$A_{cant} = b_{cant} . h_{top} = 68,58 . 5,97 = 409,42\ mm^2$ ✓ C

$A_{web} = d . h_{web} = 38,84 . 9,47 = 367,81\ mm^2$ ✓ D

$A_{bot} = b . h_{bot} = 107,32 . 5,89 = 632,11\ mm^2$ ✓ E

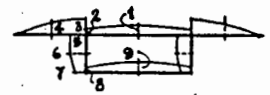

FIGURE 3.2.10 : Points of cross-section where K_{26} is defined

At 1 ; $\tau_{dwr}(600) = 1289,63.10^{-6} . \frac{108,08}{5,97} = 0,023\ N/mm^2$ ✓

At 2 ; $\tau_{dwr}(600) = 1289,63.10^{-6} . \frac{-52,10}{5,97} = -0,011\ N/mm^2$ ✓

At 3 ; $\tau_{dwr}(600) = 1289,63.10^{-6} . \frac{671,05}{5,97} = 0,145\ N/mm^2$ ✓

At 4 ; $\tau_{dwr}(600) = 1289,63.10^{-6} . \frac{400,98}{5,97} = 0,087\ N/mm^2$ ✓

At 5 ; $\tau_{dwr}(600) = 1289,63.10^{-6} . \frac{-723,15}{9,47} = -0,098\ N/mm^2$ ✓

At 6 ; $\tau_{dwr}(600) = 1289,63.10^{-6} . \frac{-631,20}{9,47} = -0,086\ N/mm^2$ ✓

At 7 ; $\tau_{dwr}(600) = 1289,63.10^{-6} . \frac{12,48}{9,47} = 0,002\ N/mm^2$ ✓

At 8 ; $\tau_{dwr}(600) = 1289,63.10^{-6} . \frac{12,48}{5,89} = 0,003\ N/mm^2$ ✓

At 9 ; $\sigma_{dwr}(600^-) = 1289,63.10^{-6}.\frac{802,62}{5,89} = 0,176\ N/mm^2$ ✓

See figure 3.2.12 for a diagram of the above stresses. ✓

At midspan ($z = 600^+$) :-

Since $\frac{d}{dz}B_{dwr}(600^+) = -\frac{d}{dz}B_{dwr}(600^-)$, it follows that the stress values at the $z = 600^+$ section are equal in magnitude but opposite in sign to those calculated above for the $z = 600^-$ section. ✓

See figure 3.2.12. for a diagram of these stresses. ✓

At ¼-span ($z = 300$) :-

The distortional warping shear stresses can be calculated at the same points of cross-section - see figure 3.2.10.

$$\sigma_{dwr}(300) = -\frac{202,54.107,32.38,84}{390,38.10^6.4(1+5,0)}.\frac{K_{28}}{h} = -90,11.10^{-6}.\frac{K_{28}}{h}\ N/mm^2$$ ✓

At 1 ; $\sigma_{dwr}(300) = -90,11.10^{-6}.\frac{108,08}{5,97} = -0,002\ N/mm^2$ ✓

At 2 ; $\sigma_{dwr}(300) = -90,11.10^{-6}.\frac{-52,10}{5,97} = 0,001\ N/mm^2$ ✓

At 3 ; $\sigma_{dwr}(300) = -90,11.10^{-6}.\frac{671,05}{5,97} = -0,010\ N/mm^2$ ✓

At 4 ; $\sigma_{dwr}(300) = -90,11.10^{-6}.\frac{400,93}{5,97} = -0,006\ N/mm^2$ ✓

At 5 ; $\sigma_{dwr}(300) = -90,11.10^{-6}.\frac{-723,15}{9,47} = 0,007\ N/mm^2$ ✓

At 6 ; $\sigma_{dwr}(300) = -90,11.10^{-6}.\frac{-631,20}{9,47} = 0,006\ N/mm^2$ ✓

At 7 ; $\sigma_{dwr}(300) = -90,11.10^{-6}.\frac{12,48}{9,47} = 0,000$ ✓

At 8 ; $\sigma_{dwr}(300) = -90,11.10^{-6}.\frac{12,48}{5,89} = 0,000$ ✓

At 9 ; $\sigma_{dwr}(300) = -90,11.10^{-6}.\frac{802,62}{5,89} = -0,012\ N/mm^2$ ✓

See figure 3.2.15 for a diagram of the above stresses. ✓

Evaluation of transverse bending stresses, f_{trb}, at the midspan and ¼-span sections :-

At midspan ($z = 600$) ;

$$M_{trb,B}(600) = \frac{E.I_{PRA}\beta_{trb}(600)}{2(1+K_{30})} = \frac{2918.4,209.-1708,26.10^{-6}}{2(1+0,969)}$$ ✓

$$= -5,329\ N\text{-}mm/mm$$ ✓

$$M_{trb,D}(600) = -\frac{K_{30}.E.I_{PRA}.\beta_{trb}(600)}{2(1+K_{30})} = -\frac{0,969.2918.4,209.-1708,26}{2(1+0,969).10^6}$$ ✓

$$= 5,162\ N\text{-}mm/mm.$$ ✓

where $K_{30} = \frac{3+\frac{b}{d}.\frac{I_{web}}{I_{top}}}{3+\frac{b}{d}.\frac{I_{web}}{I_{bot}}} = \frac{3+\frac{107,32}{38,84}.\frac{83,460}{20,212}}{3+\frac{107,32}{38,84}.\frac{83,460}{20,083}} = 0,969$ ✓

Therfore, the stresses can be found as follows :-

at top of web, in flange $f_{trb}(600) = \frac{6}{5{,}97^2} \cdot -5{,}329 = \mp 0{,}897$ N/mm²

at top of web, in web $f_{trb}(600) = \frac{6}{9{,}47^2} \cdot -5{,}329 = \mp 0{,}357$ N/mm²

at bot. of web, in web $f_{trb}(600) = \frac{6}{9{,}47^2} \cdot 5{,}162 = \pm 0{,}345$ N/mm²

at bot. of web, in flange $f_{trb}(600) = \frac{6}{5{,}89^2} \cdot 5{,}162 = \pm 0{,}893$ N/mm²

See figure 3.2.13 for a diagram of the above stresses.

At ¼-span ($z = 300$) ;

$$M_{trb,B}(300) = \frac{2918 \cdot 4{,}209 \cdot -55{,}64 \cdot 10^{-6}}{2(1+0{,}969)} = -0{,}174 \text{ N-mm/mm}$$

$$M_{trb,D}(300) = -\frac{0{,}969 \cdot 2918 \cdot 4{,}209 \cdot -55{,}64 \cdot 10^{-6}}{2(1+0{,}969)} = 0{,}168 \text{ N-mm/mm}$$

Therefore, the stresses can be found as follows :-

at top of web, in flange $f_{trb}(300) = \frac{6}{5{,}97^2} \cdot -0{,}174 = \mp 0{,}029$ N/mm²

at top of web, in web $f_{trb}(300) = \frac{6}{9{,}47^2} \cdot -0{,}174 = \mp 0{,}012$ N/mm²

at bot. of web, in web $f_{trb}(300) = \frac{6}{9{,}47^2} \cdot 0{,}168 = \pm 0{,}011$ N/mm²

at bot of web, in flange $f_{trb}(300) = \frac{6}{5{,}89^2} \cdot 0{,}168 = \pm 0{,}029$ N/mm²

See figure 3.2.16 for a diagram of the above stresses.

ANALYSIS : MODEL NO. 3 LOADCASE 2

THE FOLLOWING CHECKS CAN BE DONE FOR THE STRESS VALUES AS WAS CALCULATED ABOVE :

Equilibrium check on $\sigma_{dwr}(600)$ values at midspan (fig 3.2.12):-

horizontal force on top flange $= \frac{5{,}97 \cdot 107{,}32}{6}(-0{,}011{,}2 + 0{,}0234) + \frac{2 \cdot 68{,}88 \cdot 5{,}97}{6}(4 \cdot 0{,}0087 + 0{,}146)$

$= 74{,}76$ N ←

horizontal force in bot. slab $= \frac{5{,}89 \cdot 107{,}32}{6}(2 \cdot 0{,}003 + 4 \cdot 0{,}176)$

$= 74{,}80$ N →

∴ resultant horizontal force on cross-section ≑ 0 as is required for a self-equilibrating stress system.

forces in webs are equal and opposite ∴ resultant vertical force ≑ 0 as is required for a self-equilibrating stress system.

vertical force in one web $= \frac{38{,}84 \cdot 9{,}47}{6}(-0{,}008 + 4 \cdot -0{,}086 + 0{,}002)$

$= -26{,}97$ N (↑ for rhs web) R ⊓ L

∴ resultant anti-clockwise moment $= -26{,}97 \cdot 107{,}32 + \left(\frac{74{,}76 + 74{,}80}{2}\right) 38{,}84$
(about mid-point of closed secⁿ)

$= 10{,}03$ N-mm ↺

This moment is negligable by comparison with the applied torsional moment of 11 595 N-mm and the $\sigma_{dwr}(600)$ stress system is therefore self-equilibrating

E.25

Equilibrium check on σ_{dwor} (600^+) values (figure 3.2.12) :-

Since the σ_{dwor} (600^+) values are equal in magnitude but opposite in sign to the σ_{dwor} (600^-) values, it follows that the stress system at this point i.e $z = 600^+$ would also be self-equilibrating.

Equilibrium check on σ_{dwor} (800) values (figure 3.2.15) :-

hor. force in top flange = $\frac{5,97 \cdot 101,32}{6}(2.0,001+4.-0,002)+\frac{2.68,58.5,97}{6}(4.-0,006-0,010)$

$= -5,28$ N $\rightarrow$

hor. force in bot. flange = $\frac{5,89 \cdot 101,32}{6}(0,000+4.-0,012)$

$= -5,06$ N $\leftarrow$

$\therefore$ resultant horizontal force on cross-section ≈ 0 as is required for a self-equilibrating stress system.

Vertical force in one web = $\frac{38,84 \cdot 9,47}{6}(0,007+4.0,006+0)$

$= 1,90$ N ($\downarrow$ for rhs web $^R\sqcap^L$ ⊗)

$\therefore$ resultant anti-clockwise moment = $1,90.101,32-\left(\frac{5,28+5,06}{2}\right).38,84$ (about mid-point of closed sec^n)

$= 3,11$ N-mm)

This moment is negligable by comparison with the applied torsional moment of 11595 N-mm and the σ_{dwor} (300) stress system is therefore self-equilibrating.

ANALYSIS : MODEL NO. 3 LOADCASE 2

Check on β_{dwor} (600) using figure 3.2.11 - i.e the f_{dwor} (600) stress values. Also check f_{dwor} (600) for equilibrium.

By anti-symmetry about the $\mathcal{C}$ ($x=0$), the resultant axial force on the cross-section is zero.

Also $M_x = 0$ by anti-symmetry.

$M_y = 2.122,24^2.5,97.0,207.\frac{1}{2}.\frac{2}{3}\uparrow + 101,32.9,47.38,84.\frac{-0,001-0,456}{2}\downarrow + \ldots$
$\ldots + 2.5,89.53,66^2.\frac{1}{2}.-0,456.\frac{2}{3}\downarrow$

$= -18,05$ N-mm $\Downarrow$

This value is small if compared to the applied loading.

$\beta_{dwor}(600) = 53,66^2.5,89.\frac{1}{2}.\frac{2}{3}.-0,456.2.38,84\downarrow + 0,001.9,47.38,84^2.101,32.\frac{1}{2}\uparrow +$
$\ldots -(0,001+0,456)\frac{1}{2}.9,47.38,84^2.\frac{2}{3}.101,32\downarrow$

$= -409,09 * 10^3$ N-mm^2

$\approx 2 * \beta_{dwor}(600)$ — see pg. 22
$(= 2 * -204,65.10^3 = -409,3 * 10^3$ N-mm$^2)$

$\therefore$ f_{dwor} (600) values were correctly derived from the β_{dwor} (600) value. Also, the f_{dwor} (600) stress system is self-equilibrating.

Check on B_{dwr} (300) value by using figure 3.2.14 - i.e the f_{dwr} (300) stress values. Also check the f_{dwr} (300) stress system for equilibrium.

By anti-symmetry about the ℄ (x=0), the resultant axial force on the cross-section is zero.

Also, $M_x = 0$ by anti-symmetry.

$M_y = 2.122,24^2.5,97. - 0,031.\frac{1}{2}.\frac{2}{3}\downarrow + 107,32.9,47.38,84.\frac{0,068-0,013}{2}\uparrow +$
$\ldots + 2.5,80.53,66^2.\frac{1}{2}.0,068.\frac{2}{3}\uparrow$

$= 10,75$ N-mm ↑

This value is small if compared to the applied loading.

$B_{dwr}(300) = 53,66^2.5,80.\frac{1}{2}.\frac{2}{3}.0,068.2.38,84\uparrow + -0,013.38,84^2.9,47.107,32\frac{1}{2}\downarrow$
$\ldots + (0,068+0,013).38,84^2.107,32.\frac{2}{3}.9,47.\frac{1}{2}$

$= 61,20$ N-mm^2 $* 10^5$

$\simeq 2 * B_{dwr}$ (300) – see page 23.
$(= 2 * 30,34 * 10^3 = 60,68 * 10^3$ N-mm$^2)$

∴ f_{dwr} (300) values were correctly derived from the B_{dwr} (300) value. Also, the f_{dwr} (300) stress system is self-equilibrating.

Units for the following diagrams are all in N/mm^2 (MPa.)

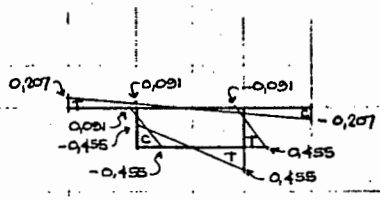

FIGURE 3.2.11: f_{dwr} at midspan

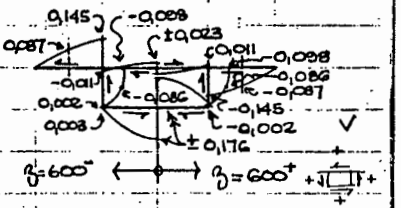

FIGURE 3.2.12: σ_{dwr} at midspan (ℓ=600⁻ and 600⁺)

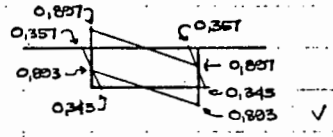

FIGURE 3.2.13: f_{trb} at midspan

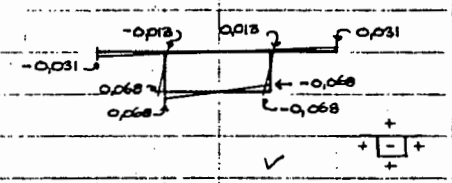

FIGURE 3.2.14: f_{dwr} at ℓ=300mm. (¼-span)

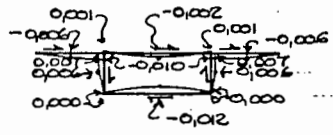

FIGURE 3.2.15: σ_{dwr} at ℓ=300mm (¼-span)

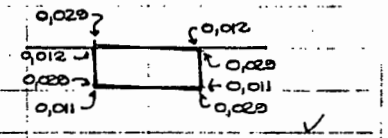

FIGURE 3.2.16: f_{trb} at ℓ=300mm. (¼-span)

ANALYSIS : MODEL NO 3 LOADCASE 2

Units for the following diagrams are all in N/mm^2 (MPa.)

THE COMBINED STRESS DIAGRAMS CAN BE PLOTTED AS FOLLOWS:

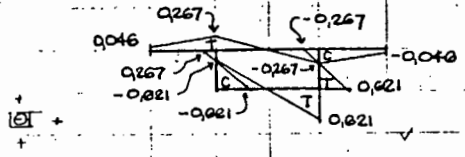

FIGURE 3.2.17: longitudinal stresses at midspan (z = 600)

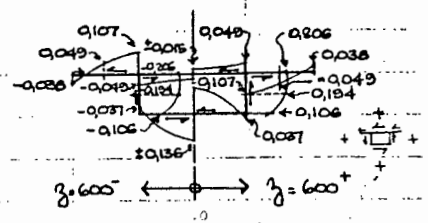

FIGURE 3.2.18: shear stresses at midspan (z = 600)

NOTE: EXTREME FIBRE STRESSES CAN BE FOUND USING FIG. 3.2.5. (DOTTED LINES)

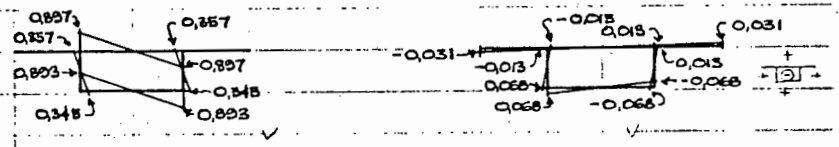

FIGURE 3.2.19: transverse bending stresses at midspan (z = 600mm.)

FIGURE 3.2.20: longit. stresses at ¼-span. (z = 300 mm.)

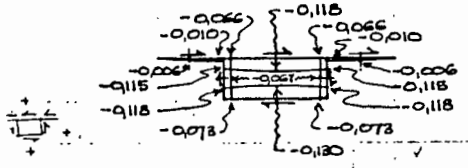

FIGURE 3.2.21: shear stresses at ¼-span (z = 300)

NOTE: EXTREME FIBRE STRESSES CAN BE FOUND USING FIGURE 3.2.9 (DOTTED LINES).

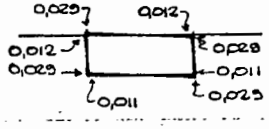

FIGURE 3.2.22: transverse bending stresses at ¼-span. (z = 300mm)

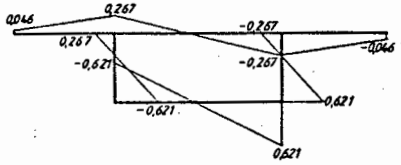

a) *Longitudinal stresses at midspan*

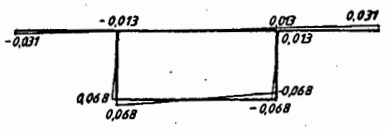

b) *Longitudinal stresses at ¼-span (z = 300 mm)*

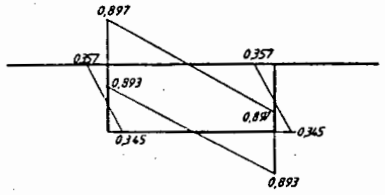

c) *Transverse bending stresses a at midspan*

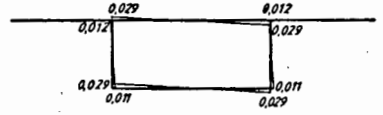

d) *Transverse bending stresses at ¼-span (z = 300 mm)*

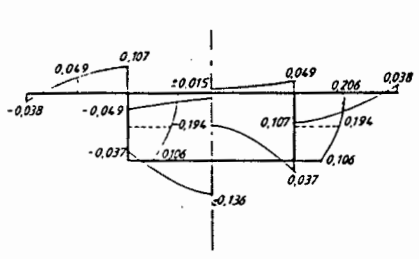

e) *Shear stresses at midspan*

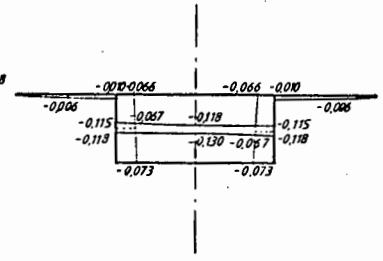

f) *Shear stresses at ¼-span (z = 300 mm)*

FIGURE 4.11: Model 3 Loadcase 2
Combined stresses from analysis